Segmental Orientation and Conformational Dynamics of Polymer Chains

by

Türkan Haliloğlu

B.S. in Chemical Engineering
BOĞAZİÇİ UNIVERSITY 1987

M.S. in Chemical Engineering
BOĞAZİÇİ UNIVERSITY 1989

Submitted to the Institute for Graduate Studies in Science and Engineering in partial fulfillment of the requirements for the degree of

Doctor
of
Philosophy

Chemical Engineering
BOĞAZİÇİ UNIVERSITY
1992

Acknowledgement

I would like to express my sincere gratitude to Doç. Dr. İvet Bahar and Prof. Dr. Burak Erman for their motivating guidance and invaluable supervision during the course of this study. Their helpful criticism in all aspects is of my great appreciation.

I would like to express my thanks to Prof. Dr. Salih Dinçer, Prof. Dr. Bahattin Baysal and Doç. Dr. Mehmet Çamurdan for their kind help and interest in this work.

Abstract

Various remarkable features of polymers, as compared with metallic and inorganic materials, arise from the fact that macromolecules can take up various conformations. The study of macromolecular conformations and dynamics is undoubtedly important in polymer science and technology from both basic and practical viewpoints. Comprehension of the configurational statistics of chain molecules leads to a rational interpretation and understanding of their physical properties. In previous studies, much effort have been devoted to dilute solutions. Though, recently there is a clear trend towards studying molecular properties in condensed systems, studies in the area of dilute solutions still remain a cornerstone of polymer characterization.

Orientational motions of segments in polymer chains depend sensitively on both intra- and intermolecular configurational characteristics of the chains, and thus are of special interest for the understanding of polymer behavior.

This thesis is mainly composed of two parts. In the first part, segmental orientation of polymers related to the chemical structure and resulting configurational characteristics of the chains are investigated using polyetylene(PE) and polyoxyethylene(POE) networks. In the calculations, the orientation of a reference vector **m** rigidly embedded in a chain of deformed network is considered. As a first step, the mean-square cosine $\langle \cos^2\theta \rangle_{\mathbf{r}}$ of the angle that **m** makes with a laboratory-fixed axis is formulated for a chain with fixed end-to-end vector **r**. A series expression including terms up to fifth inverse power of n, where n is the number of bonds in the network chain, is obtained for

$\langle\cos^2\theta\rangle_r$. Next, the corresponding averages over all chains of a network and the associated orientation function S, which is macroscopically observed are found in terms of (i) unperturbed chain moments readily obtainable by the rotational isomeric state scheme(RIS) (ii) the extension ratio λ for uniaxially deformed networks. Such a rigorous expression for S is particularly useful for relatively short chains and for moderate to large deformations that can not satisfactorily be accounted for by the existing simpler formulations. Thus, we estimate ranges of extension ratios λ to which the conventional first order approximation may be confidently applied. Calculations are performed for PE and POE chains of n = 21, 51 and 101 bonds which are generated by Monte Carlo simulation. The results are compared with those obtained by previous theoretical approaches. These comparisons demonstrate the importance of the adoption of higher order terms in the serial expansion of the orientation function for $\lambda \geq 1.8$

In the second part , static and dynamic correlations between bond conformations and reorientations are examined by Brownian dynamics simulations for polymer chains with fixed ends. Polyethylenelike model chains are considered. Rates of rotational isomeric transitions and time evolution of orientational correlations are analyzed for various extensions of the chain. The relatively more extended chain exhibits the higher mobility in the short-time scale but possesses lower effective rate of rotational isomerization. This follows from a hazard analysis covering ranges up to 10 ns. The time decays of bond orientational correlations are reproducible by stretch exponential functions with exponent almost independent of chain extension. The imposition of deformation by fixing chain ends, affects the orientational mobility of the chain down to the scale of individual bonds which may be observed from the biased evolution of time-dependent distribution functions for bond spatial reorientations. The analysis is also extended to the study of local orientational motions as seen by a

laboratory fixed-observer. Time-dependent joint probability distribution functions for orientations of a vector affixed to a polymer chain are expressed in terms of double spherical harmonics. An expansion of the distribution function up to the second order harmonics accurately reproduces the results of Brownian dynamics simulations for a 49 bond polyethylene chain whose end-to-end separation is fixed at different extensions. Various functions related to the anisotropy of segmental dynamics such as the mobility, orientation-mobility correlation, directivity of mobility and the sense of mobility are examined and observed to be strongly dependent on the degree of chain extension.

ÖZET

Makromoleküllerin birçok önemli özellikleri, metaller ve inorganik maddelerle karşılaştırıldığında, konformasyonal dönüşümlere sahip olmalarının bir sonucudur. Polimer bilim ve teknolojisinde moleküler konformasyonların ve makromoleküler dinamiğin incelenmesi temel ve pratik görüşler açısından önemlidir. Zincir moleküllerinin konfigürasyon istatistiğinin incelenmesi, oluşturduğu polimerin özelliklerinin anlaşılmasına ve yorumlanmasına olanak sağlar.

Polimer zincirlerinde yönlenme hareketleri zincirin hem molekül içi hem de moleküller arası konfigürasyonal karakteristiklerine bağlıdır. Bu tez çalışması iki bölümden oluşmaktadır. Birinci bölümde polimer zincirlerinin yapılarına ve onun sonucu konfigürasyon karakteristiklerine bağlı olarak yerel(segmental) yönlenmesi polietilen(PE) ve polioksietilen (POE) ağyapılarında incelenmektedir. Hesaplamalarda deformasyona uğramış ağyapıda bir zincire yerleştirilmiş bir referans vektörünün yönlenmesi düşünülmüştür. İlk adım olarak, **m** vektörünün sabit bir eksenle yaptığı açının karelerinin ortalaması $\langle\cos^2\theta\rangle_r$, konum vektörü (end-to-end vector) **r** olan bir polimer zinciri için ifade edilir. Ardından bir ağyapının bütün zincirlerine karşılık gelen ortalamalar ve ilgili yönlenme fonksiyonu, i) dönme izomerleri modeli ile elde edilen serbest zincirin momentleri ile ve ii) tek yönlü deformasyona uğramış ağyapılardaki çekme oranları ile ifade edilir. Yönlenme fonksiyonunun elde edilen şekli, özellikle kısa zincirler ve yüksek deformasyon oranlarında gerçeğe yakın sonuçlar vermektedir. Hesaplamalar Monte Carlo simülasyon yöntemi ile elde edilmiş n = 21, 51 ve 101 bağdan oluşan PE ve POE zincirleri için yapılmıştır. Birinci

derece yaklaşımın uygulanabileceği zincir boyutları ve çekme oranları belirlenmiştir. Sonuçlar Monte Carlo simülasyon sonuçları ve önceki teorik yaklaşımlarla karşılaştırılmıştır. Bu karşılaştırılmalar çekme oranı $\lambda \geq 1.8$ olan durumlarda yönlenme fonksiyonu için yüksek mertebeden yaklaşımın önemini göstermektedir.

Bu tez çalışmasının ikinci bölümünde Brownian Dinamik simülasyon yöntemi ile tek yönlü değişik derecelerde deformasyona uğramış polimer zincirlerinin statik ve dinamik özellikleri araştırılmıştır. Bu amaçla model PE zincirlerinin simülasyonu yapılmıştır. Dönme izomerleri arasındaki geçiş hızları ve yönlenme korelasyonlarının zaman içindeki gelişimi değişik oranlarda çekilen zincirler için incelenmiştir. En fazla deformasyona uğrayan zincirin kısa-zaman ölçeğinde en fazla hareketliliğe sahip olduğu gözlenmektedir; ancak aynı zincir *hazard* analiz yönteminden elde edilen sonuçlara göre en düşük etkin dönme izomerizasyon hızını göstermektedir. Bağ vektörlerinin zaman içinde sönmesini gösteren eğriler Kollrauch-Williams-Watts(stretched-exponential) fonksiyonlarına uymaktadır. Zincir uçlarını sabit tutmak üzere uygulanan deformasyon, zincir bağlarının ölçeğinde dahi etki etmektedir. Yerel yönlenme hareketleri, sabit bir eksenden izeyebilmek üzere, küresel harmonik(spherical harmonics) serisi ile ifade edilmiş zamana bağlı olasılık dağılım fonksiyonları ile incelenmiştir. Bu serinin ikinci dereceye kadar açılmış terimleri Brownian Dinamik sonuçları ile karşılaştırılmıştır. Yerel zincir dinamiğindeki yönlenmeyi ifade eden fonksiyonlar farklı oranlarda çekilmiş zincirler için hesaplanmış ve çekme oranlarına büyük ölçüde bağımlı oldukları gözlenmiştir.

TABLE OF CONTENTS

Page

List of Figures

Page

Page

List of Tables

List of Symbols

A_i (t) : Gaussianly distributed stochastic force per unit mass

C(t) : orientation-mobility correlation

D(t) : directivity of mobility

$D^k_{ml}(\Omega_0)$: Wigner rotation matrices of Ω_0

$E\{\Phi\}_r$: configurational energy of the configuration $\{\Phi\}_r$

$\mathbf{I}_3$: the identity matrix of order 3

k_B: Boltzmann constant

$\mathbf{l}_i$: the bond vector between atoms i-1 and i

l_i : the magnitude of bond vector

m : a unit vector rigidly affixed to a chain

m_i : mass of particle i

M(t) : mean mobility amplitude

$M_1(t)$: first orientational autocorrelation function of bond vectors

$M_2(t)$: second orientational autocorrelation function of bond vectors

$M_i(t)_{norm}$: normalized orientational autocorrelation function of bond vectors

N : the number of Kuhn segments in a chain

p_t : probability of trans state for a given bond

p_{g+} : probability of gauche$^+$ state for a given bond

p_{g-} : probability of gauche$^-$ state for a given bond

$P_{\mathbf{r}}(\omega)$: equilibrium probability distribution of the polar direction ω

$P_{\mathbf{r}}(\Omega, t; \Omega_0, t_0)$: joint probability of orientation Ω at time t and Ω_0 at time t_0 in a chain with fixed **r**

q : Fourier transform variable

$q_{\mathbf{r}}(\omega, t; \omega_0, t_0)$: conditional probability of occurrence of the orientation ω at time t, given that the orientation at time t_0 is ω_0 in a chain with fixed **r**

$q_{\xi\eta}$: the conditional probability of occurrence of isomeric state η for bond i, given that i-1 is in the state ξ

$\mathbf{r}$: end-to-end separation vector of a chain

r : magnitude of $\mathbf{r}$

R : gas constant

$\mathbf{r}_0$: end-to-end vector of a chain in undeformed state

$\mathbf{r}_i$: position vector of particle i

r_{max} : the maximum end-to-end separation

S : orientation function

$S(t)$: sense of mobility

T : absolute temperature

U : statistical weight matrix

V : total conformational potential

$V_b(l_i)$: bond stretching potential

$V_\theta(\theta_i)$: bond angle bending potential

$V_\phi(\phi_i)$: bond torsional potential

$Y^m{}_k(\Omega_0)$: spherical harmonics of functions Ω_0

Z : configurational partition function

$Z_\mathbf{r}$: configurational partition function for a chain with fixed end-to-end vector $\mathbf{r}$

α : reorientation angle

β : exponent in the stretched exponential function

ε : strain

θ, ϕ : the polar and azimuthal angles of a vector

θ_i : the supplemental bond angle between the bonds i and i+1

λ_h : transition rate from asymptotic slope of hazard plot

λ : extension ratio

λ_{tg} : transition rate from trans to one of the gauche states

λ_{gt} : transition rate from one of gauche states to the trans

ξ : friction coefficient

τ : characteristic time of stretched exponential expression

τ_q : the angle between the X axis and $\mathbf{q}$(see Figure 2.2a)

Φ : the angle between $\mathbf{m}$ and $\mathbf{r}$(see Figure 2.2a)

ϕ_i: the torsional angle of bond vector $\mathbf{l}_i$

$\{\Phi\}_{\mathbf{r}}$: configuration of a chain with fixed end-to-end vector $\mathbf{r}$

χ, ψ, ω : three Euler angles(see Figure 2.2a)

$\Omega(\omega, t)$: spherical polar angles

∇_i : gradient operator, the partial derivative with respect to the position vector $\mathbf{r}_i$

Chapter I

Introduction

This thesis is mainly composed of two studies of segmental orientation in polymer chains. In the first part, segmental orientation in uniaxially deformed networks, polyethylene(PE) and polyoxyethylene(POE) have been investigated.

The existing theoretical characterization of segmental orientation in polymeric chains which are subject to an external disturbance is based almost entirely on the freely jointed chain model. Although this model conveniently leads to simple analytical expressions for segmental orientation, its inadequacy to reflect the effects of the real chemical structure of a polymeric system is a serious weakness. Recent developments in spectroscopic techniques, in particular the use of dynamic infrared spectroscopy[1] and deuterium NMR spectroscopy[2], permit very accurate measurements of segmental orientation in polymeric systems in deformed state. The degree of accuracy of these two techniques is unprecedented by any of the conventional techniques in this field.

On the theoretical side, the general formulation of the problem of segmental orientation in real chains has been outlined in the pioneering work of Nagai[3]. Calculation methods for segmental orientation according to rotational isomeric scheme for real chains were later improved by Flory[4] in a form that is suitable for the study of birefringence. The formulations of both Nagai and Flory lead to an expression in the form of series expansion containing various-order moments of the chain end-to-end vector and related trigonometric variables. For sufficiently long chains, i.e., chains containing more than 100 bonds, the first term

of the series gives a reasonable accuracy. However, as the number of bonds decreases, more terms of the series are required for accuracy. The specific aim of this study is to give a more rigorous expression for the orientation function so as to include several powers of 1/n, where n is the number of bonds of the chain. By the use of such an expression, the relative contributions of first and second order approximations are assessed. It should be noted, at this point that the original paper of Nagai contains some minor printing mistakes in the expression for orientation and not all of the sixth-order terms are included therein. The treatment by Flory, on the other hand, is developed only for birefringence and is not exactly suitable for the study of segmental orientation. The present treatment may thus be regarded as an improvement and completion of the previous formulations of Nagai and Flory.

Within the context of the first part, in Section II, the theory is applied to uniaxially deformed PE and POE networks and the importance of contribution of higher order terms to segmental orientation is examined. Calculations have been performed for PE and POE network chains of n = 21, 51 and 101.

In the second part, Brownian Dynamics simulations have been performed for the investigation of equilibrium and dynamic properties of uniaxially deformed polymer chains. Internal orientational and conformational correlations in deformed polymer chains with fixed end-to-end separation are studied as a first step. Previous theoretical considerations indicate that polymers with fixed ends are subject to distinct conformational statistics, depending on the degree of extension or perturbation of the chain.[4] Similarly, the local reorientational and conformational dynamics of deformed chains is expected to be altered due to the imposition of spatially constrained ends. Examination of the distribution of conformational states and their time evolution in chains with fixed end-to-end

separation **r** is expected to give some insights as to the intrinsic orientational characteristics of deformed network chains.

A potentially useful tool to study high frequency motions and associated dynamic properties in polymeric systems is the Brownian dynamics (BD) simulation technique.[5] The time evolution of particles in BD method is described by coupled Langevin differential equations or alternatively stochastic difference equations which are shown to be equivalent to the Fokker-Planck description of particle diffusion.[6,7] Earlier studies using this technique adopted simple model chains such as one-dimensional bistable oscillators.[8,9] Studies of more realistic moderate size chains with fixed bond lengths and bond angles were soon performed by Fixman using generalized coordinates,[6,7] by Pear and Weiner,[10,11] and Levy et al.[12] In the BD study of conformational transitions by Helfand, Wasserman and Weber[13,14] bond stretching and bond angle bending were incorporated as possible degrees of freedom in addition to bond torsional mobility. BD has thereafter proved to be a mathematically convenient method to treat several problems involving (i) static properties such as end-to-end distribution functions in various regimes,[15] surface adsorption,[16] and collapse transition produced by modulating intermolecular interactions,[17] and (ii) dynamic phenomena such as relaxation of various correlation functions, transitions between rotational conformers,[13,14,18] chain diffusion,[7,19] cyclization.[20] Also, the time evolution of internal relaxational modes and dynamic light scattering functions have been recently investigated by BD method,[21] following the formalism introduced by Ermak and McCammon[22] which considers the effect of fluctuating hydrodynamic interactions.

In this study, BD simulations are performed using the polyethylenelike model chain of Helfand, Wasserman and Weber.[13,14]A similar mathematical

formalism has been recently adopted by Adolf and Ediger[23] to analyze the role of cooperativity in conformational transitions of polyisoprene. The ends of the chains investigated in the present study are held fixed in space, to mimic the state of deformed chains following the affine network model. The simulations are repeated for various end-to-end separations to assess the influence of chain extension (or compression) on the conformational and orientational behavior of the chain. Results of BD simulation are used to study the internal orientational dynamics of deformed polyethylene model chains as a function of their end-to-end separation. The rate of transitions between isomeric states and bond orientational auto- and cross-correlations are observed to be strongly affected by the perturbation of chain dimensions. Conformational correlation functions are evaluated for backbone bonds and the autocorrelation functions, $M_1(t)$ and $M_2(t)$ associated with the reorientation of bond vectors are analyzed.

The analysis is extended to study the local orientational motions in polymer chains by the use of time-dependent probability distribution functions . The anisotropy of segmental dynamics in polymer chains has been investigated some years ago in terms of double spherical harmonics by Tao[24] and Jarry and Monnerie.[25] These authors formulated the time-dependent orientation distribution for vectors affixed to chains in a form suitable for the study of local chain dynamics by polarized fluorescence experiments. In recent years, interest has been refocussed on the problem of the anisotropy of local static and dynamic orientational correlations following the developments in deuterium NMR spectroscopy.[26] The present treatment tests the adequacy of spherical harmonics series expansion of the joint distribution function for chains with fixed ends at various extensions. The analysis carried out for the investigation of internal orientational dynamics of PE chains in Section 3.2 is extended to the study of local orientational motions in deformed chains as seen by a laboratory-fixed

observer at a given orientation with respect to the chain vector. Time-dependent joint probability functions in the form of a double spherical harmonics series are developed for the orientation of bond vectors. The coefficients of this series are evaluated numerically for a polyethylene chain of 49 bonds using the results of the Brownian dynamics simulation described in detail in Sections 3.1 and 3.2.

Finally in Section 3.4, the simulation results have been exploited for the calculation of some experimental measurable functions; the mean mobility, orientational-mobility amplitude correlations, directivity of mobility and the sense of mobility.

Chapter II

Segmental Orientation in Uniaxially Deformed Networks: A High Order Approximation for Finite Chains and Large Deformations

The second Legendre function S, also termed as the orientation function, is defined by

$$S = [\, 3 < \cos^2\theta > - 1 \,] / 2 \qquad (2.1)$$

Segmental orientation in deformed networks may be analyzed at different levels of approximation. The simplest and the most commonly employed model is the Kuhn model[32] relating the orientation function to the number of Kuhn segments in network chains and to the applied state of uniaxial deformation. It is given according to the expression

$$S = (1/5N)\,(\lambda^2 - \lambda^{-1}) \qquad (2.2)$$

where N is the number of Kuhn segments of the chain and λ is the extension ratio defined as the ratio of the final macroscopic length of the network under uniaxial extension to its length in the reference state. The variable λ also identifies the extension ratio of each chain at the microscopic level because eq 2.2 is based on the affine network model where the ends of the network chains deform affinely with macroscopic dimensions. Equation 2.2 constitutes

the first term of a series expression for the freely jointed chain. Under larger degrees of extension of the network, higher order terms in 1/N and λ are needed which have been derived by Roe and Krigbaum[31] and Walasek.[33] Inasmuch as eq 2.2 and its higher order approximations[31,33] are based on the freely jointed chain, they give only a qualitative idea on segmental orientation in deformed network chains. The shortcomings of eq 2.2 when applied to real chains have been recently indicated.[34,35]

In a more realistic approximation, the front factor 1/5N in eq 2.2 may be replaced by the coefficient

$$D_o = (3 < r^2\cos^2\Phi >_o / < r^2 >_o - 1) /10 \qquad (2.3)$$

obtained[3,4] according to a more rigorous description of the chain structure than the freely jointed one. This expression characterizes the orientation of any vector which is rigidly affixed to any point of the chain. Φ is the angle between the vector of interest and the chain end-to-end vector. Angular brackets denote the ensemble average and the subscript zero indicates that the averaging is performed for chains in the unconstrained state. The statistical averages in eq 2.2 may conveniently be evaluated according to the RIS scheme as has been indicated by Nagai[3] and Flory.[4] Thus, for a chain of n bonds, within the validity of the RIS scheme, eq 2.2 represents the exact first term, linear in 1/n, that replaces the front factor of 1/5N of the Kuhn approximation in eq 2.2. Its derivation rests on the two assumptions that (i) the chains are long and (ii) the macroscopic deformation imposed on the network is low. The higher order terms required when the chains become shorter and the deformations larger have been given by Nagai[3] and Flory[4]. In the following sections, the formulation of Nagai and Flory has been generalized[36] to finite chains and large deformations.

The affine network model of rubber elasticity is adopted. The choice of a network for describing segmental orientation is only for convenience of visualizing the chains in equilibrium in the deformed state. We therefore assume each chain to extend between two active junctions that displace affinely with the macroscopic deformation. The treatment may be applied to systems other than networks by suitably assuming two points on the chain to deform affinely and calculating the state of segmental orientation between those two points. In this respect the present treatment focuses only on intramolecular contributions to segmental orientation. Intermolecular contributions imposed by the local anisotropic environment of a given segment are not considered.

As a first step, following Nagai's earlier treatment , the mean square cosine $\langle\cos^2\theta\rangle_{\mathbf{r}}$ of the angle that **m** makes with a laboratory-fixed axis is formulated for a chain vector with fixed end-to-end vector **r**. An expression including terms up to fifth inverse power of n, where n is the number of bonds in the network chain, is obtained for $\langle\cos^2\theta\rangle_{\mathbf{r}}$. Next the corresponding averages over all chains of a network and the associated orientation function S, are found in terms of (i) unperturbed chain moments readily obtainable by the rotational isomeric scheme(RIS) (ii) the extension ratio for uniaxially deformed networks.

2.1Theory

One configuration of a single chain is shown in Figure 2.1. Oxyz represents a laboratory fixed coordinate system. The two ends of the chain at O and A represent points fixed in space. In a network, those are the two junction points at the termini of a network chain. They are assumed to displace affinely

with the macroscopic deformation. **r** in the figure represents the end-to-end vector of the chain in the deformed state, which, in the undeformed state, is equal to $\mathbf{r}_0$. For simple elongation along the x-direction, using the deformation gradient tensor λ, we have

$$\mathbf{r} = \lambda \mathbf{r}_0 \tag{2.4}$$

where

$$\lambda = \begin{bmatrix} x/x_0 & 0 & 0 \\ 0 & y/y_0 & 0 \\ 0 & 0 & z/z_0 \end{bmatrix} = \begin{bmatrix} \lambda & 0 & 0 \\ 0 & \lambda^{-1/2} & 0 \\ 0 & 0 & \lambda^{-1/2} \end{bmatrix} \tag{2.5}$$

with x_0, y_0, z_0, and x, y, z denoting the components of $\mathbf{r}_0$ and **r**, respectively, and λ representing the extension ratio.

In Figure 2.1, **m** represents a unit vector rigidly affixed to the chain at a given point. It makes an angle θ with the x-axis as shown. In the present treatment, **m** may represent the direction of any sequence of bonds in the chain or it may refer to a specific label attached to the chain. Identification of **m** with one of the principal components of the optical polarizability tensor provides the basis for the analysis of strain birefringence[4] whereas in the treatment of dichroic ratio it is identified with the absorption transition moment of the excited group. We are interested in the orientation of **m** as the network deforms and the ends of the chain displace affinely with macroscopic strain.

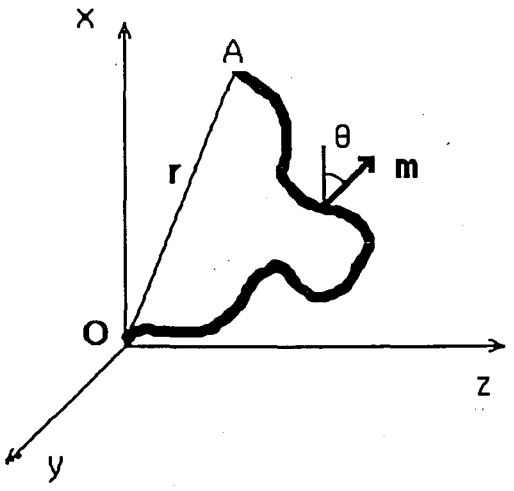

Figure 2.1 Schematic representation of a chain OA with end-to-end vector **r**. The vector **m** is rigidly affixed to the chain and makes an angle θ with the laboratory fixed x-axis.

The orientation of **m** will be calculated in two stages: In the first stage, we consider only a single chain whose end-to-end vector **r** is fixed in space, and calculate the average $< \cos^2\theta >_{\mathbf{r}}$ over all configurations of that chain. Here, the subscript **r** refers to the averaging over all configurations at fixed **r**. In the second stage, we find the average $< \cos^2\theta >$ over all chains of the system. Here, the subscript **r** is deleted inasmuch as the constraint of fixed **r** is removed.

2.1.1 Average Orientation of Bond Vectors with respect to Stretch Direction in Deformed Chains

Calculation of $< \cos^2\theta >_{\mathbf{r}}$

We follow a procedure similar but not identical to the one adopted by Nagai[3] and Flory.[4] The average $< \cos^2\theta >_{\mathbf{r}}$ is expressed by

$$< \cos^2\theta >_r = Z_r^{-1} \int \cos^2\theta \exp (- E \{ \phi \}_r / kT) \, d\{\phi\}_r \tag{2.6}$$

where, $E \{ \phi \}_r$ is the energy of the configuration $\{ \phi \}_r$ which is defined by a set of skeletal bond rotations. The subscript **r** in $d\{ \phi \}_r$ indicates that the integration is carried out over only those configurations that possess the specified end-to-end vector **r**. It should be understood that the whole configurational space is referred to, whenever the subscript **r** is omitted. k is the Boltzmann factor, T is the absolute temperature. Z_r is the configuration partition function for a chain with fixed **r**, defined as

$$Z_r = \int \exp (- E \{ \phi \}_r / kT) \, d\{ \phi \}_r \tag{2.7}$$

Denoting the integral in the right-hand side of eq 2.6 by f (**r**), we have

$$f (\mathbf{r}) \equiv \int \cos^2\theta \exp (- E \{ \phi \}_r / kT) \, d\{\phi\}_r = < \cos^2\theta >_r Z_r \tag{2.8}$$

The Fourier transform f (**q**) of f (**r**) is

$$f (\mathbf{q}) = \int e^{ - i\mathbf{q} \cdot \mathbf{r}} < \cos^2\theta >_r Z_r \, d\mathbf{r} \tag{2.9}$$

$$= \int_r \int_{\chi,\psi,\omega} \int_{\{\phi\}_r} \cos^2\theta \exp (- E\{ \phi \}_r / kT) \, e^{ - i\mathbf{q} \cdot \mathbf{r}} \sin\chi \, d\chi \, d\psi \, d\omega \, d \{ \phi \}_r \, dr \tag{2.10}$$

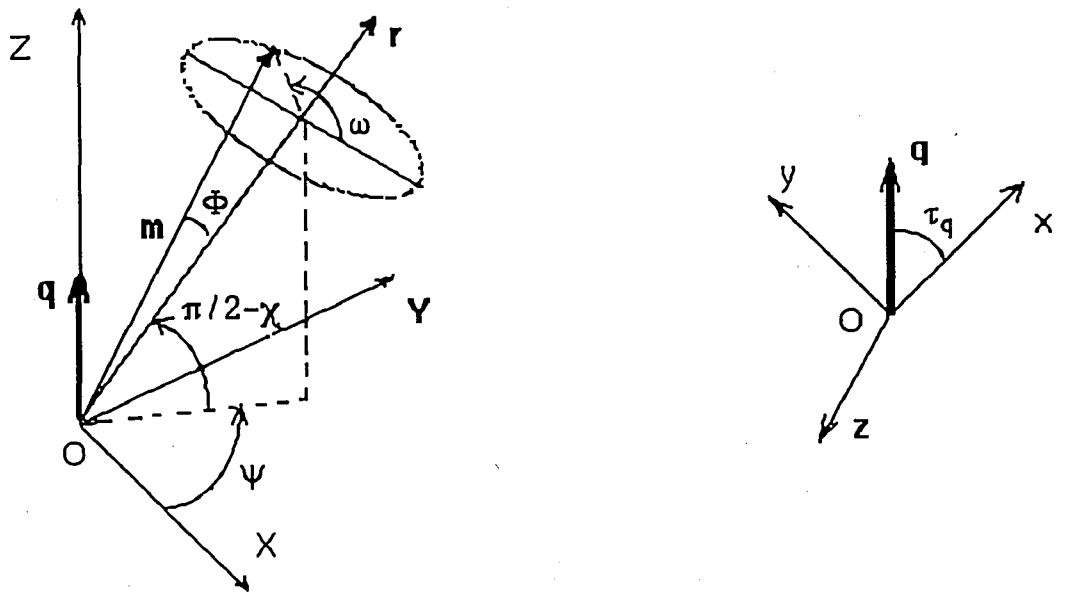

Figure 2.2 (a) The representation of **m** and **r** in the XYZ coordinate system in which the Z-axis is parallel to the transform variable **q**. Φ is the angle between **m** and **r**. ψ, χ and ω are the three Euler angles. (b) Position of the transform variable **q** with respect to the laboratory fixed frame xyz. τ_q is the angle it makes with the x-axis.

Here **q** is the transform variable, r is the magnitude of **r** and χ, ψ and ω are the three Euler angles defined in Figure 2.2. In this figure, XYZ is a new Cartesian coordinate system with the Z axis parallel to **q** and the X axis is in the xZ plane. The X axis makes an acute angle with x. χ and ψ are the polar and azimuthal angles, respectively, locating **r** relative to **q** along the polar axis Z. ω gives the rotation of the plane defined by **m** and **r** from the plane of **r** and Z. Using

$$\int_r \int_{\chi,\psi,\omega} \int_{\{\phi\}_r} d\{\phi\}_r \sin\chi \, d\chi \, d\psi \, d\omega \, dr = 8\pi^2 \int_r \int_{\{\phi\}_r} d\{\phi\}_r \, dr$$

$$= \int_r \int_{\{\phi\}_r} d\{\phi\}_r \, dr = \int_{\{\phi\}} d\{\phi\} \qquad (2.11)$$

Equation 2.9 may be rewritten as

$$f(\mathbf{q}) = (8\pi^2)^{-1} \int_{\{\phi\}} \cos^2\theta \exp(-E\{\phi\}/kT)\, e^{-i\mathbf{q}\cdot\mathbf{r}} \sin\chi \, d\chi \, d\psi \, d\omega \, d\{\phi\} \qquad (2.12)$$

Let Φ denote the angle between **m** and **r** as shown in Figure 2.2a. The laboratory fixed system Oxyz is shown in part b of the same figure. The components of **q** along the x, y and z axes are indicated as q_x, q_y and q_z. The angle between the x axis and **q** is shown by τ. From the scalar product of **m** with the x axis, both of them being expressed in the frame XYZ, it is possible to write $\cos\theta$ in terms of χ, ψ, ω, Φ and τ as

$$\cos\theta = \sin\tau [\sin\chi\cos\psi\cos\Phi + (\cos\chi\cos\psi\cos\omega - \sin\psi\sin\omega)\sin\Phi]$$

$$+ \cos\tau [\cos\chi\cos\Phi - \sin\chi\cos\omega\sin\Phi] \qquad (2.13)$$

The substitution of eq 2.13 into eq 2.12 and integration over χ, ψ and ω, at fixed $\{\phi\}$, leads to the series expression

$$f(\mathbf{q}) = \frac{1}{3}\int \left[[1 - \frac{(qr)^2}{3!} + \frac{(qr)^4}{5!} - \frac{(qr)^6}{7!} + \frac{(qr)^8}{9!} + \ldots] - \frac{1}{2}(3\cos^2\tau - 1)(3\cos^2\Phi - 1) \right.$$

$$x\left[\frac{(qr)^2}{5.3!}-\frac{(qr)^4}{7.5.3!}+\frac{(qr)^6}{9.7.5!}-\frac{(qr)^8}{11.9.7!}\right]\Big]\exp(-E/kT)\,d\{\phi\} \tag{2.14}$$

where q is the magnitude of **q**. Expressing the internal configuration variables in terms of the configurational averages of the various quantities, we obtain

$$f(\mathbf{q})=\frac{Z}{3}\left\{\left[1-\frac{\langle r^2\rangle_0 q^2}{3!}+\frac{\langle r^4\rangle_0 q^4}{5!}-\frac{\langle r^6\rangle_0 q^6}{7!}+\frac{\langle r^8\rangle_0 q^8}{9!}\right]\right.$$

$$-\frac{1}{2}(3q_x^2-q^2)\left[\frac{1}{5.3}(3\langle r^2\cos^2\Phi\rangle_0-\langle r^2\rangle_0)-\right.$$

$$\frac{q^2}{7.5.3!}(3\langle r^4\cos^2\Phi\rangle_0-\langle r^4\rangle_0)+\frac{q^4}{9.7.5!}(3\langle r^6\cos^2\Phi\rangle_0-\langle r^6\rangle_0)$$

$$\left.-\frac{q^6}{11.9.7!}(3\langle r^8\cos^2\Phi\rangle_0-\langle r^8\rangle_0)+\ldots\right] \tag{2.15}$$

where the subscript zero appended to angular brackets refers to the averaging of the chains in the unperturbed state and Z is the configuration partition function for the free chain. Eq 2.15 is identical in form to the expression which was given by Flory up sixth order terms. Following the procedure adopted by Flory, multiplication of the denominator of eq 2.15 by exp ($\langle r^2\rangle_0 q^2/6$) and the numerator by the series expansion of this expression leads to

$$f(\mathbf{q})=\frac{Z}{3}\exp(-\langle r^2\rangle_0 q^2/6)\{1+[\eta_2(\langle r^2\rangle_0/3)+\eta_4(\langle r^2\rangle_0/3)^2 q^2$$

$$+\eta_6(\langle r^2\rangle_0/3)^3 q^4+\eta_8(\langle r^2\rangle_0/3)^4 q^6+\ldots](q^2-3q_x^2)$$

$$+[g_4(<r^2>_0/3)^2 q^4+g_6(<r^2>_0/3)^3 q^6+g_8(<r^2>_0/3)^4 q^8+...]\}$$

(2.16)

where

$$\eta_2 \equiv \frac{1}{10}\left(\frac{3<r^2\cos^2\Phi>_0}{<r^2>_0}-1\right)$$

$$\eta_4 \equiv \frac{1}{20}\left[\left(\frac{3<r^2\cos^2\Phi>_0}{<r^2>_0}-1\right)-\frac{3}{7}\left(\frac{3<r^4\cos^2\Phi>_0}{<r^2>_0^2}-\frac{<r^4>_0}{<r^2>_0^2}\right)\right]$$

(2.17)

$$\eta_6 \equiv \frac{1}{80}\left[\left(\frac{3<r^2\cos^2\Phi>_0}{<r^2>_0}-1\right)-\frac{6}{7}\left(\frac{3<r^4\cos^2\Phi>_0}{<r^2>_0^2}-\frac{<r^4>_0}{<r^2>_0^2}\right)\right.$$
$$\left.+\frac{1}{7}\left(\frac{3<r^6\cos^2\Phi>_0}{<r^2>_0^3}-\frac{<r^6>_0}{<r^2>_0^3}\right)\right]$$

$$\eta_8 \equiv \frac{1}{480}\left[\left(\frac{3<r^2\cos^2\Phi>_0}{<r^2>_0}-1\right)-\frac{9}{7}\left(\frac{3<r^4\cos^2\Phi>_0}{<r^2>_0^2}-\frac{<r^4>_0}{<r^2>_0^2}\right)\right.$$
$$+\frac{3}{7}\left(\frac{3<r^6\cos^2\Phi>_0}{<r^2>_0^3}-\frac{<r^6>_0}{<r^2>_0^3}\right)-\frac{3}{77}\left.\left(\frac{3<r^8\cos^2\Phi>_0}{<r^2>_0^4}-\frac{<r^8>_0}{<r^2>_0^4}\right)\right]$$

and

$$g_4 \equiv -\left(\frac{1}{2!\,2^2}\right)\left[1-\frac{3<r^4>_0}{5<r^2>_0^2}\right]$$

$$g_6 \equiv -\left(\frac{1}{3!\,2^3}\right)\left[3\left(1-\frac{3<r^4>_0}{5<r^2>_0^2}\right)-\left(1-\frac{3^2<r^6>_0}{5\cdot 7<r^2>_0^3}\right)\right]$$

(2.18)

$$g_8 \equiv -\left(\frac{1}{4!\,2^4}\right)\left[\,6\left(1-\frac{3<r^4>_0}{5<r^2>_0^2}\right)-4\left(1-\frac{3^2<r^6>_0}{5\cdot7<r^2>_0^3}\right)+\left(1-\frac{3^3<r^8>_0}{5\cdot7\cdot9<r^2>_0^4}\right)\right]$$

The inverse Fourier transform of eq 2.9 yields the required average

$$<\cos^2\theta>_r = (2\pi)^{-3} Z_r^{-1} \int f(\mathbf{q})\, e^{i\,\mathbf{q}\cdot\mathbf{r}}\, d\mathbf{q} \tag{2.19}$$

Substituting from eq 2.16 into eq 2.19, writing $\mathbf{q}\cdot\mathbf{r}$ as $x\,q_x + y\,q_y + z\,q_z$ and performing the integrations lead to

$$<\cos^2\theta>_r = (Z/Z_r)\,(3/<r^2>_0^3)^{1/2}\,(1/2\pi)^{3/2}\exp(-3r^2/2<r^2>_0)\left\{1+\right.$$

$$\left.\alpha_1\eta_2+\alpha_2\eta_4+\alpha_3\eta_6+\alpha_4\eta_8+\beta_1 g_4+\beta_2 g_6+\beta_3 g_8\right\} \tag{2.20}$$

where

$$\alpha_1 \equiv 3\,(3x^2-r^2)/<r^2>_0$$

$$\alpha_2 \equiv 3^2\left(\frac{7}{3}-\frac{r^2}{<r^2>_0}\right)(3x^2-r^2)/<r^2>_0$$

$$\alpha_3 \equiv 3^3\left(7-6\frac{r^2}{<r^2>_0}+\frac{r^4}{<r^2>_0^2}\right)(3x^2-r^2)/<r^2>_0 \tag{2.21}$$

$$\alpha_4 \equiv 3^4\left(\frac{77}{3}-33\frac{r^2}{<r^2>_0}+11\frac{r^4}{<r^2>_0^2}-\frac{r^6}{<r^2>_0^3}\right)(3x^2-r^2)/<r^2>_0$$

and

$$\beta_1 \equiv 15 - 30\,\frac{r^2}{\langle r^2\rangle_0} + 9\,\frac{r^4}{\langle r^2\rangle_0^2}$$

$$\beta_2 \equiv 105 - 315\,\frac{r^2}{\langle r^2\rangle_0} + 189\,\frac{r^4}{\langle r^2\rangle_0^2} - 27\,\frac{r^6}{\langle r^2\rangle_0^3} \qquad (2.22)$$

$$\beta_3 \equiv 945 - 3780\,\frac{r^2}{\langle r^2\rangle_0} + 3402\,\frac{r^4}{\langle r^2\rangle_0^2} - 972\,\frac{r^6}{\langle r^2\rangle_0^3} + 81\,\frac{r^8}{\langle r^2\rangle_0^4}$$

The ratio Z_r / Z is equal to the distribution function $W(\mathbf{r})$ of the chain end-to-end vector. The latter may be expressed as a series expansion as derived by Nagai,[3] which, upon substitution of the variables defined in eqs 2.18 and 2.22, takes the simple form

$$Z_r / Z = W(\mathbf{r}) = (2\pi \langle r^2\rangle_0 / 3)^{-3/2} \exp\{-3r^2 / 2\langle r^2\rangle_0\}\,[\,1 + \beta_1 g_4 + \beta_2 g_6 + \beta_3 g_8 + \ldots]$$

(2.23)

By inserting eq 2.23 into eq 2.20 the following expression is obtained for the average of $\langle \cos^2\theta \rangle_r$ of the unit vector **m**

$$\langle \cos^2\theta \rangle_r = \frac{1}{3}(1 + \beta_1 g_4 + \beta_2 g_6 + \beta_3 g_8 + \ldots)^{-1}(1 + \alpha_1\eta_2 + \alpha_2\eta_4 + \alpha_3\eta_6 + \alpha_4\eta_8 + \beta_1 g_4 + \beta_2 g_6 + \beta_3 g_8 + \ldots)$$

(2.24)

Equation 2.24 may be approximated by expanding the first term in parenthesis as

$$< \cos^2\theta >_r \equiv \frac{1}{3} (1 - \beta_1 g_4 - \beta_2 g_6 - \beta_3 g_8) (1 + \alpha_1 \eta_2 +$$

$$+ \alpha_2 \eta_4 + \alpha_3 \eta_6 + \alpha_4 \eta_8 + \beta_1 g_4 + \beta_2 g_6 + \beta_3 g_8)$$

$$= \frac{1}{3} + (1 - \beta_1 g_4 - \beta_2 g_6 - \beta_3 g_8) \sum_{i=1}^{4} [\alpha_i \eta_{2i} / 3] \qquad (2.25)$$

2.1.2 Average Orientation of Bond Vectors with respect to Stretch Direction in Free Chains

Calculation of $< \cos^2 \theta >$

The expression given by eq 2.25 is an average for a single chain of the network having its two ends fixed. For relating the segmental orientation to that observed in experiments, we have to average eq 2.25 over all orientations and magnitudes of the end-to-end chain vectors. In eq 2.25 the coefficients η_i and g_i include statistical averages which have already been performed, as apparent from eqs 2.17 and 2.18. Averaging over the ensemble of chains has therefore to be carried out only for the terms comprising α_i and β_i. The latter includes ratios of the form $r^m / < r^2 >_0^{m/2}$, and α_i includes both those ratios and other terms of the form $3 x^2 / < x^2 >_0 - r^2 / < r^2 >_0$. If the powers of r are written in terms of the x, y and z components, a representative term whose ensemble average has to be taken will have the form $x^p y^q z^r$, where x, y and z are the components of the end-to-end vector in the deformed state. According to the affine deformation assumption, they are related to those in the undeformed state by

$$x^p y^q z^r = \lambda_x^p \lambda_y^q \lambda_z^r x_0^p y_0^q z_0^r$$

(2.26)

Here λ_x, λ_y and λ_z are the x, y, z components of λ. Representing the polar and azimuthal angles of a chain end-to-end vector by ϑ and φ, the undeformed components may in turn be expressed as

$$\begin{aligned} x_0 &= r_0 \cos\vartheta \\ y_0 &= r_0 \sin\vartheta \cos\varphi \\ z_0 &= r_0 \sin\vartheta \sin\varphi \end{aligned}$$

(2.27)

Substitution of eq 2.27 into 2.26 and averaging over both r_0 and the trigonometric functions leads to

$$< x^p y^q z^r > = \lambda_x^p \lambda_y^q \lambda_z^r < r^{p+q+r} >_0 Q(p,q,r)$$

2.28)

where,

$$Q(p,q,r) = (4\pi)^{-1} \int_{\varphi=0}^{2\pi} \int_{\vartheta=0}^{\pi} \cos^p\vartheta \sin^{q+r+1}\vartheta \cos^q\varphi \sin^r\varphi \, d\varphi \, d\vartheta$$

(2.29)

The application of the above integrations to isotropic, unperturbed chains leads to the averages of unperturbed dimension and of α_i, β_i and $\alpha_i\beta_j$ which are listed in the Appendix A. Those averages are inserted in eq 2.25 to yield the average $<\cos^2\theta>$ over all **r**. It is convenient to organize the latter on the basis of increasing powers of λ. Following the arguments given by Nagai[3] and Flory,[4] it can be shown that the coefficients g_i and η_i scale with the number n of segments in a chain as follows:

$$g_4 , \eta_2 \sim n^{-1}$$

$$g_6 , g_8 , \eta_4 , \eta_6 \sim n^{-2} \qquad (2.30)$$

$$\eta_8 \sim n^{-3}$$

Accordingly, $<\cos^2\theta>$ may be rearranged as

$$<\cos^2\theta> = \frac{1}{3}[\,1 + D_1(\lambda^2 - \lambda^{-1}) + D_2(\lambda^4 + \frac{1}{3}\lambda - \frac{4}{3}\lambda^{-2}) +$$

$$+ D_3(\lambda^6 + \frac{3}{5}\lambda^3 - \frac{8}{5}\lambda^{-3}) + D_4(\lambda^8 + \frac{5}{7}\lambda^5 + \frac{12}{35}\lambda^2 - \frac{8}{35}\lambda^{-1} - \frac{64}{35}\lambda^{-4}) + \cdots] \qquad (2.31)$$

where

$$D_1 = 2\eta_2 + 14\eta_4 + 126\eta_6 + 1386\eta_8 - 30\eta_2 g_4 -$$

$$- 210\eta_2 g_6 - 1890\eta_2 g_8 - 210\eta_4 g_4 - 1890\eta_6 g_4$$

$$D_2 = -\frac{18}{5}(\eta_4 + 18\eta_6 + 297\eta_8 - 10\eta_2 g_4 - 105\eta_2 g_6 - \qquad (2.32)$$

$$- 1260\eta_2 g_8 - 85\eta_4 g_4 - 900\eta_6 g_4)\frac{<r^4>_0}{<r^2>_0^2}$$

$$D_3 = \frac{54}{7}(\eta_6 + 33\eta_8 - \eta_2 g_4 - 21\eta_2 g_6 -$$

$$- 378\eta_2 g_8 - 17\eta_4 g_4 - 258\eta_6 g_4)\frac{<r^6>_0}{<r^2>_0^3}$$

$$D_4 = 18\,(\eta_2 g_6 + 36\,\eta_2 g_8 + \eta_4 g_4 + 28\,\eta_6 g_4)\,\frac{<r^8>_0}{<r^2>_0^4}$$

It should be noted that in eq 2.32, the leading term of D_1 is of order n^{-1}, those of D_2 and D_3 are of order n^{-2}, and that of D_4 is of order n^{-3}.

2.1.3 Orientation function

Substitution of eq 2.31 into eq 2.1 yields

$$S = \frac{1}{2}[\,D_1(\lambda^2 - \lambda^{-1}) + D_2(\lambda^4 + \frac{1}{3}\lambda - \frac{4}{3}\lambda^{-2}) + D_3(\lambda^6 + \frac{3}{5}\lambda^3 - \frac{8}{5}\lambda^{-3}) + D_4(\lambda^8 + \frac{5}{7}\lambda^5 + \frac{12}{35}\lambda^2 - \frac{8}{35}\lambda^{-1} - \frac{64}{35}\lambda^{-4}) + \cdots] \tag{2.33}$$

Inasmuch as the next coefficient D_5 will include terms of the order n^{-3}, eq 2.33 can not be regarded as complete up to the third order. Accordingly, calculations in the ensuing section are confined only to the first and second order approximations.

The orientation function in the small deformation limit may be obtained from eq 2.33 by factoring out the conventional small strain expression $\varepsilon = \lambda - 1$ and letting $\lambda = 1$. The result takes the form

$$S = \frac{3}{2}(D_1 + \frac{7}{3}D_2 + \frac{21}{5}D_3 + \frac{33}{5}D_4)\,\varepsilon \tag{2.34}$$

2.2 Segmental Orientation in Polyethylene Networks.

2.2.1 Statistical Characterization of the Polyethylene(PE) Chain and Monte Carlo Chain Generation

The statistics of PE chain has been investigated before.[4] The chain has a quite simple structure which is represented as a linearly connected sequence of groups, the identities of individual atoms being ignored. The planar form of the chain is depicted in Figure 2.3. The chain can be represented as $H(-CH_2CH_2)_xH$ in a closed form, where x stands for the number of repeat units. Considering pairwise interdependence of backbone bonds, following RIS formalism, two equivalent statistical weight matrices are required to account for the pairwise dependent bond rotational potentials in each repeat unit.

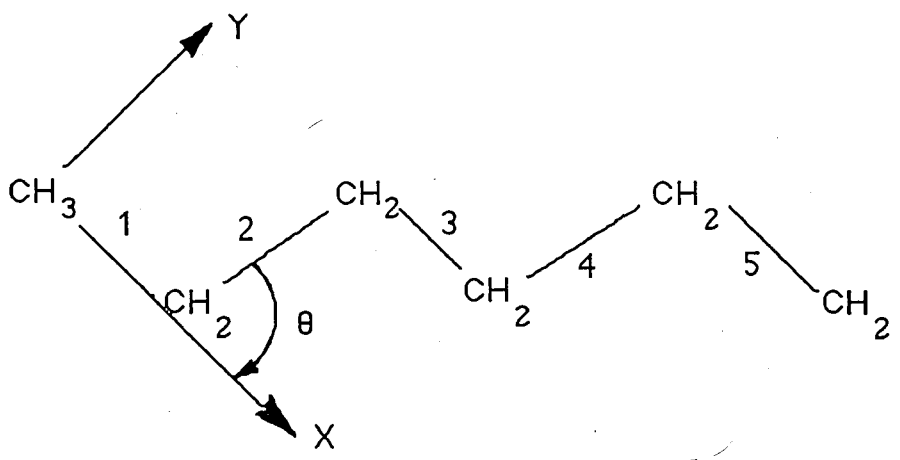

Figure 2.3 The planar form of a polyetylene(PE) chain

The first few bonds of the chain are represented in Figure 2.3. Local coordinate systems for skeletal bonds are defined in the conventional way; x axis lies along the i^{th} bond, y axis lies in the plane determined by bonds i and i-1 and

z axis in the way completing the right-handed system. 0^{th} atom is placed at the origin. The length of the CC bond is 1.53 Å and the supplemental bond angle ∠ CCC is 68^0. Isomeric rotations of the bonds are described in terms of three rotational states, *trans* (t), *gauche*$^+$ (g^+), and *gauche*$^-$ (g^-) which stand respectively for 0^0, $+112^0$, -112^0 rotations. The statistical weight matrices for the pair of backbone bonds is denoted by **U** and defined as

$$\mathbf{U} = \begin{bmatrix} 1 & \sigma & \sigma \\ 0 & \sigma & 0 \\ 1 & 0 & \sigma \end{bmatrix} \tag{2.35}$$

Here the parameter σ is calculated from the general expression

$$\sigma = \exp(-E_\sigma / RT) \tag{2.36}$$

where R is the gas constant, T is the absolute temperature and E_σ is 0.5 kcal/mol. For a chain of X units of the form $(-CH_2CH_2-)_X$, the configurational partition function Z is found from multiplication of the statistical weight matrices **U** as

$$Z = \mathbf{J}^*(\mathbf{U})^{2x-1}\mathbf{J} \tag{2.37}$$

where $\mathbf{J}^* \equiv$ row(1 0 0)

$\mathbf{J} \equiv$ col(1 1 1)

Monte Carlo Chain Generation:

The various moments of the form $\langle r^{2m}\rangle_0$ and $\langle r^{2m}\cos 2\phi\rangle_0\rangle$, with m=1-3, which appear in eqs 2.17-2.18, may in principle, be evaluated according to the matrix generation scheme of the RIS model. However, the analytical calculation

of the moments higher than the second becomes prohibitively difficult and recourse to Monte Carlo methods becomes imperative.

Conditional Monte Carlo technique with bond isomeric state probabilities deduced from the RIS model has been employed in generating chains of n=21, 51 and 101 bonds. In general, the conditional probability $q_{\zeta\eta;i}$ of occurrence of isomeric state η for bond i, given that bond i - 1 is in state ζ, is found from

$$q_{\zeta\eta;i} = p_{\zeta\eta;i} / \Sigma p_{\zeta\eta;i} \tag{2.38}$$

where the summation extends over all states accessible to bond i and the joint probability $p_{\zeta\eta;i}$ of states $\zeta\eta$ for the respective bonds i - 1 and i, is evaluated from

$$p_{\zeta\eta;i} = Z^{-1}\mathbf{J}^{*}\left[\prod_{h=2}^{i-1}\mathbf{U}_h\right]\mathbf{U}'_{\zeta\eta;i}\left[\prod_{j=i+1}^{n-1}\mathbf{U}_j\right]\mathbf{J} \tag{2.39}$$

Here $\mathbf{U}_{\zeta\eta;i}$ is the matrix obtained by equating all elements of $\mathbf{U}_i$ to zero, with the exception of the element $\zeta\eta$. Clearly, in the index notation which is adopted for convenience in eq 2.39, the matrix $\mathbf{U}_2,....,\mathbf{U}_{n-1}$ is identified with **U.**

The following variable were recorded for each generated chain:

i) The vector $\mathbf{r}_i$ connecting the zeroth atom to the ith atom, along the backbone.

ii) The angle Φ_i between the central bond vector $\mathbf{l}_i$ and the end-to-end vector **r**, which is obtained from

$$\Phi_i = \cos^{-1}[(\mathbf{l}_i.\mathbf{r})/l_i\, r] \qquad (2.40)$$

Here l_i and r is the magnitude of the vectors $\mathbf{l}_i$ and $\mathbf{r}_i$ and the dot stands for the scalar product.

iii) The vectors $r^{2m}=(\mathbf{r}.\mathbf{r})^{m}$ and $(r^{2m}\cos^2\phi)$, with m = 1-4 (2.41)

The above information obtained for each generated chain is combined to determine the ensemble averages $\langle r^{2m}\rangle_0$ and $\langle r^{2m}\cos^2\phi\rangle_0$ overall sets of generated chains of a given size.

2.2.2 Calculations and Discussion

Calculations were performed for polyethylene (PE) for a quantitative assessment of the relative importance of higher order approximations,in the evaluation of average orientations. Calculations involve two major steps in parallel with the theoretical presentation above: First, chains with constant **r** have been explored. The exact dependence of $\langle \cos^2\theta \rangle_r$ on **r** has been determined from Monte Carlo simulations and compared with the predictions of eq 2.24. In the second stage of calculations, all network chains have been considered and the degree of orientation has been investigated as a function of extension ratio, by adopting both first and second order dependences on 1/n, for comparison. The results from the two sets of calculations are separately presented and discussed in the following.

2.2.2.1 Orientation in a Chain with Fixed End-to-End Separation

Monte Carlo (MC) simulations are used in the present work for two purposes: First, it is possible to obtain an exact value for $< \cos^2 \theta >_r$ as a function of **r**, provided that a sufficiently large number of chains is generated. Secondly, MC chains are used for the determination of moments of the form $< r^{2m} \cos^2 \theta >_o$, $< r^{2m} >_o$, with m = 1-4, which will be required for the evaluation of η_i and g_j in eq 2.24. In particular, evaluation of averages with usual generator matrix technique of the RIS formalism, is prohibitively difficult when m is larger than 2, and MC calculations are indispensable.

PE chains generated by the conditional Monte Carlo method are classified according to the magnitude of their end-to-end vectors, and the average square cosine of the angle between the central bond and the vector **r** is evaluated for each subset of chains lying in a given interval of $r \pm \Delta r$. The resulting $< \cos^2 \theta >_r$ values are plotted as a function of r / r_{max} in Figures 2.4-2.6, for the respective cases n = 21, 51 and 101. r_{max} refers to the maximum end-to-end separation, i.e. that of the all trans configuration. The final point at $r / r_{max} = 1$ is calculated for the central bond in a fully extended chain of n = 21, 51 and101 bonds as $< \cos^2 \theta >_r$ = 0.717, 0.699 and 0.694, respectively. Results from MC simulations for each of the successive intervals are shown by the empty circles. In order to end up with a reliable number of chains in each interval, generation of a set of $\sim 10^5$ chains is required for a given n. It is observed in Figure 2.4 that $< \cos^2 \theta >_r$ values for n=21, which are connected by a curve to guide the eye, are subject to considerable fluctuations.The latter are not due to uncertainties or scattering in the properties of the generated chains but to a systematic reproducible effect

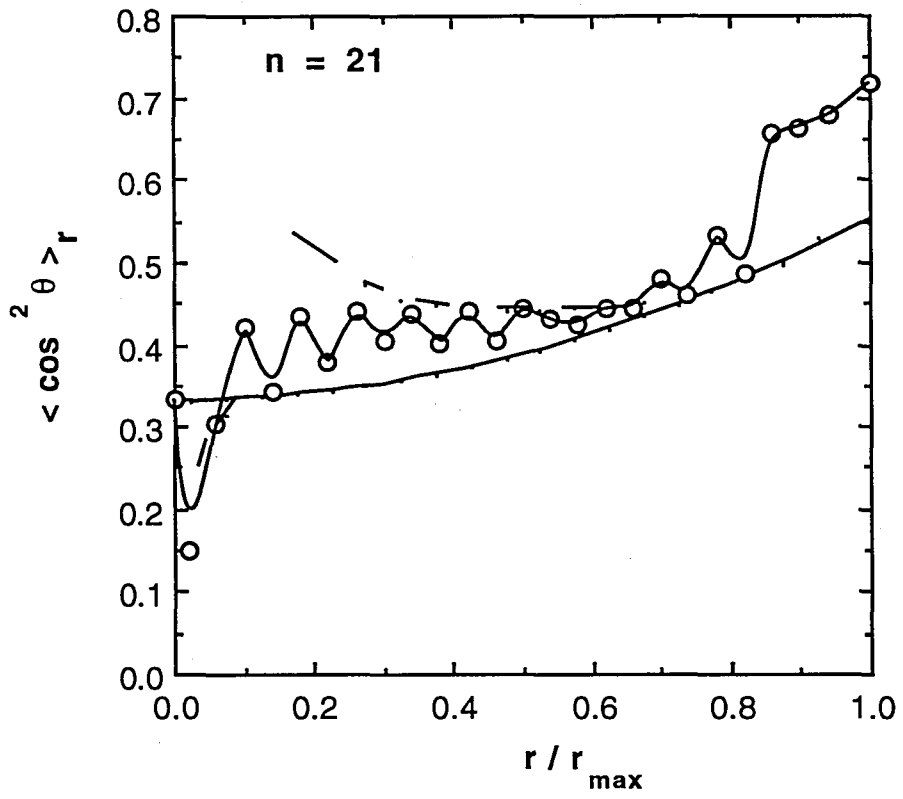

Figure 2.4 Dependence of $< \cos^2 \theta >_r$ on r / r max for n = 21.The circles are results from MC simulations. The curve through the circles is drawn to guide the eye. The lower solid curve is theoretically obtained by using the first order approximation. The discontinuous curve is found from eq 2.24. The discontinuous portion is indicated by the dashed curve.

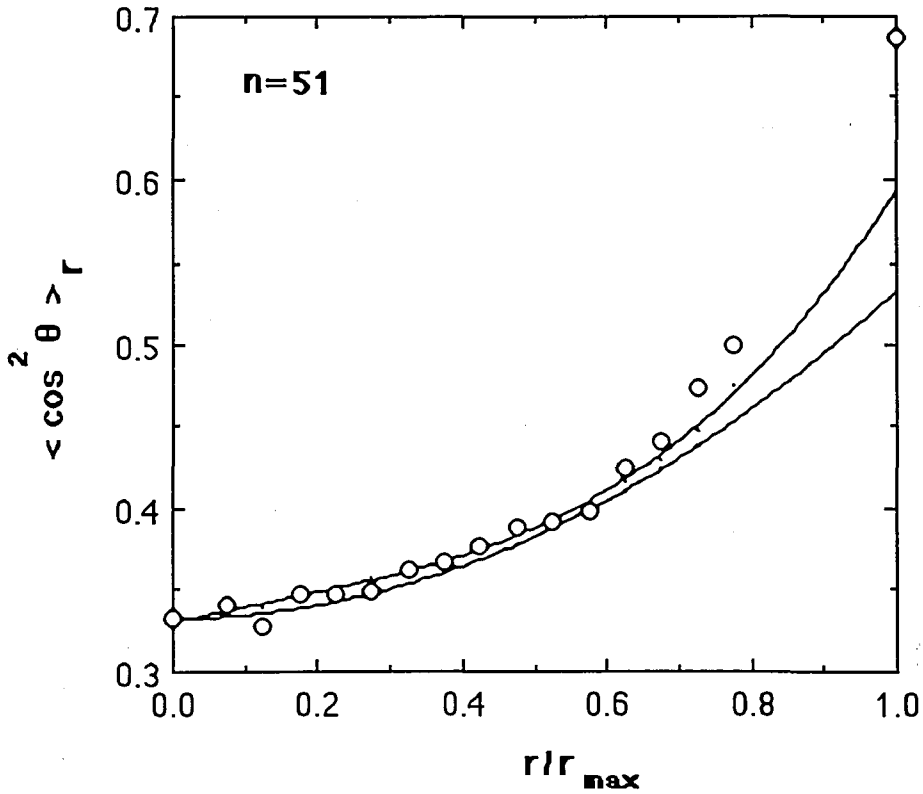

Figure 2.5 Dependence of $< \cos^2 \theta >_r$ on r / r max for n = 51.The circles are results from MC simulations. The lower solid curve is obtained by using the first order approximation. The upper curve is found from eq 2.24.

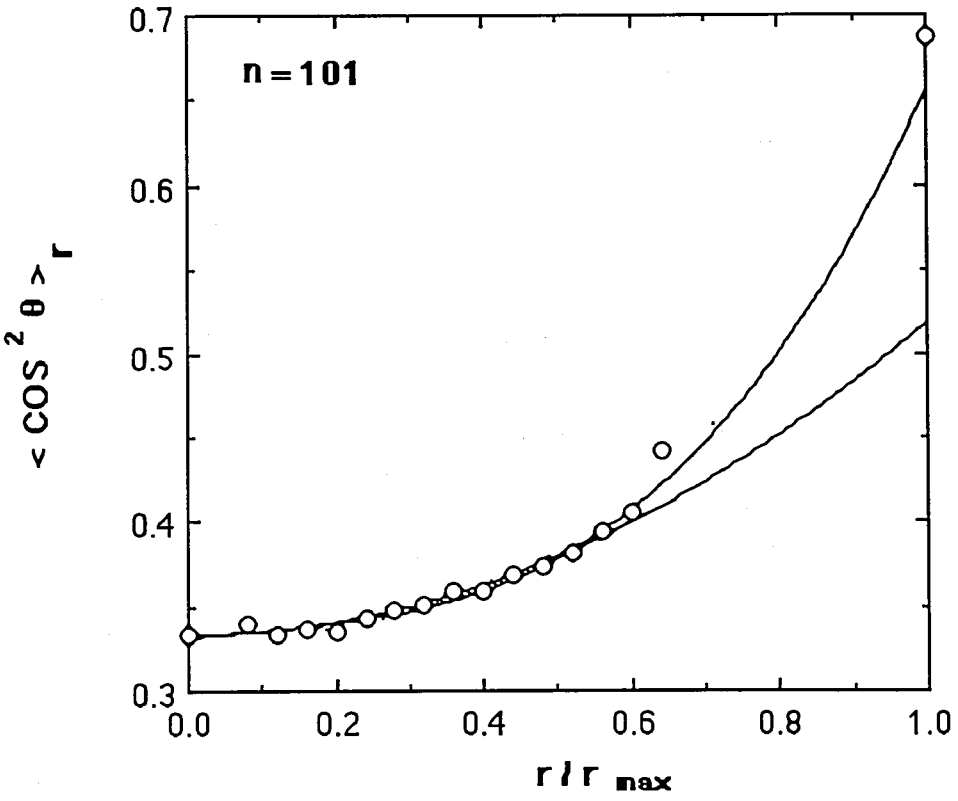

Figure 2.6 Dependence of $< \cos^2 \theta >_r$ on r / r max for n = 101.The circles are results from MC simulations. The lower solid curve is obtained by using the first order approximation. The upper curve is found from eq 2.24.

which may be attributed to small chain length. Similar fluctuations, though considerably weakened in amplitude, are discernible in longer chains, as may be seen in Figures 2.5 and 2.6.

For comparative purposes, the theoretical curves obtained with (i) the first order approximation where $< \cos^2 \theta >_r = 1 / 3 + \alpha_1 \eta_2 / 3$ and (ii) the more complete expression given by eq 2.24, are shown by in Figures 2.4-2.6. Comparison of the theory with MC simulations is made possible by identifying the direction of the end-to-end vector with the x-axis. In all cases the lower curves represent the first order approximation whereas the upper curves are obtained from eq 2.24. The extrapolation of the latter to $r / r_{max} = 1$ has been carried out with the help of best fitting third order polynomials. From the observation of Figures 2.5 and 2.6, it is noted that in the case of longer chains the two approaches are both satisfactory, although eq 2.24 exhibits a better agreement with the real behavior which is indicated by MC simulations. The deviation between the two approaches is particularly apparent at more extended configurations. For n = 21, however, the first order approximation curve lies definitely below the MC simulation points, regardless of r / r_{max} and is not adequate for data interpretation. In this respect, the approach (ii) follows more closely the MC simulations, apart from a singularity near $r / r_{max} = 0.2$, due to the vanishing of the denominator in eq 2.24. This region is shown by the dashed portion of the curve.

2.2.2.2 Orientation as a Function of Extension Ratio

The dependence of S on λ is shown in Figure 2.7 for n= 21. The solid curve is obtained from eq 2.33 by retaining the linear term only, i.e., by adopting

$$D_1 = 2\,\eta_2$$

$$D_2 = D_3 = D_4 = 0 \qquad (2.42)$$

The dashed curve in Figure 2.7 is obtained for the second order approximation by the use of the following expressions for D_i's in eq 2.33

$$D_1 = 2\,\eta_2 + 14\,\eta_4 + 126\,\eta_6 - 30\,\eta_2 g_4$$

$$D_2 = -\frac{18}{5}\,(\eta_4 + 18\,\eta_6 - 10\,\eta_2 g_4)\,\frac{<r^4>_0}{<r^2>_0^2}$$

$$D_3 = \frac{54}{7}\,(\eta_6 - \eta_2 g_4)\,\frac{<r^6>_0}{<r^2>_0^3} \qquad (2..43)$$

$$D_4 = 0$$

The results of the first and second order approximations shown in Figure 2.7 for n = 21 are very close to each other for $1 < \lambda < 1.75$. In this range, the second order approximation predicts a slightly smaller S values than the linear one. Above λ =1.75, however, the second order approximation for S increases very sharply to full orientation at about $\lambda = 2.8$. It may be concluded from Figure 2.7 that for short polyethylenelike chains (n ≈21), the first order approximation to orientation given by the very simple expression

$$S = \frac{1}{2}\,D_1\,(\lambda^2 - \lambda^{-1}) \qquad (2.44)$$

is satisfactory for relatively small strains. However, the identification of the front factor in eq 2.44 with the Kuhn expression of 1/5N, with N indicating the number

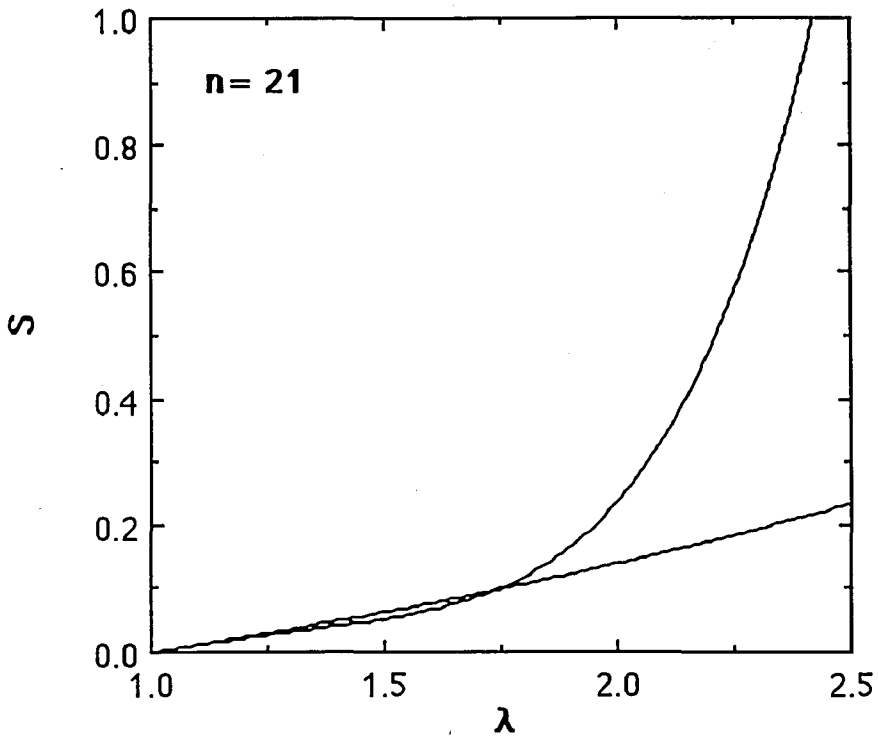

Figure 2.7 Dependence of the orientation function S on extension ratio λ for a chain with 21 bonds. The lower curve is obtained from the linear expression given by eq 2.44. The upper curve is from the second order expression obtained by inserting the coefficients given by eq 2.43 into eq 2.33.

of Kuhn segments in the network chain, is not acceptable as has been demonstrated previously.[28] For a polyethylene chain of n = 21 bonds, one Kuhn segment contains about 10-22 C-C bonds depending on the definition of the Kuhn length.[4,29] Thus,1/5N assumes values between 0.1 - 0.2 while the present calculations predict a value of .02 for $D_1/2$.

Results of calculations of S for n = 101 are shown in Figure 2.8 as a function of λ . The upper curve obtained by the second order approximation departs from the results of the linear approximation, the lower curve, around λ = 2. $D_1/2$ is 0.004 for this chain and deviates strongly from the Kuhn approximation.

It may be concluded from the form of eq 2.33 that S has to converge to the expression given by eq 2.44 in the limit of very large n. The strong deviation of the two curves from each other in Figure 2.8 indicates, however, that n = 101 is a value much lower than that required for eq 2.44 to be strictly valid. It may be interesting to note the abruptness of the deviation of the second order curves in Figures 2.7 and 2.8 from the respective first order ones. The marked rise of the curves in the second order approximation results from the dominance of the λ^6 term with increasing extension. This type of behavior at higher strains is distinctly exhibited by the recent results of infrared dichroism measurements in high cis-1,4-polybutadiene networks.[30]

A comparison of eq 2.31 with the results of Roe and Krigbaum[31] for finite freely jointed chains shows that the functions containing the λ's are identical in the two works and both formulations exhibit strong resemblances. However, the coefficient D_3 of eq 2.31 is of order n^{-2} whereas the corresponding coefficient in the work of Roe and Krigbaum is of order n^{-3}. It may thus be concluded that the

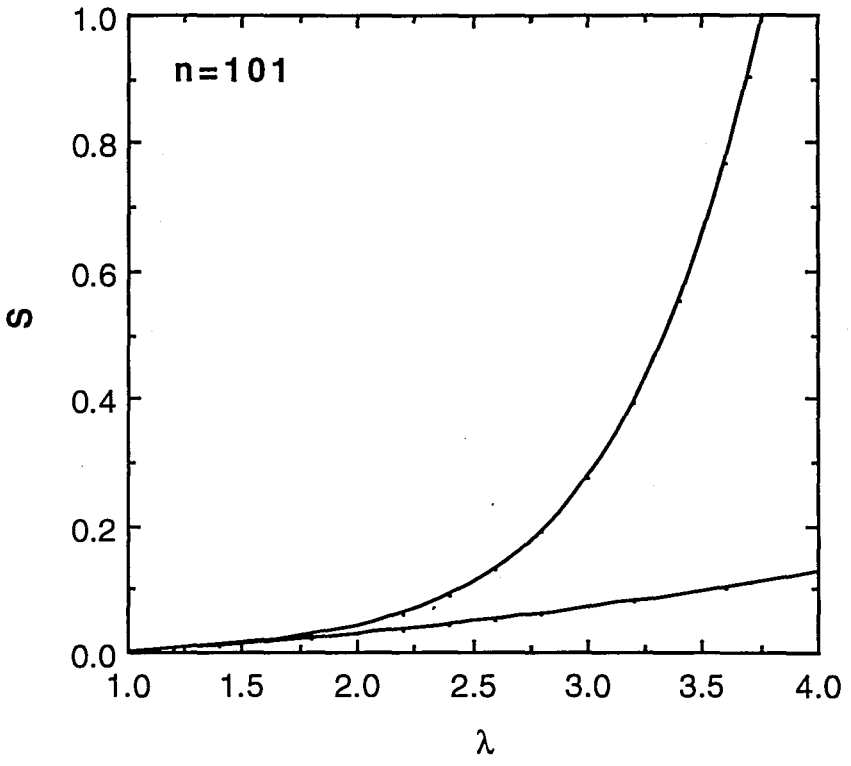

Figure 2.8 Dependence of the orientation function S on extension ratio λ for a chain with 101 bonds. See legend for Figure 2.7.

present study does not converge to that of Roe and Krigbaum in the limit of freely jointed chains.

2.2.2.3 Orientation in the Small-strain Limit

Calculations of the values of S / ε from eq 2.34 by retaining only terms of order n^{-1} leads to 0.1176, 0.0525, and 0.0243 for n=21, 51, and 101, respectively. When terms of order n^{-2}, i.e., second order terms, are included, the above values become, respectively, 0.1253, 0.0546, and 0.0255. This comparison shows that the contribution of the second order terms to S / ε is 6.6%, 4.0 % and 5.1 % for n=21, 51 and 101, respectively. Thus it may be concluded that in the small strain limit , the term S / ε which may be referred to as the orientational modulus, is satisfactorily represented by

$$S/\varepsilon = \frac{3}{10}\left(\frac{3\langle r^2\cos^2\Phi\rangle_0}{\langle r^2\rangle_0} - 1\right) \qquad (2.45)$$

The above equation is particularly useful in interpreting results from infrared dichroism experiments recently developed by Noda et. al.[1], which allow for very precise determination of S / ε.

2.3 Segmental Orientation in Polyoxyethylene Networks

2.3.1 Statistical Characteristics of the POE Chain

The statistics of the POE has previously been investigated by various authors[4,37-39]. The chain presents a relatively simple structure having x repeat units, each of them comprising three backbone bonds of the type C-C, C-O and O-C. On the premise of pairwise interdependence of backbone bonds, following RIS formalism, three statistical weight matrices are required to take account of the neighbor dependence of bond rotational potentials. From structural point of view, POE presents intermediate characteristics between polyethylene and polyoxymethylene. Yet, the preferred conformations for the three polymeric chains differ markedly. In the former, the *trans* conformation is of lower energy than the *gauche*; the reverse holds for the latter. On the other hand, analysis of chain conformation in POE suggests a preference for *trans* rotations about the C-O and O-C bonds while it is well established from previous spectroscopic studies and theoretical analysis that *gauche* states are preferred about the C-C bonds.

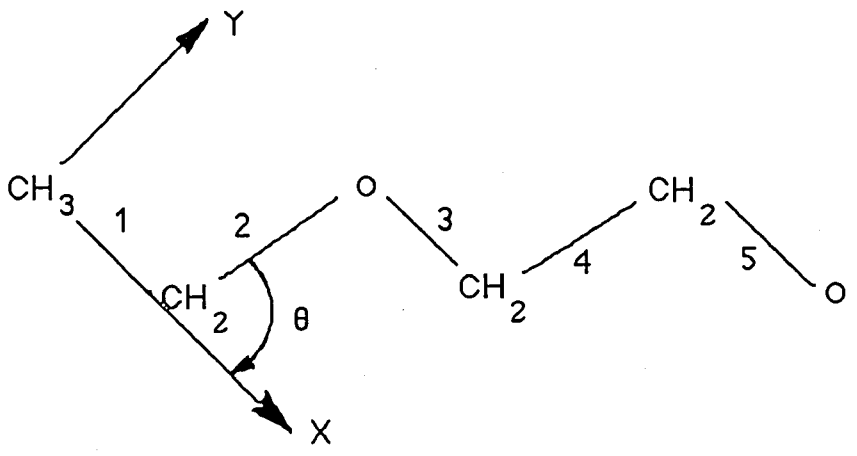

Figure 2.9 Schematic representation of the first five bonds in polyoxyethylene. The X and Y axes of the local coordinate system appended to the first bond are explicitly shown. θ represents the supplemental bond angle and the numbers affixed to the bonds indicate their indices.

The first few bonds of the chain are shown in Figure 2.9. Backbone bonds are indexed as indicated. Local coordinate systems for skeletal bonds are defined as previously described for PE. The length of the bonds in the backbone are l_{cc}=1.53 Å, and l_{co}=1.43 Å. The supplemental bond angles ∠ COC and ∠ OCC are nearly the same and equal to θ=68.5°. Isomeric rotations of the bonds are described in terms of three rotational states, *trans* (*t*), *gauche*$^+$ (g^+) and *gauche*$^-$ (g^-) with respective torsional angles of 0°, +110°, -110°.[10] The statistical weight matrices for the pairs of bonds (CC, CO), (CO, OC) and (OC, CC) are denoted by $\mathbf{U}_a$, $\mathbf{U}_b$ and $\mathbf{U}_c$, respectively. They read

$$\mathbf{U}_a = \begin{bmatrix} 1 & \sigma & \sigma \\ 1 & \sigma & \sigma\omega \\ 1 & \sigma\omega & \sigma \end{bmatrix}$$

$$\mathbf{U_b} = \begin{bmatrix} 1 & \sigma & \sigma \\ 1 & \sigma & \sigma\omega' \\ 1 & \sigma\omega' & \sigma \end{bmatrix}$$

$$\mathbf{U_c} = \begin{bmatrix} 1 & \sigma' & \sigma' \\ 1 & \sigma' & \sigma'\omega \\ 1 & \sigma'\omega & \sigma' \end{bmatrix} \qquad (2.46)$$

Here the parameter α ($\alpha = \sigma, \sigma', \omega$ or ω') is found from the general expression

$$\alpha = \exp (- E_\alpha / RT) \qquad (2.47)$$

where R is the gas constant, T is the absolute temperature, and E_α assumes the values 0.90, -0.45, 0.39 kcal/mol and ∞ for α equal to σ, σ', ω and ω' , respectively.[38] For a chain of x units (or 3x-1 bonds) of the form $H(-CH_2CH_2O)_xH$, which will be investigated in the following, the configurational partition function Z is found from the serial multiplication of the statistical weight matrices as

$$Z = \mathbf{J^*} (\mathbf{U_a}\, \mathbf{U_b}\, \mathbf{U_c})^{x-1}\, \mathbf{J} \qquad (2.47)$$

2.3.2 Calculations and Discussion

The ensemble averages determined from Monte Carlo simulations are used in eqs 2.17, 2.18 to evaluate the parameters $\eta_2 = D_0$, η_4, η_6 and g_4 which are then inserted into eqs 2.32 to calculate the coefficients D_1, D_2 and D_3 for n = 21, 51 and 101. A list of averages resulting from Monte Carlo simulations at 303 K is presented in Table 2.1, for the cases n = 21, 51 and 101. Each average is obtained from a set of 50000 sample chains. The deviation from each mean on

TABLE 2.1

Values of the various Averages Appearing for POE

	n		
	21	51	101
$< \overline{\cos^2\Phi} >_o$	.3694(±0.0007)	0.3518(±0.0002)	0.3422(±0.0001)
$< r^2 \overline{\cos^2\Phi} >_o$	70.68(±0.20)	174.18(±0.64)	343.86(±0.96)
$10^{-4} < r^4 \overline{\cos^2\Phi} >_o$	1.678(±0.011)	12.96(±0.10)	55.04(±0.17)
$10^{-7} < r^6 \overline{\cos^2\Phi} >_o$	0.4519(±0.0049)	12.25(±0.14)	117.8(±0.1)
$< r^2 >_o$	175.4(±0.4)	469.6(±1.6)	989.6(±2.8)
$10^{-4} < r^4 >_o$	4.00(±0.02)	34.72(±0.25)	155.97(±0.63)
$10^{-7} < r^6 >_o$	1.05(±0.01)	32.03(±0.34)	328.79(±1.00)

TABLE 2.2

Values of the Coefficients D_0, D_1, D_2 and D_3 for POE

	n		
	21	51	101
$10^{-3} D_o$	20.905(±0.024)	8.938(±0.027)	4.241(0.000)
$10^{-2} D_1$	11.160(±0.160)	2.186(±0.035)	0.837(±0.055)
$10^{-3} D_2$	-46.67(±0.95)	-3.17(±0.31)	-0.02(±0.27)
$10^{-3} D_3$	9.344(±0.133)	1.046(±0.068)	0.12(±0.18)

the basis of two groups of 25000 chains are indicated in parentheses in the table. The deviations in the coefficients D_2 and D_3 for n = 101 indicate that Monte Carlo calculations of the stated sample size cannot be reliably used for their absolute determination. However, calculations presented below indicate that the effect of those deviations on S is of secondary importance. In fact, less than 6 % error in the absolute values of S is found to result from those uncertainties, throughout the range of extension ratios investigated.

The coefficients D_0, D_1, D_2 and D_3 are given in Table 2.2 for the three values of n. The entries in the parenthesis indicate again the deviation from each mean when two groups of 25000 chains are used instead of one 50000. The dependence of the coefficients on the number of chains generated is displayed in Figures 2.10-2.13. In general, the fluctuations in the curves become relatively unimportant when the number of chains generated exceeds 20000.

The coefficients D_0, D_1, D_2 and D_3 obtained by Monte Carlo simulations are inserted into eq 2.33 to evaluate the orientation function in terms of the extension ratio. In Figures 2.14-2.17 the reduced orientation function [S] defined as

$$[S] = S / (\lambda^2 - \lambda^{-1}) \qquad (2.49)$$

is presented. Figure 2.14 displays the variation of [S] with the number of chains generated for n = 21, 51 and 101, for $\lambda = 2$. When the number of chains used is more than 20000, the fluctuations in [S] are indeed negligibly small and the values of [S] calculated using two sets of 25000 generated chains lie within 1, 2 and 6% of each other for n = 21, 51 and 101, respectively.

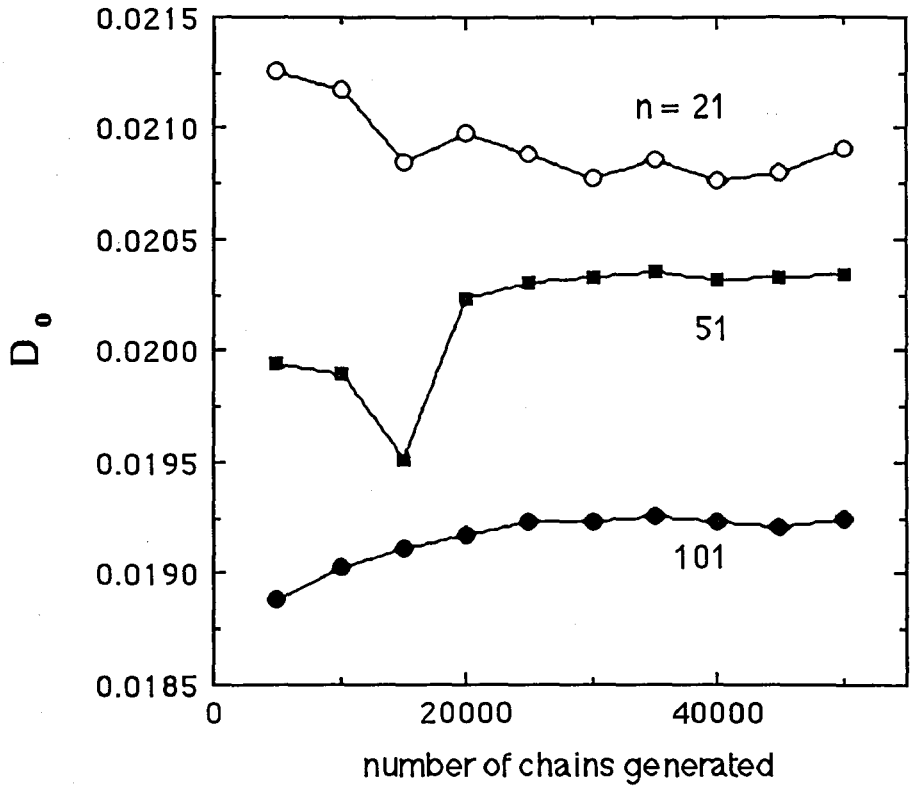

Figure 2.10 The variation of D_0 values with the number of chains generated for n = 21, 51, 101. In order to present all three curves on the same graph, the D_0 values for n = 51 and n = 101 are shifted up by adding a constant to each. The constant is 0.0114 for n = 51 and 0.015 for n = 101.

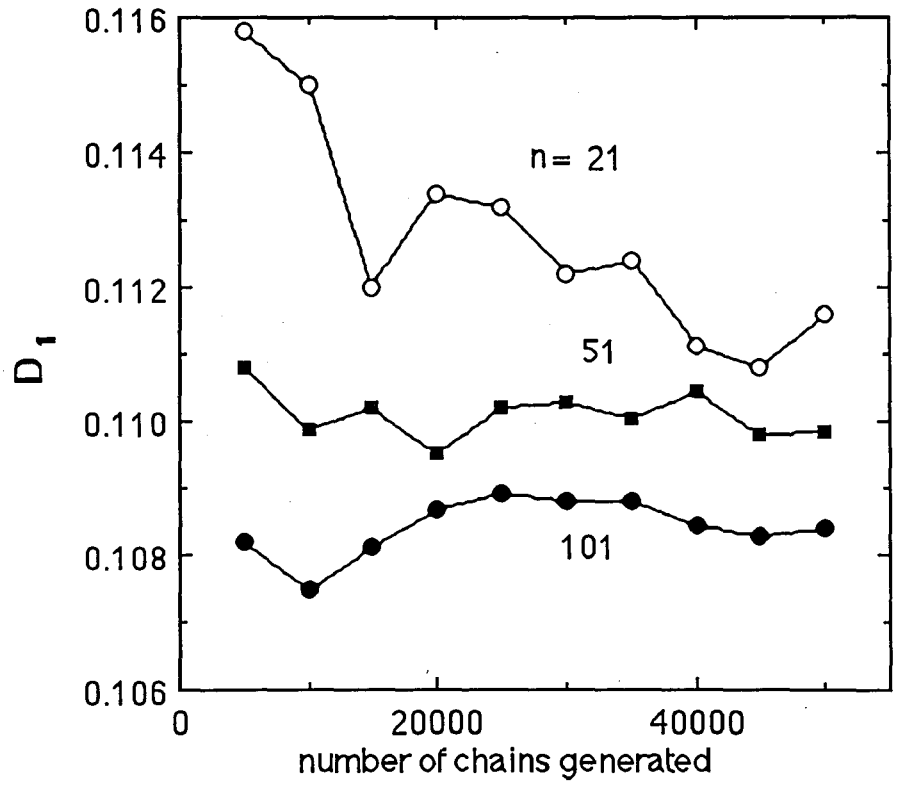

Figure 2.11 The variation of D_1 values with the number of chains generated for n = 21, 51, 101. The curves for n = 51 and n = 101 are shifted up by adding a constant to each. The constant is 0.087 for n = 51 and 0.10 for n = 101.

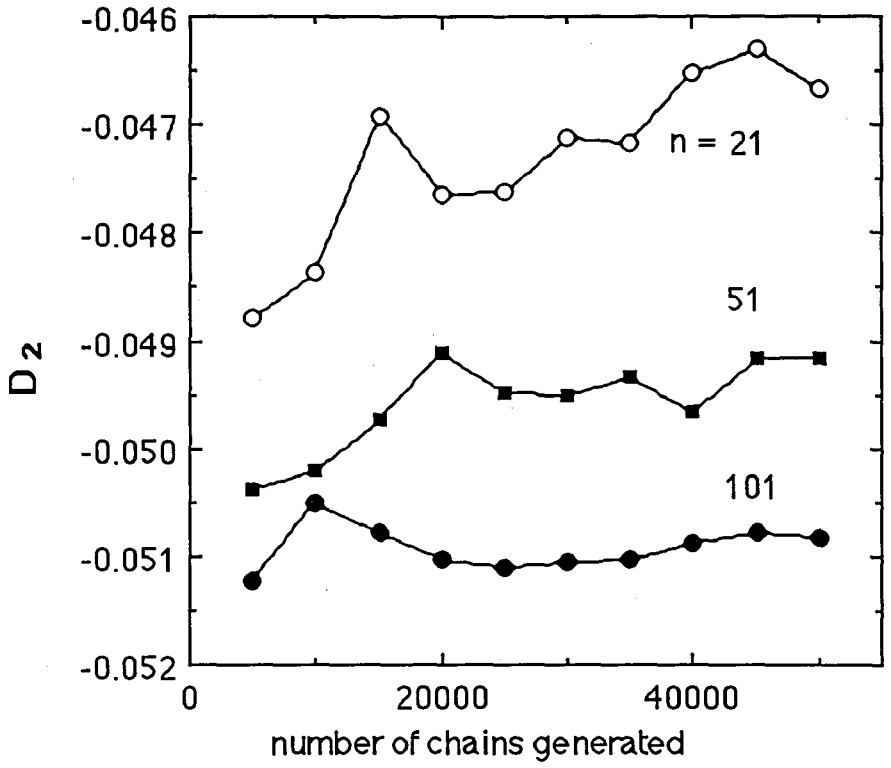

Figure 2.12 The variation of D_2 values with the number of bonds generated for n = 21, 51, 101. The curves for n = 51 and n = 101 are shifted up by adding a constant to each. The constant is -0.046 for n = 51 and -0.0508 for n = 101.

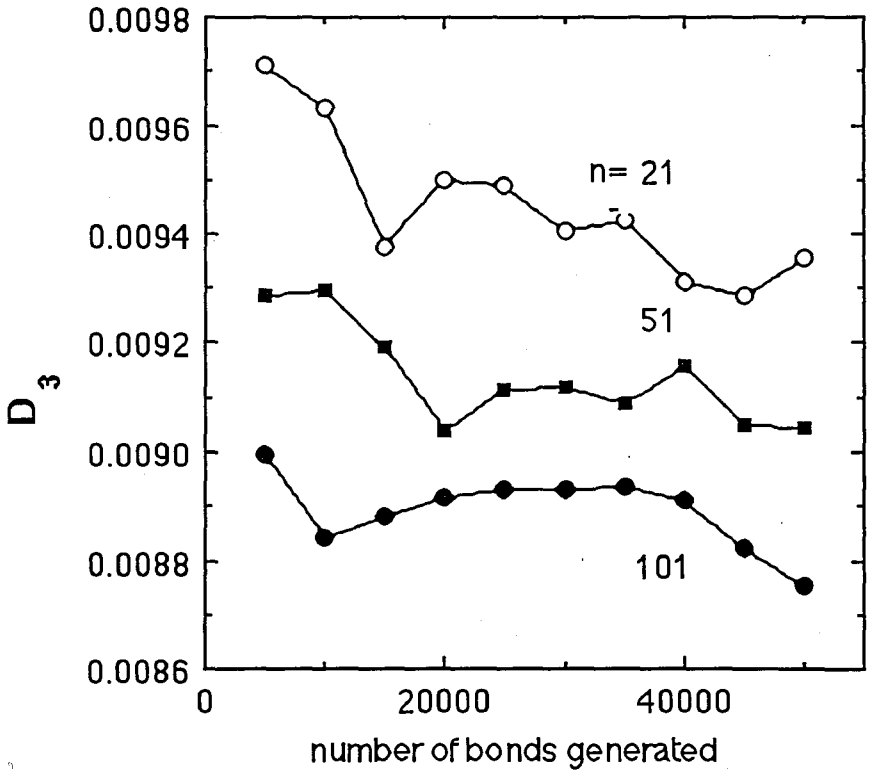

Figure 2.13 The variation of D_3 values with the number of bonds generated for n = 21, 51, 101. The curves for n = 51 and n = 101 are shifted up by adding a constant to each. The constant is 0.008 for n = 51 and 0.00879 for n = 101.

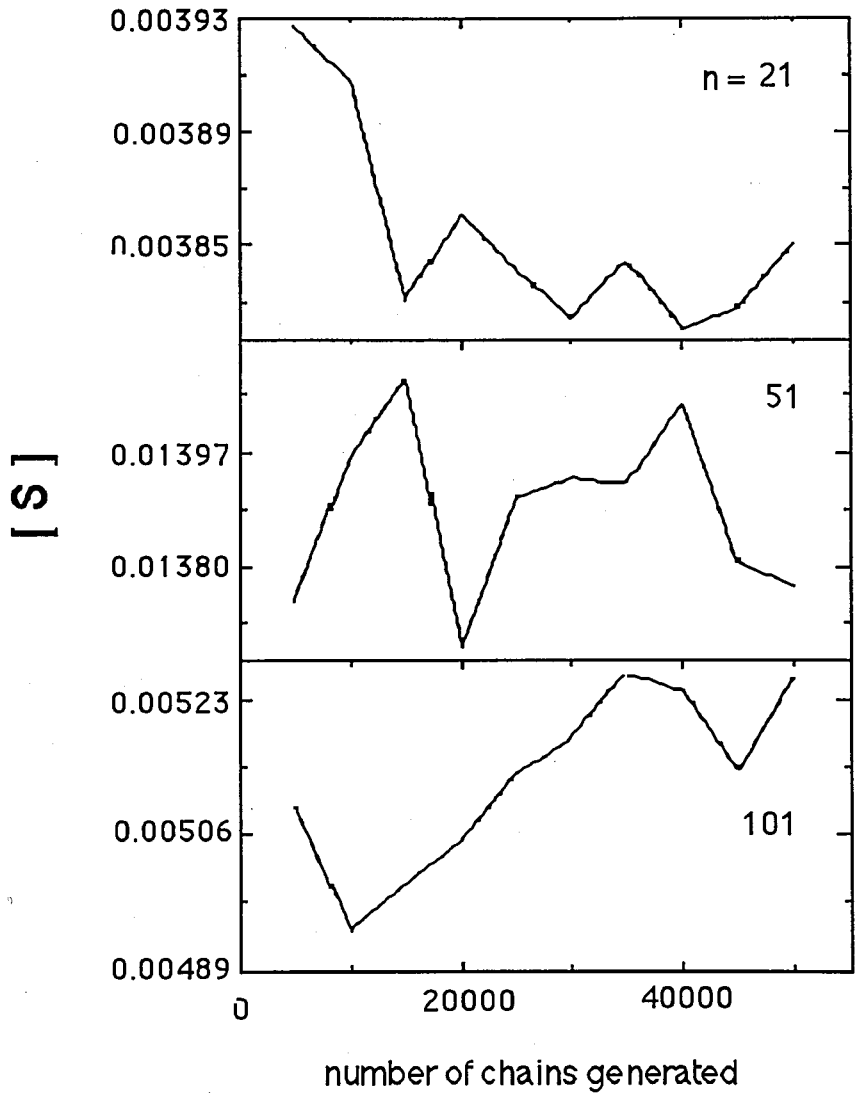

Figure 2.14 The dependence of the reduced orientation function [S] at $\lambda = 2$ on the number of chains generated for n = 21, 51 and 101.

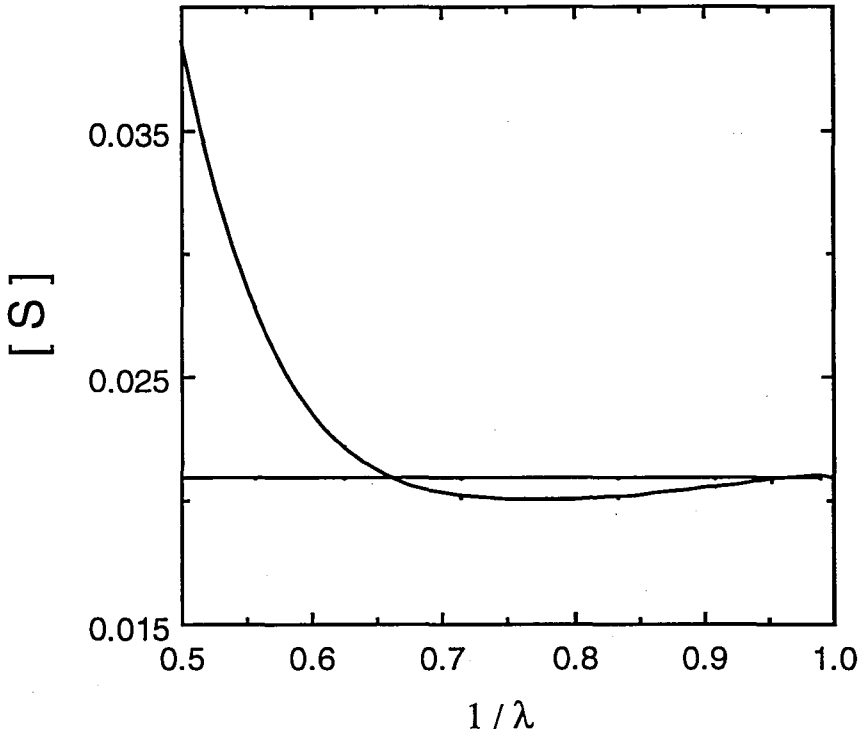

Figure 2.15 Reduced orientation function $[S] = S / (\lambda^2 - \lambda^{-1})$ as a function of the inverse extension ratio $1/\lambda$, for a chain of $n = 21$ bonds, at $T = 303$ K. The horizontal line represents the first order approximation and the higher curve results from the second order approximation which includes the contributions of both terms of order $1/n$ and $1/n^2$.

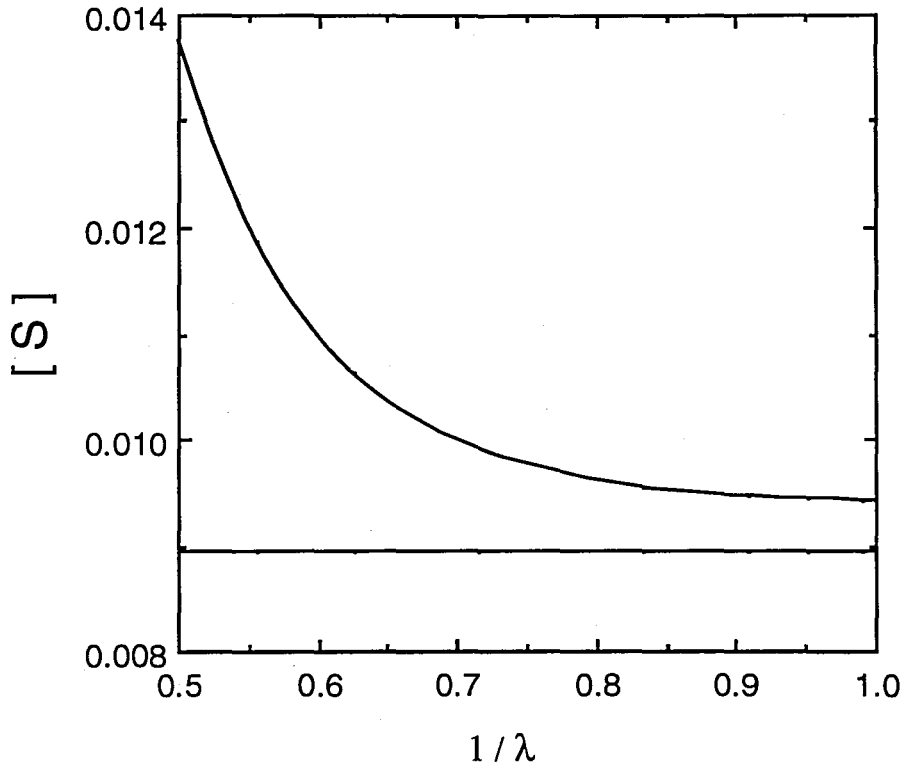

Figure 2.16 Reduced orientation function $[S] = S / (\lambda^2 - \lambda^{-1})$ as a function of the inverse extension ratio $1/\lambda$, for a chain of n = 51 bonds, at T = 303 K. See legend to Figure 2.15.

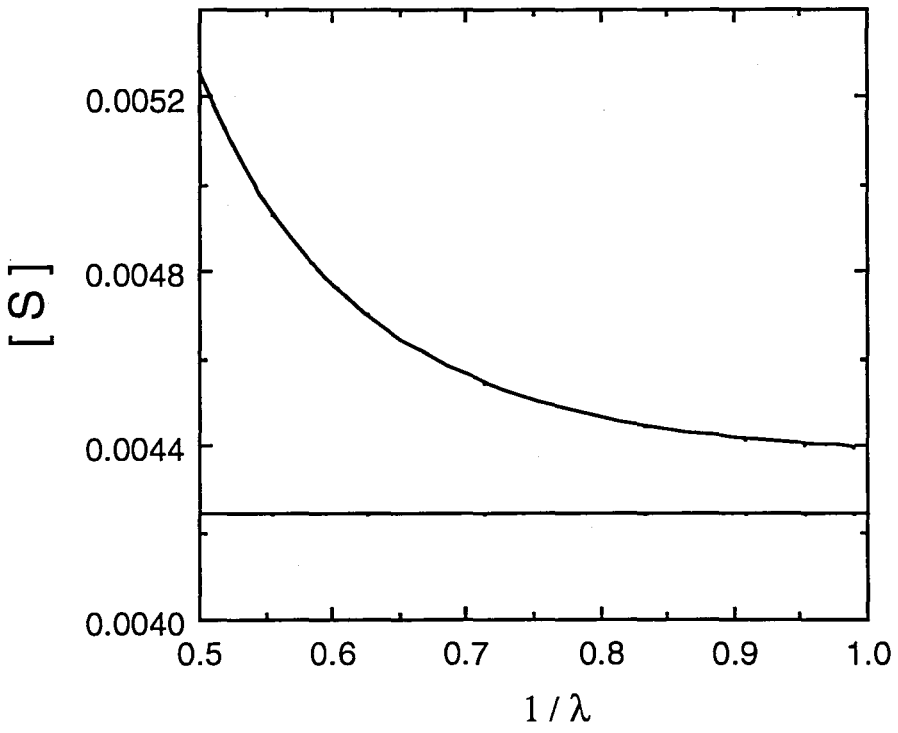

Figure 2.17 Reduced orientation function [S] = S / (λ^2 - λ^{-1}) as a function of the inverse extension ratio 1/λ, for a chain of n = 101 bonds, at T = 303 K. See legend to Figure 2.15.

Figures 2.15-2.17 illustrate the change in [S] as a function of the inverse extension ratio $1/\lambda$ for n = 21, 51 and 101, respectively. The horizontal line represents results for the first order approximation whereas the upper curve is obtained for the second order approximation in all of the three figures. Comparison of the ordinate scales in the three figures indicates, as expected, that longer chains are less oriented at a given λ. For small degrees of deformation, the first and the second order approximations are rather close to each other. For n = 20, in the range $\lambda < 1.5$, the second order approximation falls below the first order approximation. It is interesting to note that this result was also obtained in the previous calculations[36,41] for polyethylene and poly(dimethyl siloxane). As λ increases, the curve for segmental orientation in the second order approximation rises abruptly. More precisely, for $\lambda = 2$ for instance, the contribution of the second order terms to segmental orientation amounts to 45% of the total [S], for n = 21. The contribution of the second order terms decreases in longer chains. In fact, it accounts for 34% and 19% of the total [S], for n = 51 and 101, respectively.

The values of D_o reported in Table 2.2 allow for the estimation of the number m_K of bonds in a Kuhn segment. Identification of the front factor 1/5N of eq 2.2 with D_o yields the value of $m_K = 2 - 2.3$. This value is much smaller than that for the polyethylene chain obtained previously.[4] On the other hand, it is noted that for POE, the estimation of m_K on the basis of the second and fourth moments of displacement vector leads[39] to $m_K = 10.3$ while the conventional approach[34] of estimating m_K from $\langle r^2 \rangle_o$ and the fully extended **r**, gives $m_K = 6.0$. The variety of values assumed by m_K depending on the method of comparison indicates that an absolute identification of a real chain by an equivalent Kuhn chain is inappropriate.

Chapter III

Brownian Dynamics Simulation of Chains with Fixed End-to-End Separation

3.1 Molecular Model and Simulation Method

Model Description

A segment AB of N bonds in a laboratory-fixed coordinate system OXYZ is considered. The two ends A and B of the chain are held fixed in space throughout the BD simulation. For mathematical convenience the first atom is assumed to coincide with the origin of the frame OXYZ, and the first bond lies along the X axis. The tetrahedrally attached second bond is in the plane XY and makes an acute angle with the X-axis, as shown in Figure 3.1. Holding the direction of the first two bonds fixed in space corresponds to eliminating the three degrees of freedom associated with the absolute spatial reorientation of the chain. This device is inconsequential for the study of the internal conformational and orientational dynamics of the chain which is of interest in the present study. The backbone atoms are indexed from 0 to N and their location with respect to the frame OXYZ are given by the position vectors $\mathbf{r}_j = (x_j, y_j, z_j)$. $\mathbf{r}_j$ may alternatively be viewed as the position vector of the i^{th} united group forming the chain, in which the hydrogen atoms or other substituents are collapsed into the backbone atom. For simplicity, the ith backbone atom or group will be referred to

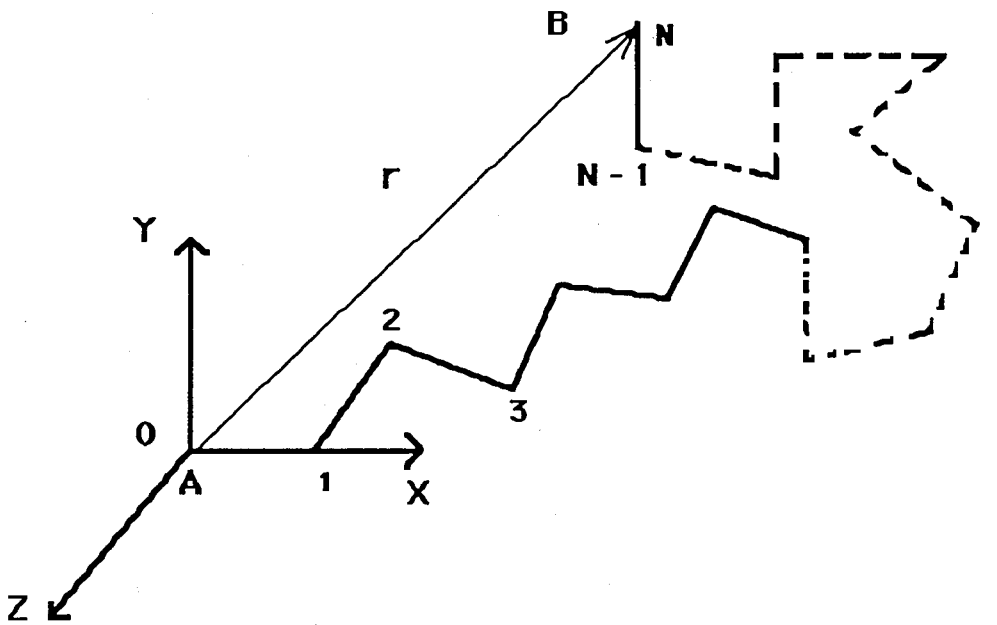

Figure 3.1 Schematic representation of a chain of N bonds in a fixed reference frame OXYZ. Atoms with indices 0, 1, 2 and N are fixed in space throughout the BD simulations of a chain of a given end-to-end separation vector **r**.

as C_i. The position vector $\mathbf{r}_N$ of the terminal atom is equal to the end-to-end vector $\mathbf{r}$ of the chain.

A short sequence of bonds between atoms C_{i-2} and C_{i+2} is shown in Figure 3.2. $\mathbf{l}_i$ is the bond vector connecting atoms i - 1 and i as

$$\mathbf{l}_i = \mathbf{r}_i - \mathbf{r}_{i-1} \qquad i = 1, \ldots\ldots, N \qquad (3.1)$$

The dot product of consecutive bond vectors defines the supplemental bond angle θ_i as

$$\theta_i = \cos^{-1}\left[\frac{\mathbf{l}_{i+1} \cdot \mathbf{l}_i}{l_{i+1}\, l_i}\right] \qquad i = 1, \ldots\ldots, N-1 \qquad (3.2)$$

where l_i is the magnitude of the vector $\mathbf{l}_i$. The torsional state of bond i is described by the dihedral angle ϕ_i which is expressed in terms of bond vectors as

$$\phi_i = \cos^{-1}\left[-\frac{(\mathbf{l}_i \times \mathbf{l}_{i-1})}{|(\mathbf{l}_i \times \mathbf{l}_{i-1})|} \cdot \frac{(\mathbf{l}_{i+1} \times \mathbf{l}_i)}{|(\mathbf{l}_{i+1} \times \mathbf{l}_i)|}\right] \qquad i = 2, \ldots\ldots, N-1 \qquad (3.3)$$

The values of 0°, 120° and -120° for ϕ_i define the respective rotational isomeric states *trans* (*t*), gauche$^+$ (g^+) and gauche$^-$ (g^-) of bond i.[1]

The chain is subject to an intramolecular conformational potential controlling the changes in the bond lengths, bond angles and bond torsions in conformity with the model chain of Helfand et al.[14] The bond stretching potential $V_b(l_i)$ for bond i is given by the harmonic function

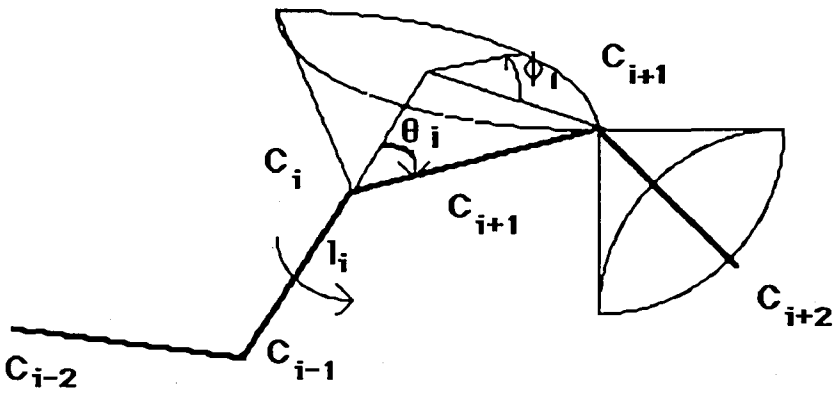

Figure 3.2 A portion of simulated chain between atoms C_{i-2} and C_{i+2} indicating the generalized coordinates l_i, θ_i and ϕ_i. l_i with $1 \leq i \leq N$ is the bond vector between atoms C_{i-1} and C_i, θ_i is the supplemental bond angle at the ith atom and is defined in the range $1 \leq i \leq N-1$, ϕ_i is the torsional angle of the bonds with indices $2 \leq i \leq N-1$.

$$V_b(l_i) = (k_b / 2)(l_i - l_0)^2 \qquad i = 1, \ldots\ldots, N \qquad (3.4)$$

where k_b is the bond-stretching force constant, and l_0 is the most probable bond length. Similarly, $V_\theta(\theta_i)$ is the bond angle bending potential which constrains the supplemental bond angle θ_i to fluctuate about θ_0 according to

$$V_\theta(\theta_i) = (k_\theta / 2)(\cos\theta_i - \cos\theta_0)^2 \qquad i = 1, \ldots\ldots, N - 1 \qquad (3.5)$$

Here k_θ is the bond angle bending force constant. The torsional motion of bond i is governed by the rotational potential $V_\Phi(\phi_i)$

$$V_\phi(\phi_i) = k_\phi \sum_{n=0}^{5} a_n \cos^n \phi_i \qquad i = 2, \ldots\ldots, N - 1 \qquad (3.6)$$

leading to three isomeric minima at the *t* and $g^{\pm}$ states. Here k_Φ is the bond torsion constant and the coefficients a_i $(0 \leq i \leq 5)$ satisfy the relationship,

$$\sum_{n=0}^{5} a_n = 0 \qquad (3.7)$$

with a_0 equal to unity. It is clear from eq 3.6 that bonds are subject to independent rotational potentials which leads to the expression

$$V_\phi(\phi_2, \ldots\ldots, \phi_{N-1}) = \sum_{i=2}^{N-1} V_\phi(\phi_i) \qquad (3.8)$$

for the rotational potential energy of the chain. Clearly, this approximation is not applicable to chains in which the rotational state of a given bond is strongly coupled to that of its close neighbors. In the case of pairwise interdependent

bonds which is commonly adopted in chain statistics, the potential given by eq 3.6 should be modified as a function of two consecutive bond dihedral angles.

The total conformational potential V of the chain is given by the additive contribution of the above three interactions as

$$V = \sum_{i=1}^{N} V_b(l_i) + \sum_{i=1}^{N-1} V_\theta(\theta_i) + \sum_{i=2}^{N-1} V_\phi(\phi_i) \qquad (3.9)$$

Brownian Dynamics Method

For a chain of N+1 atoms each of equal mass m, the Brownian motion of the i^{th} atom is given by the Langevin equation

$$m \frac{d^2 \mathbf{r}_i}{dt^2} = -\xi \frac{d\,\mathbf{r}_i}{dt} - \nabla_i V + m\,\mathbf{A}_i(t) \qquad (3.10)$$

which in the high-friction limit reduces to the equation of motion

$$\beta \frac{d\mathbf{r}_i}{dt} = -\,m^{-1}\,\nabla_i V + \mathbf{A}_i(t) \qquad (3.11)$$

In eqs 3.10 and 3.11, ξ is the friction coefficient, β is defined as the ratio ξ / m, ∇_i is the gradient operator indicating the partial derivative with respect to the position vector $\mathbf{r}_i$, and $\mathbf{A}_i(t)$ is the Gaussianly distributed stochastic force per unit mass with zero mean and covariance matrix

$$< \mathbf{A}_i(t)\,\mathbf{A}_j(t') > = (2\beta k_B T / m)\,\delta_{ij}\,\delta(t - t')\,\mathbf{I}_3 \qquad (3.12)$$

Here k_B is the Boltzmann constant and T is the absolute temperature, I_3 is the identity matrix of order 3. Explicit expressions for the stretching, bending and torsional forces resulting from the negative gradient of the potential V are given in the Appendix B.

In the present model the hydrodynamic interactions between carbon centers transmitted by the surrounding medium, and the intermolecular interactions between non bonded chain units leading to excluded volume effect have not been included. The contribution of these interactions to the rapid conformational relaxation processes in polymeric chains presently investigated is expected to be negligibly small .

The Brownian dynamics simulation is performed by the numerical integration of the 3(N+1) equations of motion given by eq 3.11 for each atom constituting the chain. The previously described[42] stochastic extension of the Runge Kutta method is adopted for that purpose and the second order approximation is used. The details of the method is given in Appendix C. The integration time step is taken as δt = 0.5 fs in conformity with previous work.[14] Thus, the simulated stochastic process is discrete and Markovian in the sense that the trajectories of particles are generated only at discrete time steps 0, δt, $2\delta t$, etc. and the state of the system at a given time $t+\delta t$ is completely determined by its state at time t .

Simulation Parameters

Simulations are carried out for polymeric chains of 49 bonds using the set of energy parameters listed in Table 3.1. The parameters for torsional parameters are proposed by Ryckaert and Bellemans[43] as representative of a

Table 3.1
Conformational Energy Parameters

k_b/m (ns^{-1})	2.5×10^9
k_θ/m (J / kg)	1.3×10^7
k_ϕ/m (J / kg)	6.634×10^5
a_0	1.0
a_1	1.3108
a_2	-1.4035
a_3	-0.3358
a_4	2.8271
a_5	-3.3885

Table 3.2
Simulation data and Results*

Run	λ	t_f (ns)	p_t	$\lambda_{tg}(ns^{-1})$
I	0.37	12.0	0.593	5.60
II	0.91	13.5	0.603	5.40
II**	0.91	13.5	0.627	2.92
III	1.38	12.5	0.641	4.58
IV	2.00	13.5	0.777	2.76

* at 400K, ** at 300K

hydrocarbon chain. The force constants for bending and bond stretching were proposed by Helfand et al.[14] as a reasonable compromise between realistic estimates leading to too fast oscillations and softer potentials allowing for larger time steps of integration. The mass m of chain atoms was taken as 0.014 kg/mol, corresponding to methylene repeat units. Similarly, the equilibrium values l_0 = 1.53 Å and $\theta_0 = 70.53^o$ of alkane chains were used. Simulations were performed with $\beta = 1.0 \times 10^5$ / ns for T = 400K in general. A few runs were repeated for 300K to estimate the effect of temperature change.

Initially, bond lengths and angles were assumed to be at their equilibrium values and bond torsional angles were assigned by the Monte Carlo technique based on the conventional rotational isomeric state[4] approach. Accordingly, a priori probabilities of rotameric states *t*, g^+ and g^- were estimated from the above rotational potential and bonds are assigned isomeric states in conformity with those probabilities. Simulations were repeated for four chains with distinct end-to-end separations listed in Table 3.2. The total duration of simulations t_f for each run are given in the third column. A given run required a CPU time of about 10-12 hours on an SGI / 35 Personal Iris. The end-to-end vector of each chain was held fixed by artificially freezing the two terminal atoms. This mathematical device permits to simulate a chain between two securely embedded junction points A and B in a deformed network, which undergoes restricted motions to the extent of rigidity imposed by its extension. The degree of extension of each chain is characterized by the ratio $\lambda = r / < r^2 >_0^{1/2}$ of its end-to-end distance r to the unperturbed chain length. Compared to the dimensions of unperturbed polyethylene chains, in which $r \equiv < r^2 >_0^{1/2} \approx 2.6$ nm for n = 48, (using the characteristic ratio[4] $C_n \approx 6.0$ in $< r^2 >_0 = C_n n l_0^2$), the simulated chains III and IV with respective end-to-end distances 3.62 and 5.23 nm have relatively expanded configurations, while the chain I with r = 0.97 nm is highly

contracted. The dimensions of the chain II with end-to-end distance r = 2.39 nm approximate those of unperturbed PE polymers.

3.2 Internal Orientational and Conformational Correlations in Deformed Polymer Chains

The simulation results have been used to study the equilibrium and dynamic properties of model PE chains described in the previous section. The following sections are organized as follows: In Section 3.2.1, the BD trajectories of bond dihedral angles are displayed for chains of various extension and the rotational isomerization rates are estimated from hazard analysis. Static and dynamic correlations between bond orientations are analyzed . The time evolution of probability distribution functions for bond dihedral angles and bond reorientation in space are obtained. In the final Section 3.2.2, concluding remarks are presented.

3.2.1 Analysis of the Trajectories

3.2.1.1 Trajectories and Equilibrium Distribution of Bond Dihedral Angles

For illustrative purposes, the changes in the dihedral angles of the central bonds in the chains I, II and IV during a BD simulation period of 1.2 ns are displayed in Figure 3.3. The preference for rotational angles centered within $\pm 30^{o}$ fluctuations about the isomeric states *t*, g^{+} and g^{-} is clearly apparent from those trajectories. It is noted that the more contracted chain exhibits steady

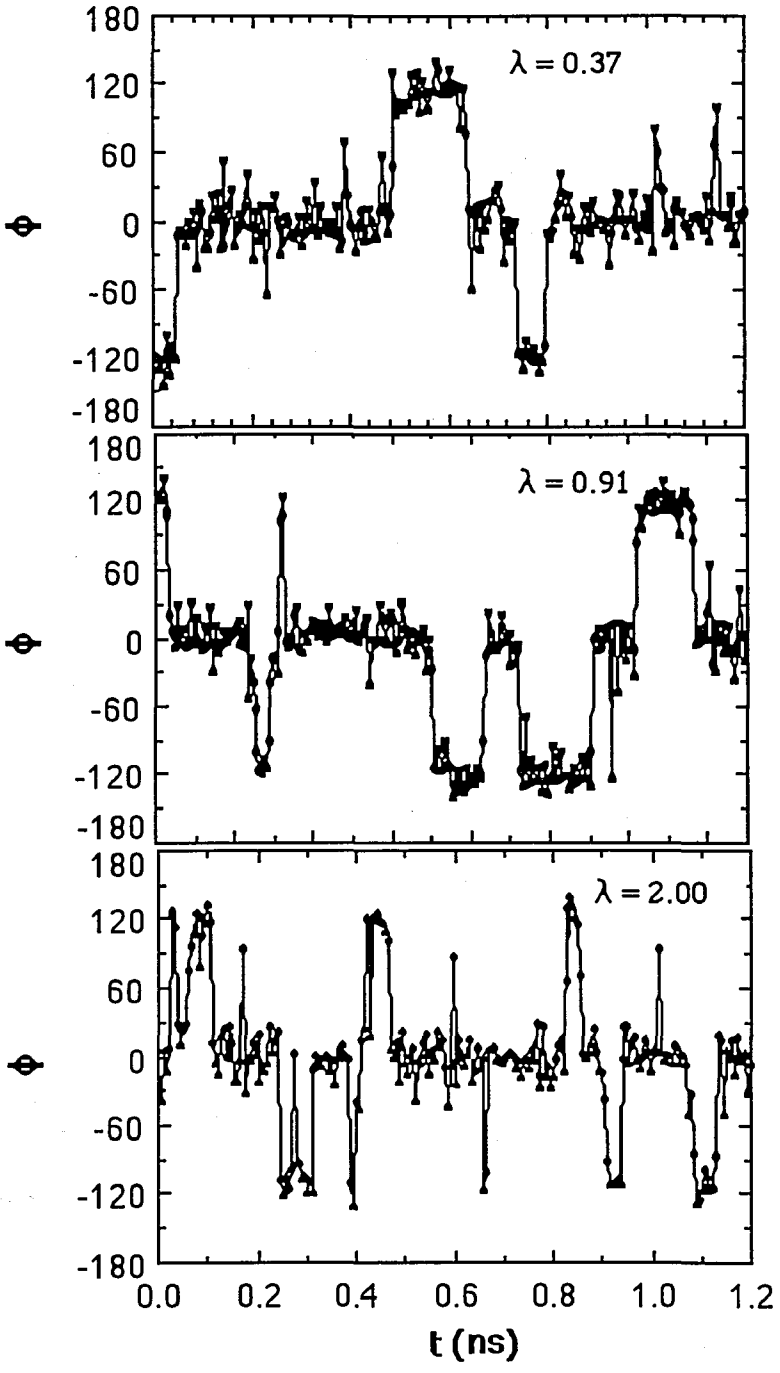

Figure 3.3 Example trajectories of 1.2 ns for dihedral angles ϕ_i of the central bonds in chains of various extensions I, II and IV with λ = 0.37, 0.91 and 2.00, respectively, at 400K.

transitions between rotamers while the highly strained chain with the largest λ is subject to fast oscillatory motions and in particular rapid back transitions restoring the bond torsional angle to the *trans* state, whenever the *gauche*$^{\pm}$ state is visited. In Figure 3.4, the isomeric transitions within the simulation period of 1.2 ns are presented for the bonds in the chains with λ = 0.37, 1.38 and 2.00.

The normalized probability distributions of dihedral angles for the chains of various extensions are displayed in Figure 3.5(a)-(d). The distributions were obtained by considering dihedral angle intervals of 20°. The weak asymmetries of the figures indicate the statistical error bounds of the BD simulations. An increased preference for the *trans* state with increasing chain extension is observed. From the integration of the probability distribution curves in the ranges $-60^{\circ} \leq \phi \leq 60^{\circ}$ and $60^{\circ} \leq |\phi| \leq 180^{\circ}$, the equilibrium probabilities of *t* and $g^{\pm}$ states, respectively, are estimated. The results are listed in the fourth column of Table 3.2. It is interesting to note from the tabulated equilibrium probabilities p_t of the *trans* state or from the curves in Figure 3.5(a)-(d) that the equilibrium distribution of rotational states is more sensitive to chain extension in the case of more stretched chains (with higher λ). The contracted chain on the other hand exhibits a distribution of dihedral angles that closely approximates that of the unperturbed chain.

3.2.1.2 Rotational Isomerization Rates

For the estimation of the rotational isomerization rates in the chains with different extensions, the hazard plots shown in Figures 3.6(a) and (b) were drawn. The cumulative hazard H(t) in the ordinate of the figures are obtained from the set of first passage times from one rotational isomeric minimum to

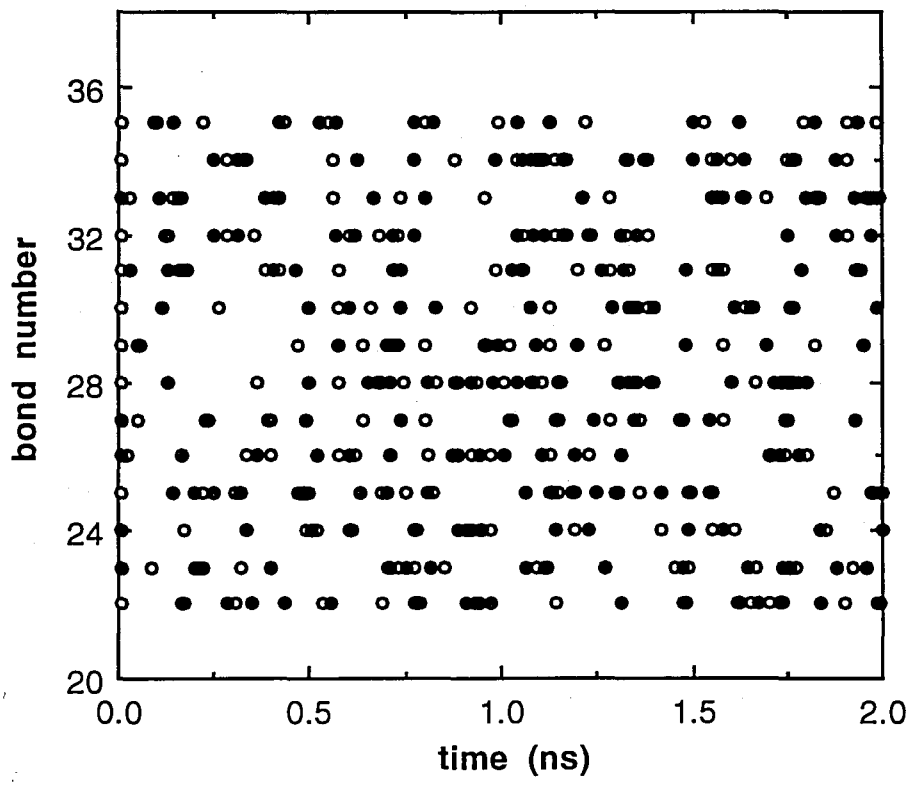

Figure 3.4 Absolute transition times(abscissa) for the various bonds. An o indicates a transition from one of the gauche states to the trans state, while ● indicates a transition from the trans state to the one of the gauches.

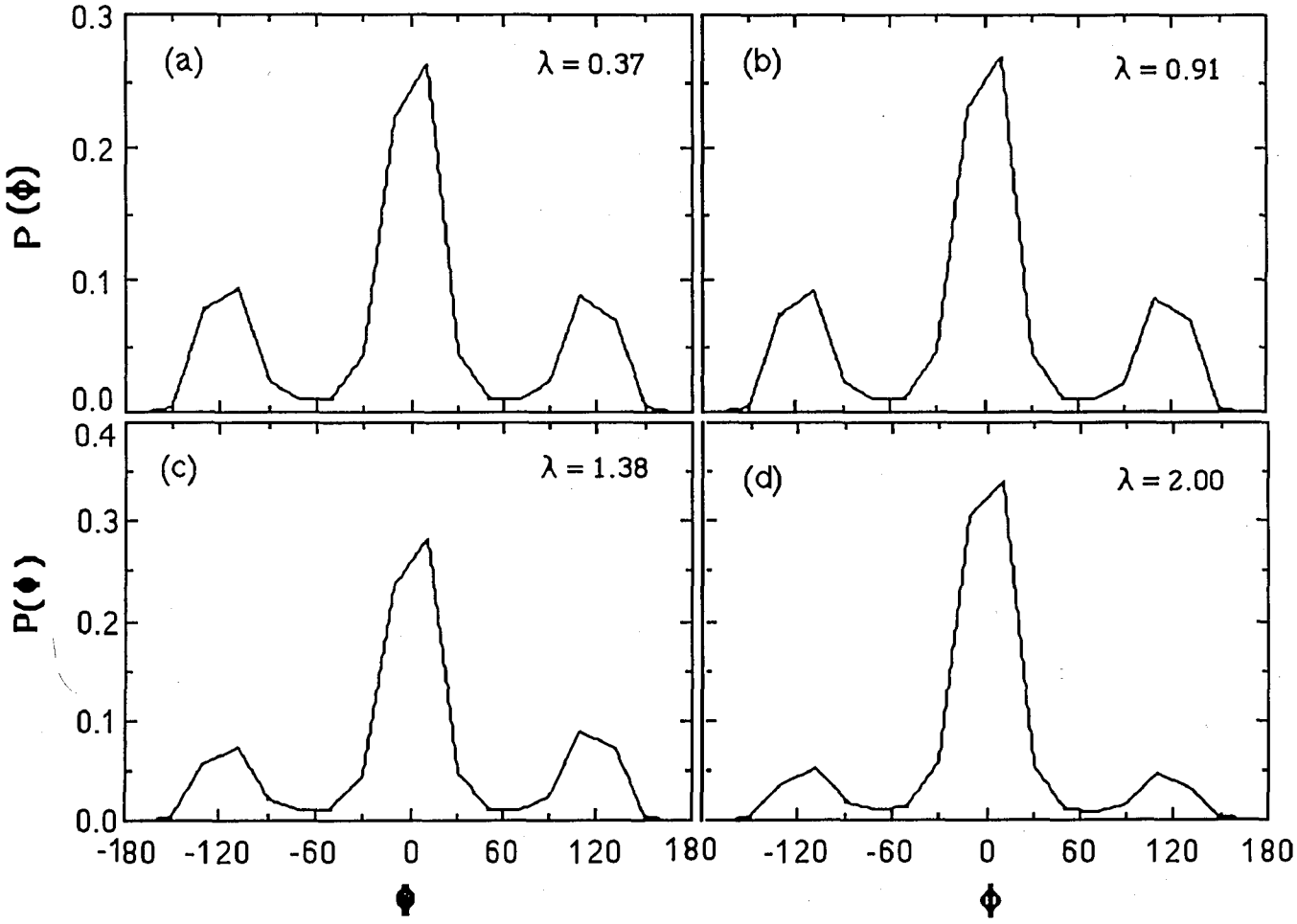

Figure 3.5(a)-(d) Equilibrium probability distribution $P(\phi_i)$ of dihedral angles of internal bonds ($5 \leq i \leq N-5$) for chains with (a) $\lambda = 0.37$, (b) $\lambda = 0.91$, (c) $\lambda = 1.38$ and (d) $\lambda = 2.00$.

another, by following the procedure previously outlined.[9] Accordingly the first passage times are organized in ascending order and the hazard rate $h(\tau_i)$ corresponding to the ith element τ_i of the set of first passage times is assigned the value $h(\tau_i) = i / (n-i)$ where n is the total number of first passages. The cumulative hazard H(t) results from the summation of the hazard rates $h(\tau_i)$ in the range $0 \leq \tau_i \leq t$. The details of the hazard analysis technique is given in Appendix D.

The asymptotic slope λ_h of the cumulative hazard is a measure of the transition rate for each chain. The slope λ_h is related to the rate of transition λ_{tg} from *trans* to one of the *gauche* states and to the reverse rate λ_{gt} by

$$\lambda_h = 2p_t \lambda_{tg} + 2p_g \lambda_{gt} = 4p_t \lambda_{tg} \qquad (3.13)$$

where the second equality follows from the principle of detailed balance. The isomerization rates λ_{tg} resulting from the least squares fits of the plots for the four chains in Figure 3.6(a) are listed in the fifth column of Table 3.2. The isomerization rates decrease with chain extension and increases with temperature.

In particular, it is noted from Figure 3.6(a) that the most stretched chain (IV) exhibits distinctly lower slope λ_h indicative of a slower transition rate compared to the other three chains. At first glance, this feature appears contradictory to the trajectories displayed in Figure 3.3. A closer examination reveals, however, that on a short time scale this chain is in fact the one which exhibits the highest mobility as illustrated in Figure 3.6(b). This figure which represents nothing else than the short time portion of Figure 3.6(a) clearly demonstrates the enhanced tendency of the chain IV to undergo high frequency

motions at short time scales. The majority of those motions are however in the form of reverse transitions forcing the bond back to its original state and do not effectively contribute to the conformational relaxation of the chain. The effective rate of isomerization is portrayed by the long time asymptotic slope of the cumulative hazards and is relatively low, as would be expected for a chain with considerably reduced degree of freedom. In the case of temperature effect, any decrease in temperature leads to the lower isomerization rates as depicted in Figure 3.6(c).

3.2.1.3 Equilibrium Correlations between Bond Orientations

The equilibrium correlation between the orientations of bonds i and j along the chain is expressed by the order parameter or orientation function S

$$S = 1/2\ (3\ (\mathbf{m}_i \cdot \mathbf{m}_j)^2 - 1) = 1/2\ (3 < \cos^2\alpha > - 1) \qquad (3.14)$$

where $\mathbf{m}_i$ and $\mathbf{m}_j$ are the unit vectors along the two bond vectors $\mathbf{l}_i$ and $\mathbf{l}_j$, and α is the angle between them. The angular brackets in eq 14 indicate both the time average for the pair of bonds i and j and the ensemble average over pairs of bonds with the fixed number j - i of intervening bonds. Figure 3.7 displays the decay of orientational cross-correlations with increasing number of intervening bonds, for the four chains of different extensions. A sharp even-odd effect which persists over a large number j-i of intervening bonds is observed in the case of stretched chains. Strongest orientational correlations, positive or negative, occur in the case of the most strained chain (IV) as expected. It is interesting to note on the other hand that the orientational behavior of the contracted chain (I) closely resembles that of the unperturbed chain (II) and the orientational correlations between bonds vanish at about j - i =5, in those chains.

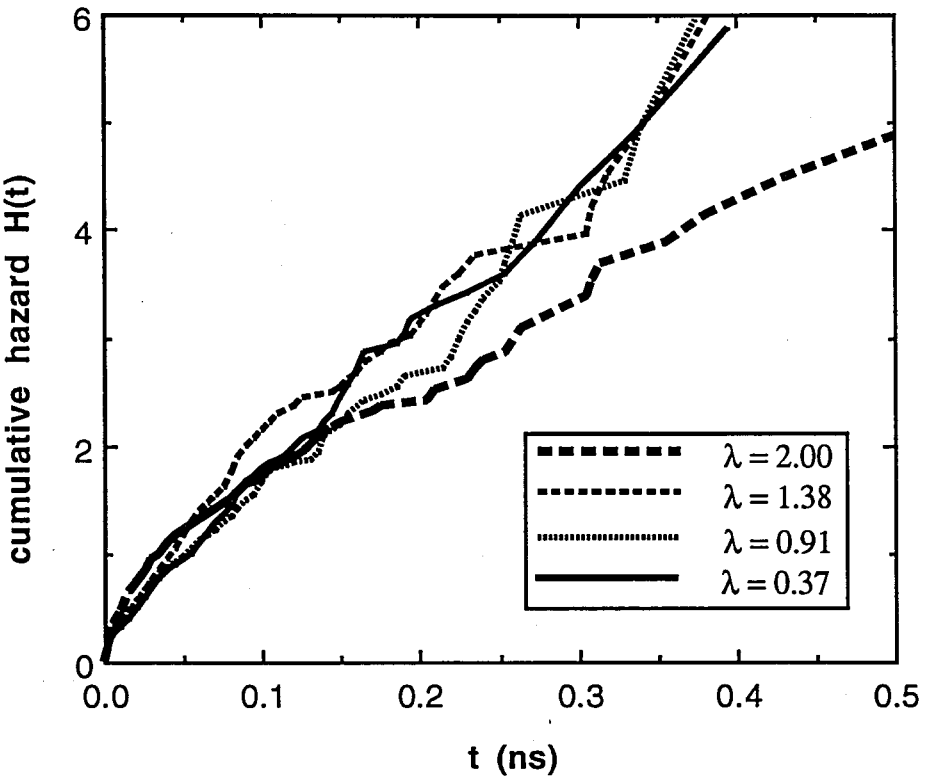

Figure 3.6(a) Time dependence of cumulative hazards H(t) for the simulated chains of various end-to-end separation, indicated in the figure. The lowest curve obtained for λ = 2.00 shows the low effective rate of isomerization of the most strained chain.

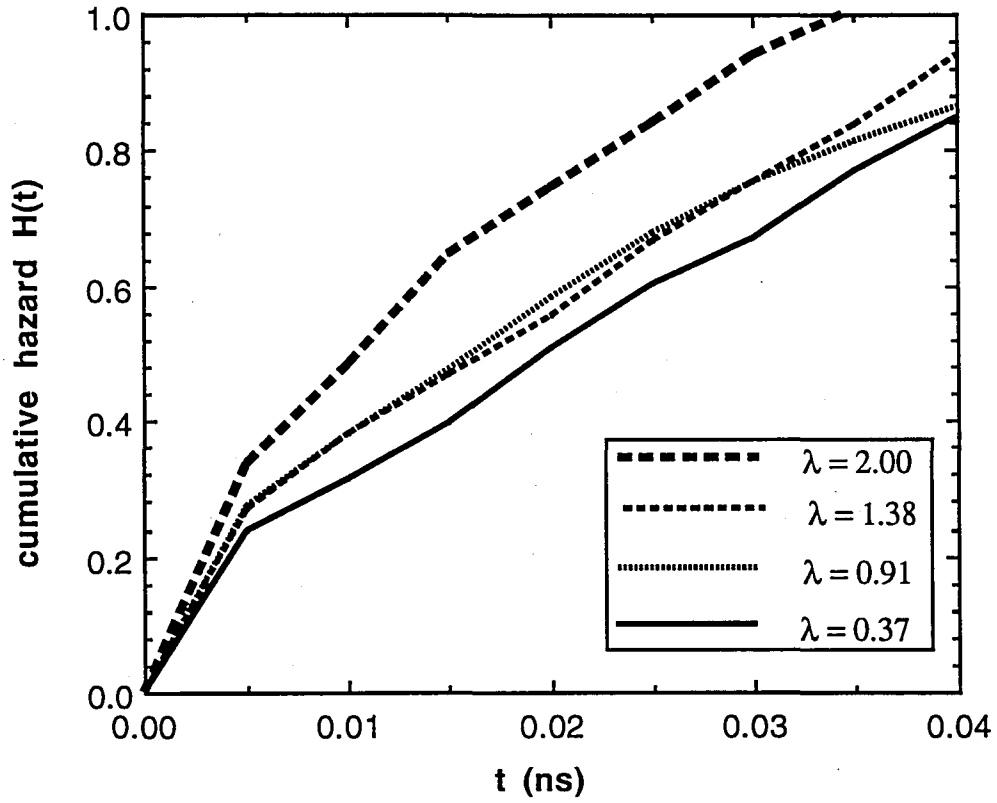

Figure 3.6(b) Short time region of the hazard plot displayed in Figure 3.6a, indicating the enhanced tendency of the bonds in the most stretched chain to undergo back transitions to their original rotameric state.

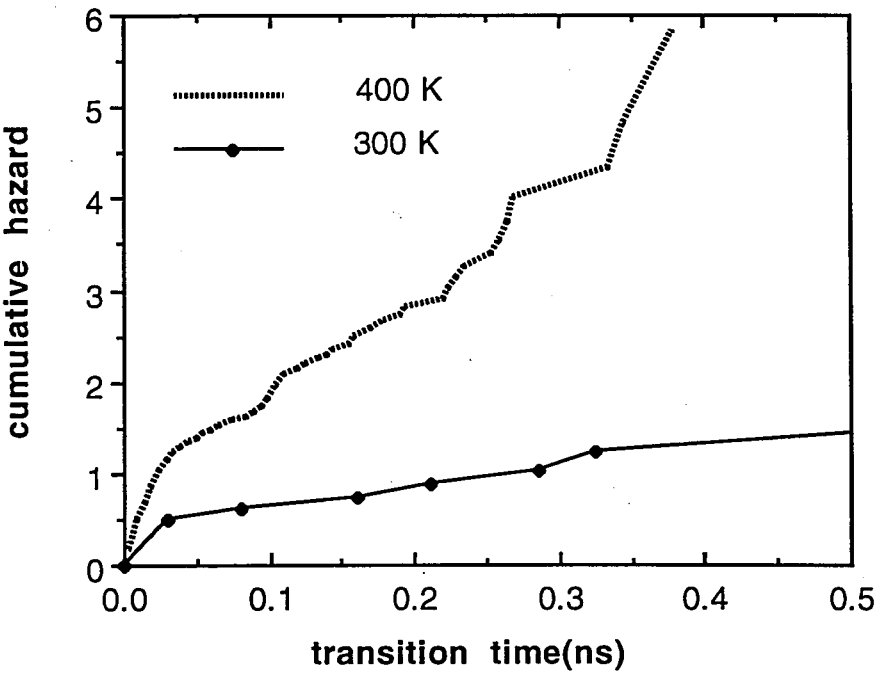

Figure 3.6(c) Time dependence of cumulative hazards H(t) for the example chain II at the two simulation temperatures, 300 and 400K is indicated in the figure. The lowest curve obtained shows the low effective rate of isomerization of the chain at the lower temperature.

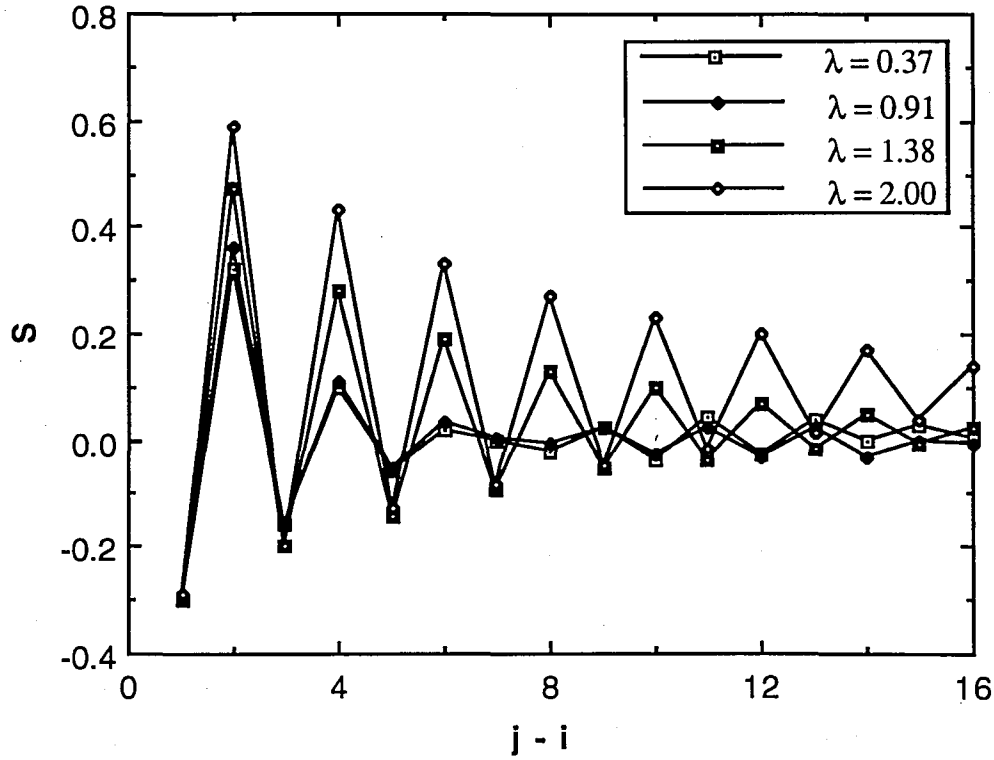

Figure 3.7 Static orientational cross-correlation function $S = 1/2\ [3\ (\mathbf{m}_i \cdot \mathbf{m}_j)^2 - 1]$ between bonds i and j as a function of the number j-i of intervening bonds, for the four chains with the indicated extensions, at 400K. A strong even-odd effect enhanced by chain extension is observed.

The influence of temperature on the degree of bond orientational correlations is illustrated in Figure 3.8. Chain II is taken up. It is observed that the orientational correlations which vanish at about j - i = 6 at 400 K are maintained until j - i $\geq$ 10 with the decrease in temperature to 300K.

An estimation of the orientational correlation distance between neighboring bonds may be performed by examining the change in the orientational cross-correlation function S with the distance separating the studied bonds. Figure 3.9 displays the variation of S with d where d is taken as the distance between the midpoints of the bonds. Results reported in Figure 3.9 are obtained by computing the average S values corresponding to intervals Δd of 0.025 nm. The curves exhibit oscillations which gradually level off with increasing d to the asymptotic values dictated by the particular chain extension. The lowest starting point reflects the almost tetrahedral bond angle between successive bonds and is not affected by chain extension. The effect of chain extension is distinguishable at longer separations. Strongest orientational correlations occur in the most stretched chain. The unperturbed chain exhibit the same behavior as the contracted chain I and is not explicitly displayed for clarity. The relative heights of the curves are in conformity with the ordering of their end-to-end separation. This dependence of S on d is characterized in all cases by a maximum correlation at a separation of about 0.12 nm, followed by a minimum at about 0.20 nm. Beyond 0.5nm approximately, orientational correlations between bonds become negligibly small unless the chain is highly strained.

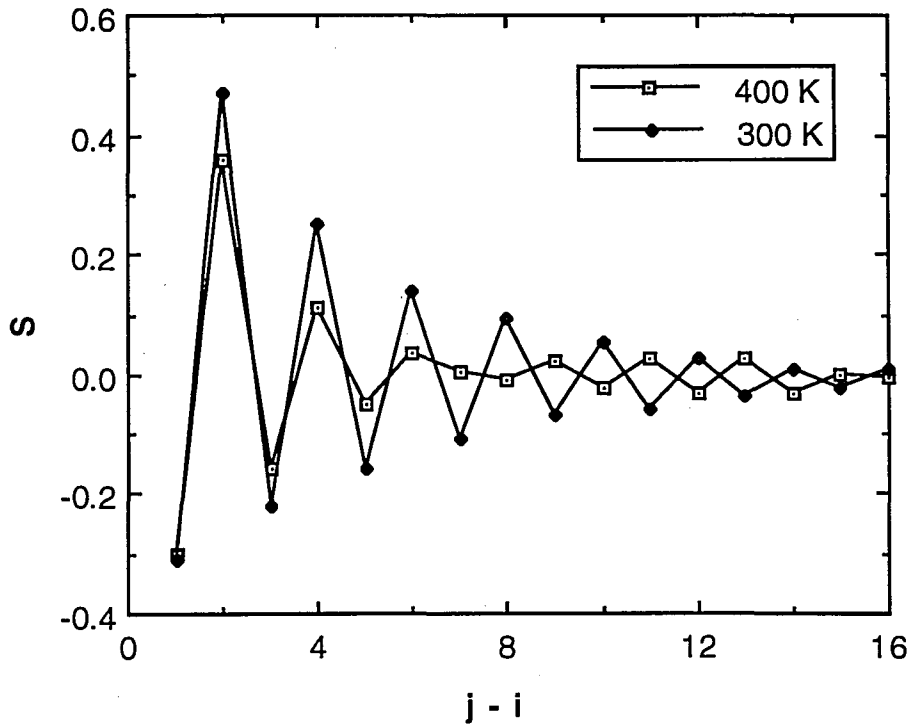

Figure 3.8 Decrease in S with increasing temperature. Results are presented for the example chain II at the two simulation temperatures 300 and 400K.

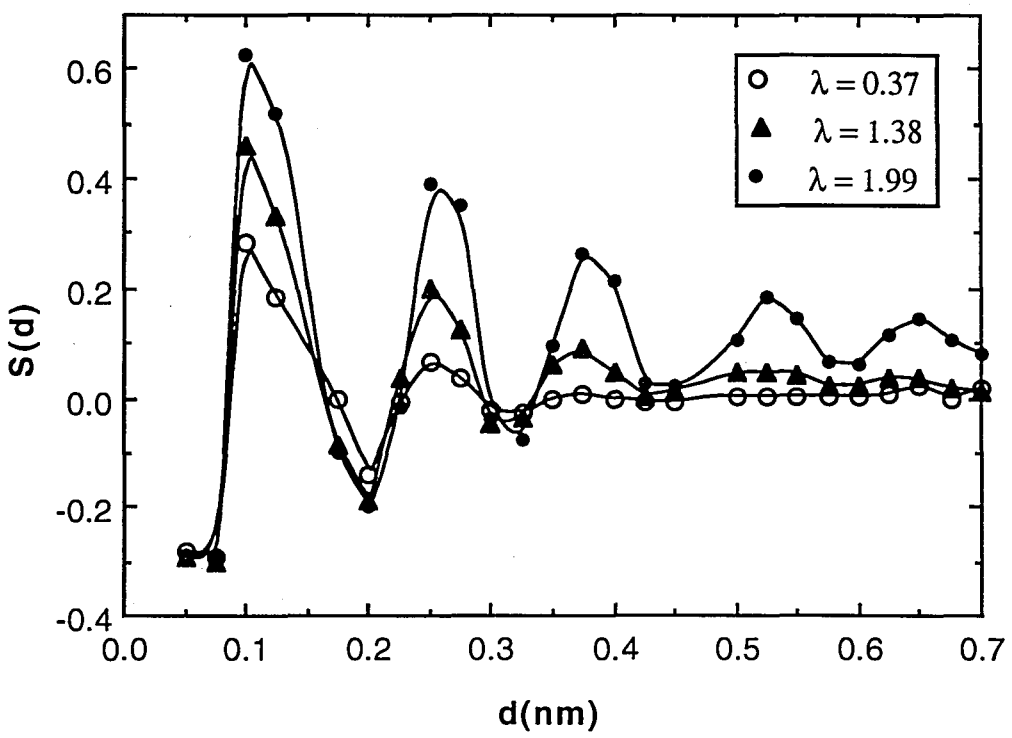

Figure 3.9 Change in equilibrium orientational correlations S between pairs of bonds with increase in their separation d. The orientational correlation length does not extend beyond 0.5 nm except for the highly strained chain.

3.2.1.4 Time Decay of Bond Orientational Autocorrelations

The first and second orientational autocorrelation functions (OACF) for a given bond i along the chain are given by the respective expressions

$$M_1(t) = \langle \mathbf{m}_i(0) \cdot \mathbf{m}_i(t) \rangle \tag{3.15}$$

and

$$M_2(t) = 1/2 \langle 3 (\mathbf{m}_i(0) \cdot \mathbf{m}_i(t))^2 - 1 \rangle \tag{3.16}$$

Here $\mathbf{m}_i(0)$ and $\mathbf{m}_i(t)$ represent the unit vectors associated with the initial and final states of the investigated bond vector. $M_1(t)$ is related to dielectric relaxation process whereas $M_2(t)$ is observed in fluorescence anisotropy, NMR and ESR experiments. In analogy to eq 3.14, the averages in eqs 3.15 and 3.16 are performed by taking both the ensemble and the time averages as

$$M_1(t) = \Delta t\,(n-2k)^{-1}\,(t_f - t)^{-1} \sum_{i=k}^{n-k} \sum_{s} \mathbf{m}_i(s\Delta t) \cdot \mathbf{m}_i(s\Delta t + t) \tag{3.17}$$

A similar expression applies to $M_2(t)$. The first summation includes all bonds devoid of end effects. The value k = 10 is safely used. The second summation is performed over discrete initial times $s\Delta t$ with spacing Δt. s is varied from 0 to $(t_f - t)/\Delta t$ for a total simulation duration of t_f, and Δt is chosen as 4900 fs. It is noted that the use of $\mathbf{m}_j(s\Delta t)$ instead of $\mathbf{m}_i(s\Delta t+t)$ in eq 3.17 yields at t = 0 the equilibrium property $\langle \cos \alpha \rangle$. Similarly, $M_2(t)$ reduces to S upon substitution of t = 0 and $j \neq i$.

The time decay of the first OACF $M_1(t)$ is displayed in Figure 3.10. The initial decay rates are comparable in the chains with different extensions but the

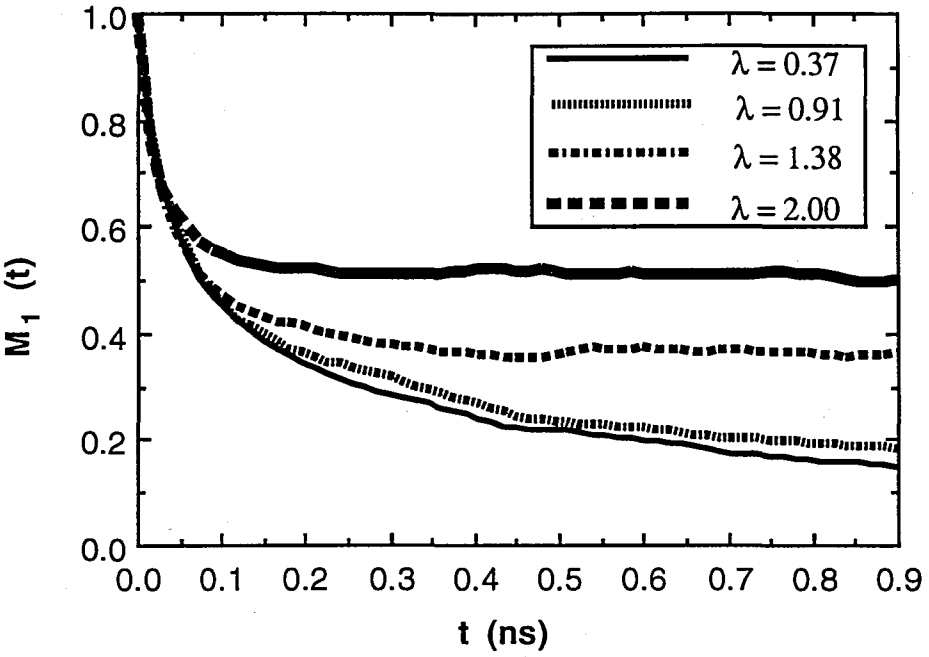

Figure 3.10 Time decay of the first orientational autocorrelation function $M_1(t)$ for internal bonds of simulated chains subject to indicated λ values. Deviations between curves arise mostly from differences between the equilibrium values asymptotically approached.

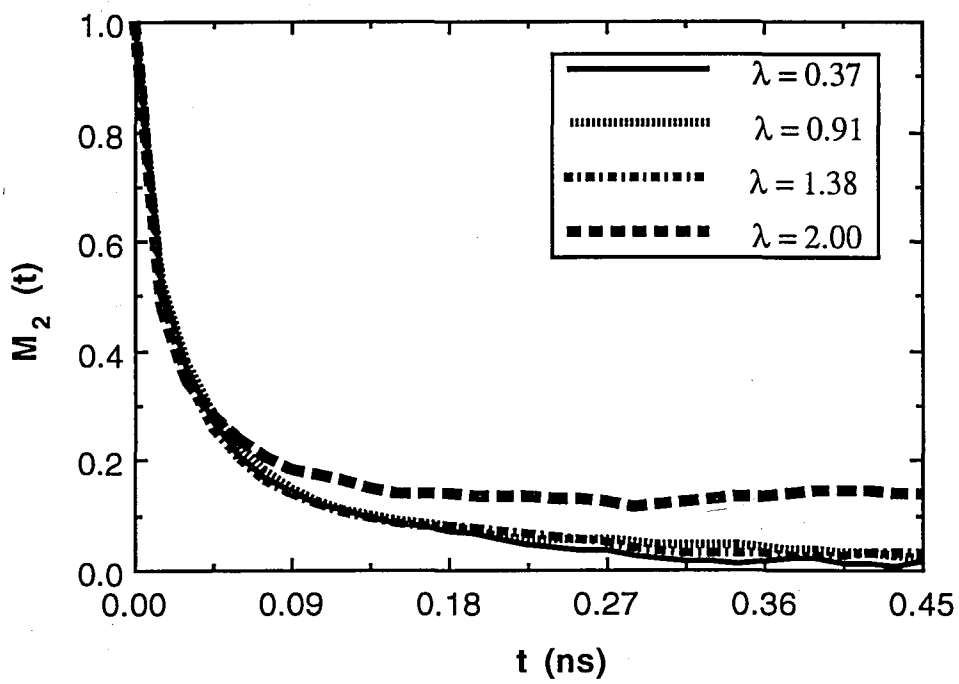

Figure 3.11 Time decay of the second orientational autocorrelation function $M_2(t)$ for internal bonds of simulated chains subject to indicated λ values.

curves gradually separate as the equilibrium values are asymptotically approached. The distinction between the respective chains are even weaker if the second OACF $M_2(t)$ is considered, as illustrated in Figure 3.11. A measure of the dynamics of the chain excluding the effect of equilibrium constraints is the normalized OACFs

$$M_i(t)_{norm} = [\, M_i(t) - M_i(\infty) \,] / [\, M_i(0) - M_i(\infty) \,] \qquad i = 1,2 \tag{3.18}$$

The time decay of the normalized first OACF is displayed in Figure 3.12. It is clearly seen that bond reorientation is fastest in the most stretched chain indicating the occurrence of fast large amplitude motions on a localized scale. As far as the overall chain is concerned, on the other hand, the asymptotic high value of $M_1(t)$ at long times in Figure 3.10 shows that the ultimate orientational relaxation is considerably limited. This is a natural consequence of the imposition an uniaxial tension holding the chain ends far above their unperturbed separation. Figure 3.12 shows that the bond reorientation is slowed down in the case of less extended chains. The influence of temperature on the bond OACF is depicted in Figure 3.13. Any increase in temperature results in faster bond reorientation.

Stretched exponential functions of the form[44]

$$M_i(t) = \exp \{- t / \tau_i)^{\beta} \} \tag{3.19}$$

with $0 \leq \beta \leq 1$ has been used in literature to approximate the time decay of correlation functions. τ_i is the characteristic time for the specific relaxation process expressed by $M_i(t)$. Eq 3.19 may be rewritten as

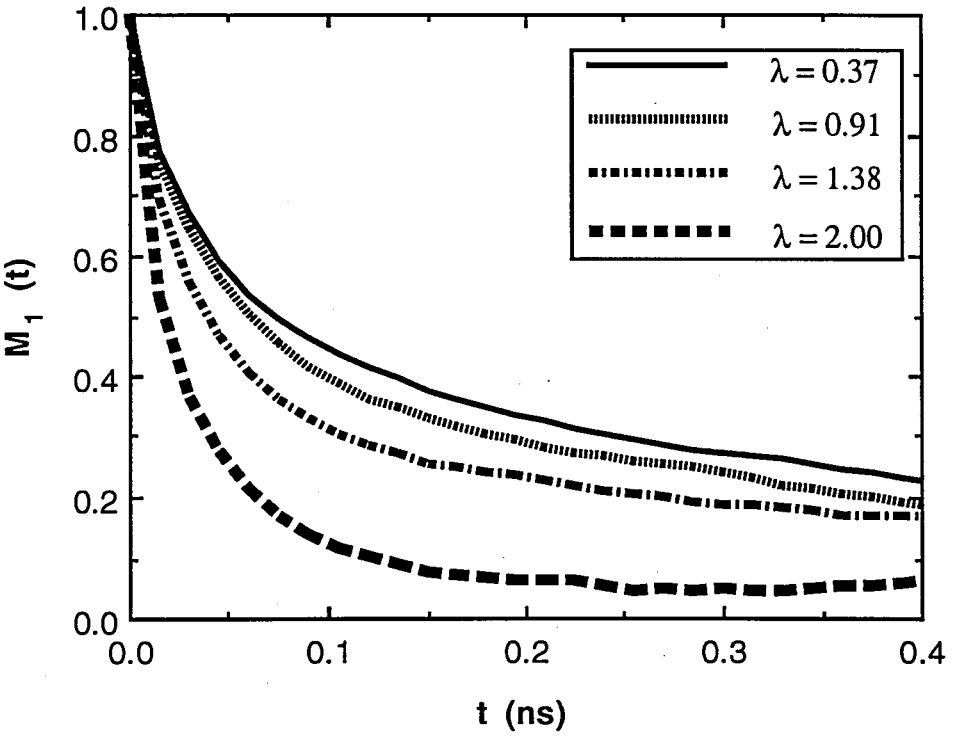

Figure 3.12 Time dependence of normalized first OACF $M_1(t)_{norm}$ which is a measure of local chain dynamics excluding equilibrium contributions. The loss of orientation of bonds occurs the fastest in the most strained chain and decreases gradually with decreasing end-to-end separation.

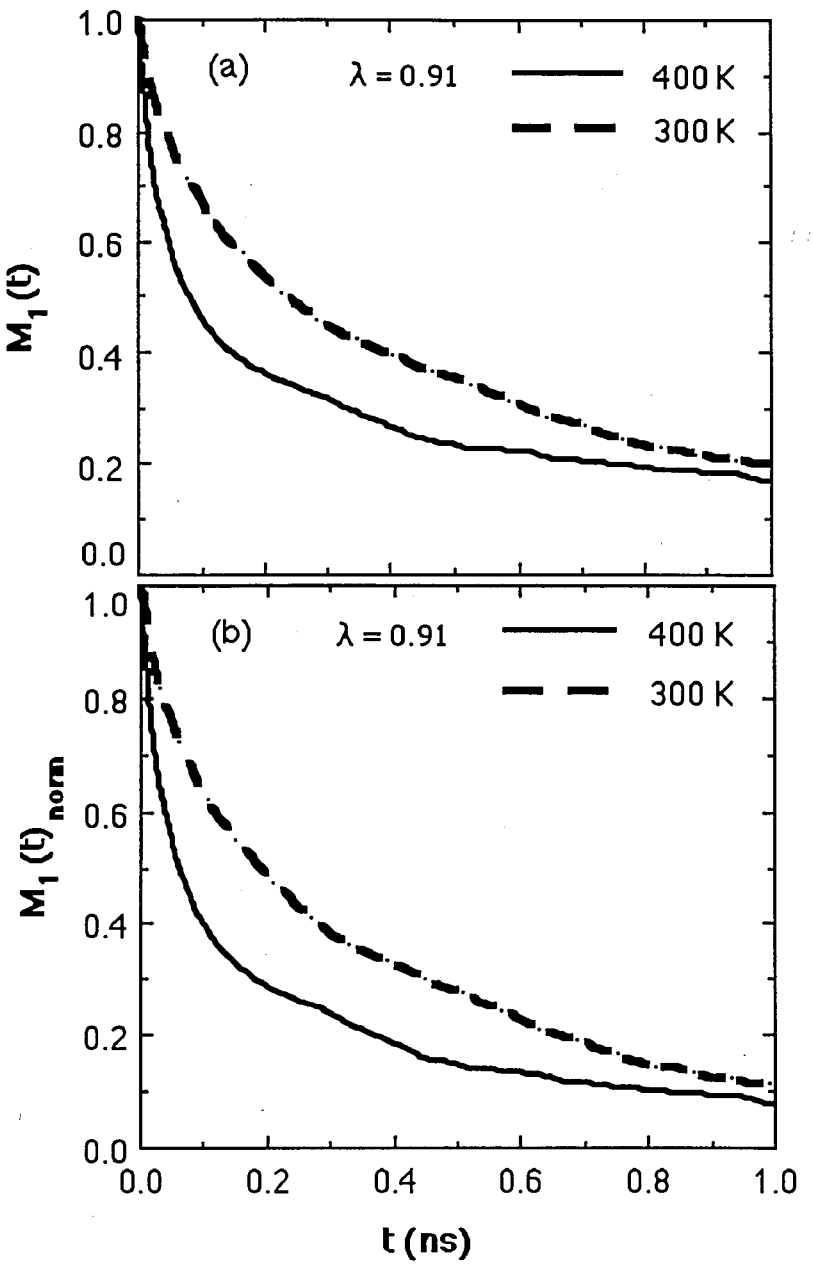

Figure 3.13 a) Time decay of the first autocorrelation function $M_1(t)$ for internal bonds of the example chain II at the two simulation temperature 300 and 400K. b) Time dependence of normalized $M_1(t)$ which is a measure of local chain dynamics excluding equilibrium contributions for the chain II at the two simulation temperature 300 and 400K.

$$\log [- \ln M_i(t)] = \beta \log t - \beta \log \tau_i \qquad (3.20)$$

which permits an easier graphical analysis of the results. Plots of log [-ln $M_i(t)$] vs. log t are presented for i = 1 and 2 of the bonds in the chains with different degrees of extension in Figures 3.14 and 3.15 respectively. Representation of $M_1(t)$ by stretched-exponential for the chain II at two simulation temperatures, 300 and 400K is given in Figure 3.16. The analysis is mostly significant in the intermediate to long time range inasmuch as a single exponential decay of correlation functions is operative in the two limits as t approaches zero or infinity. That the OACFs may be fairly well represented by stretched exponentials is seen from the approximately straight lines resulting from BD simulations. The exponents calculated from the slopes of the curves in Figure 3.14 vary in the range 0.46±0.03, smoothly increasing with chain extension. An exponent of β = 0.55±0.04 is obtained on the other hand from the best fitting lines in Figure 3.15. The dependence on chain extension is mostly manifested by the vertical shifting of the curves which is directly related to the characteristic time τ_i. It is noted that the characteristic times τ_1 associated with the first OACF exhibit a definite dependence on chain extension whereas those corresponding to $M_2(t)$ are relatively insensitive. Table 3.3 gives a summary of the exponents and characteristic times resulting from the BD trajectories of the four chains. A ratio of τ_1 / τ_2 of about 4 is obtained for the unperturbed chain. This ratio is found to decrease with increasing chain extension. Correlation times for the decay of $M_1(t)$ and $M_2(t)$ may alternatively be estimated from the times corresponding to 1/e of their full relaxation. The correlation times obtained by this method exhibit the same dependence on chain extension. The ratio τ_1 / τ_2 is found to decrease linearly with chain extension, irrespective of the method of estimation of characteristic or correlation times, as illustrated in Figure 3.17.

Table 3.3

Stretched Exponential Parameters for Bond OACFs*

Run	λ	τ_1 (ns)	β	τ_2 (ns)	β
I	0.37	0.178	0.453	0.030	0.586
II	0.91	0.137	0.469	0.030	0.578
II**	0.91	0.324	0.674		
III	1.38	0.087	0.454	0.027	0.554
IV	2.00	0.026	0.467	0.020	0.513

* at 400K, ** at 300K

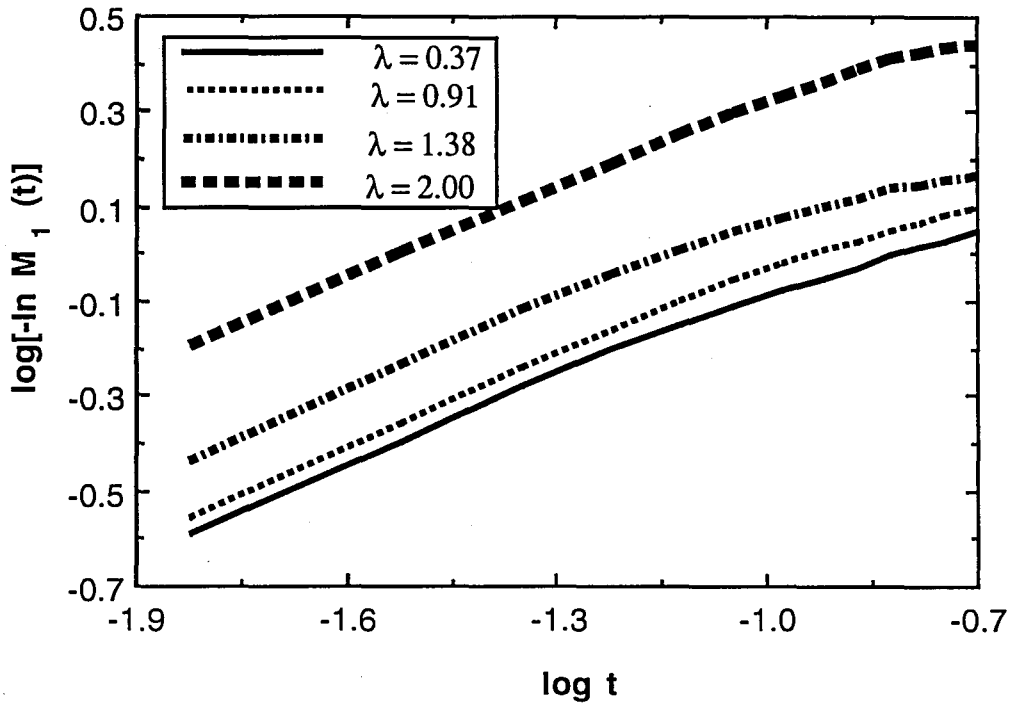

Figure 3.14 Comparison of the time dependence of $M_1(t)$ with the stretched exponential form according to eq 3.20. Best fitting lines yield exponents $\beta = 0.45 \pm 0.03$ and the characteristic times listed in Table 3.3.

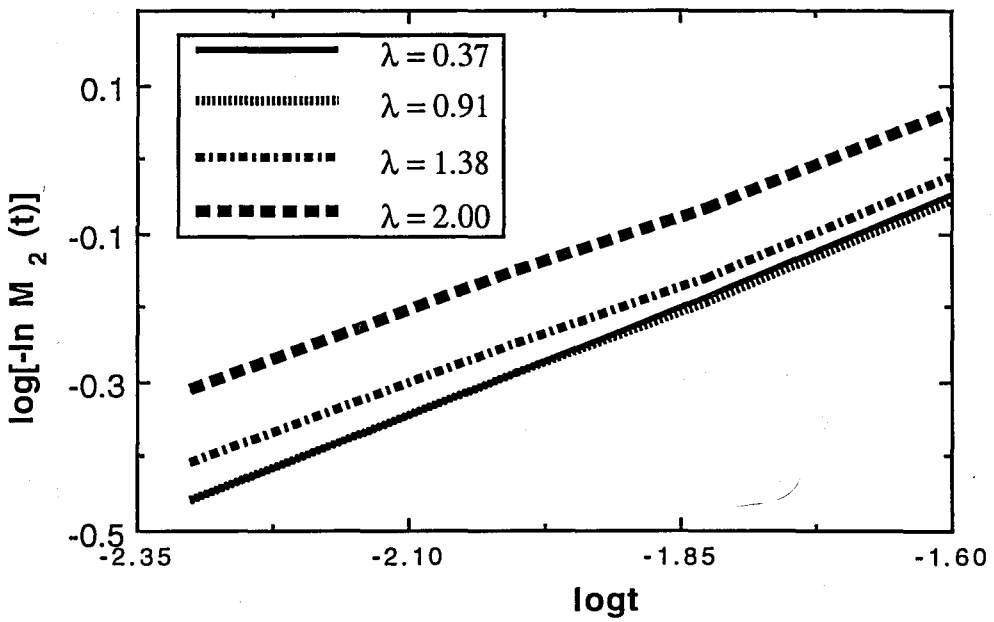

Figure3.15 Comparison of the time dependence of $M_2(t)$ with the stretched exponential form. Exponents $\beta = 0.55 \pm 0.04$ are obtained from the best fitting lines. The characteristic times and exponents for the four runs are listed in Table 3.3.

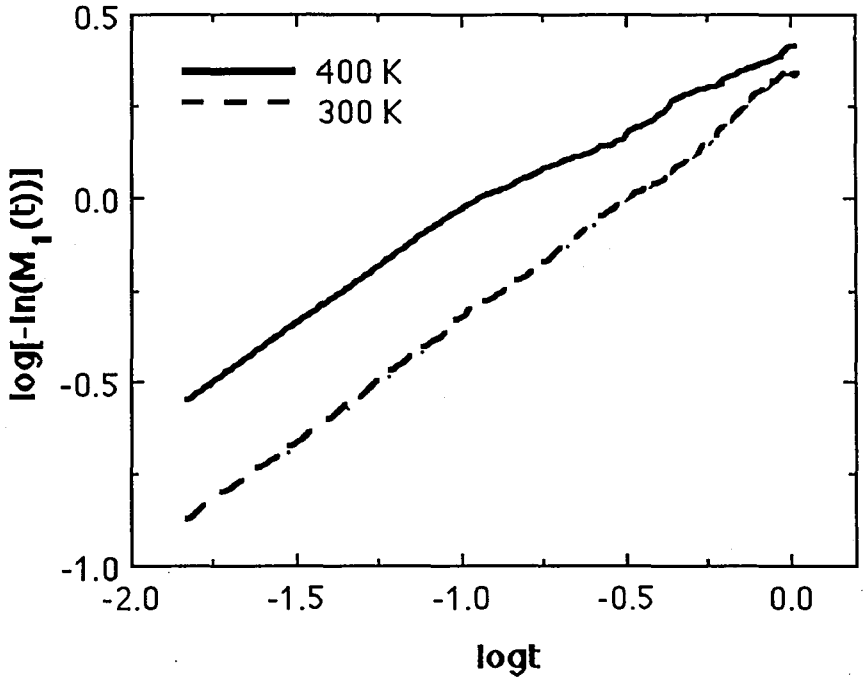

Figure 3.16 Comparison of the time dependence of $M_1(t)$ with the stretched exponential form according to eq 3.20 for the chain II at the two simulation temperature, 300 and 400K. Exponents β and the characteristic times obtained from best fitting lines are listed in Table 3.3.

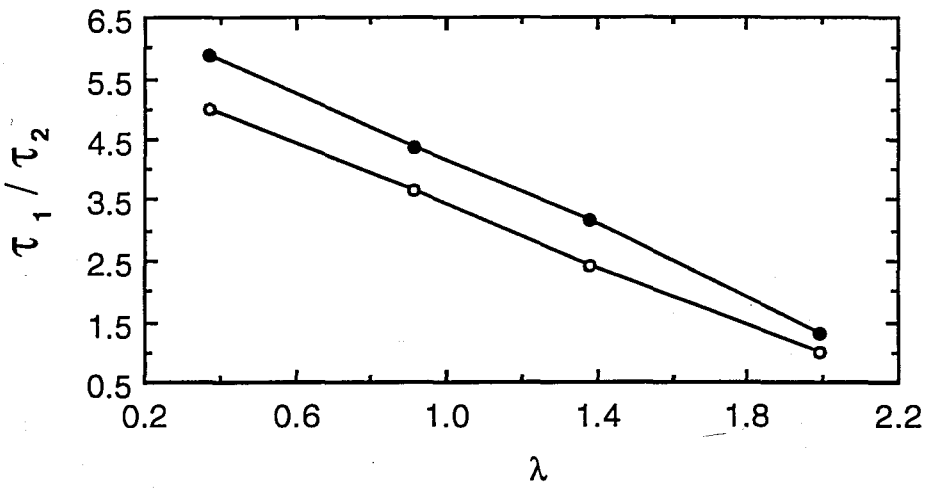

Figure 3.17 Dependence of the ratio τ_1 / τ_2 on chain extension. τ_1 and τ_2 are obtained both from (i) the best fitting stretched exponentials (filled circles) and (ii) the 1/e points of full decays of OACFs (empty circles). Linear decrease of τ_1 / τ_2 with chain extension is observed irrespective of the method of approach.

3.2.1.5 Distribution of Bond Rotation and Reorientation Angles

Following the approach adopted by Takeuchi and Roe[45,46] for a detailed description of the time evolution of relaxational processes in polymers, time-dependent distribution functions is considered in the following. The evolution of bond torsional motions is described by the probability distribution function $P(|\Delta\phi|, \Delta t)$ associated with the absolute changes in dihedral angles $|\Delta\phi|$ occurring within the time interval Δt. Similarly, $P(\Delta\alpha, \Delta t)$ represents the probability that a given bond undergoes a spatial reorientation of angle $\Delta\alpha$ during a time span Δt.

Figures 3.18(a)-(d) display the distribution functions $P(|\Delta\phi|, \Delta t)$ of bond torsional motions obtained for the four chains of various extensions. The λ values corresponding to each of the parts (a)-(d) is indicated. The curves are drawn for Δt = 0.005, 0.060 and 1.765 ns in each case. The distribution functions are not normalized but rescaled such that $P(|\Delta\phi| = 0^0, \Delta t) = 1$ for each of the chosen Δt values. Initially the distribution function $P(|\Delta\phi|, \Delta t)$ is a dirac function with the pike at $|\Delta\phi| = 0$. With increase in the elapsed time the distribution is expected to broaden towards larger $|\Delta\phi|$ values. However, the broadening does not occur in a gaussian form but instead a second peak centered about $|\Delta\phi| = 110^0$ appears which is indicative of the probable transition to another rotational isomeric state. In fact, the change in the torsional angle exactly reflects the rotational difference between the *trans* and *gauche* states of either sign in PE chains. At long times the equilibrium distribution of dihedral angles is gradually approached as revealed from the comparison of the uppermost curves in Figure 3.18(a)-(d) with those of Figure 3.5(a)-(d).

Figures 3.19(a)-(d) display the evolution of bond reorientation in space. The distribution curves $P(\Delta\alpha, \Delta t)$ are obtained from the angular displacement $\Delta\alpha$

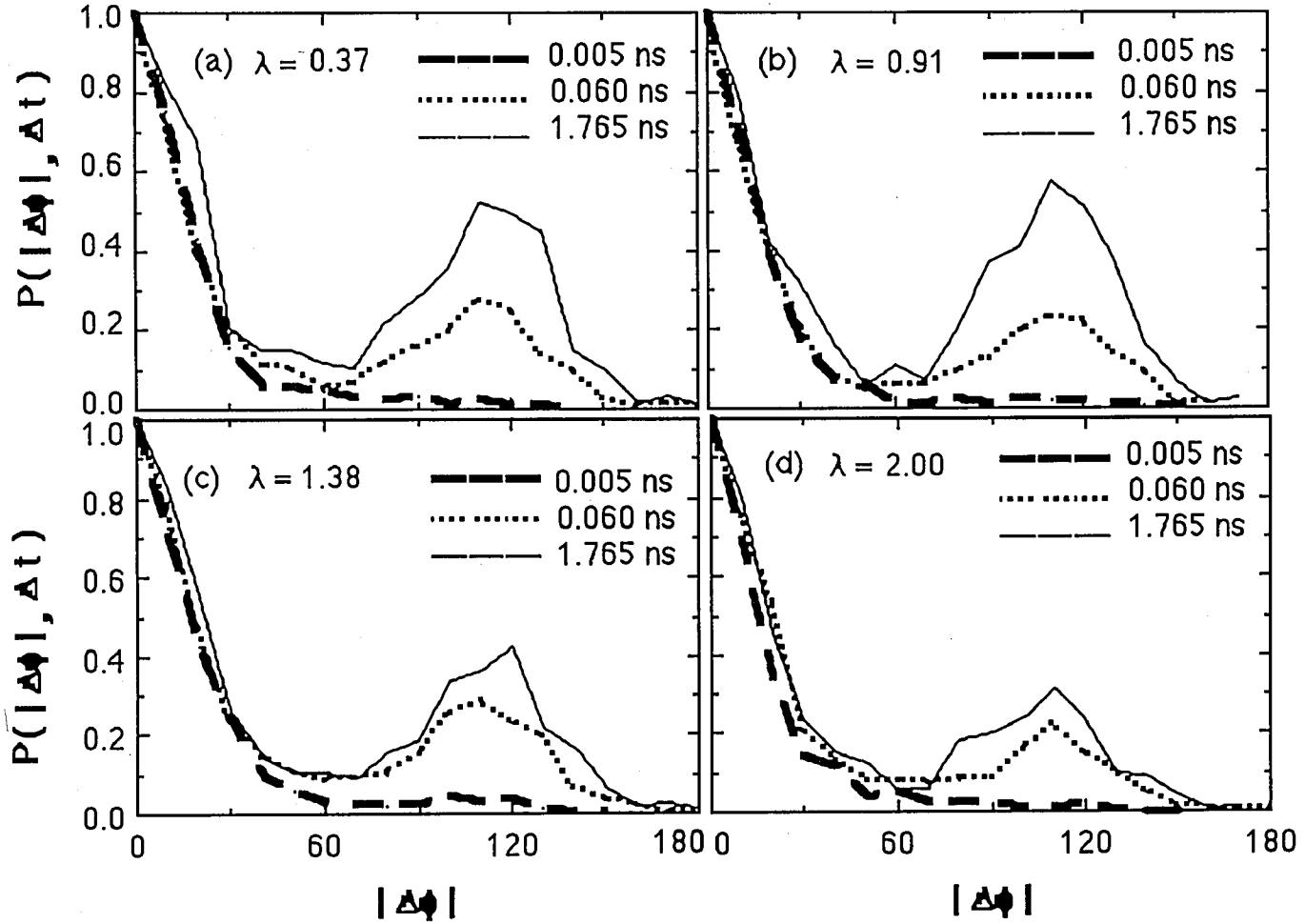

Figure 3.18(a)-(d) Distribution function $P(|\Delta\phi|, \Delta t)$ of obsolute changes in dihedral angles within respective time intervals Δt of 0.005, 0.06 and 1.765 ns, for (a) $\lambda = 0.37$ (b) $\lambda = 0.91$ (c) $\lambda = 1.38$ and (d) $\lambda = 2.00$. The distribution functions are rescaled such that $P(|\Delta\phi|\ \Delta t) = 1$

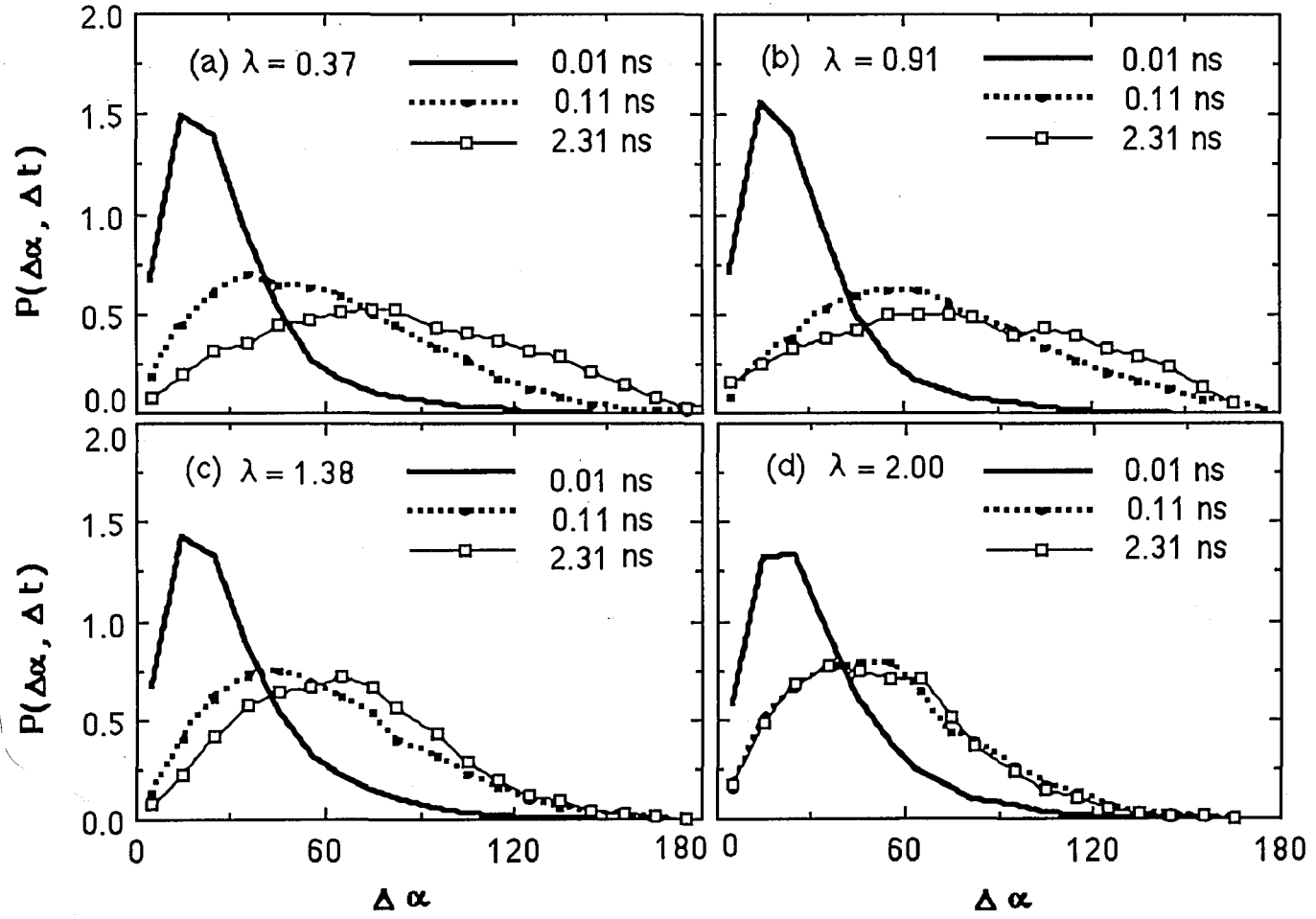

Figure 3.19 (a)-(d). Normalized probability distribution P ($\Delta\alpha$ Δt) for the orientation of bond vectors by an angle $\Delta\alpha$ within the time intervals of $\Delta t = 0.01, 0.11$ and 2.31 ns for (a) $\lambda = 0.37$ (b) $\lambda = 0.91$ (c) $\lambda = 1.38$ and (d) $\lambda = 2.00$.

of bond vectors in space, by considering the same bond during two successive times with a delay of Δt. Curves are drawn for Δt = 0.01, 0.11 and 2.31ns. For an unbiased distribution of spatial reorientation the distribution curves should evolve from a dirac function at $\Delta t = 0$ to the functional form 1/2 sin $\Delta\alpha$ at long times. This is not the case as the chains are subject to fixed end-to-end separations that certainly constrain bond spatial reorientations. The unperturbed chain and the compressed chain obey comparable dynamics and approach the equilibrium distribution 1/2 sin $\Delta\alpha$ at long times, which is indicated by the dotted curve in parts (a) and (b) of the figure. The bonds in the stretched chains however exhibit smaller $\Delta\alpha$ values on the average, decreasing with chain extension. This clearly demonstrates the influence of the deformation of chain ends on the orientational mobility of the chain even at the scale of individual bonds.

3.2.2 Concluding Remarks

In the present study, BD simulation method has been employed for a systematic analysis of chain extension on the conformational and orientational dynamics of polymer chains. The picture of spatially frozen chain ends is conveyed by the classical model of network chains in which the junctions deform affinely with the macroscopic strain. A more realistic model would consider a distribution of end-to-end separations in the deformed state and the possible fluctuations of the constrained domains. Restriction of the analysis to fixed chain ends is a mathematical simplicity which is adopted for computational efficiency.

The hazard analysis of BD trajectories demonstrates that with increasing extension and decreasing temperature the effective isomerization rates

decrease. The highly strained chain undergoes rapid rotational jumps though those are mostly in the form of back transitions forcing the bonds back to their original states and hence not contributing effectively to the conformational relaxation of the chain. Examination of the equilibrium correlations between bonds within the four chains of different extensions reveal the strong even-odd effect dominating the static cross-correlations, in agreement with previous work[47] The correlation length is about 0.5nm in the unperturbed or weakly perturbed state but is larger in the highly stretched chain.

Dynamic orientational autocorrelations of bonds are described by the functions $M_1(t)$ and $M_2(t)$ differing in correlation times by a factor of about 4 in the case of unperturbed chains. This factor is found to decrease linearly with increasing end-to-end separation. Recent MD simulations of n-alkanes in the bulk state by Takeuchi and Roe[45] yield a value of about 3 for the ratio τ_1 / τ_2 of the correlation times associated with $M_1(t)$ and $M_2(t)$ for bond reorientation. The small difference between the present results and those from MD simulations may be attributed to the influence of intermolecular constraints which are not presently considered. In fact, with increasing constraints at the chain ends, i.e. with increasing **r**, the ratio τ_1 / τ_2 is found to decrease linearly and approaches almost unity (indicative of large jump motions) in the highly strained chain. Previous analytical treatment based on the dynamic rotational isomeric states formalism leads[48] to a ratio of about 1-1.5 which follows from the discrete 120° amplitude jumps inherently present in that approach.

The exponents β which satisfactorily reproduce the time decay $M_1(t)$ and $M_2(t)$ are found to assume the values 0.46 ± 0.03 and 0.55 ± 0.04, respectively. For polyisoprene, recent BD simulations lead to $\beta \approx 0.6$ for $M_2(t)$ while $\beta \approx 0.4$ for $M_1(t)$ as measured in dielectric experiments and interpreted theoretically.[49] It is

interesting to note that the exponents in the two different chains, polyethylene and polyisoprene, show comparable qualitative and quantitative dependence on the type of orientational autocorrelation function considered.

Time-dependent probability distribution functions describing the evolution of rotational and reorientational motions of the bonds indicate that the amplitudes of *rotational* motions are not affected by chain extension but their occurrence is reduced. Thus the location of the second peak in the distribution functions of Figure 3.18 remains unchanged at about $\Delta\phi = 112^{\circ}$ when increasing deformation but its height is reduced. The amplitudes of bond *reorientational* motions on the other hand are significantly diminished upon stretching of the chain as observed from the shift of the maxima in Figure 3.19 to lower values with increasing chain extension. Thus the long time peak shifts from 90° for the unperturbed chain, to less than 60° for the highly strained chain.

3.3 Time-Dependent Probability Distribution Functions for Orientational Motions of Segments in Polymer Chains.

In this part, the adequacy of the joint probability distribution function in terms of spherical harmonics has been tested for chains with fixed ends at various extensions. The sections under this subject are organized as follows:

In Section 3.2.1, the serial expression for the time-dependent probability distribution function is given. The coefficients of this series are evaluated from simulations for chains of various extensions in Section 3.3.1 and the series are developed up to the second order terms in the spherical harmonics and the analytical expressions are compared with the results from Brownian dynamics simulations in Sections 3.3.2 and 3.3.4. Graphical analysis of the probability distribution functions have been carried out to indicate the suitability of the closed form expressions for an effective description of local orientational dynamics of polymer chains in Section 3.3.3 and concluding remarks has been represented in the final Section 3.3.5 within the content of this part.

3.3.1 Distribution Function for Segmental Orientation

The z-axis of the laboratory-fixed coordinate system is chosen along the direction of the end-to-end vector **r**. The n'th atom is kept fixed along the z-axis.The zeroth atom of a 49 bond chain is located at the origin. The z-axis chosen in this manner forms an axis of cylindrical symmetry about which all configurations of the chain are equally accessible. The orientational dynamics of

a vector **m**, shown in Figure 3.20, is analyzed. **m** is assumed to be rigidly affixed to a point along the chain. The axes shown in the figure are parallel to the respective axes of the laboratory-fixed coordinate system. The state of separation of the two ends of the chain is represented by the parameter λ defined as the ratio of the fixed end-to-end distance **r** to the root mean-square distance of the end-to-end vector of the unperturbed chain. Four different values of extension ratios λ are considered in this study as shown in the third line of Table 3.4.

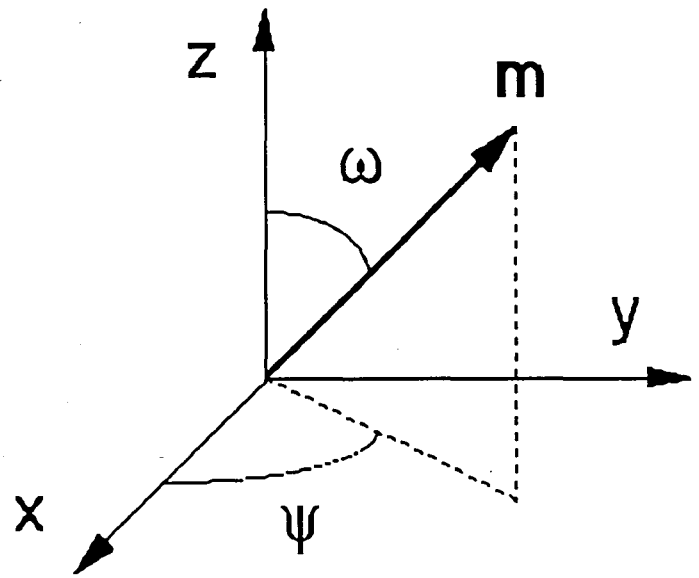

Figure 3.20 Orientation of the vector **m** with respect to the laboratory-fixed frame xyz, defined by the polar angle ω and the azimuthal angle ψ.

The instantaneous orientation of **m** may be described by spherical polar angles $\Omega = (\omega, \psi)$ where ω is the angle between the z-axis and **m**, and ψ is the angle between the x-axis and the projection of **m** on the xy-plane. The joint probability of orientation Ω at time t and Ω_0 at time t_0 for the vector **m** is denoted as $p_r(\Omega, t; \Omega_0, t_0)$ for a chain with end-to-end separation **r**. This probability may be expressed in terms of a double spherical harmonics series as

$$p_r(\Omega, t; \Omega_0, t_0) = \sum_{k=0}^{\infty} \sum_{l=0}^{\infty} \sum_{m=-k}^{k} \sum_{n=-l}^{l} a_{kl}^{mn} Y_k^m(\Omega_0) Y_l^n(\Omega)^* \qquad (3.21)$$

where $Y_k^m(\Omega_0)$ are the spherical harmonics given by[50]

$$Y_k^m(\Omega) = Y_k^m(\omega, \psi) = (-1)\left[\frac{(2k+1)(k-m)!}{4\pi (k+m)!}\right] P_k^m(\cos\omega)\, e^{im\psi} \qquad (3.22)$$

with $P_k^m(\cos\omega)$ expressed in terms of the Legendre polynomial $P_k(\cos\omega)$ of degree k as

$$P_k^m(\cos\omega) = (\sin^2\omega)\,]\frac{d^m}{dx^m} P_k(\cos\omega) \qquad (3.23)$$

$P_k(\cos\omega)$ is equal to $(\cos\omega)$ and $(3/2\cos^2\omega - 1/2)$ for k = 1 and 2, respectively. The details are given Appendix E. The superscript * in eq 3.21 denotes the complex conjugate, and a_{kl}^{mn} is the coefficient obtained as

$$a_{kl}^{mn} = \langle Y_k^m(\Omega_0) Y_l^n(\Omega)^* \rangle_r \qquad (3.24)$$

$$= \int_{\Omega} \int_{\Omega_0} p_r(\Omega, t; \Omega_0, t_0) Y_k^m(\Omega_0) Y_l^n(\Omega)^* \, d\Omega_0 \, d\Omega \qquad (3.25)$$

where, $d\Omega = \sin\omega \, d\omega \, d\psi$ and $d\Omega_0 = \sin\omega_0 \, d\omega_0 \, d\psi_0$ and the variable ω and ψ vary in the ranges $0 \le \omega \le \pi$, $0 \le \psi \le 2\pi$. The angular brackets with the subscript **r** denote the time average over all possible configurations of the chain with fixed **r**.

We define the probability function $p_r(\Omega, t; \Omega_0, t_0)$ in eq 3.21 as the probability obtained for a single chain with fixed **r** along the z-axis. In adopting

this definition, we pay attention to directivity along the chain by assuming that the two ends of the chain are distinguishable. We make this choice in the interest of interpreting our computer simulation results obtained for the single chain. This choice of averaging does not obtain, for example, in spectroscopic experiments where the two ends of chains are not distinguishable and odd powers of cos ω necessarily vanish when t = 0. This point will further be discussed below.

The following relations exist between the coefficients of eq 3.21 from cylindrical symmetry:

$$a_{kl}^{mn} = a_{kl}^{-m-n} = a_{kl}^{m}\delta_{mn} \tag{3.26}$$

where δ_{mn} is the Kronecker delta. With these definitions, eq 3.21 may be written up to the second order terms in the spherical harmonics as

$$p_r(\Omega, t; \Omega_0, t_0) = \frac{1}{16\pi^2}\left[1 + \sum_{i=1}^{9} < f_i >_r f_i\right] \tag{3.27}$$

where the nine functions f_i are given as

$$f_1 = (3/2)^{1/2} \ (\cos\omega + \cos\omega_0)$$

$$f_2 = \frac{1}{2} \ (5/2)^{1/2} \ [(3\cos^2\omega_0 - 1) + (3\cos^2\omega - 1)]$$

$$f_3 = \frac{1}{4} \ (30)^{1/2} \ [\cos\omega_0 (3\cos^2\omega - 1) + \cos\omega (3\cos^2\omega_0 - 1)]$$

$$f_4 = 3\cos\omega_0 \cos\omega$$

$$f_5 = \frac{5}{4} (3 \cos^2 \omega_0 - 1) (3 \cos^2 \omega - 1) \qquad (3.28)$$

$$f_6 = \frac{3}{2} 2^{1/2} \sin \omega_0 \sin \omega \cos (\psi - \psi_0)$$

$$f_7 = \frac{15}{2} 2^{1/2} \sin \omega_0 \cos \omega_0 \sin \omega \cos \omega \cos (\psi - \psi_0)$$

$$f_8 = \frac{3}{2} (5)^{1/2} [\sin \omega_0 \cos \omega_0 \sin \omega + \sin \omega \cos \omega \sin \omega_0] \cos (\psi - \psi_0)$$

$$f_9 = \frac{45}{24} 2^{1/2} \sin^2 \omega_0 \sin^2 \omega \cos 2 (\psi - \psi_0)$$

The averages appearing in eq 3.27 are defined as

$$< f_i >_r = \int_{\Omega} \int_{\Omega_0} f_i \, p_r (\Omega, t; \Omega_0, t_0) \, d\Omega_0 \, d\Omega \qquad (3.29)$$

For an ensemble of chains with indistinguishable ends for which the z-axis may equally be directed from the n'th atom to the zero'th atom, the averages $< f_i >_r$ containing odd powers of cos ω_0 should reduce to zero, thus leaving the four averages $< f_2 >_r$, , $< f_5 >_r$, $< f_6 >_r$ and $< f_9 >_r$.

Evaluation of the nine functions $< f_i >_r$ completely describes the probability distribution function up to the second order terms in the spherical harmonics.

3.3.2 Evaluation of $< f_i >_r$ from Brownian Dynamics Simulation Data

In this section, the averages $< f_i >_r$ are evaluated from trajectories of the vector **m** over sufficiently long time ranges by using the Brownian dynamics simulations of the preceding work, Section 3.1, for a polyethylene chain at four different degrees of extension, λ. The vector **m** is chosen in the present study as a unit vector along backbone carbon-carbon bond. All calculations throughout the paper are based on the average behavior of the central 20 bond vectors of the chain. The total duration of the four simulations are shown in the second line of Table 3.3. Time steps of 5 femtoseconds were used in simulations. The averages are calculated for the four runs by using eq 3.22. The first two averages, $< f_1 >_r$ and $< f_2 >_r$ are independent of time inasmuch as they depend only on the instantaneous values of ω and the simulations are performed at steady state conditions. Their dependence on the degree of extension are shown in Figure 3.21. The filled circles in the figure represent the $< f_1 >_r$ values obtained from simulations. The empty circles are for $< f_2 >_r$. The solid line is obtained for $< f_2 >_r$ from a previous Monte Carlo study, Section 2.2, of orientation in deformed polyethylene chains. The points and the curves indicate the good agreement between Brownian dynamics simulations and the Monte Carlo calculations. Small differences between the results of the two methods may be attributed to the fact that the bond orientational potentials were taken to be pairwise dependent in the Monte Carlo calculations while they are assumed to be independent in the present Brownian dynamics simulations. The curve as well as the empty circles in the figure exhibit the dominant $\lambda^2 - 1/\lambda$ behavior of the orientation function.

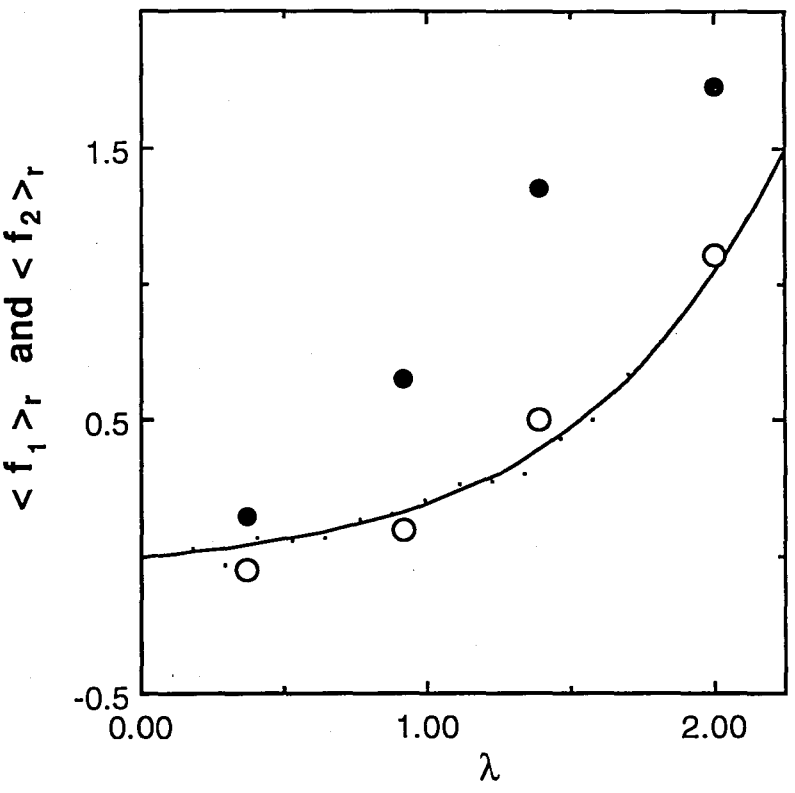

Figure 3.21 Dependence of the coefficients $\langle f_1 \rangle_r$ and $\langle f_2 \rangle_r$ defined in eqs 3.28 and 3.29, on the extension ratio λ. The filled and empty circles are computed for $\langle f_1 \rangle_r$ and $\langle f_2 \rangle_r$, respectively from Brownian dynamics simulations of 49-bond chains. The curve was obtained[6] for $\langle f_2 \rangle_r$ in a recent Monte Carlo study of orientation in deformed PE chains.

The decay of the functions $< f_3 >_r$ and $< f_4 >_r$ with time are presented in Figures 3.22-a and 3.22-b, respectively, for the four different degrees of extension. In Figure 3.22-a, the curves display different relaxational behavior at different degrees of extension. Strongest time dependence is observed for the intermediate extension of $\lambda = 1.38$. The highly compressed chain exhibits only a small amount of decay. The dependence of $< f_4 >_r$ on strain presented in Figure 3.22-b exhibits on the other hand, a systematic pattern such that the highly stretched chain rapidly decays to its asymptotic value while both the magnitude and the rate of decay for the highly compressed chain are significant. The behavior of $< f_5 >_r$ and $< f_6 >_r$ are shown in Figures 3.23-a and 3.23-b, respectively. Both functions depend strongly on time and extension. For a given λ, $< f_5 >_r$ asymptotically converges to the square of the corresponding $< f_2 >_r$ as dictated by the expressions given in eq 3.28. The decay curves for the functions, $< f_7 >_r$ and $< f_8 >_r$ are displayed in Figures 3.24-a and b. The values of $< f_8 >_r$ for $\lambda = 1.38$ and 2.00 are very close to each other which is representative of a saturation effect at higher levels of stretching. Large reduction in the values of $< f_8 >_r$ upon compression to $\lambda = 0.37$ should also be noted. Finally, the decay curves for $< f_9 >_r$ are given in Figure 3.25. The strain dependence of these curves exhibits the same trend as that of $< f_8 >_r$.

3.3.3 Graphical Presentation of the Distribution Functions

In order to illustrate some features of the distribution functions, the surfaces generated from eq 3.27 for $p_r(\Omega, t; \Omega_0, t_0)$ are plotted in Figures 3.26 and 3.27 for vectors with specific initial orientation Ω_0 in chains of different extensions. The reorientational behavior of two major class of vectors, namely those parallel and perpendicular to the direction of stretch are investigated in Figures 3.26 and

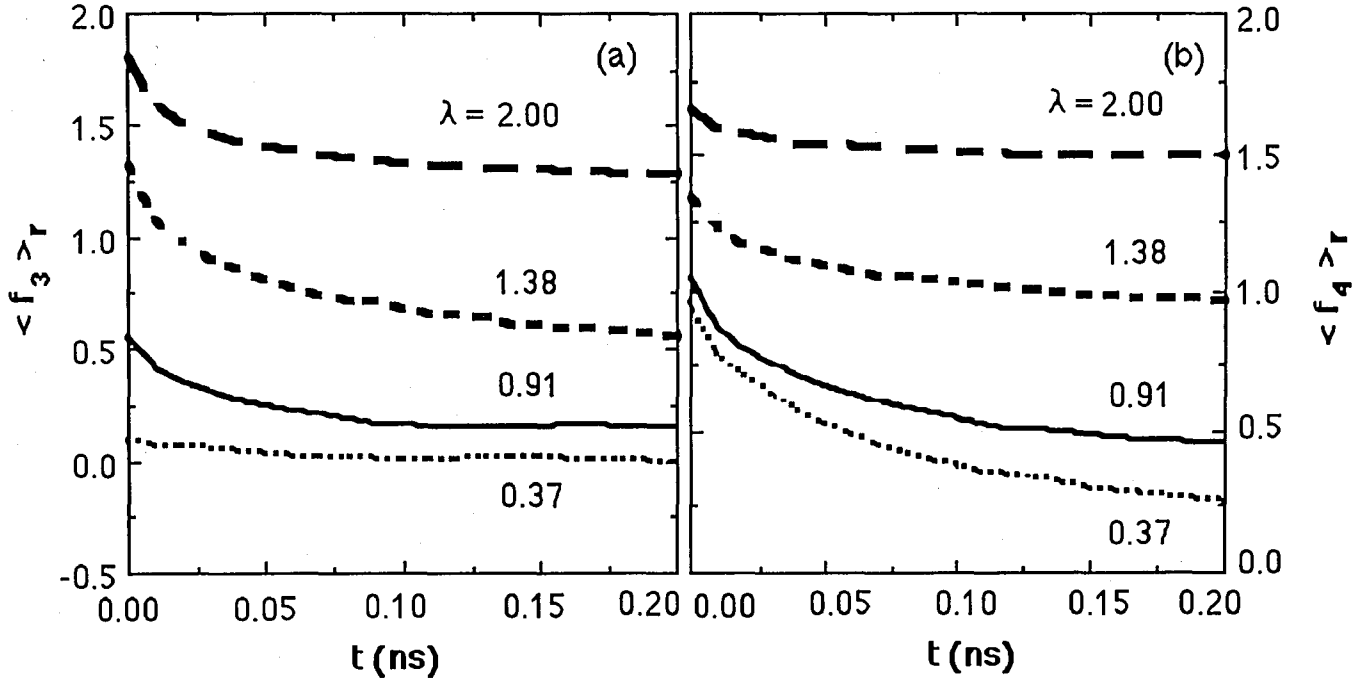

Figure 3.22(a-b) Time decay of the coefficients $< f_3 >_r$ (left) and $< f_4 >_r$ (right) defined in eqs 3.28 and 3.29, obtained from BD trajectories of deformed 49-bond chains with the indicateed degrees of extension, at 400K.

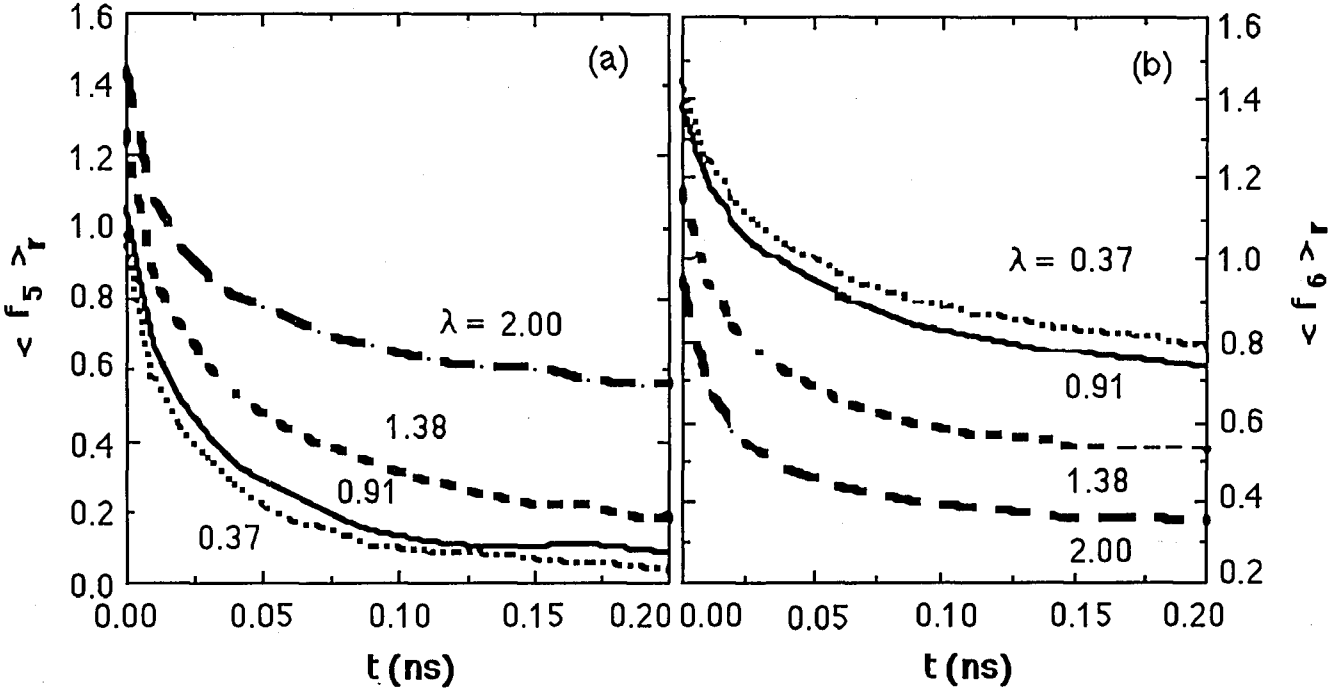

Figure 3.23(a-b) Time decay of the coefficients $< f_5 >_r$ (left) and $< f_6 >_r$ (right). See legend to Figure 3.22.

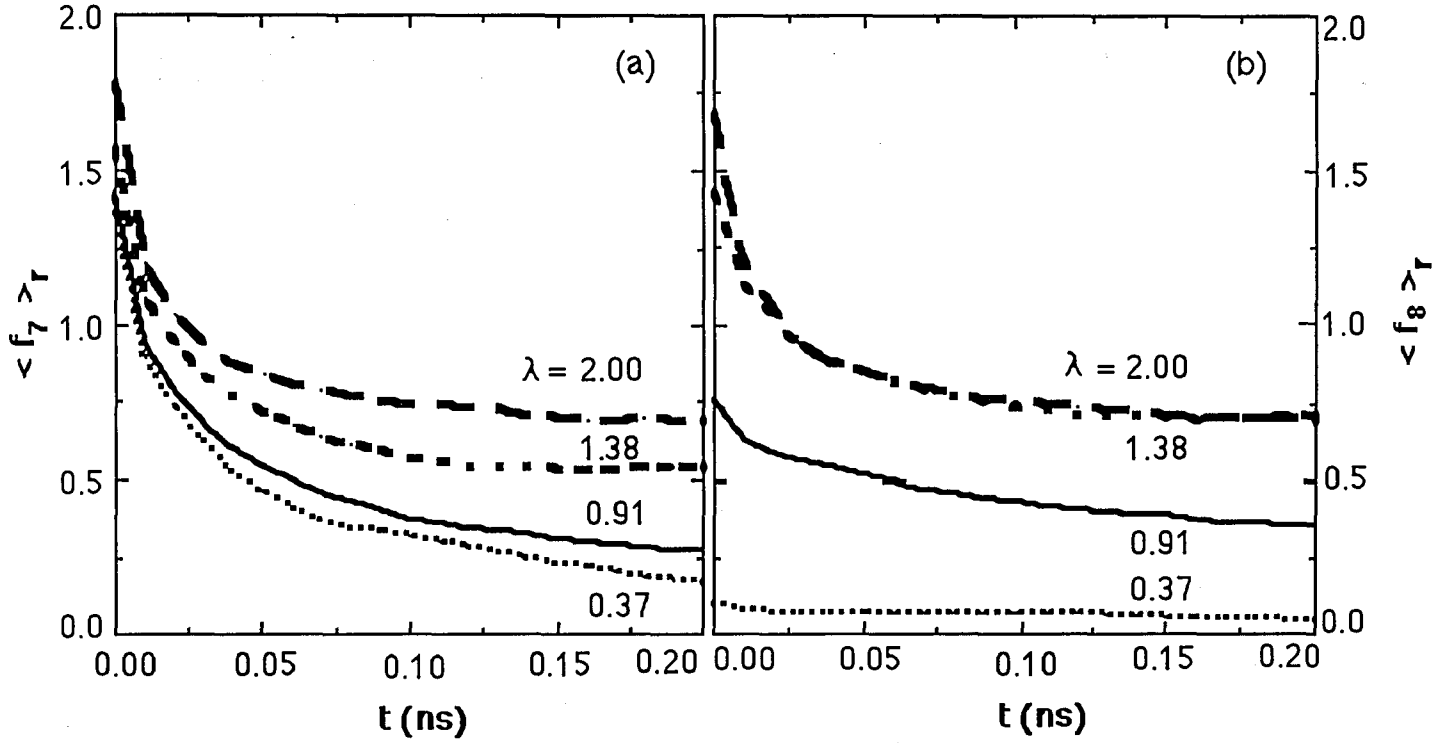

Figure 3.24(a-b) Time decay of the coefficients $< f_7 >_r$ (left) and $< f_8 >_r$ (right). See legend to Figure 3.22.

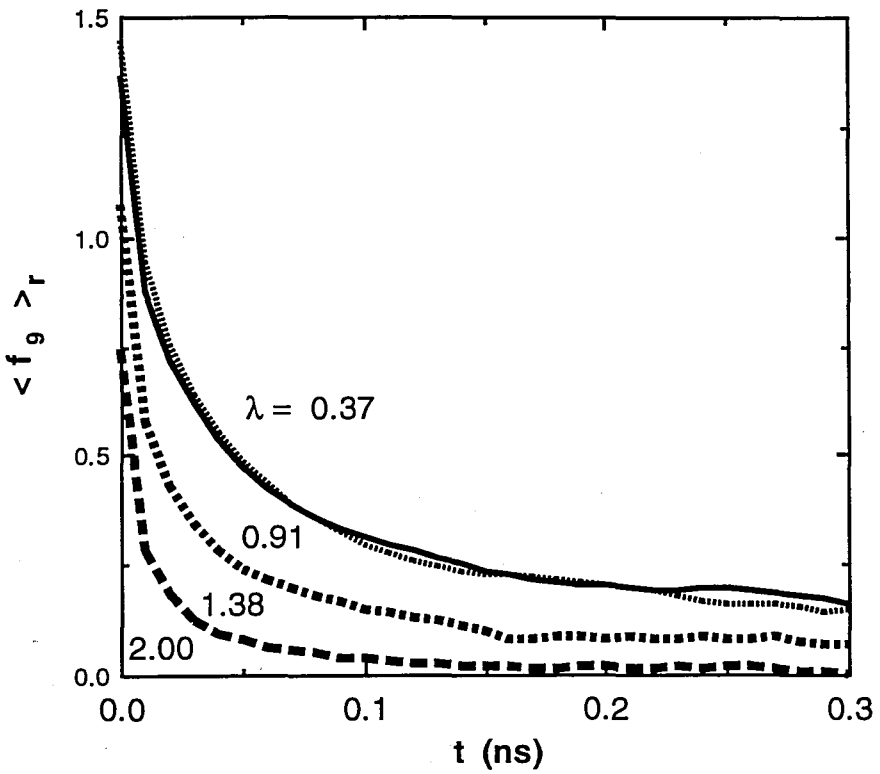

Figure 3.25 Time decay of the coefficient $\langle f_9 \rangle_r$. See legend to Figure 3.22.

3.27, respectively. Inasmuch as the conformational transitions in chains with fixed end-to-end separation conform with a stationary process, the elapsed time $t - t_0$ rather than the two absolute times t_0 and t, is of importance. The value $t - t_0 = 0.5$ ns is considered in most of the calculations. This time is of the order of the relaxation time for the reorientational motions of **m**. For economy of space, results for the two extreme cases of deformation, $\lambda = 0.37$ and $\lambda = 2.00$, are displayed in parts (a) and (b) of the figures.

In Figures 3.26(a) and (b) , the normalized probability surfaces for those vectors which were originally parallel to the z-axis, i. e., $\omega_0 = 0°$ are shown for the two extension ratios (a) $\lambda = 0.37$ and (b) $\lambda = 2.00$, at $t - t_0 = 0.5$ ns. The surface remains constant along the ψ axis, indicating that a vector originally along the z-axis may result in any direction around the end-to-end vector, with equal probability. This is a natural consequence of the cylindrical symmetry about the z-axis. The dependence on ω on the other hand may be observed from a given cross-section of constant ψ. The stronger tendency of alignment along the stretch direction in the highly extended chain is clearly observable. The time evolution of a given probability surface may be seen from the comparison of Figures 3.26(a) and 3.26(c), on the other hand, which are obtained for the respective time intervals $t - t_0 = 0.5$ and 1.5 ns, for the compressed chain. With increasing time, the distribution of ω approaches the equilibrium distribution of orientations with respect to the z-axis which will be reconsidered below.

In Figures 3.27(a) and (b) , the probability surfaces calculated from eq 3.27 are shown for bond vectors which were originally perpendicular to the z-axis and parallel to the x-axis, i. e., $\omega_0 = 90°$ and $\psi_0 = 0°$. The extension ratios $\lambda = 0.37$ and 2.00 are considered in parts (a) and (b), respectively, with the same time interval of 0.5 ns. The general sloping down of the surface as ψ increases from

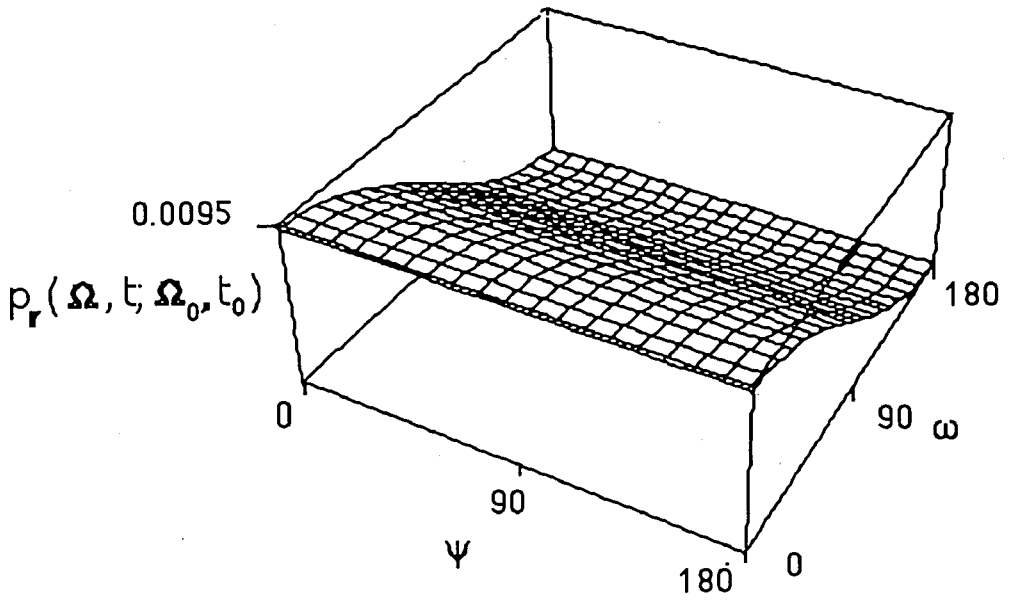

Figure 3.26(a) Time-dependent orientational probability distribution function $p_r(\Omega, t; \Omega_0, t_0)$ as a function of $\Omega = (\omega, \psi)$ calculated from eq 3.27 for bond vectors originally along the z-axis ($\omega_0 = 0^o$) in the chain subject to the extension ratio $\lambda = 0.37$, at $t - t_0 = 0.5$ ns.

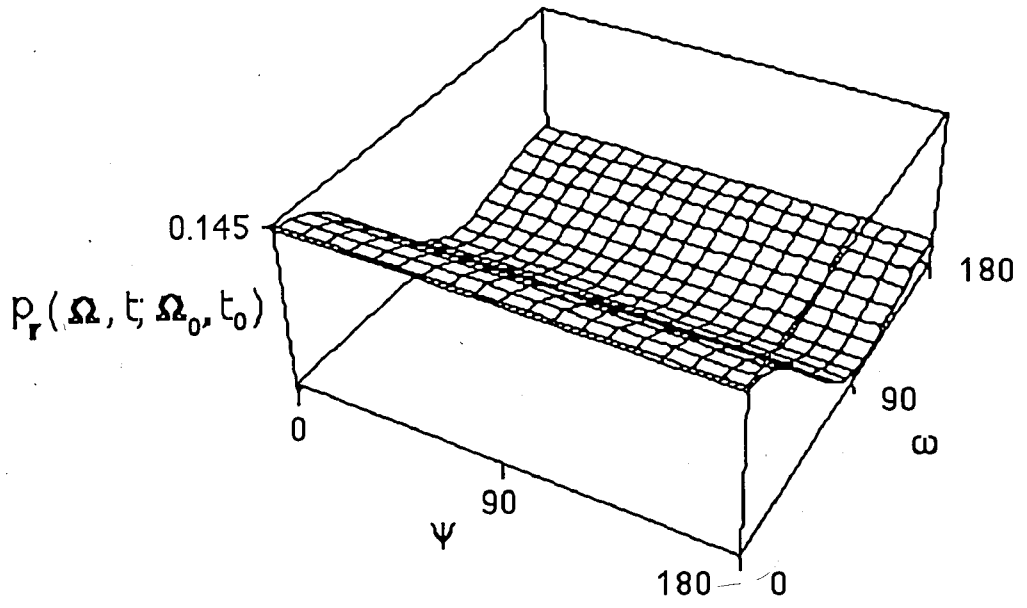

Figure 3.26(b) Probability surface $p_r(\Omega, t; \Omega_0, t_0)$ for $\omega_0 = 0^o$, $t - t_0 = 0.5$ ns and $\lambda = 2.00$.

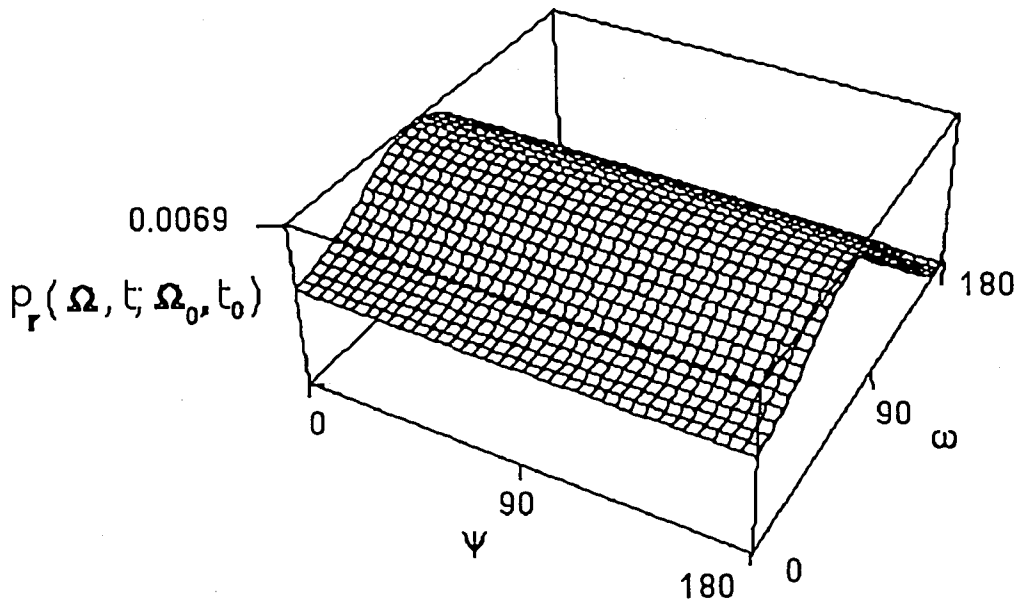

Figure 3.26(c) Probability surface $p_r(\Omega, t; \Omega_0, t_0)$ for $\omega_0 = 0^o$, $t - t_0 = 1.5$ ns and $\lambda = 0.37$.

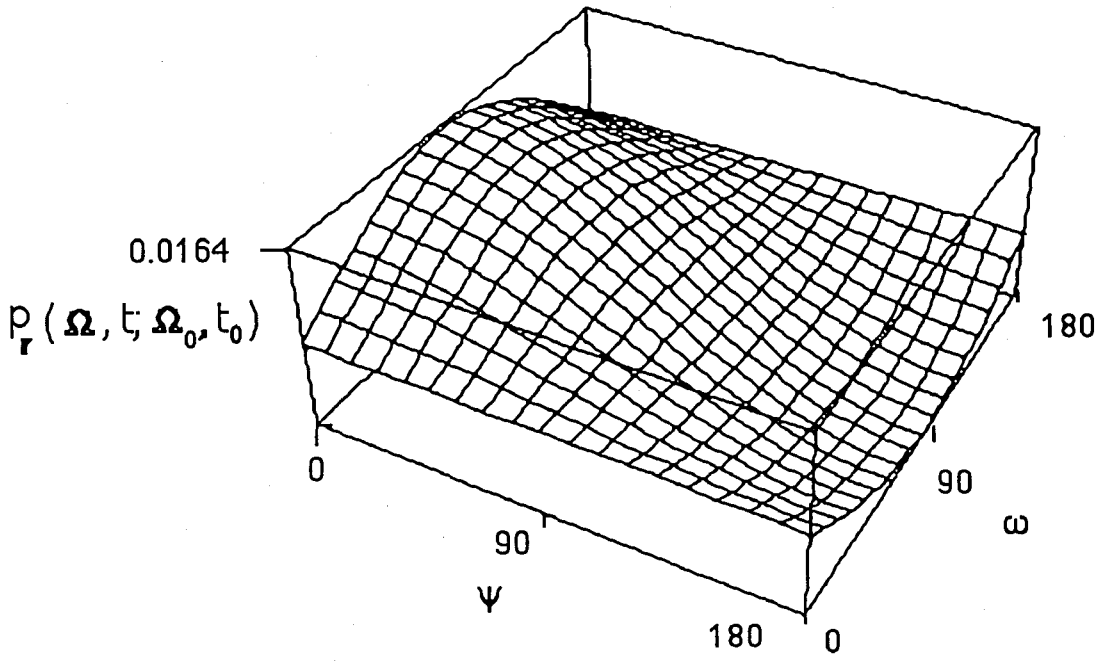

Figure 3.27(a) Probability surface $p_r(\Omega, t; \Omega_0, t_0)$ as a function of $\Omega = (\omega, \psi)$ calculated for bond vectors originally perpendicular to the z-axis in the compressed chain. $\Omega_0 = (\omega_0, \psi_0) = (90^0, 0^0)$, $\lambda = 0.37$, and $t - t_0 = 0.5$ ns.

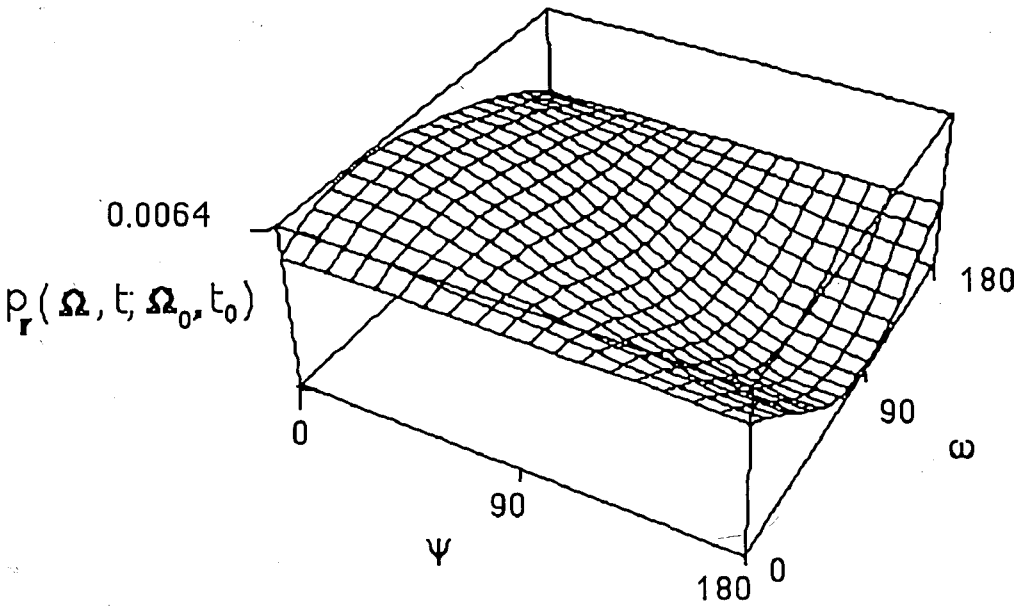

Figure 3.27(b) Probability surface $p_r(\Omega, t; \Omega_0, t_0)$ for $(\omega_0, \psi_0) = (90^0, 0^0)$, $t - t_0 = 0.5$ ns and $\lambda = 2.00$.

0° to 180° indicates that the vectors **m** did not have sufficient time to spread out in the xy-plane during the time interval of 0.5 ns. The higher ordinate value observed in part (b) is again indicative of the enhanced tendency of the vectors perpendicular to the stretch direction in the highly extended chain, to escape their original orientation and to align along the preferred directions $\omega = 0°$ and 180°. It is noted that the sense 0° is preferred rather than 180°. This is due to the fact that the two senses $\pm\mathbf{r}$ of the end-to-end vector are *distinguishable* for the presently investigated bond vectors. Bond vectors exhibit a higher tendency to be oriented along $+\mathbf{r}$ sense, unless the chain is infinitely long.

In Figures 3.28(a)-(c), the dependence of the probability surface on the polar angles ω_0 and ω of **m**, irrespective of the azimuthal angles ψ_0 and ψ, are shown. The resulting surfaces represent the probability $p_r(\omega, t; \omega_0, t_0)$ of the time-delayed joint event $(\omega, t; \omega_0, t_0)$. Summation over the azimuthal angles corresponds to integration of eq 3.27 with respect to these two variables. Performing the integrations leads to the joint probability, $p_r(\omega, t; \omega_0, t_0)$ of the polar angles of **m** as

$$p_r(\omega, t; \omega_0, t_0) = \frac{1}{4}\left[1 + \sum_{i=1}^{5} < f_i >_r \, f_i\right] \qquad (3.30)$$

The surface are obtained by summing all occurrences of **m** over the full range of azimuthal angles, $0° \le \psi_0 \le 360°$ and $0° \le \psi \le 360°$, for $t - t_0 = 0.5$ ns in parts (a) and (b), and for $t - t_0 = 1.5$ ns in part (c). Comparison of Figures 3.28(a) and (b) obtained for $\lambda = 0.37$ and 2.00 respectively, reveals the pronounced effect of chain extension on the time-delayed joint probability of polar angles. The relatively diffuse distribution of polar angles in the compressed chain is strongly sharpened and biased towards low values of (ω, ω_0) with increasing extension,

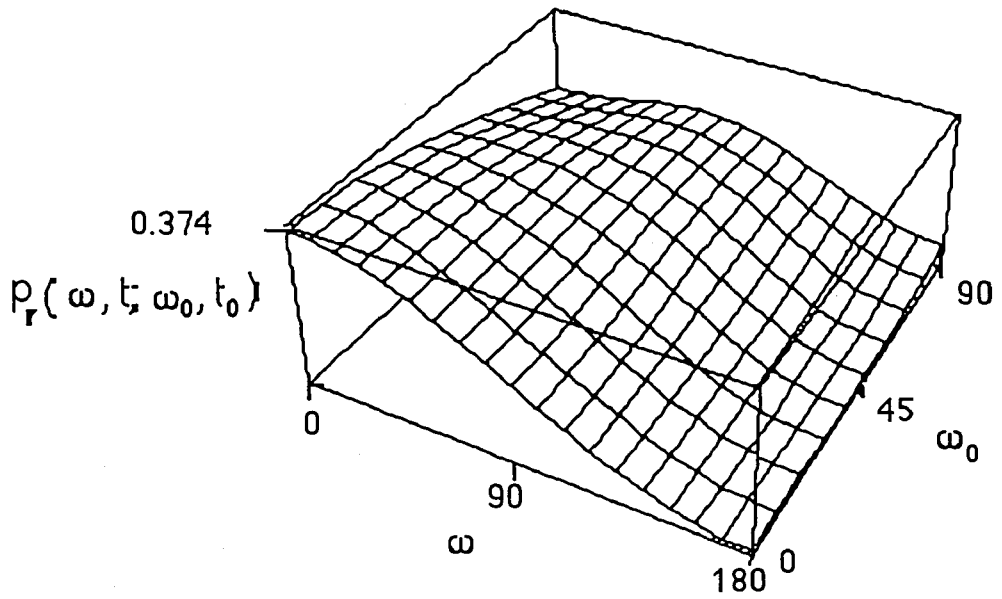

Figure 3.28(a) Dependence of the probability distribution function $p_r(\omega, t; \omega_0, t_0)$ given by eq 3.29 on the polar angles ω_0 and ω, for bond vectors in the highly compressed chain with $\lambda = 0.37$ at the time interval $t - t_0 = 0.5$ ns.

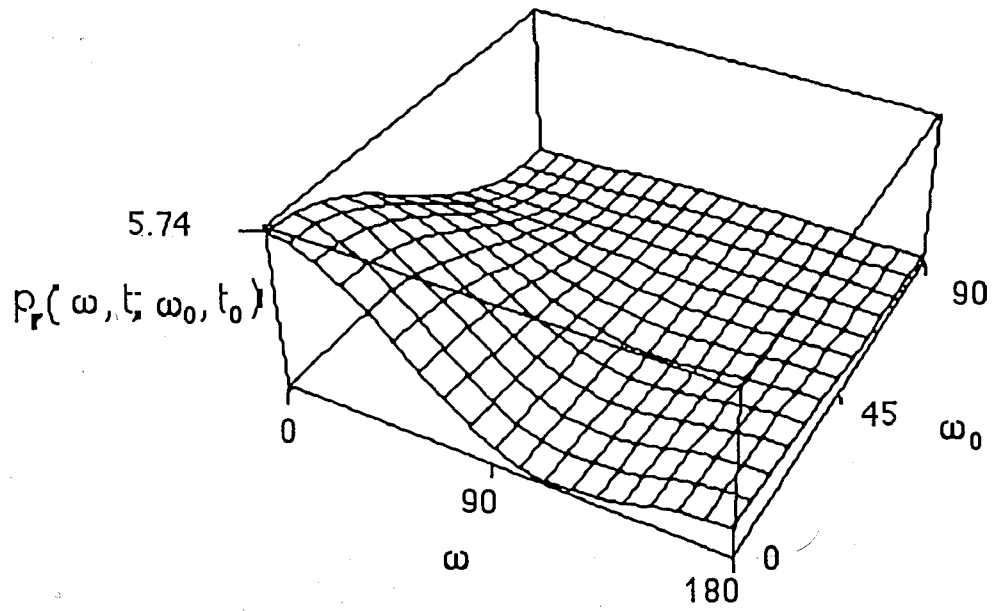

Figure 3.28(b) Probability surface $p_r(\omega, t; \omega_0, t_0)$ for $t - t_0 = 0.5$ ns and $\lambda = 2.00$.

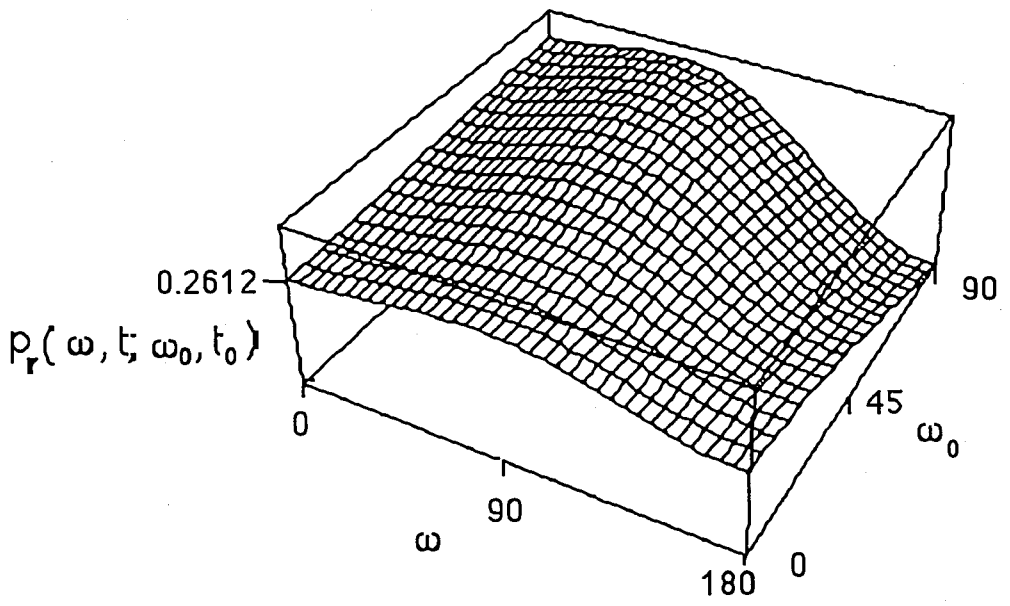

Figure 3.28(c) Probability surface $p_r(\omega, t; \omega_0, t_0)$ for $t - t_0 = 1.5$ ns and $\lambda = 0.37$.

as expected. Comparison of Figures 3.28(a) and (c) on the other hand, displays the time evolution of the same probability surface obtained for $\lambda = 0.37$. The probability distribution obtained at long times in Figure 3.28(c) indicates that the equilibrium state $(\omega,\omega_o) = (90, 90)$ corresponding to transverse orientations of bond vectors with respect to the z-axis is relatively favored in the case of compressed chains. One may better visualizes the distributions by considering the intersections of the surface by planes perpendicular to the ω_0 axis. The curves obtained in this manner show the probability of occurrence of the final orientation ω for a vector **m** which was initially at ω_0. Thus, the plane at $\omega_0 = 0°$ in Figure 3.28(c) shows that bonds which were originally along the direction of the end-to-end vector **r** will acquire a broad distribution of orientations after 1.5 ns. Similarly, the plane at $\omega_0 = 90°$ shows that bonds which were originally perpendicular to **r** will orient more along the direction of **r** and much less in the direction of **-r**, in agreement with the implications of Figure 3.27(b) discussed above.

3.3.4 Comparison between Numerical and Analytical Results

The curves shown in Figure 3.29 are obtained from eq 3.30 for the four values of λ and the time interval $t - t_0 = 0.5$ ns. The ordinate values represent the conditional probabilities $q_r(\omega, t; \omega_0, t_0)$ which are defined as

$$q_r(\omega, t / \omega_0, t_0) \equiv \frac{p_r(\omega, t; \omega_0, t_0) \sin\omega}{\int_0^{\pi} p_r(\omega, t; \omega_0, t_0) \sin\omega \, d\omega} = \frac{p_r(\omega, t; \omega_0, t_0) \sin\omega}{p_r(\omega_0, t_0)} \qquad (3.31)$$

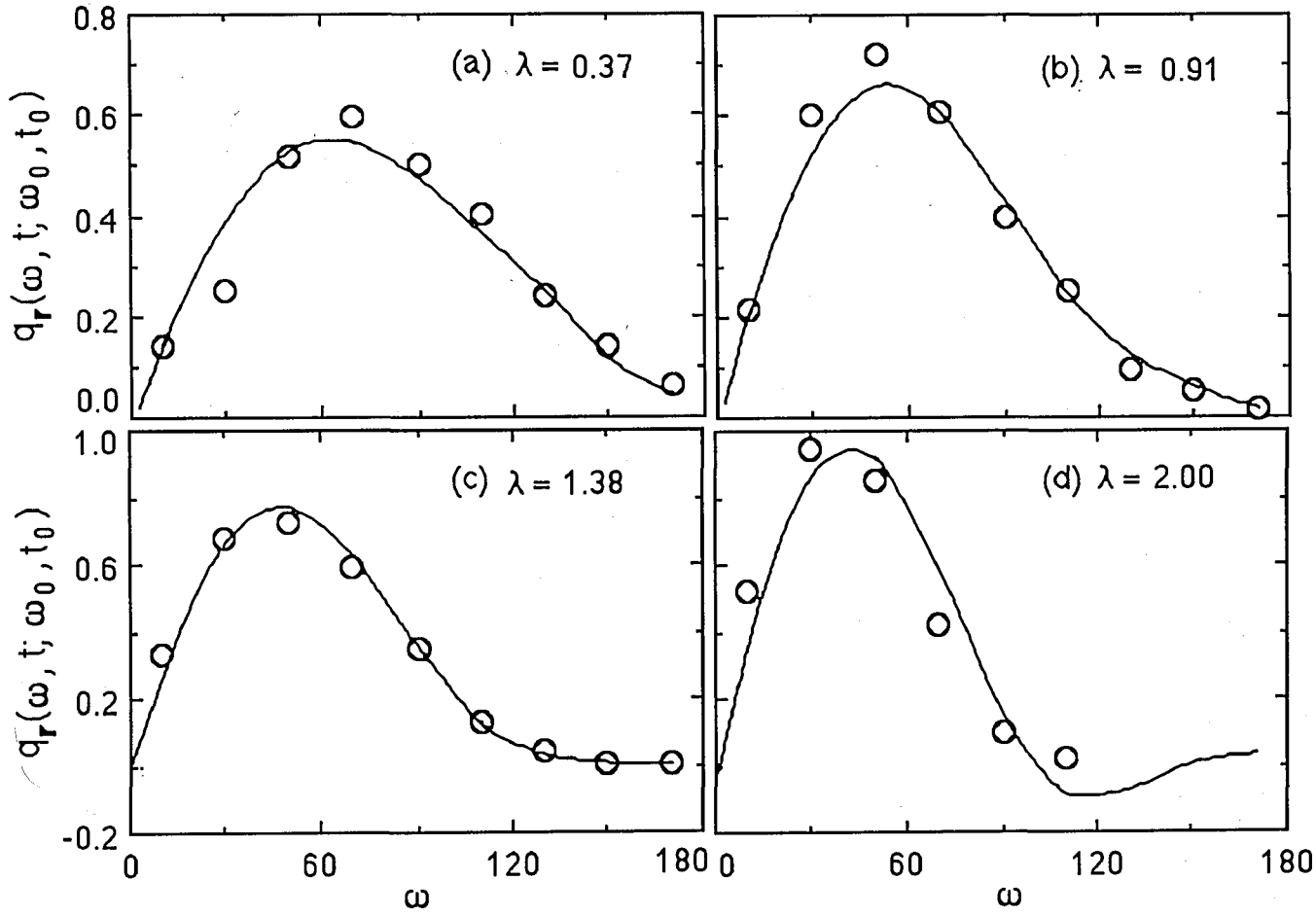

Figure 3.29 Time-dependent conditional probability $q_r(\omega, t; \omega_0, t_0)$ of occurance of the polar angle ω at the end of $t-t_0 = 0.5$ ns for bond vectors originally along $\mathbf{r}$, in chains with different degrees of extension. The emty circles are the results from BD trajectories and the curves are calculated using eq 3.30 and 3.31.

$q_r(\omega, t; \omega_0, t_0)$ gives the probability of occurrence of the orientation ω at time t, given that the studied vector makes initially an angle ω_0 with the direction of extension. Thus, the surface represents the time-delayed normalized distribution of polar angles for those bonds which were originally along **r**. The points are the results from Brownian dynamics simulations, obtained from direct counting of the joint event $(\omega_0 \pm \Delta\omega_0, t_0 ; \omega \pm \Delta\omega, t)$, with $t - t_0 = 0.5$ ns and $\omega_0 = 0°$. In order to have a sufficiently large population, the intervals in the counting process were taken as $\Delta\omega_0 = \Delta\omega = 10°$. The agreement between the simulation results and the analytical expression is remarkable although the latter is truncated after the second order terms. Negative values of the probability in part (d) indicate that the second order approximation becomes insufficient as the degree of stretching becomes large. As expected, the curves become more sharply peaked and their maxima shift to smaller values of ω upon stretching. However the shift is relatively small and moves from about 60° for $\lambda = 0.37$ to 40° for $\lambda = 2.00$.

Further integration of eq 3.30 over the polar angle ω_0 after multiplying by sin ω_0 results in the equilibrium probability distribution $p_r(\omega)$ of the polar directions as

$$p_r(\omega) = \frac{1}{2}[\,1 + 3 \langle \cos\omega \rangle \cos\omega + \frac{5}{4}(3\langle \cos^2\omega \rangle - 1)(3\cos^2\omega - 1)\,] \qquad (3.32)$$

This quantity represents the equilibrium distribution of bond orientations with respect to the end-to-end vector **r**, inasmuch as **r** coincides with the z-axis. Predictions of eq 3.32 are compared in Figure 3.30 with results of Brownian dynamics simulations for the four different degrees of stretching. The good agreement between the numerical and analytical results confirms once again the

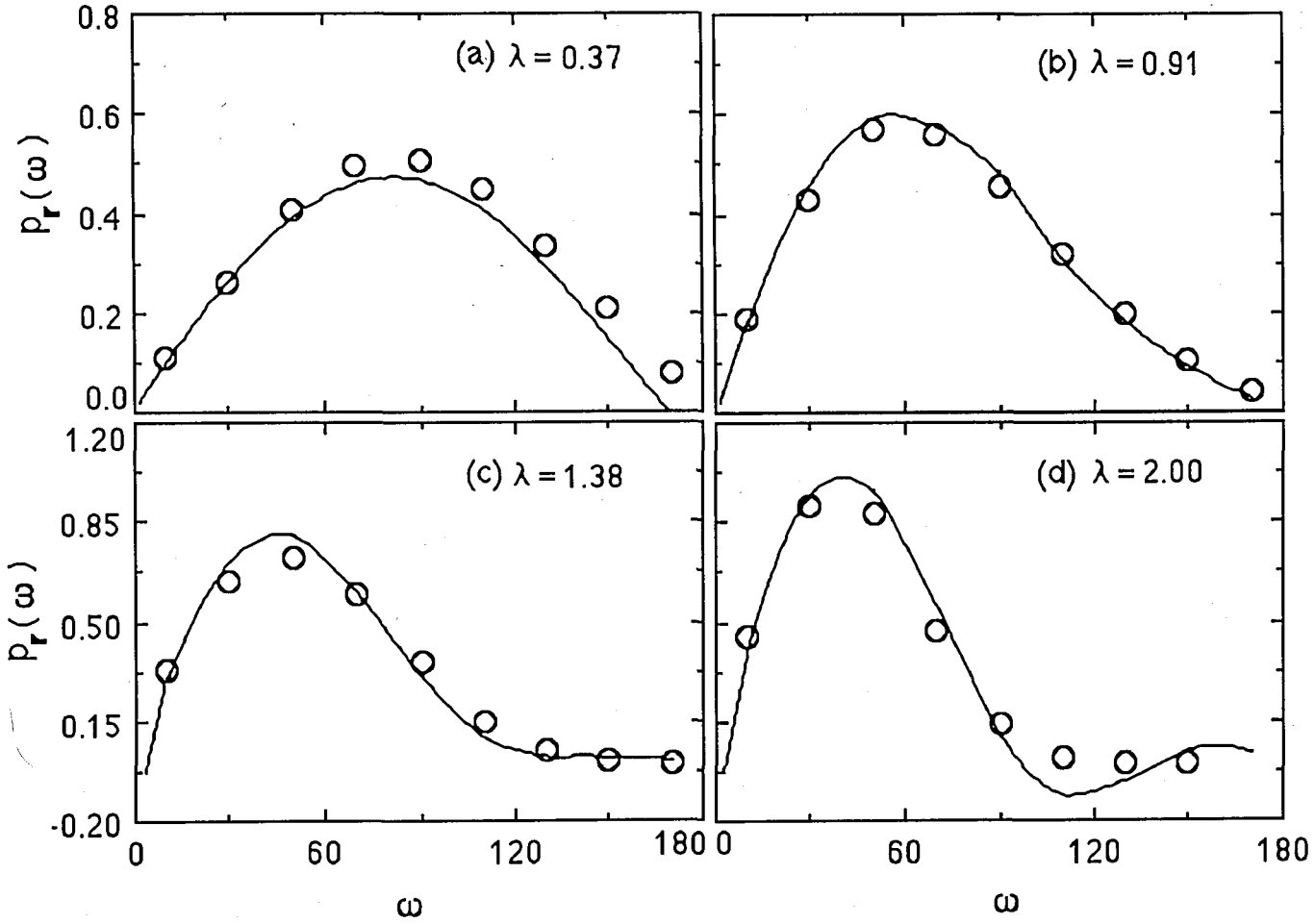

Figure 3.30 Normalized equilibrium probability distribution function $p_r(\omega)$ of the polar angle in chains with different degrees of extension. The empty circles are the results frm BD trajectories and the curves are calculatedfrom eq 3.32.

suitability of the second-order expansion of time-dependent distribution functions in terms of spherical harmonics for an effective description of local orientational behavior of the chain.

3.3.5 Concluding Remarks

Series expansions has been widely used in chain statistics for representing the probability distribution functions associated with the equilibrium conformational properties of polymer chains. A common example is the Hermite polynomials series employed for the distribution of the end-to-end separation vector **r**. Monte Carlo chain generation technique is conveniently used to determine the moments which appear in the coefficients of these series expansions. In analogy to this common procedure of equilibrium statistics, a series expansion is proposed in the present work for the time-dependent joint probability distribution of spatial orientations of vectorial quantities rigidly embedded in polymer chains. Brownian dynamics simulation method is used in this case instead of Monte Carlo technique, for the estimation of the time-dependent averages appearing in the coefficients of a spherical harmonics series. Comparison of the predictions of the series with the results from Brownian dynamics simulations confirms that the truncated series expansion may be safely employed for a quantitative analysis of local orientational dynamics in deformed chains. Brownian dynamics simulation rests on the assumption of a Markoff process. The present calculations show that this Markoff process may accurately be described by a second order series in spherical harmonics.

Present calculations were performed for deformed chains of 49 bonds. The analysis demonstrates that truncation of the series after the second order

spherical harmonics is suitable for an accurate description of the local orientational dynamics in those chains. For longer chains subject to weak deformation, the chain segments enjoy a higher degree of flexibility and on a local scale the orientation behavior of bond vectors approaches an unbiased distribution. As a result, the coefficients with odd-powered averages in the series will be vanishingly small and only the contributions from the remaining terms will survive, leading to much simpler expressions.

The description of local orientational dynamics by a closed form expression for time-delayed joint probability function allows for the prediction of the dynamic behavior of specific vectors observed in various experimental techniques. Examples are C-H bond vectors in NMR relaxation, transition moment vectors in fluorescence polarization, dipole moments in dielectric relaxation, etc. For the application of the presently developed probability distribution formalism to those specific vectorial quantities, it is sufficient to know the spatial orientation of those vectors with respect to the chain vector. Thus, the use of analytical expressions for time-dependent orientational distribution functions may avoid repetitive simulations and may be particularly useful as a substitute for extensive computational analysis.

Inasmuch as the coefficients in the series are evaluated in a semi-empirical way, based on BD trajectories, it should be noted that the expressions for the time-dependent distribution functions suffer from the same limitations as those inherently present in the simulation techniques. Absence of intramolecular effects such as bond rotational interdependence and volume exclusion, and neglect of intermolecular contributions such as specific solvent effects and hydrodynamics interactions are the main assumptions present in the BD simulations which are readily reflected upon the distribution functions.

3.4 Orientational Mobility in Uniaxially Deformed Networks

3.4.1 Introduction of an Internal Coordinate System for the Orientation of vectors.

Orientational motions of segments in polymers depend sensitively on both intra- and intermolecular configurational characteristics of the chains, and thus are of special interest for the understanding of polymer behavior. In a previous sections, results of Brownian dynamics (BD) simulations were used to study the orientational dynamics of deformed polyethylene model chains as a function of their end-to-end separation. On the basis of the cylindrical symmetry of polymers about the direction of extension, time-dependent joint probability functions expanded in terms of double spherical harmonics were developed. The anisotropy of segmental dynamics in terms of spherical harmonics was originally investigated by Tao[24] and Jarry and Monnerie[25] some years ago. These authors formulated the time-dependent orientational distribution for vectors affixed to chains in a form suitable for studying local chain dynamics by polarized fluorescence experiments. Recent developments in deuterium NMR spectroscopy[51] have refocussed the interest on the problem of the anisotropy of local static and dynamic orientational correlations.

The initial orientation of a vector **m** rigidly affixed to the chain is described by the set $\Omega_0 = \{\omega_0, \psi_0\}$, with respect to the laboratory fixed frame Oxyz, as shown in Figure 3.31-a. At time t, the orientation of **m** is given by $\Omega = \{\omega, \psi\}$. For spectroscopic reasons, the orientation of **m** at time t relative to its previous

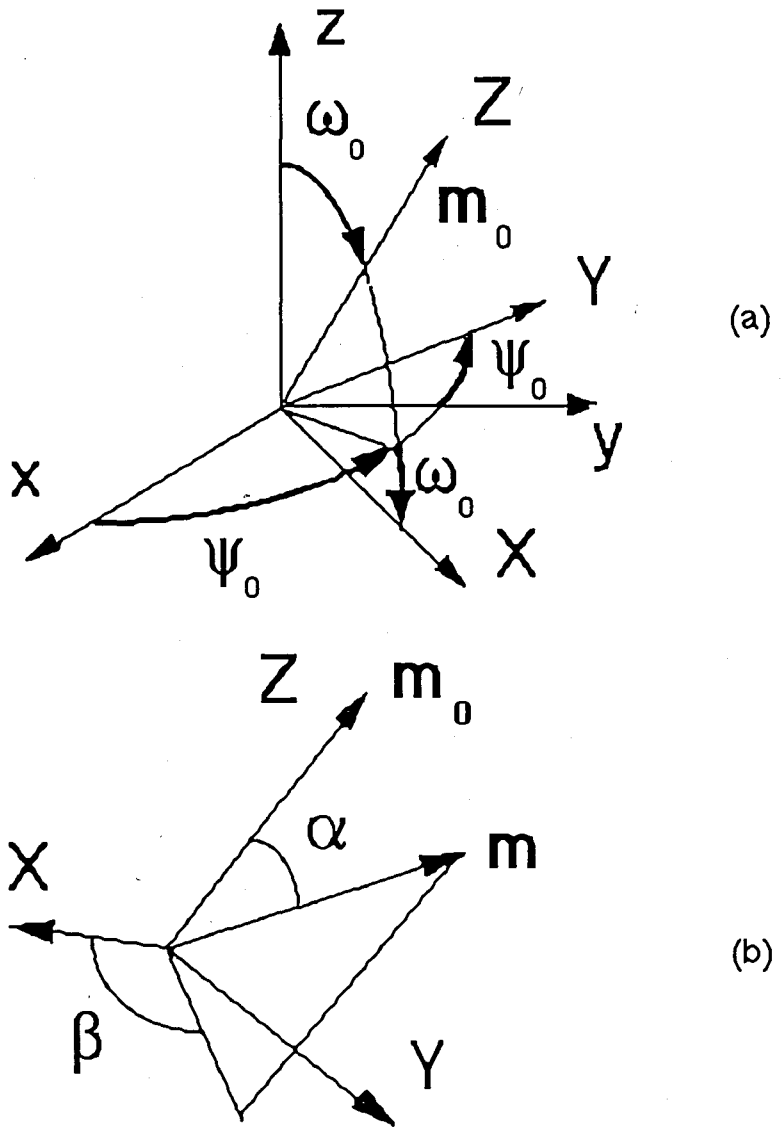

Figure 3.31 Coordinate systems defining the orientation of $\mathbf{m}_0$. Oxyz is the laboratory-fixed frame with the z-axis along the direction of uniaxial deformation. The frame OXYZ defines the internal reorientation of **m**, in terms of the polar and azimuthal angles α and β, respectively, as shown in part (b). The Z-axis is directed along $\mathbf{m}_0$ and makes an angle ω_o with the z-axis. The intersection of the XZ-plane with the xy-plane makes an angle of ψ_0 with the x-axis, and the Y-axis always remains in the xy-plane.

orientation may be desirable. This requires the introduction of an internal coordinate system, OXYZ, shown in Figure 3.31-a. Following the definition of Jarry and Monnerie[25] the Z-axis is chosen to coincide with the initial direction of the **m**, thus making an angle ω_0 with the z-axis.The intersection of the XZ-plane with the xy-plane makes an angle of ψ_0 with the x-axis, and the Y-axis always remains in the xy-plane. The instantaneous orientation of **m** is shown in Figure 3.31-b with the angles α and β denoting the polar and azimuthal angles, respectively, relative to the OXYZ coordinate system.

The spherical harmonics[50] $Y_k^m(\Omega)$ appearing in the time-dependent joint distribution function may be expressed in terms of the internal reorientation variables $\Gamma = \{\alpha, \beta\}$ by the use of Wigner rotation matrices $\overline{D}^k_{m\mu}(\Omega_0)$ as

$$Y_k^m(\Omega) = \sum_{\mu=-k}^{+k} \overline{D}^k_{m\mu}(\Omega_0)\, Y_k^\mu(\Gamma) \qquad (3.33)$$

The details of the Wigner rotation matrices[25] and the spherical hrmonics $Y^m{}_k(\Omega)$ up to the second order, rotated the way $\Omega_0(\omega_0, \psi_0)$ are given in Appendix G. These Wigner matrices are used for the elimination of the set $\Omega = \{\omega, \psi\}$ in favor of $\Gamma = \{\alpha, \beta\}$ and $\Omega_0 = \{\omega_0, \psi_0\}$. Four physically meaningful functions characterizing mobility result from this elimination:

3.4.2 Orientational Mobility Functions

3.4.2.1 The Mean Mobility-Amplitude

$$M(t) = \frac{1}{2} (3 < \cos^2 \alpha > - 1) \qquad (3.34)$$

M(t) is also referred to as the second orientational autocorrelation function of **m**. Time decay of M(t) has been obtained from BD simulations for polyethylene chains with the four different extension ratios, λ = 0.37, 0.91, 1.38, and 2.00 in Section 3.2.1.4 and depicted in Figure 3.11.

3.4.2.2 The Orientation-Mobility Amplitude Correlation

$$C(t) = \frac{1}{4} < (3 \cos^2 \omega_0 - 1) (3 \cos^2 \alpha - 1) > \qquad (3.35)$$

This function reflects the correlations between the original orientation of **m** and its mobility. At long times, the two terms in parenthesis become independent and C(t) may therefore be written as a product of two functions. Thus, the orientation-mobility correlations may be described in terms of the difference R(t)

$$R(t) = C(t) - \frac{1}{4} < (3 \cos^2 \omega_0 - 1) > < (3 \cos^2 \alpha - 1) > \qquad (3.36)$$

If R(t) = 0, the mobility of **m** is uncorrelated with its direction. If directions parallel to **r** have less mobility than the perpendicular directions, then R(t) > 0. Otherwise R(t) is negative. In Figure 3.32, the time dependences of R(t) calculated from BD

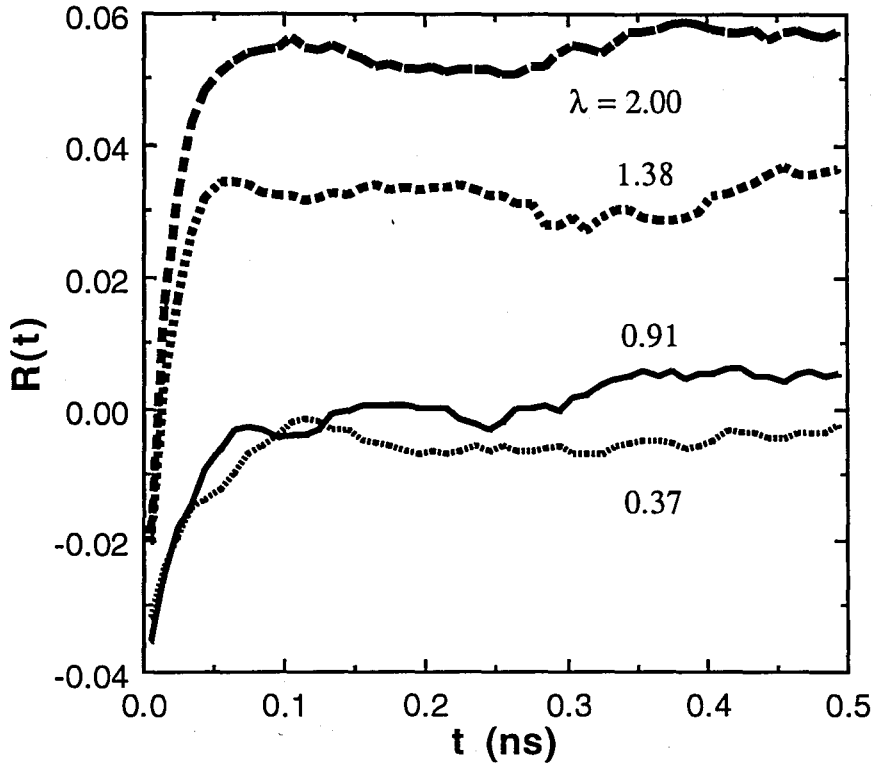

Figure 3.32 Time dependence of R(t), defined by eq 3.35, for chains with the indicated extension ratios. R(t) describes the orientation-mobility amplitude correlations C(t) of bond vectors in deformed chains relative to the case of chains in which the original orientation of bond vectors is independent of their motion amplitude.

simulations are shown for four different extension ratios. For very short times (≤0.01 ns) R(t) is negative and therefore the bonds along directions perpendicular to **r** are relatively more mobile. For the highly compressed chain with $\lambda = 0.37$, R(t) remains negative for all times. For the chain with $\lambda = 0.91$, which is closest to the unperturbed state, R(t) rapidly becomes zero and oscillates about this value. R(t) is positive for all times, for $\lambda = 1.38$ and 2.00.

3.4.2.3 The Directivity of Mobility

$$D(t) = \frac{3}{4} < \sin^2 \omega_0 \sin^2 \alpha_0 \cos 2\beta > \qquad (3.37)$$

This function may best be described following Jarry and Monnerie, in terms of two planes P and P' shown in Figure 3.33-a. D(t) differentiates between motions contained in such planes. The P-plane is defined as the plane that contains $\mathbf{m}_0$ and the laboratory-fixed z-axis. Motions of **m** with $\beta = 0$ or π are confined to this plane. The P'-plane contains $\mathbf{m}_0$ and is perpendicular to the P-plane. Motions of **m** with $\beta = -\pi/2$ or $\pi/2$ are confined to this plane. If the vector moves in the P-plane, $\cos 2\beta = 1$ and D(t) is positive. If it moves in the P'-plane, $\cos 2\beta = -1$ and D(t) is negative.

Results of calculations for D(t) based on BD simulations are presented in Figure 3.34. For the chain with $\lambda = 0.37$ D(t) is close to zero or slightly negative, indicating the absence of a strongly preferred directivity. For $\lambda = 0.91$, D(t) remains small but positive for all times, indicating that motions in planes containing the fixed end-to-end vector are more intense than those in other planes. Upon further stretching of the chain, D(t) becomes strongly positive and motions in the P-plane dominate.

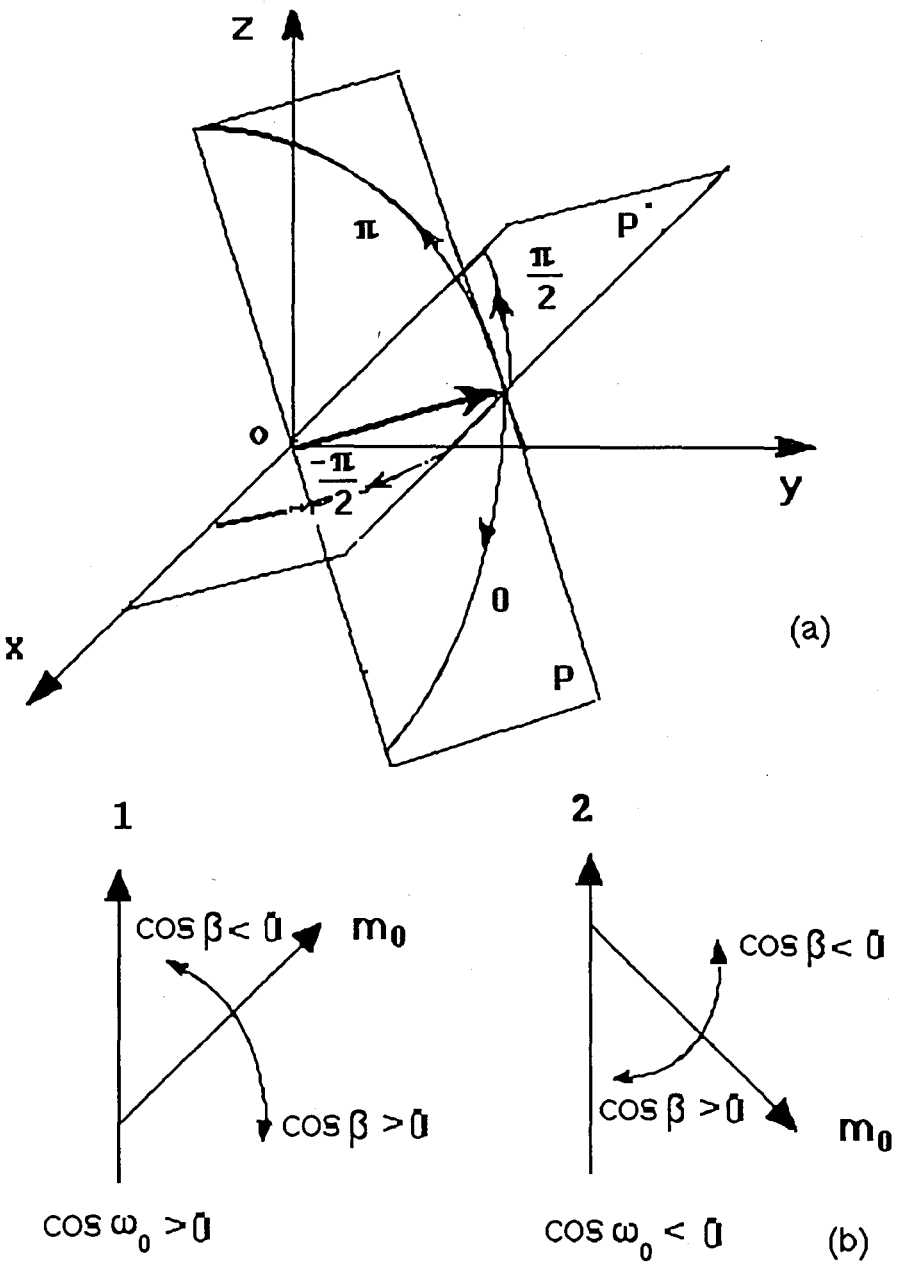

Figure 3.33 (a) Definition of planes P and P'. The P-plane is defined as the plane that contains $\mathbf{m}_0$ and the laboratory-fixed z-axis. The P'-plane contains $\mathbf{m}_0$ and is perpendicular to the P-plane. (b) Diagrams 1 and 2 illustrate the movements leading to positive or negative values for the terms involved in eq 3.38 defining the sense S(t) of mobility.

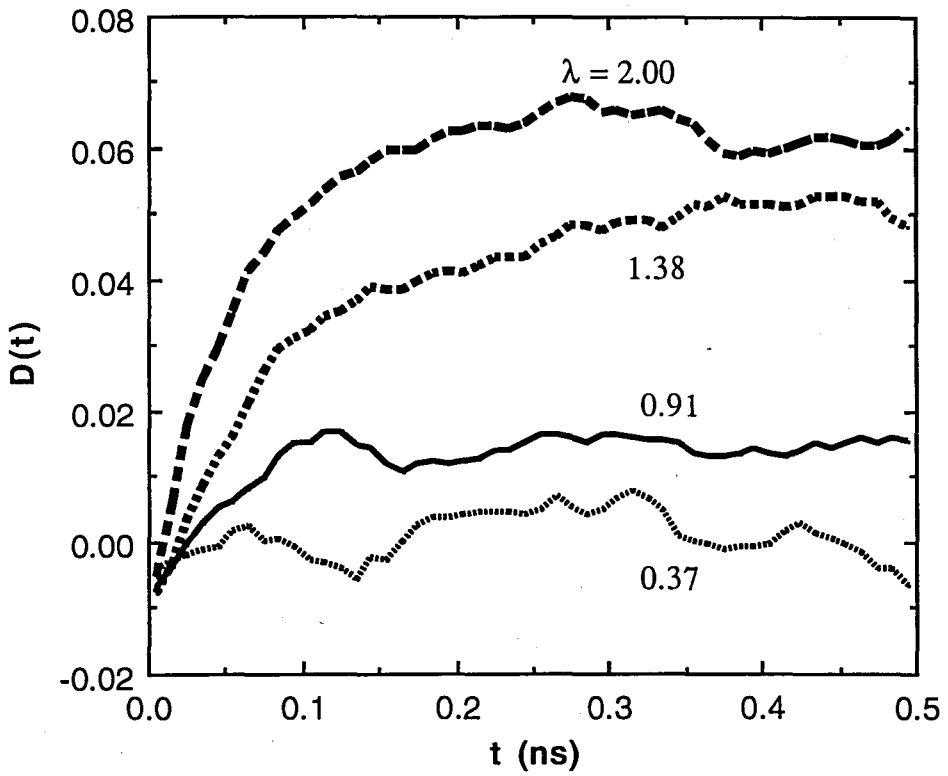

Figure 3.34 Time dependence of directivity of mobility D(t) of **m** for chains with different extension ratios.

3.4.2.4 The Sense of Mobility

$$S(t) = 3 < \sin \omega_0 \cos \omega_0 \sin \alpha \cos \alpha \cos \beta > \qquad (3.38)$$

This function distinguishes between motions of **m** towards the direction of stretch or away from it. The sign of S(t) depends on the signs of cos ω_0 and cos β. The latter is positive if $\mathbf{m}_0$ rotates away from the laboratory-fixed z-axis and is negative otherwise, as shown in Figure 3.33-b. Similarly, cos ω_0 is positive if $\mathbf{m}_0$ makes an angle less than 90° with **r** and is negative otherwise.

In Figure 3.35 values of S(t) calculated from BD simulations are presented for the four different values of the extension ratio. For all extensions S(t) is negative and this negativity becomes more pronounced as the chain is stretched. Since bonds making an angle less than 90° with the z-axis are more populated, the cos ω_0 term will contribute to S(t) with a positive sign. One may conclude from this, therefore, that cos β should be negative, i.e., motions of the bonds directed towards the z-axis are more intense than those away from it. This tendency is weakest in the case of compressed chains.

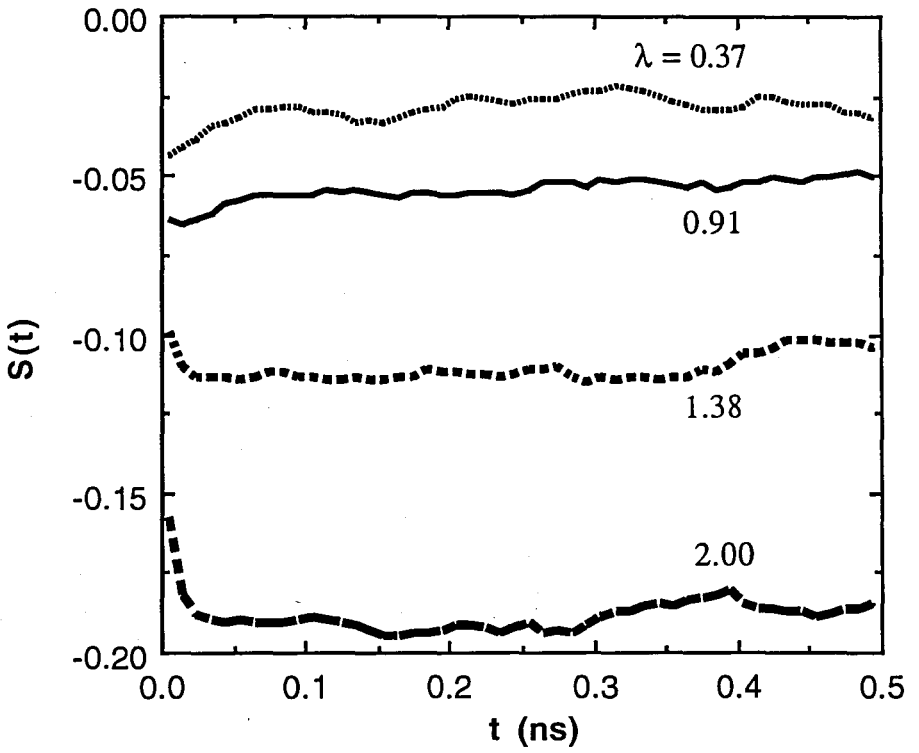

Figure 3.35 Time dependence of sense of mobility S(t) of **m**, for chains with different extension ratios.

Chapter IV

Conclusion and Recommendations

4.1 Conclusion

In the present study, the segmental orientation and the conformational dynamics of polymer chains have been investigated and the following conclusions are reached:

i) For segmental orientation in uniaxially deformed PE and POE networks, the specific aim was to obtain a more rigorous expression for the orientation function, which includes several powers of 1/n. By the use of such an expression, the relative contributions of the first and second order approximations to segmental orientation are assessed. It has been found that the new formulation is particularly useful for relatively short chains and for moderate to large deformations . Calculations performed for PE and POE chains of n = 21, 51 and 101 gave the ranges of extension ratios λ to which the conventional first-order approximation may be confidently applied. Results compared with those obtained from simulations demonstrate the importance of a higher order approximation for the orientation function in the range $\lambda \geq 1.8$.

ii) In the Brownian Dynamics simulation study , the inner orientational and conformational correlations in deformed polymer chains with fixed end-to-end separation were investigated for polymer chains with fixed ends. Rates of rotational isomeric transitions and time evolution of orientational correlations for

various stretch ratios of model PE show that the more extended chains exhibit the highest mobility in the short-time scale but possess the lowest effective rate of rotational isomerization as follows from a hazard analysis within the time span of 10 ns. The stretched-exponential functions with exponent almost independent of chain extension reproduce the time decays of bond orientational correlations. The evolution of rotational and reorientational motions of the bonds described by the time-dependent probability distribution functions shows that the amplitudes of rotational motions are not affected by chain extension but their occurrence is reduced. The distribution of reorientational angles is biased towards lower orientational angle values upon stretching of the chain. This is an indication of the effect of deformation of chain ends on the orientational mobility of the bonds in the chain.

iii) The adequacy of double spherical harmonics functions for the time-dependent probability distribution functions of orientational motions has been tested for describing the orientation of bond vectors. The coefficients of the serial expansion have been evaluated from BD simulations. The results show that truncation of the series after the second order harmonics reproduces the results of BD simulations for a 49 bond PE chain whose ends are held fixed at various extensions, and consequently it is suitable for the description of local orientational dynamics in those chains.

iv) The anisotropy of segmental dynamics has been described by four physically meaningful functions such as mean-mobility amplitude term, orientational-mobility correlation, directivity and the sense of mobility using the results of BD simulation. Strong dependence of those properties on chain extension has been observed.

4.2 Recommendations for Future Developments

The analysis carried out to assess the importance of higher order approximation in the evaluation of the orientation function S may be repeated for networks with a variety of chemical structure to understand the ranges of extension ratio and the size of chains to which the first order approximation may be applied.

In the BD simulations of uniaxially deformed PE chains in dilute solutions, hydrodynamic interactions and excluded volume effects have been ignored for the computational simplicity. For future study, with increase in the computational facilities, contributions of those effects to the equilibrium and dynamic properties of the polymer chains in condensed systems may be investigated. The simulation program may be adopted for different model polymer chains by changing the energy parameters and their properties may be investigated comparatively . In all of the simulations, rotational transitions between isomeric states are based on independent bond rotational potential and thus pentane effects have been neglected. Use of an energy potential governing pairwise dependence on rotational potential may lead to a more realistic description of the polymer chain.

The present work has been performed for deformed polymer chains. Deformation induces the concept of anisotropy of the properties of those polymers and thus indicates the importance of physically meaningful functions which are experimentally measurable as well. The optical and mechanical anisotropy in oriented polymeric materials may be studied in terms of the orientation of the structural units by suitable refinement in the simulation program and efficient manipulation of the simulation data.

References

1. Noda,I.,Dowrey, A.E., Marcott,C.,(i)"Fourier Transform Infrared Characterization" Ed., M. Ishida, Plenum: New York (1987). (ii) Appl. Spectroscopy **42** (1948).
2. Dubault, A., Deloche, B., J. Herz , "Investigation of Segmental Orientation in Polymeric Systems by NMR Spectroscopy", Polymer, **25**, 1405 (1984).
3. Nagai, K., "Photoelastic Property of Cross-Linked Amarphous Polyetylene", J. Chem. Phys. 1964, **40**, 2818 (1964).
4. Flory, P. J., "Statistical Mechanics of Chain Molecules", Interscience : New York (1969).
5. Allen, M. P.,Tildesley, D. J., " Computer Simulation of Liquids", Oxford University Press (1989).
6. Fixman, M., "Simulation of Polymer Chains", J. Chem. Phys. **69,** 1527 (1978).
7. Fixman, M., "Simulation of Polymer Dynamics", J. Chem. Phys. **69,** 1538 (1978).
8. Weiner, J. H., Pear, M. R., "Brownian Dynamics Study of Polymer Chains ", Macromolecules **10**, 317 (1977).
9. Helfand, E., "Brownian Dynamics Study of Conformational Transitions",J. Chem. Phys. **69**, 1010 (1978).
10. Pear, M. R., Weiner, J., " Brownian Dynamics Study of Polymer Chain of Linked Rigid Bodies", J. Chem. Phys. **71**, 212 (1979).
11. Pear, M. R., Weiner, J. H., "Brownian Dynamics Study of Polymer Chain of Linked Rigid Bodies. II. Results for Longer Chains" J. Chem. Phys. **72**, 3939 (1980).
12. Levy, R. M., Karplus, M., Mc Cammon, J. A.," Diffusive Langevin Dynamics of Model Alkanes", Chem. Phys. Lett. **65**, 338(1979).

13. Helfand, E., Wasserman, Z. R., Weber, T. A.,"Brownian Dynamics Study of Polymer Conformational Transitions", J. Chem. Phys. **70**, 2016 (1979).

14. Helfand, E., Wasserman, Z. R., Weber, T. A.,"Brownian Dynamics Study of Conformational Transitions", Macromolecules **13**, 526(1980).

15. Bishop, M., Clarke, J. H. R., "Brownian Dynamics Study of the End-to-End Distribution Function of Two-Dimensional Linear Chains in Different Regimes", J. Chem. Phys. **91**,6345 (1989).

16. Bishop, M., Clarke, J. H. R., " Brownian Dynamics Study of Surface Adsorption of a Linear Polymer in Different Regimes", J. Chem. Phys. **93**, 1455 (1990).

17. Bishop, M., Michels, J. P. C., "The Collapse Transition in Three-Dimensional Linear and Ring Polymers", J. Chem. Phys. **84**, 447 (1986).

18. Helfand, E., Wasserman, Z. E., Weber, T. A., J. Skolnick, J., Runnels, J. H., " The Kinetics of Conformational Transitions", J. Chem. Phys. **75**, 4441(1981).

19. Fixman, M., "Dynamics of Stiff Polymer Chains", J. Chem. Phys. **78**, 1954 (1983).

20. Garcia Fernandez, J. L., Rey, A., Freire, J. J., Fernandez de Piérola, I., "Cyclization Dynamics of Flexible Polymers", Macromolecules **23**,2057(1990).

21. Rey, A., Freire, J. J., Garcia de la Torre, J., " Brownian Dynamics of a Flexible Polymer. Internal modes and Quasielastic Scattering Function", J. Chem.Phys. **90**, 2035 (1989).

22. Ermak, D. L., Mc Cammon, J. A.," Brownian Dynamics with Hydrodynamic Interactions", J. Chem. Phys. **69**, 1352 (1978).

23. Adolf, D. B., Ediger, M. D., "Brownian dynamics Simulations of Local Motions in Polyisoprene",Macromolecules **24**, 5834 (1991).

24. Tao, T., Biopolymers **8**, 609 (1969).

25. Jarry,J. P., Monnerie,L.,"Orientation and MolecularDynamics in Uniaxial Polymers", J. Polym. Sci. Polym. Phys. Ed. **16**, 443 (1978).

26. Spiess, H. W., " NMR Spectroscopy in Polymers", Advances in Polymer Science **66**, 23-58(1985).

27. Haliloglu, T., Bahar, I., Erman, B., "Orientational and Conformational Correlations in Deformed Polymer Chains with Fixed End-to-End Separation: A Brownian Dynamics Simulation Study", J. Chem. Phys. submitted (1992).

28. Erman, B.,Bahar, I. ,"Stochastic Treatment of Conformational Transitions of Polymer Chains", Macromolecules **21**, 457 (1987).

29. Yoon, D. Y., Flory, P. J., "Moments and Distribution Function for Polymer Chains of Finite Length",J. Chem. Phys. **61**, 5366 (1974).

30. Amram, B., Bokobza, L., Monnerie, L., J. P. Queslel, J. P.," Mobility of Macromolecular Chains as Sudied by Excimer Fluorescence", Polymer **29**, 1155(1988).

31. Roe, R. J., Krigbaum, W. R., " Orientation Distribution Function of Statistical Segments in Deformed Polymer Networks", J. Appl. Phys. **35**, 2215 (1964).

32. Kuhn, W., Grun, F., Kolloid-Z. **101**, 248 (1942).

33. Walasek, J., " Segmental Orientation in Deformed Networks", J. Polym. Sci., Part B: Polym. Phys. **26**, 1907 (1988).

34. Erman, B., Monnerie, L., " Segmental Orientation and Mobility in Deformed Amorphous Polymeric Networks", Macromolecules **18**, 1985 (1985).

35. Erman, B., Bahar, I., "Effects of Chain Structure and Network Constitution on Segmental Orientation in Deformed Amorphous Networks", Macromolecules **21**, 452 (1988).

36. Erman, B., Haliloglu, T., Bahar, I., Mark, J. E., "Segmental Orientation in Uniaxially Deformed Networks: A Higher Order Approximation for Finite Chains and Large Deformations", Macromolecules,**24**, 901 (1991).

37. Mark, J. E., Flory, P. J., "The Configuration of the Polyoxyethlene Chain", J. Am. Chem. Soc. **87**, 1415 (1965).

38. Abe, A., Mark, J. E., "Conformational Energies of Polyoxides",J. Am. Chem. Soc. **98**, 6468 (1976).

39. Abe, A., Kennedy, J. W., Flory, P. J., " Persistence Vectors and Higher Moment Tensors of Polyoxialkanes", J. Polymer. Science Polym. Phys. Ed. **14**,1337 (1976).

40. Curro, J. G., Mark, J. E., "Distribution Functions for Plyoxide Chains", J. Chem. Phys. **82**, 3820 (1985).

41. Erman, B., Bahar, I., Monnerie, L., in preparation.

42. Helfand, E., "Numerical Integration of Stochastic Differential Equations", J. Bell Syst. Tech. ,**58,** 2289 (1979).

43. Ryckaert, J. P., Bellemans, A.," Molecular Dynamics in Short-Chain Systems", Chem. Phys. Lett. **30**, 123 (1975).

44. Williams, G., Adv. Polym. Sci. **33**, 59 (1979).

45. Takeuchi, H., Roe, R. J., " Molecular Dynamics Simulation of Local Chain Motion in Bulk Amorphous Polymers", J. Chem. Phys. **94**, 7446 (1991).

46. Takeuchi, H., Roe, R. J.," Molecular Dynamics Simulation of Local Chain Motion in Bulk Amorphous Polymers.II.", J. Chem. Phys. **94**, 7458 (1991).

47. Bahar, I., Erman, B., " Anisotropy of Static and Dynamic Orientational Correlations in N-alkanes",J. Chem. Phys. **88**, 1228 (1988).

48. Bahar, I., Erman, B., Monnerie, L., "Comparison of Dynamic Rotational Isomeric State Results with Previous Expressions for Local Chain Motion", Macromolecules **22**, 431 (1989).

49. Bahar, I., Erman, B., Kremer, F., Fischer, E. W., "Segmental Motions of cis-Polyisoprene in the Bulk State: Interpretation of Dielectric Relaxation Data", Macromolecules **25**, 816 (1992).

50. G. Arfken "Mathematical Methods for Physicists", Academic Press:San Diego, California (1985).

51. Rose, M. E., "Elementary Theory of Angular Momentum" John Wiley& Sons: New York(1957)

52. Bury, K. V., "Statistical Models in Applied Science", Wiley: New York (1975). Mann, N. R., Schafer, R. E., Singpurwalla, N. D., "Methods for Statistical Analysis of Reliability and Life Data", Wiley: New York(1974).

Appendix A

Performing the integrations indicated in eq 2.26, the averages shown in eq 2.25 are obtained up to the eight order as

$$< x^2 >_0 = < y^2 >_0 = < z^2 >_0 = < r^2 >_0 / 3$$

$$< x^4 >_0 = < y^4 >_0 = < z^4 >_0 = < r^4 >_0 / 5$$

$$< x^6 >_0 = < y^6 >_0 = < z^6 >_0 = < r^6 >_0 / 7$$

$$< x^8 >_0 = < y^8 >_0 = < z^8 >_0 = < r^8 >_0 / 9$$

$$< x^2 y^2 >_0 = < x^2 z^2 >_0 = ... = < r^4 >_0 / 15$$

$$< x^2 y^4 >_0 = < x^2 z^4 >_0 = ... = < r^6 >_0 / 35$$

$$< x^2 y^6 >_0 = < x^2 z^6 >_0 = ... = < r^8 >_0 / 63$$

$$< x^4 y^4 >_0 = < x^4 z^4 >_0 = ... = < r^8 >_0 / 105$$

$$< x^2 y^2 z^2 >_0 = \qquad < r^6 >_0 / 60$$

$$< x^4 y^2 z^2 >_0 = < y^4 x^2 z^2 >_0 = \ .... = < r^8 >_0 / 315 \qquad \text{(A.1)}$$

The terms not shown in eq A.1 are readily obtained from symmetry. The use of these averages leads to the following averages of α_i, β_i and $\alpha_i\beta_j$

$$< \alpha_1 > = 2 \Lambda_2$$

$$< \alpha_2 > = 14 \Lambda_2 - \frac{6}{5} \frac{< r^4 >_0}{< r^2 >_0^2} \Lambda_4$$

$$< \alpha_3 > = \Lambda_2 - \frac{108}{5} \frac{< r^4 >_0}{< r^2 >_0^2} \Lambda_4 + \frac{54}{7} \frac{< r^6 >_0}{< r^2 >_0^3} \Lambda_6$$

$$< \alpha_4 > = 1386 \Lambda_2 - \frac{1782}{5} \frac{< r^4 >_0}{< r^2 >_0^2} \Lambda_4 + \frac{1782}{7} \frac{< r^6 >_0}{< r^2 >_0^3} \Lambda_6 - 18 \frac{< r^8 >_0}{< r^2 >_0^4} \Lambda_8$$

$$\langle \alpha_1\beta_1 \rangle = 30\,\Lambda_2 - 12\,\frac{\langle r^4 \rangle_0}{\langle r^2 \rangle_0^2}\,\Lambda_4 + \frac{54}{7}\,\frac{\langle r^6 \rangle_0}{\langle r^2 \rangle_0^3}\,\Lambda_6$$

$$\langle \alpha_1\beta_2 \rangle = 210\,\Lambda_2 - 378\,\frac{\langle r^4 \rangle_0}{\langle r^2 \rangle_0^2}\,\Lambda_4 + 162\,\frac{\langle r^6 \rangle_0}{\langle r^2 \rangle_0^3}\,\Lambda_6 - 18\,\frac{\langle r^8 \rangle_0}{\langle r^2 \rangle_0^4}\,\Lambda_8 \qquad \text{(A.2)}$$

$$\langle \alpha_1\beta_3 \rangle = 1890\,\Lambda_2 - 4536\,\frac{\langle r^4 \rangle_0}{\langle r^2 \rangle_0^2}\,\Lambda_4 + 2916\,\frac{\langle r^6 \rangle_0}{\langle r^2 \rangle_0^3}\,\Lambda_6 - 648\,\frac{\langle r^8 \rangle_0}{\langle r^2 \rangle_0^4}\,\Lambda_8$$

$$\langle \alpha_2\beta_1 \rangle = 210\,\Lambda_2 - 306\,\frac{\langle r^4 \rangle_0}{\langle r^2 \rangle_0^2}\,\Lambda_4 + \frac{918}{7}\,\frac{\langle r^6 \rangle_0}{\langle r^2 \rangle_0^3}\,\Lambda_6 - 18\,\frac{\langle r^8 \rangle_0}{\langle r^2 \rangle_0^4}\,\Lambda_8$$

$$\langle \alpha_3\beta_1 \rangle = 1890\,\Lambda_2 - 3240\,\frac{\langle r^4 \rangle_0}{\langle r^2 \rangle_0^2}\,\Lambda_4 + \frac{13932}{7}\,\frac{\langle r^6 \rangle_0}{\langle r^2 \rangle_0^3}\,\Lambda_6 - 504\,\frac{\langle r^8 \rangle_0}{\langle r^2 \rangle_0^4}\,\Lambda_8$$

where

$$\Lambda_2 = \lambda^2 - \lambda^{-1}$$

$$\Lambda_4 = 3\lambda^4 + \lambda - 4\lambda^{-2} \qquad \text{(A.3)}$$

$$\Lambda_6 = \lambda^6 + \frac{3}{5}\lambda^3 - \frac{8}{5}\lambda^{-3}$$

$$\Lambda_8 = \lambda^8 + \frac{5}{7}\lambda^5 + \frac{12}{35}\lambda^2 - \frac{8}{35}\lambda^{-1} - \frac{64}{35}\lambda^{-4}$$

Appendix B Details of Flexible Chain Formalism

The position vector $\mathbf{r}_i$ of the ith atom is a function of the generalized coordinates l_i, l_{i+1}, θ_{i-1}, θ_i, θ_{i+1}, ϕ_{i-1}, ϕ_i, ϕ_{i+1} and ϕ_{i+2}, as follows from the examination of eqs 1-3. Thus, the gradient of the overall potential V with respect to $\mathbf{r}_i$ may be written as

$$\nabla_i V = \nabla_i \left[\sum_{k=i}^{i+1} V_b(l_k) + \sum_{k=i-1}^{i+1} V_\theta(\theta_k) + \sum_{k=i-1}^{i+2} V_\phi(\phi_k) \right] \qquad \text{(B.1)}$$

It should be noted that in eq A.1 and in the following equations the potential or the force having an undefined generalized coordinate as the argument (such as $V_\theta(\theta_k)$ with $k < 1$ or $k \geq N$) is implicitly accepted to be equal to zero. Replacing in eq A.1 the negative gradients of the potential functions V_ζ (with ζ = b, θ or ϕ) by the forces $\mathbf{F}_\zeta$ and inserting the results into the equation of motion 3.11, leads to

$$\beta \, d\mathbf{r}_i / dt = m^{-1} \left[\sum_{k=i}^{i+1} \mathbf{F}_b(l_k) + \sum_{k=i-1}^{i+1} \mathbf{F}_\theta(\theta_k) + \sum_{k=i-1}^{i+2} \mathbf{F}_\phi(\phi_k) \right] + \mathbf{A}_i(t) \qquad \text{(B.2)}$$

The bond stretching forces which are associated with the deformation of the lengths of bonds i and i+1 are given by

$$\mathbf{F}_b(l_i) = - k_b (1 - l_0 / l_i) \mathbf{l}_i \qquad 1 \leq i \leq N \qquad \text{(B.3)}$$

and

$$\mathbf{F}_b(l_{i+1}) = k_b (1 - l_0 / l_i) \mathbf{l}_{i+1} \qquad 2 \leq i \leq N - 1 \qquad \text{(B.4)}$$

On the other hand, the bond bending forces on atom i arising from the distortions of the angles θ_{i-1}, θ_i and θ_{i+1} are given respectively by

$$\mathbf{F}_\theta(\theta_{i-1}) = -K_{\theta\, i-1}\left[\mathbf{l}_{i-1} - d^{i}_{i-1}\,\mathbf{l}_i/l_i^{2}\right] \qquad 2 \le i \le N \qquad \text{(B.5)}$$

$$\mathbf{F}_\theta(\theta_i) = -K_{\theta i}\left[\mathbf{l}_{i+1} - \mathbf{l}_i + d^{i+1}_{i}(\mathbf{l}_{i+1}/l_{i+1}^{2} - \mathbf{l}_i/l_i^{2})\right] \qquad 2 \le i \le N-1 \qquad \text{(B.6)}$$

and

$$\mathbf{F}_\theta(\theta_{i+1}) = K_{\theta i+1}\left[\mathbf{l}_{i+2} - d^{i+2}_{i+1}\,\mathbf{l}_{i+1}/l_{i+1}^{2}\right] \qquad 2 \le i \le N-2 \qquad \text{(B.7)}$$

Here $K_{\theta m}$ and d^{k}_{m} are defined as

$$K_{\theta m} \equiv k_\theta \frac{(\cos\theta_m - \cos\theta_0)}{l_m\, l_{m+1}} \qquad \text{(B.8)}$$

and

$$d^{k}_{m} \equiv \mathbf{l}_m \cdot \mathbf{l}_k \qquad \text{(B.9)}$$

In order to write the rotational potential forces $\mathbf{F}_\phi(\phi_m)$, $i-1 \le m \le i+2$, in a more concise form, the following variables are introduced

$$a^{k}_{j} = \left[l_j^2\, l_k^2 - (d^{k}_{j})^2\right] \qquad \text{(B.10)}$$

$$A_1(i,j,k) = (d^{i}_{j}\,\mathbf{l}_j - l_j^2\,\mathbf{l}_i)(d^{k}_{i}\,l_i^2 - d^{k}_{j}\,d^{i}_{j})(a^{i}_{j})^{-1} + (l_j^2\,\mathbf{l}_k - d^{k}_{j}\,\mathbf{l}_j) \qquad \text{(B.11)}$$

$$A_2(i,j,k) = (d^{i}_{j}\mathbf{l}_j - l_j^2\,\mathbf{l}_i)(d^{j}_{k}\,l_i^2 - d^{j}_{i}\,d^{i}_{k})(a^{i}_{j})^{-1} + (\mathbf{l}_i\,d^{j}_{k} - \mathbf{l}_k\,d^{i}_{j}) \qquad \text{(B.12)}$$

Using those variables, the bond rotational forces read

$$F_\phi(\phi_{i-1}) = K_{\phi\, i-1}\ A_1\ (i,\ i-1,\ i-2) \qquad 3 \le i \le N \qquad \text{(B.13)}$$

$$F_\phi\,(\phi_i) = K_{\phi\, i}\ [\ A_2\ (\ i,\ i-1,\ i+1)\ -\ A_1\ (i+1,\ i,\ i-1) + A_2\ (i,\ i+1,\ i-1)]$$
$$3 \le i \le N-1 \qquad \text{(B.14)}$$

$$F_\phi\,(\phi_{i+1}) = -\ K_{\phi i+1}\ [\ A_2\ (i+1,\ i,\ i+2)\ -\ A_1\ (i,\ i+1,\ i+2) + A_2\ (i+1,\ i+2\ ,\ i)\ ]$$
$$3 \le i \le N-2 \qquad \text{(B.15)}$$

and

$$F_\phi\,(\phi_{i+2}) = -\ K_{\phi i+2}\ A_1\ (i+1,\ i+2,\ i+3) \qquad 3 \le i \le N-3 \qquad \text{(B.16)}$$

where the proportionality constant $K_{\phi m}$ is defined as

$$K_{\phi\, m} \equiv -\ k_\phi\ (a^m_{m-1}\ a^{m+1}_m)^{-1/2}\ [\ \sum_{i=1}^{5}\ i\ a_i\ \cos^{i-1}\phi_m\ ] \qquad \text{(B.17)}$$

Appendix C Hazard Analysis

In hazard analysis, at the beginning of a simulation, a "clock" equal to zero is set and the number of time steps required for a transition is counted for the particle to first reach the bottom of the opposite well. Then the clock is again set to zero and the next reaction time is measured and so on. The reaction times, except the first one, are the first passage times from one minimum to the other. Thus a set of n reaction times is obtained. These are arranged in ascending order,

$$t_{(1)} \leq t_{(2)} \leq \ldots\ldots \leq t_{(n)}$$

forming what is called a set of order statistics. The statistical method employed have mostly been developed in the field of reliability analysis.[52]

In hazard analysis, the hazard rate h(t) defined such that h(t)dt is the probability that a system which has survived a time t since its last transition will undergo a transition at time between t and t+dt. Cumulative hazard is defined as follows:

$$H(t) = \int_0^t h(t')dt' \qquad \text{C.1}$$

The probability of transition occurring in a time less than t since the last is

$$P(t) = 1 - \exp[-H(t)] \qquad \text{C.2}$$

and the probability density of transition at t is

$$P(t) = dP/dt = h(t)\exp[-H(t)] \qquad C.3$$

The data is best depicted in a hazard plot, a plot of the n transition times vs expectation values of the corresponding cumulative hazards. The expectation of cumulative hazard at the time of the k^{th} ordered transition is,

$$\overline{H}_k = \sum_{l=0}^{k-1} \frac{1}{n-l} \qquad C.4$$

as a function of k only.

The slope of the hazard plot gives the reaction rate. What is measured is a composite of all processes, trans going to either one of gauches or vice versa:

$$\lambda = 2p_t\lambda_{tg}+2p_g\lambda_{gt} \qquad C.5$$

where λ_{tg} is the rate of transition from trans to one of the gauches, λ_{gt} is the reverse rate, p_t is the fraction of trans, and p_g is the fraction in one of the gauches. From the detailed balance:

$$p_t\lambda_{tg} = p_g\lambda_{gt}$$

so that

$$\lambda_{tg} = \lambda/4p_t \qquad C.6$$

Appendix D Extended Runge-Kutta Method for Integration of Stochastic Differential Equations

The Langevin equation by which the dynamics of model polyethylene chains are simulated is a stochastic differential equation. A stochastic differential equation does not have a definite solution as in the case of deterministic differential equations. An extension of the Runge-Kutta method for the integration of stochastic differential equations was presented in a previous study by Helfand.[42] He showed that this technique produces results which are statistically correct to the k^{th} order in the time step s.

General form of stochastic differential equation occurring in Brownian motion theory is as follows:

$$\frac{dx}{dt} = f(x)+A(t) \qquad \text{D.1}$$

Here the A(t) are Gaussianly distributed random variables with mean zero and covariance(white-noise)

$$\langle A(t)A(t')\rangle = \xi\delta(t-t') \qquad \text{D.2}$$

and it is related to the wiener processes(Brownian motion processes)

$$w_0(t) = \int_0^t A(t')\,dt' \qquad \text{D.3}$$

which has correlation

$$\langle [w_0(t)] \rangle = \xi t \qquad \text{D.4}$$

A stochastic differential equation does not have a definite solution. Numerical integration means generation of statistically representative trajectory values of x at discrete times: x(o), $x(s_1)$, $x(s_1+s_2)$. The process defined in D.1 is Markovian. Thus the process is completely specified by the conditional probability density function $P(x, s / x_0, 0)$ which gives the probability density of observing x at time s, given the value x_0 of the variable at time zero. What is searched for is a method of selecting a value x_s with statistics correct to k^{th} order in s. That means that the moments $\langle x_s^q \rangle$ are all correctly given to $O(s^k)$. An approximation algorithm involves generation of some random numbers.

Eq D.1 may be written in an integrated form by iteration and Taylor series expansion:

$$x = x_0 + \int_0^s f(x) + w_0(s) \qquad \text{D.5}$$

Here f(x) can be extended as

$$f(x) = f_0 + f_0'(x-x_0) + \ldots\ldots \frac{1}{p!} f_0^{(p)} (x-x_0)^p \qquad \text{D.6}$$

for all points of x_0 accessible to the trajectory. To develop an iteration solution, x is substituted in the integral in eq D.5 and f(x) is expanded in the power series(eq D.6):

$$x(s) = x_0 + \int_0^s ds_1 \{x_0 + \int_0^{s1} ds_2 f[x_0+\ldots] + w(s_1)\} + w_0(s) \qquad \text{D.7}$$

$$= x_0+sf_0+1/2s^2f_0\,f_0'+1/6s^3(f_0f_0'^2+f_0^2f_0'')+ S$$

with

S stands for the stochastic part. The statistics of the stochastic part of the trajectory are embodied in the moments of S. $f_0^{(n)}$ denotes the n^{th} derivative of f evaluated at x_0.

The aim of many numerical procedure is to present an algorithm which, when expanded in s, matches the series(eq D.7) to a given order, k, in s. Furthermore, the use of the derivatives of f is avoided. In the extension of the Runge-Kutta theory one goes from initial condition x_0 to x(s) in k stages by the procedure presented below:

$$g_1 = f(x_0 + s^{1/2}\xi^{1/2}\lambda_1.\mathbf{Z})$$

$$g_2 = f(x_0 + s\beta_{21}g_1 + s^{1/2}\xi^{1/2}\lambda_2.Z)$$

.

$$g_k = f(x_0 + s\beta_{k1}g_1 +...+ s\beta_{k,k-1}g_{k-1} + s^{1/2}\xi^{1/2}\lambda_k.\mathbf{Z}) \qquad \text{D.8}$$

.

$$x_s=x_0 + s(A_1g_1 +...+ A_kg_k) + s^{1/2}\xi^{1/2}\lambda_0.\mathbf{Z}$$

The parameters A's, B's and λ's are to be selected such that an expansion of eq D.8 in powers of S matches the nonstochastic and the moments of the stochastic term S through order k of eq D.7. **Z** is a vector of Gaussian random variables with mean zero and variance unity, generated for each time step s. The number of Gaussian variables is determined such that there are a sufficient number of parameters to satisfy these equations. g_k represents the k^{th} order perturbation for f. In the case of $\xi = 0$, the ordinary differential equation is recovered from eq D.8. For detailed intermediate steps, the reader is suggested to read the paper by Helfand.[42]

In the second order approximation of the extended Runge-Kutta method, the stages of the numerical procedure applied in the Brownian Dynamics simulation program for the solution of the Langevin equation(eq 3.11) are given below:

$$g_1 = f(x_0)$$
$$g_2 = f(x_0 + sg_1 + s^{1/2}\xi^{1/2} Z) \qquad \text{D.9}$$
$$x_s = x_0 + s(1/2\, g_1 + 1/2\, g_2) + s^{1/2}\xi^{1/2}Z$$

with the solution set of parameters:

$$A_1 = A_1 = 1/2$$
$$\beta_{21} = 1 \qquad \text{D.10}$$
$$\lambda_0 = 1,\ \lambda_1 = 0,\ \lambda_2 = 1$$

evaluated from the solution of the following equations:

$$A_1 + A_2 = 1$$
$$A_2 B = 1/2$$
$$\lambda_0^2 = 1 \qquad \text{D.11}$$
$$(A_1\lambda_1 + A_2\lambda_2)\,\lambda_0 = 1/2$$
$$A_1\lambda_1^2 + A_2\lambda_2^2 = 1/2$$

g_1 and g_2 are the first and the second order perturbation of f which is the total conformational potential force calculated of the polymer chain in the simulation program. Z is a single Gaussian random variable and generated using the Function Gauss in the program for each time step s. ξ is equated to

$2\beta k_B T/m$, given as the coefficient of the covariance of the Gaussianly distributed force in eq 3.12.

Appendix E Spherical Harmonics

The solutions to (1) Laplace's equation, (2) Helmholtz's or the space-dependence of the classical wave equation, and (3) the Schrödinger wave equation in central force fields

$$\nabla^2\Psi + k^2\Psi = 0 \qquad \text{E.1}$$

are called the solid spherical harmonics[50] $r^l Y_l^m(\omega, \psi)$, where r, ω, ψ are three spherical coordinates. The angular dependence of eq E.1 in the separation of variables results in the surface spherical harmonics $Y_l^m(\omega, \psi)$ of function of spherical angles ω and ψ.

Azimuthal dependence(ψ) produces the solution

$$\Phi(\Psi) = e^{-1m\psi}, e^{1m\psi} \qquad \text{E.2}$$

which satisfies the orthogonality condition:

$$\int_0^{2\pi} e^{-im_1\psi} e^{-im_2\psi} d\psi = 2\pi\, \delta_{m_1, m_2} \qquad \text{E.3}$$

and results in

$$\Phi_m = \frac{1}{2\pi} e^{im\psi} \qquad \text{E.4}$$

which is orthonormal with respect to integration over the azimuthal angle ψ .

Polar dependence (ω) leads to the Legendre functions,

$$P_n^m(\cos\omega) = \frac{1}{2^n n!}(1-x^2)^{m/2}\frac{d^{m+n}}{dx^{m+n}}(x^2-1)^n \qquad -n \le m \le n \qquad \text{E.5}$$

and normalizing the associated Legendre function results in the orthonormal function

$$P_n^m(\cos\omega) = \sqrt{\frac{2n+1}{2}\frac{(n-m)!}{(n+m)!}}\ P_n^m(\cos\omega) \qquad -n \le m \le n \qquad \text{E.6}$$

The product of $\Phi_m(\psi)$ which is orthonormal with respect to the azimuthal angle ψ, and $P^m{}_n(\cos\omega)$ which is orthonormal with respect to the polar angle ω gives the spherical harmonics which are functions of two angles and orthonormal to the spherical surface:

$$Y_n^m(\Omega) = Y_n^m(\omega, \psi) = (-1)^m\left[\frac{(2n+1)(n-m)!}{4\pi(n+m)!}\right]^{1/2} P_n^m(\cos\omega)\, e^{im\psi} \qquad \text{E.7}$$

The complete orthogonality integral becomes:

$$\int\int Y^{m_1}_{n_1}(\omega, \psi)\, Y^{m_2}_{n_2}(\omega, \psi)\, \sin\omega d\omega\, d\psi = \delta_{n_1,n_2}\ \delta_{m_1,m_2} \qquad \text{E.8}$$

These functions takes the name "spherical harmonics", because; they are defined over the surface of a sphere with ω, the polar angle and ψ, the azimuth. The "harmonic" is included because solutions of Laplace's equation were called harmonic functions and $Y^m{}_n(\omega, \psi)$ is the angular part of such solution.

The spherical harmonics of function $\Omega(\omega, \psi)$ obtained up to the second order terms using eqs E.6 and E.7 are given below:

$$Y^0_0(\Omega) = \left(\frac{1}{4\pi}\right)^{1/2}$$

$$Y^0_1(\Omega) = \left(\frac{3}{4\pi}\right)^{1/2}\cos\omega$$

$$Y^0_2(\Omega) = \left(\frac{5}{16\pi}\right)^{1/2}(3\cos^2\omega-1) \qquad \text{E.9}$$

$$Y^1_2(\Omega) = (-1)\left(\frac{15}{8\pi}\right)^{1/2}(\cos\omega \sin\omega)\, e^{-i\psi}$$

$$Y^2_2(\Omega) = \left(\frac{15}{32\pi}\right)^{1/2}(\sin^2\omega)\, e^{-i2\psi}$$

$$Y^{-1}_2(\Omega) = -Y^1_2(\Omega)$$

$$Y^{-2}_2(\Omega) = Y^2_2(\Omega)$$

The completeness property is the most important property of the spherical harmonics. By this property, any function can be expanded in a uniformly convergent double spherical harmonics. Thus, the joint probability distribution function $p_{\mathbf{r}}(\Omega, t; \Omega_0, t_0)$ of orientation Ω at time t and Ω_0 at time t_0 for the vector **m** for a chain with end-to-end separation **r** is expressed in terms of a double spherical harmonics series. The coefficients of this series are defined as $a^{mn}{}_{kl} = \langle Y^m{}_k(\Omega_0)\ Y^n{}_l(\Omega)\rangle_{\mathbf{r}}$ and by the use cylindrical symmetry, $a^{mn}_{kl} = a^{-m-n}_{kl} = a^{m}_{kl}\delta_{mn}$, the functions f_m (m = 0-9) up to the second order terms in the joint probability distribution function, $p_{\mathbf{r}}(\Omega, t; \Omega_0, t_0)$ given in eq 3.28 are obtained from $a^k{}_{lm}$'s as follows:

$$f_0 = a^0_{00}$$

$$f_1 = \frac{1}{\sqrt{2}} (a^0_{01} + a^0_{10})$$

$$f_2 = \frac{1}{\sqrt{2}} (a^0_{02} + a^0_{20})$$

$$f_3 = \frac{1}{\sqrt{2}} (a^0_{12} + a^0_{21})$$

$$f_4 = a^0_{11} \qquad \text{E.10}$$

$$f_5 = a^0_{22}$$

$$f_6 = \sqrt{2}\, a^1_{11}$$

$$f_7 = \sqrt{2}\, a^1_{22}$$

$$f_8 = \sqrt{2}\, a^1_{12}$$

$$f_9 = \sqrt{2}\, a^2_{22}$$

Appendix F Wigner Matrices

The introduction of α and β (defined in Figure 3.31) into the spherical harmonics $Y^m_k(\Omega)$ of angular function of Ω has been performed using the Wigner matrices:[51]

$$Y^m_k(\Omega)=\sum_{\mu=-k}^{+k} \overline{D}^k_{m\mu}(\psi_0, \omega_0, 0)Y^\mu_k(\Gamma) \qquad \text{F.1}$$

where $\overline{D}^k_{m\mu}$ are the Wigner matrices, with the argument Ω_0 denoting the three Euler angles ω_0, ψ_0 and 0 and $Y^m_k(\Gamma)$ are the spherical harmonics of angular function $\Gamma(\alpha,\beta)$. The point Ω is the same point in space as Γ but measured relative to the rotated coordinate system rather than relative to the initial system. This rotated system is specified by the three Euler angles: ψ_0, ω_0 and 0. Eq F.1 rotates the coordinates. The first two Euler angles ψ_0 and ω_0 define a new polar axis, Z (Figure 3.31) and a new zero of azimuth. (The third Euler angle 0 corresponds to a rotation about new polar axis and irrelevant here). The Wigner matrices in eq F.1 is obtained by the following expression:

$$D^j_{km}(\psi_0, \omega_0, 0) = e^{-i\psi_0}\sum_s (-)^s \frac{[(j+k)!(j-m)!(j+k)!(j-m)!]^2}{s!(j-s-k)!(j+m-s)!(k+s-m)!} X \left(\cos\frac{\omega_0}{2}\right)^{2j+m-k-2s}\left(\cos\frac{\omega_0}{2}\right)^{m-k+2s} \qquad \text{F.2}$$

where the sum is over the values of the integer s for which the factorial argument are greater than or equal to zero and the spherical harmonics. $Y^m_k(\Gamma)$ may readily be obtained from eq E.9 by replacing the spherical angles ω and ψ with α and β.

The spherical harmonics $Y^m_k(\Omega)$ up to the second order rotated the way $\Omega_0(\omega_0, \psi_0)$ by the use of Wigner matrices $\overline{D}^k_{m\mu}$ are given below:

$$Y^0_1(\Omega) = \left(\frac{1}{4\pi}\right)^{1/2}$$

$$Y^0_1(\Omega) = \left(\frac{3}{\pi}\right)^{1/2}(1/2\ \cos\omega_0\cos\alpha - \sin\omega_0\sin\alpha\ \cos\beta)$$

$$Y^1_1(\Omega) = e^{-i\psi_0}\left(\frac{3}{2\pi}\right)^{1/2}(\ \sin\omega_0\cos\beta + (1/2)\cos\omega_0\sin\alpha\ \cos\beta) \qquad \text{F.3}$$

$$Y^0_2(\Omega) = \left(\frac{5}{4\pi}\right)^{1/2}\{(3\cos^2\omega_0-1)\ ((3\cos^2\alpha_0-1)/4 + (3/4)\ \sin^2\omega_0\ \sin^2\alpha\ \cos2\beta)$$
$$-3\ \sin\omega_0\cos\omega_0\ \sin\alpha\ \sin\beta\}$$

$$Y^2_2(\Omega) = e^{-2i\psi_0}\left(\frac{15}{32\pi}\right)^{1/2}\{(\ \sin\omega_0\ \cos\omega_0\sin^2\alpha\ \cos2\beta) + (2-4\sin^2\omega_0\ )\ \sin\alpha\ \cos\alpha\ \cos\beta$$
$$-\ \cos\omega_0\ \sin\omega_0(3\cos^2\alpha-1)\}$$

$$Y^2_2(\Omega) = e^{-2i\psi_0}\left(\frac{15}{32\pi}\right)^{1/2}\{(1-(1/2)\sin^2\omega_0\ )\ \sin^2\alpha\ \cos2\beta + (\ \sin\omega_0\ \cos\omega_0\ \sin\alpha\ \cos\alpha\ \cos\beta$$
$$+\ \sin^2\alpha_0(3\cos^2\alpha-1)]\}$$

$$Y^{-1}_1(\Omega) = -Y^1_1(\Omega)$$

$$Y^{-1}_2(\Omega) = -Y^1_2(\Omega)$$

$$Y^{-2}_2(\Omega) = Y^2_2(\Omega)$$

The rotated spherical harmonics $Y^m_k(\Omega)$ placed in eq 3.24 lead to the coefficients of the probability distribution function in terms of new angles α and β. After manipulation among these coefficients, following experimental measurable functions come up:

$$1/\sqrt{5}\,\frac{a^2_{02}}{a^0_{00}} = C + D - S \qquad \text{F.4}$$

$$6/5\,\frac{a^2_{22}}{a^0_{00}} + 1/5\,\frac{a^0_{22}}{a^0_{00}} = M - 2C + (1/2)D + 3S \qquad \text{F.5}$$

$$1/5\,\frac{a^0_{22}}{a^0_{00}} + 2/5\,\frac{a^1_{22}}{a^0_{00}} - 2/5\,\frac{a^2_{22}}{a^0_{00}} = M \qquad \text{F.6}$$

where

$$M = \langle(3\cos^2\alpha - 1)/2\rangle \qquad \text{F.7}$$

is the mobility amplitude term,

$$C = \langle(3\cos^2\omega_0-1)(3\cos^2\alpha-1)/4\rangle \qquad \text{F.8}$$

is the orientation-mobility amplitude correlation term,

$$D = (3/4)\langle\sin^2\omega_0\sin^2\alpha\cos2\beta\rangle \qquad \text{F.9}$$

is the directivity of mobility,

and

$$S = 3\langle\sin\omega_0\cos\omega_0\sin\alpha\,\cos\alpha\,\cos\beta\rangle \qquad \text{F.10}$$

the sense of mobility.

Appendix G

1. Simple Flow Diagram for BD Simulation
2. Monte Carlo Simulation Program for Chain Generation
3. BD Simulation Program
4. Data File for BD Simulation Program
5. Simulation Output from BD Simulation

Simple Flow Diagram for BD Simulation

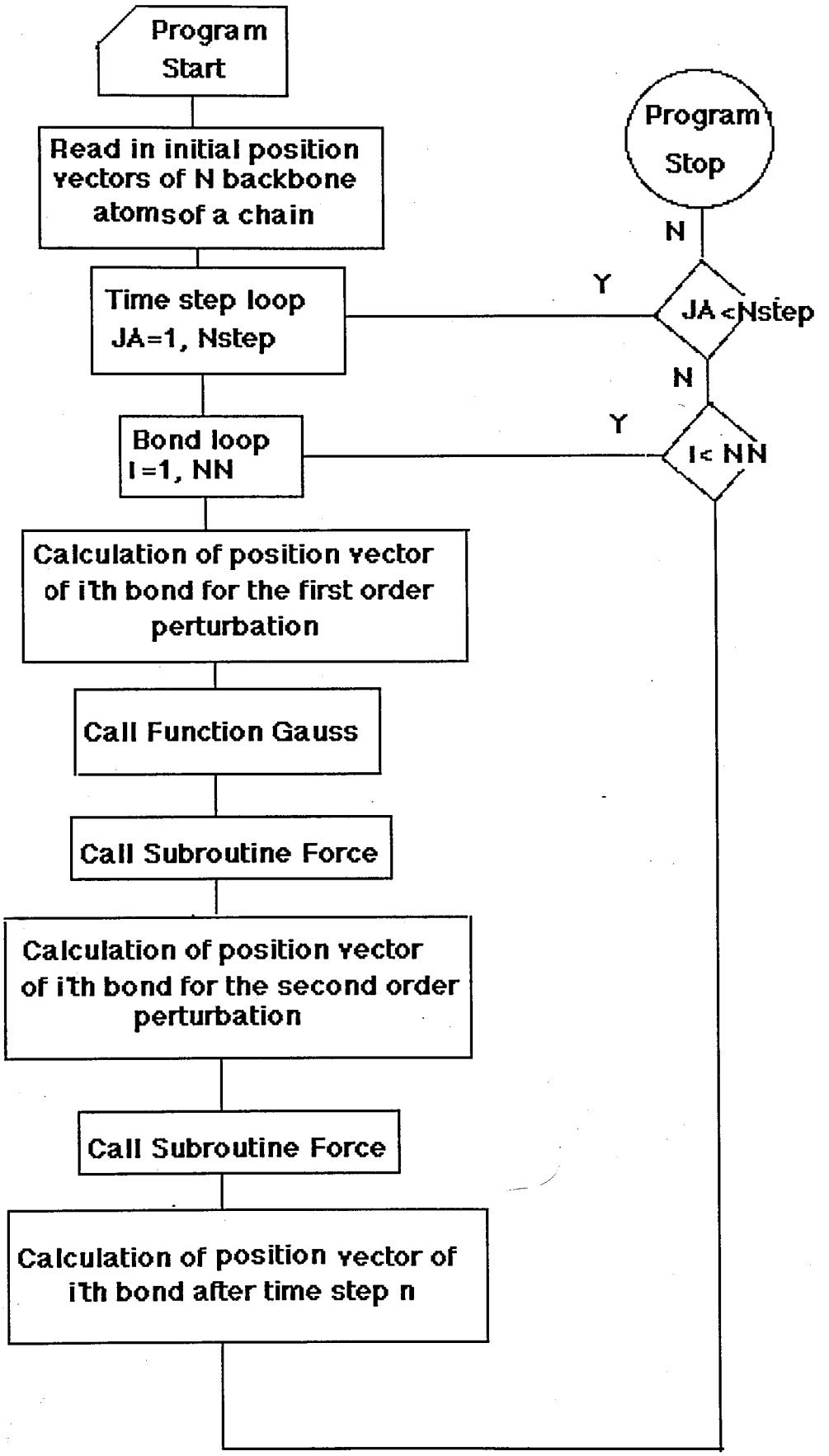

Basic Outline of the Program BROWNIAN DYNAMICS

1. Program starts
2. Program reads in the initial position vectors of NN atoms of a chain generated by Monte Carlo simulation
3. Initialization of arrays
4. Beginning of the main program
5. Start of time-step loop(JA=1,NSTEP)
6. Start of bond loop(I =1,NN)
7. Calculation of the position vector of $(i)^{th}$ atom for the first order perturbation
8. Call Function Gauss; it returns a normal variate of zero mean and unit covariance.
9. Call Function Force; it returns the total force (TFX, TFY, TFZ), acting on the $(i)^{th}$ atom after first order perturbation
10. Calculation of the position vector of $(i)^{th}$ atom for the second order perturbation
11. Call Subroutine Force; it returns the total force (TFX, TFY, TFZ), acting on $(i)^{th}$ atom after second order perturbation
12. Calculation of new position vector of $(i)^{th}$ atom at JA'th time step
13. End of bond loop(next I)
14. End of time loop(next JA)
15. Program stops.

Routines Supplied

Subroutine Force: It returns the total (TFX, TFY, TFZ) acting on $(i)^{th}$ atom due to the bond stretching, bond bending and bond rotational potential.

Function Gauss: It returns a uniform random variable with zero mean and unit variance.

Subroutine RAN2: It returns a uniform random number between 0 and 1.

```
C     Monte Carlo Simulation Program for Chain Generation

      program mc
      dimension u(101,3,3),p(101,3,3),q(3,3),cs(3)
      dimension rowj(3),colj(3),row(3),prod(3),ps(101,3)
      dimension r(101,3),t(3,3),tt(3,3),fi(101),sm(3,3)
      dimension d1(101),d2(101),d3(101),d4(101),d5(101)
      dimension d6(101),end(3),vm(3)
      data  esig,eom,epsi,n,temp/0.5,2.0,0.0,50,140./
      data ngen,tr,gp,gm,theta/10,0.,120.,-120.,68./
      data r2avg,r4avg,r6avg,r8avg/0.,0.,0.,0./
      data sum1,sum2,sum3,sum4/0.,0.,0.,0./
      open(2,file ='out mc',status='new')
      idum=-25
      write(2,*)'idum=',idum
      cs2avg=0.
      r2cs=0.
      r4cs=0.
      r6cs=0.
      r8cs=0.
      theta=theta*3.141592654/180.
      gp=gp*3.141592654/180.
      gm=gm*3.141592654/180.
      tr=tr*3.141592654/180.
      do 1 i=1,3
      rowj(i)=0.
1     colj(i)=1.
      rowj(1)=1.
      temp=temp+273.
      rg=1.987e-03
      sigma=exp(-esig/temp/rg)
      omeg=exp(-eom/temp/rg)
      psi=exp(-epsi/temp/rg)
      dis=((1-sigma*(psi+omeg))**2.+8*sigma)**0.5
      hlam1=0.5*(1+sigma*(psi+omeg)+dis)
      hlam2=0.5*(1+sigma*(psi+omeg)-dis)
      hlam3=sigma*(psi-omeg)
      z=(1-hlam2)/(hlam1-hlam2)*hlam1**(n-1)
      z=z+(-1+hlam1)/(hlam1-hlam2)*hlam2**(n-1)
      write(2,*)'partition fn from eigs=',z
      do 2 i=2,n-1
      u(i,1,1)=1.
      u(i,1,2)=sigma
      u(i,1,3)=sigma
      u(i,2,1)=1.
      u(i,2,2)=sigma*psi
      u(i,2,3)=sigma*omeg
      u(i,3,1)=1.
      u(i,3,2)=sigma*omeg
2     u(i,3,3)=sigma*psi
c     write(2,*) 'statistical weight matrix for bond 2'
```

```
c       do 12 i=1,3
c12     write(2,*)(u(2,i,j),j=1,3)
c
c
c               calculation of equilibrium probabilities for interdependent pairs
c               starting from (2,3) pair up to (n-2,n-1)pair.
                do 1000 nbond=3,n-1
                do 10 kk=1,3
                do 10 ll=1,3
                do 20 i=1,3
                do 20 j=1,3
20              u(nbond,i,j)=0.
                u(nbond,kk,ll)=u(2,kk,ll)
                do 3 i=1,3
3               row(i)=rowj(i)
                do 801 ii=2,n-1
                do 4 i=1,3
                prod(i)=0.
                do 5 k=1,3
5               prod(i)=prod(i)+row(k)*u(ii,k,i)
4               continue
                do 6 i=1,3
6               row(i)=prod(i)
801             continue
10              p(nbond,kk,ll)=(row(1)+row(2)+row(3))/z
                do 21 i=1,3
                do 21 j=1,3
21              u(nbond,i,j)=u(2,i,j)
c               write(2,*)'probs for bond ',nbond
c               do 221 i=1,3
c221            write(2,*)(p(nbond,i,j),j=1,3)
1000            continue
c
c
c               for the pair (2,3) we use the following ranges
                ra1=p(3,1,1)
                ra2=ra1+p(3,1,2)
                ra3=ra2+p(3,1,3)
                ra4=ra3+p(3,2,1)
                ra5=ra4+p(3,2,2)
                ra6=ra5+p(3,2,3)
                ra7=ra6+p(3,3,1)
                ra8=ra7+p(3,3,2)
c
c
c               Calculation of cond probs and ranges for the remaining bonds
                do 1001 i=4,n-1
                do 22 j=1,3
22              ps(i-1,j)=p(i,j,1)+p(i,j,2)+p(i,j,3)
                do 23 k=1,3
                do 23 l=1,3
23              q(k,l)=p(i,k,l)/ps(i-1,k)
                d1(i)=q(1,1)
```

```
                d2(i)=d1(i)+q(1,2)
                d3(i)=q(2,1)
                d4(i)=d3(i)+q(2,2)
                d5(i)=q(3,1)
1001            d6(i)=d5(i)+q(3,2)
c1001                   write(2,*)i,d1(i),d2(i),d3(i),d4(i),d5(i),d6(i)
c               write(2,*)'buraya geldim'
c
c               Chain Generation
                do 13 iter=1,ngen
                do 40 i=1,3
                do 41 j=1,3
41              tt(i,j)=0.
40              tt(i,i)=1.
                r(1,1)=1.53
                r(1,2)=0.
                r(1,3)=0.
                fi(1)=0.
                call transf(t,b,theta)
                call mult(t,tt,sm)
                do 46 i=1,3
46              r(2,i)=r(1,i)+1.53*tt(i,1)
                call ran2(idum,ran)
c               write(2,*)'random # for the pair (2 3)=',ran
                a=ran
                if (a.gt.ra8) then
                fi(2)=gm
                fi(3)=gm
                else
                if (a.gt.ra7) then
                fi(2)=gm
                fi(3)=gp
                else
                if (a.gt.ra6) then
                fi(2)=gm
                fi(3)=tr
                else
                if (a.gt.ra5) then
                fi(2)=gp
                fi(3)=tr
                else
                if (a.gt.ra4) then
                fi(2)=gp
                fi(3)=gp
                else
                if (a.gt.ra3) then
                fi(2)=gp
                fi(3)=tr
                else
                if (a.gt.ra2) then
                fi(2)=tr
                fi(3)=gm
                else
```

```
            if (a.gt.ra1) then
            fi(2)=tr
            fi(3)=gp
            else
            fi(2)=tr
            fi(3)=tr
            endif
            endif
            endif
            endif
            endif
            endif
            endif
            endif
c           write(2,*)'fi(2)=',fi(2),' fi(3)=',fi(3)
            do 15 ij=2,3
            b=fi(ij)
            call mult(t,tt,sm)
            do 47 i=1,3
47          r(ij+1,i)=r(ij,i)+1.53*tt(i,1)
15          continue
            nbond=3
17          nprev=nbond
            nbond=nbond+1
            call ran2(idum,ran)
            a=ran
            if (fi(nprev).eq.tr) then
            if(a.le.d1(nbond)) fi(nbond)=tr
            if(a.gt.d2(nbond)) fi(nbond)=gm
            if(a.gt.d1(nbond).and.a.le.d2(nbond)) fi(nbond)=gp
            endif
            if (fi(nprev).eq.gp) then
            if(a.le.d3(nbond)) fi(nbond)=tr
            if(a.gt.d4(nbond)) fi(nbond)=gm
            if(a.gt.d3(nbond).and.a.le.d4(nbond)) fi(nbond)=gp
            endif
            if (fi(nprev).eq.gm) then
            if(a.le.d5(nbond)) fi(nbond)=tr
            if(a.gt.d6(nbond)) fi(nbond)=gm
            if(a.gt.d5(nbond).and.a.le.d6(nbond)) fi(nbond)=gp
            endif
            b=fi(nbond)
c           write(2,*)'a=',a,'fi=',fi(nbond),'for ',nbond
            call transf(t,b,theta)
            call mult(t,tt,sm)
            DO 446 iii=1,3
446         r(nbond+1,iii)=r(nbond,iii)+1.53*tt(iii,1)
            write(2,*)'r(',nbond,')=',(r(nbond,k),k=1,3),NGEN
            if(nbond.eq.(n-1)) go to 99
            go to 17
c
c
c           Calc of contribution of each generated chain to avg properties
```

```
c99         write(2,*)'chain',iter,'is generated'
99          do 18 i=1,3
            im=(n-1)/2+1
            in=(n-1)/2
            vm(i)=r(im,i)-r(in,i)
            end(i)=r(n,i)
c           write(2,*) vm(i),end(i)
18          cs(i)=vm(i)*end(i)

            endsq=end(1)**2+end(2)**2+end(3)**2
c           write(2,*)'endsq=',endsq
            do 19 i=1,3
19          cs(i)=cs(i)/1.53/endsq**.5
            csfi=cs(1)+cs(2)+cs(3)
            cssq=csfi**2
c           write(2,*)'cos fi=',csfi,' cos2fi=',cssq
            cs2av=cs2av+cssq
            r2cs=r2cs+endsq*cssq
            r4cs=r4cs+endsq**2.*cssq
            r6cs=r6cs+endsq**3.*cssq
            r8cs=r8cs+endsq**4.*cssq
            r2avg=r2avg+endsq
            r4avg=r4avg+endsq**2.
            r6avg=r6avg+endsq**3.
            r8avg=r8avg+endsq**4.
c           write(2,*)'  cos2 th =',cs2av
c           write(2,*)'  r2 cos2 th =',r2cs
c           write(2,*)'  r4 cos2 th=',r4cs
c           write(2,*)'  r6 cos2 th =',r6cs
c           write(2,*)'  r8cos2 th =',r8cs
c           write(2,*)'  r2  =',r2avg
c           write(2,*)'  r4  =',r4avg
c           write(2,*)'  r6  =',r6avg
c           write(2,*)'  r8  =',r8avg
13          continue
            cs2av=cs2av/ngen
            r2cs=r2cs/ngen
            r4cs=r4cs/ngen
            r6cs=r6cs/ngen
            r8cs=r8cs/ngen
            r2avg=r2avg/ngen
            r4avg=r4avg/ngen
            r6avg=r6avg/ngen
            r8avg=r8avg/ngen
            write(2,*)' < cos2 th >=',cs2av
            write(2,*)' < r2 cos2 th >=',r2cs
            write(2,*)' < r4 cos2 th >=',r4cs
            write(2,*)' < r6 cos2 th >=',r6cs
            write(2,*)' < r8cos2 th >=',r8cs
            write(2,*)' < r2  >=',r2avg
            write(2,*)' < r4  >=',r4avg
            write(2,*)' < r6  >=',r6avg
            write(2,*)' < r8  >=',r8avg
```

```
c
c
      close(2)
      stop
      end
      SUBROUTINE transf(t,b,theta)
      DIMENSION t(3,3)
      t(1,1)=COS(theta)
      t(1,2)=SIN(theta)
      t(1,3)=0.
      t(2,1)=SIN(theta)*COS(b)
      t(2,3)=SIN(b)
      t(2,2)=-COS(theta)*COS(b)
      t(3,1)=SIN(theta)*SIN(b)
      t(3,2)=-COS(theta)*SIN(b)
      t(3,3)=-COS(b)
      RETURN
      END
      SUBROUTINE mult(t,tt,sm)
      DIMENSION t(3,3),tt(3,3),sm(3,3)
      DO 21 I=1,3
      DO 21 K=1,3
21    sm(I,K)=tt(I,1)*t(1,K)+tt(I,2)*t(2,K)+tt(I,3)*t(3,K)
      DO 65 I=1,3
      do 65 K=1,3
65    tt(I,K)=sm(I,K)
      RETURN
      end
      subroutine ran2(idum,ran)
      parameter (m=714025,ia=1366,ic=150889,rm=1./m)
      dimension ir(97)
      data iff/0/
      if(idum.lt.0.or.iff.eq.0) then
      iff=1
      idum=mod(ic-idum,m)
      do 11 j=1,97
      idum=mod(ia*idum+ic,m)
      ir(j)=idum
11    continue
      idum=mod(ia*idum+ic,m)
      iy=idum
      endif
      j=1+(97*iy)/m
      if(j.gt.97.or.j.lt.1)pause
      iy=ir(j)
      ran=iy*rm
      idum=mod(ia*idum+ic,m)
      ir(j)=idum
      return
      end
```

```
C*************************************************************************
C                    Brownian Dynamics Simulation Program
C*************************************************************************

C  Program Brownian Dynamics integrates the Langevin equation by the
C  extended second order Runge-Kutta method. Program simulates the
C  dynamics of the model Pe chains with the fixed end-to-end separation. A
C  flexible chain model is adopted. The intramolecular forces due to the bond
C  stretching, bond bending and the bond rotation are included. It reads in
C  the initial coordinates of NN  atoms of a chain  generated by Monte Carlo
C Simulation. In the simulation, excluded volume effects and hydrodynamic
C  interactions are ignored.

C*************************************************************************
C*************************************************************************

C      CONSTANTS

C      A1,A2,B,elam: CONSTANTS IN EXTENTED RUNGE KUTTA
C      PSIG=2*BET*KB*T/MASS
C      NN: # OF BONDS IN THE CHAIN
C      NSTEP: # OF INCREMENTS, NBOND= # OF BONDS+4(NN+4)
C      CKL,CKTH, CKF : FORCE CONSTANTS OF BOND STRETCHING,
C       BOND BENDING AND BOND TORSION
C      CTH, CEL: BOND BENGING ANGLE(TETRAHEDRAL) AND BOND C
C                  LENGTH OF CC BOND
C      CA0,CA1,CA2,CA3,CA4,CA5 : CONSTANTS IN ROTATIONAL
C                                    POTENTIAL
C      BET=E/M;  E: FRICTION COEFFICIENT, M: MASS
C      S:  TIME INCREMENTS
C      CUBL=.153 NM/SQR(3.):  X,Y,Z INTERCEPTS OF THE BOND OF
C      LENGTH .153 NM
C      AVGN: AVAGADRO'S NUMBER
C      EKB: BOLTZMANN CONSTANT

C*************************************************************************

C      UNITS

C      BET(1/NS)
C      MASS(KG/MOL)
C      CKL/MASS(1/NS**2)
C      CKTH/MASS(J/KG)
C      CKFY/MASS(J/KG)
C      CTH(DEG)
C      CEL(NM)

C*************************************************************************

C      RRX(I), RRY(I), RRZ(I): x, y, z components of positon vector of i'th bond
                                  0≤i≤nn
```

```
C       RSX(I), RSY(I), RSZ(I)
C       and
C       RFX(I), RFY(I), RFZ(I): x, y, z components of positon vector of i' th bond
                                for manipulation in intermediate steps
C       DMAG: magnitude of end-to-end vector r
C       TGAUSX, TGAUSY, TGAUSZ: gaussian random variable in 3D
C       FY(I): rotation angle of i' th bond
C       TS(I),GPS(I), GMS(I): counters for t, g+ and g- respectively
C       LC: counter for  number isomeric transitions
C       TFX(I), TFY(I), TFZ(I): x, y, z components of total force due to bond
C                               stretching, bond bending and rotational potential
C       ELX(I), ELY(I), ELZ(I): x, y, z components of bond vector i
C       ELM(I): magnitude of bond vector i
C       D(K,L): dot product of k' th and l' th bond vectors
C       TH(I): bond angle of ı' th bond
C       ELCX(I), ELCY(I), ELCZ(I): x, y, z componens of cross product of i' th
C                                  and i -1' th bond vectors
C       ELCM(I): magnitude of cross products of i' th and i - 1' th bond vectors
C       ELCD(I): dot product of cross products i ' th and i - 1 ' th bond  and
C                cross products i - 1' th and i - 2 ' th bond vectors
C       GPM(I): to distinguish plus(+) and minus(-) rotation angles of i ' th bond
C       EKTH(I):  term for bond bending force
C       EX(I), EY(I), EZ(I): x, y, z components of term in bond bending and bond
C                            torsion force
C       ACAX, ACAY. ACAZ  and
C       ACBX, ACBY. ACBZ and
C       ACCX, ACCY. ACCZ  and
C       ACOMX, ACOMY, ACOMZ: x, y, z components of terms İn bond torsion
C                                  force
C       AAZ1, AAZ2, AAZ3: terms in bond torsion force
C       FYC: term in bond torsion force
C       FFYX(I), FFYY(I), FFYZ(I): x, y, z components of derivative of cosf(i)
C       FYX(I), FYY(I), FYZ(I): x, y, z components of ROTATIONAL bond  force
C       FLX(I), FLY(I), FLZ(I): x, y, z components of bond BENDİNG force
C       FTHX(I), FTHY(I), FTHZ(I): x, y, z components of bond ANGLE force

C*******************************************************************************
C*******************************************************************************

      PROGRAM BROWNIAN DYNAMICS

      DOUBLE PRECISION RRX(200),RRY(200),RRZ(200)
      DOUBLE PRECISION TFX(200),TFY(200)
      DOUBLE PRECISION TFZ(200),G1X(200),G1Y(200)
      DOUBLE PRECISION G1Z(200),G2X(200),G2Y(200)
      DOUBLE PRECISION G2Z(200),RFX(200),RFY(200),sumer(300)
      DOUBLE PRECISION RFZ(200),FY(100),TH(100),er(300)
      DOUBLE PRECISION TS(100),GPS(100),GMS(100),CORSM(100)
      DOUBLE PRECISION RSX(200),RSY(200),RSZ(200),G(200)
      DOUBLE PRECISION CORX(100,11),CORY(100,11),CORZ(100,11)
```

```
      DOUBLE PRECISION B,EKB,AVGN,TEMP,BET,EMASS,A1,A2,ELAM,P
      DOUBLE PRECISION CKTH,CKL,CKFY
      DOUBLE PRECISION CEL,CTH,CA0,CA1
      DOUBLE PRECISION CA2,CA3,CA4,CA5,CUBL,S

      COMMON CKTH,CKL,CKFY,CEL,CTH
      COMMON CA0,CA1,CA2,CA3,CA4,CA5

      INTEGER AX,AY,AZ,BX,BY,BZ,CX,CY,CZ,DX,DY,DZX
      INTEGER APX,APY,APZ,BPX,BPY,BPZ,CPX,CPY,CPZ,DPX,DPY,DPZ

      OPEN(7,FILE='fbl522.dat2')

      OPEN(8,FILE='fbl522.out4')
      OPEN(9,FILE='fbl522.out5')
      OPEN(10,FILE='fbl522.out6')


      READ(7,*)idum,B,EKB,AVGN,TEMP,BET,EMASS,A1,A2
      READ(7,*)ELAM,NSTEP,NN,S,CKTH,CKL,CKFY,CEL,CTH
      READ(7,*)CA0,CA1,CA2,CA3,CA4,CA5

      PSIG=2.*BET*EKB*TEMP/EMASS*AVGN
      CUBL=CEL/3.**.5

      WRITE(8,*)'IDUM',IDUM,' KB',EKB,' TEMP',TEMP
      WRITE(8,*)'*************************************************'
      WRITE(8,*)'BET',BET,' MASS',EMASS,' A1',A1,' A2',A2,'B',B
      WRITE(8,*)'*************************************************'
      WRITE(8,*)'NSTEP',NSTEP,' NN',NN,' S',S,'CKTH',CKTH,'CKL',CKL
      WRITE(8,*)'*************************************************'
      WRITE(8,*)'CKFY',CKFY,'CEL',CEL,'CTH',CTH,'CA5',CA5
      WRITE(8,*)'*************************************************'
      WRITE(8,*)'CA0',CA0,'CA1',CA1,'CA2',CA2,'CA3',CA3,'CA4',CA4
      WRITE(8,*)'*************************************************'
      WRITE(8,*)'PSIG',PSIG,'CUBL',CUBL
      WRITE(8,*)'*************************************************'


C     INITIALIZE THE ARRAYS

      LC=0.
      ns=0.

      DO 1411 K=1,NBONC+8
      TS(K)=0.
      GPS(K)=0.
      GMS(K)=0.
      RRX(K)=0.
      RRY(K)=0.
      RRZ(K)=0.
      RSX(K)=0.
      RSY(K)=0.
```

```
      RSZ(K)=0.
      G1X(K)=0.
      G1Y(K)=0.
      G1Z(K)=0.
      G2X(K)=0.
      G2Y(K)=0.
      G2Z(K)=0.
      RFX(K)=0.
      RFY(K)=0.
      RFZ(K)=0.
      G(K)=0.
1411  CONTINUE

      do 1119 i=1,300
      sumer(i)=0
      er(i)=0
1119  continue

C     NN=NUMBER OF BONDS IN THE CHAIN, NN IS SHIFTED BY FOUR
C     TO NBONC FOR EASE OF COMPUTATION

      nbonc=nn+4
      do 645 i=5,nbonc
      read(7,*)rrx(i),rry(i),rrz(i)
645   continue

      DO 624 I=5,NBONC
      RSX(I)=RRX(I)
      RSY(I)=RRY(I)
      RSZ(I)=RRZ(I)

c     WRITE(2,50)RSX(I),RSY(I),RSZ(I)
624   CONTINUE

50    FORMAT(3F20.16)

C     MAGNITUDE OF THE END-TO-END VECTOR OF THE CHAIN

      DMAG=((RRX(NBONC))**2+(RRY(NBONC))**2
     +  +(RRZ(NBONC))**2)**.5

      WRITE(2,*)'DMAG',DMAG


      WRITE(2,*)'************************************************'
      WRITE(2,*)'BOND',' TRANS',' GAUCHE +',' GAUCHE-'
      WRITE(2,*)'************************************************'


C     BEGINNING OF THE MAIN PROGRAM

C     START OF TIME-STEP LOOP
```

```
      DO 101 JA=1,NSTEP


      WRITE(2,*)'*************************************************'
      WRITE(2,*)'NSTEP',JA
      WRITE(2,*)'*************************************************'

C     START OF BOND LOOP

      DO 890 I=5,NBONC
      RRX(I)=RSX(I)
      RRY(I)=RSY(I)
      RRZ(I)=RSZ(I)
890   CONTINUE


      DO 1002 I=1,NBONC
      RFX(I)=RRX(I)
      RFY(I)=RRY(I)
      RFZ(I)=RRZ(I)
C     WRITE(2,*)RFX(I),RFY(I),RFZ(I)
1002  CONTINUE

C     START OF BOND LOOP

      DO 102 I=5,NBONC
C
      DO 302 K=1,1

      RFX(I-K)=RRX(I-K)
      RFY(I-K)=RRY(I-K)
      RFZ(I-K)=RRZ(I-K)
302   CONTINUE

      PSIG=2.*BET*EKB*TEMP/EMASS*AVGN
C
C     DO 1001 K=1,NBONC
C     WRITE(2,*)'RFX',RFX(K),K,' RFY',RFY(K),' RFZ',RFZ(K),'I',I
C1001       CONTINUE
C

C     FUNCTION GAUSS RETURNS A NORMAL RANDOM VARIATE

      TGAUSX=GAUSS(idum)
      TGAUSY=GAUSS(idum)
      TGAUSZ=GAUSS(idum)

C     write(6,*)'ga',tgausx,tgausy,tgausz,i,ja

C     SUBROUTINE FORCE RETURNS THE TOTAL FORCE(TFX, TFY, TFZ)
C     ACTING ON (I)TH ATOM AFTER  FIRST PERTURBATION

      CALL FORCE (nbonc,JA,I,RFX,RFY,RFZ,TFX,TFY,TFZ,FY)
```

```
      PSIG=2.*BET*EKB*TEMP/EMASS*AVGN

C     TO KEEP END ATOMS FIXED

      if(i.eq.5.or.i.eq.nbonc)then
      tfx(i)=0
      tfy(i)=0
      tfz(i)=0
      psig=0
      endif

      G1X(I)=1./BET*TFX(I)
      G1Y(I)=1./BET*TFY(I)
      G1Z(I)=1./BET*TFZ(I)

C     POSITION VECTOR OF (I)TH ATOM AFTER FIRST PERTURBATION


      RFX(I)=RFX(I)+G1X(I)*S*B+S**.5*PSIG**.5*ELAM*TGAUSX/BET
      RFY(I)=RFY(I)+G1Y(I)*S*B+S**.5*PSIG**.5*ELAM*TGAUSY/BET
      RFZ(I)=RFZ(I)+G1Z(I)*S*B+S**.5*PSIG**.5*ELAM*TGAUSZ/BET

       IF(JA.EQ.NB)THEN
      SUMFY=SUMFY+COS(FY(I)*3.141592654/180.)
C      WRITE(2,*)COS(FY(I)*3.14/180),I
       ENDIF

C     TO SET A COUNTER TO ASSES THE TIME-STEPS THAT EACH ATOM
C     SURVIVES IN THE STATES T,G+, G-

      IF(JA.EQ.1)THEN
      WRITE(8,*)' FY',FY(I),' I',I,' JA',JA
      ENDIF
      IF(FY(I).LE.60.0.AND.FY(I).GE.-60.0) THEN
      TS(I)=TS(I)+1
      IF(TS(I).EQ.1) THEN
      LC=LC+1
c     WRITE(2,*)I, TS(I), GPS(I), GMS(I),' NSTEP', JA,' LC', LC
      GPS(I)=0
      GMS(I)=0
      ENDIF
      ENDIF
C
      IF(FY(I).GT.60.0) THEN
      GPS(I)=GPS(I)+1
      IF(GPS(I).EQ.1) THEN
      LC=LC+1
c      WRITE(2,*)I,  TS(I), GPS(I), GMS(I),' NSTEP', JA,' LC', LC
      TS(I)=0
      GMS(I)=0
      ENDIF
      ENDIF
```

```
      RSX(I)=RRX(I)+S*(A1*G1X(I)+A2*G2X(I))
     + +S**.5*PSIG**.5*ELAM*TGAUSX/BET
      RSY(I)=RRY(I)+S*(A1*G1Y(I)+A2*G2Y(I))
     + +S**.5*PSIG**.5*ELAM*TGAUSY/BET
      RSZ(I)=RRZ(I)+S*(A1*G1Z(I)+A2*G2Z(I))
     + +S**.5*PSIG**.5*ELAM*TGAUSZ/BET


102   CONTINUE

C     EEND OF BOND LOOP

      jt=jtt*1000
       if(ja.eq.jt)then
      write(6,*)'ja',ja
      if(ja.lt.300000)then
      go to 8011
      endif
      if(ja.ge.300000.and.ja.lt.600000)then
      go to 5080
      endif
      if(ja.ge.600000)then
      go to 5090
      endif

8011  DO 2510 K=15,35
      WRITE(8,*)RSX(K),RSY(K),RSZ(K),K,ja

2510  CONTINUE

       go to 2090


5080  DO 2610 K=15,35
      WRITE(9,*)RSX(K),RSY(K),RSZ(K),K,ja

2610  CONTINUE

      go to 2090


5090  DO 2710 K=15,35
      WRITE(10,*)RSX(K),RSY(K),RSZ(K),K,ja

2710  CONTINUE


      endif
2090   if(ja.gt.jt)then
      jtt=jtt+1
      endif
```

```
C
      IF(FY(I).LT.-60.0) THEN
      GMS(I)=GMS(I)+1
      IF(GMS(I).EQ.1) THEN
      LC=LC+1
c     WRITE(2,*)I, TS(I), GPS(I), GMS(I),' NSTEP', JA,' LC', LC
      TS(I)=0
      GPS(I)=0
      ENDIF
      ENDIF
C


      do 789 k=1,20
      er(k)=k*20-200
789   continue

      do 9999 k=1,20
      if(fy(i).lt.er(k+1).and.fy(i).ge.er(k))then
      sumer(k)=sumer(k)+1
      endif
9999  continue

C     SUBROUTINE FORCE RETURNS THE TOTAL FORCE(TFX, TFY, TFZ)
C     ACTING ON (I)TH ATOM AFTER  SECOND  PERTURBATION

      CALL FORCE (nbonc,JA,I,RFX,RFY,RFZ,TFX,TFY,TFZ,FY)

      PSIG=2.*BET*EKB*TEMP/EMASS*AVGN

C     TO KEEP END ATOMS FIXED

       if(i.eq.5.or.i.eq.nbonc)then
      tfx(i)=0
      tfy(i)=0
      tfz(i)=0
      psig=0
      endif
      G2X(I)=1./BET*TFX(I)
      G2Y(I)=1./BET*TFY(I)
      G2Z(I)=1./BET*TFZ(I)
C
C     WRITE(2,*)'OLD COORDINATES OF THE CHAIN'
C     WRITE(2,*)'RSX',RSX(I),'I',I,'NSTEP',JA
C     WRITE(2,*)'RSY',RSY(I),'I',I,'NSTEP',JA
C     WRITE(2,*)'RSZ',RSZ(I),'I',I,'NSTEP',JA
C     WRITE(2,*)'*******************************************'
C     ENDIF
C     ENDIF


C     NEW COORDINATES OF  (I)TH BOND AFTER JA'TH TIME STEP
```

```
101   CONTINUE

C     END OF TIME-STEP LOOP

      DO 2910 K=5,NBONC
      WRITE(8,*)RSX(K),RSY(K),RSZ(K)
2910  CONTINUE
C
55    FORMAT(3F19.15)
      DO 2921 K=5,NBONC
      WRITE(8,*)TS(K),GPS(K),GMS(K)
2921  CONTINUE
C
      DO 8887 K=1,50
      write(6,*)sumer(k), k, er(k)
      write(8,*)sumer(k), k, er(k)
8887  continue

C
      CLOSE(2)
      CLOSE(8)
      CLOSE(1)
C
      STOP
      END


C     SUBROUTINE FORCE RETURNS THE TOTAL
C     FORCE(TFX,TFY,TFZ)ACTING ON(I)TH ATOM DUE TO THE BOND
C     STRETCHING, BOND BENDING AND BOND ROTATIONAL
C     POTENTIAL. THAT IS THE FORCE ON THE ATOM(I) DUE TO THE
C     PRESENCE OF THE CARTESIAN COORDINATE Xi,Yi, Zi  IN THE
C     GENERALIZED COORDINATES Li+k, THi+k AND  Fi+k,
C      k=0,1 for Li+k, bond length
C      k=0-2 for THi+k, bond angle
C      k=0-3 for Fi+k, bond torsional angle


      SUBROUTINE FORCE(nbonc,JA,I,RFX,RFY,RFZ,TFX,TFY,TFZ,FY)

      DOUBLE PRECISION RFX(200),RFY(200),RFZ(200),EKTH(10)
      DOUBLE PRECISION EKFY(10),ELX(10),ELY(10),ELZ(10)
      DOUBLE PRECISION ELM(10),ELCX(10),ELCY(10)
      DOUBLE PRECISION ELCZ(10),ELCM(10),ELCD(10),TH(100)
      DOUBLE PRECISION FY(100),EX(10),EY(10),EZ(10)
      DOUBLE PRECISION D(150,150),A(150,150),FLX(10),FLY(10)
      DOUBLE PRECISION FLZ(10),FTHX(20),FTHY(20),FTHZ(20)
      DOUBLE PRECISION FFYX(10),FFYY(10),FFYZ(10),FYX(10)
      DOUBLE PRECISION FYY(10),FYZ(10),GPM(100)
      DOUBLE PRECISION TFX(200),TFY(200),TFZ(200),FAYY(100)
```

```
      DOUBLE PRECISION ACAX,ACAY,ACAZ,ACBX,ACBY,ACBZ,ACCX
      DOUBLE PRECISION ACCY,ACCZ,ACOMX,ACOMY,ACOMZ,ACOM

      DOUBLE PRECISION CKTH,CKL,CKFY,CEL,CTH,CA0,CA1
      DOUBLE PRECISION CA2,CA3,CA4,CA5,P,FYC
      DOUBLE PRECISION AAX1,AAX2,AAY1,AAY2,AAZ1,AAZ2

      REAL MA(3),NA(3),LA(3)

      COMMON CKTH,CKL,CKFY,CEL,CTH
      COMMON CA0,CA1,CA2,CA3,CA4,CA5


      ni=i+3
      if(i.eq.nbonc)then
      ni=i
      endif
      if(i.eq.nbonc-1)then
      ni=i+1
      endif
      if(i.eq.nbonc-2)then
      ni=i+2
      endif
      if(i.eq.nbonc-3)then
      ni=i+3
      endif

C     INITIALIZE THE ARRAYS

      DO 5001 K=I-3,ni
      GPM(K)=0.
      FTHX(K)=0.
      FTHY(K)=0.
      FTHZ(K)=0.
      FYX(K)=0.
      FYY(K)=0.
      FYZ(K)=0.
      FFYX(K)=0.
      FFYZ(K)=0.
      FFYY(K)=0.
      ELCX(K)=0.
      ELCY(K)=0.
      ELCZ(K)=0.
      ELCM(K)=0.
      ELX(K)=0.
      ELY(K)=0.
      ELZ(K)=0.
      ELM(K)=0.
      TH(K)=0.
      ELCD(K)=0.
      FY(K)=0.
      FAYY(K)=0
      EKTH(K)=0.
```

```
      EX(K)=0.
      EY(K)=0.
      EZ(K)=0.
      FLX(K)=0.
      FLY(K)=0.
      FLZ(K)=0.0
      TFX(K)=0.
      TFY(K)=0.
      TFZ(K)=0.
      EKFY(K)=0.
5001   CONTINUE
C
      MA(1)=0.
      NA(1)=0.
      LA(1)=0.
      MA(2)=0.
      NA(2)=0.
      LA(2)=0.
C
      DO 5002 K=I-3,ni
      DO 5003 L=I-3,ni
      D(K,L)=0.
      D(L,K)=0.
      A(K,L)=0.
      A(L,K)=0.
5003   CONTINUE
5002   CONTINUE

C     BOND VECTOR OF (I)TH ATOM,L

      DO 101 K=I-2,ni
      ELX(K)=RFX(K)-RFX(K-1)
      ELY(K)=RFY(K)-RFY(K-1)
      ELZ(K)=RFZ(K)-RFZ(K-1)
c     WRITE(2,*)'ELX',ELX(K),ELY(K),ELZ(K),'K',k,'ni',ni
101    CONTINUE
C     WRITE(2,*)'***********************************************'


C     MAGNITUDE OF BOND VECTOR,L

      may=i-2
      if(i.eq.5.or.i.eq.6)then
       may=5
      endif

      DO 102 K=may,ni
      ELM(K)=(ELX(K)**2+ELY(K)**2+ELZ(K)**2)**.5
c     WRITE(2,*)'ELM',ELM(K),'ni',ni
102    CONTINUE
C     WRITE(2,*)'***********************************************'

C     DOT PRODUCT OF (I)TH AND (I-1)TH BOND VECTORS
```

```
C       DEFINITION FOR D(I, J), DOT PRODUCT OF (I)TH AND (J)TH CC
        VECTORS

192     if(i.lt.6)then
        go to 199
        endif
        may=i-2
      if(i.eq.6)then
      may=5
        endif
        DO 108 K=may,ni-1
        DO 109 L=K+1,ni
        D(K,L)=ELX(K)*ELX(L)+ELY(K)*ELY(L)+ELZ(K)*ELZ(L)
        D(L,K)=D(K,L)
c       WRITE(2,*)'D',D(K,L),'K',K,'L',L
109     CONTINUE
108     CONTINUE
C       WRITE(2,*)'***********************************************'
C
C       THE ANGLE BETWEEN (I)TH AND (I-1)TH BOND VECTORS

        may=i-1
        if(i.eq.6)then
        may=5
        endif

        DO 501 K=may,ni
        TH(K)=(ACOS(D(K,K-1)/(ELM(K)*ELM(K-1))))*180./3.141592654
c       WRITE(2,*)'TH',TH(K),K
501     CONTINUE
C       WRITE(2,*)'THK***********************************************'
C

        if(i.lt.7)then
        go to 197
        endif



C       CROSS PRODUCT OF (I) AND (I-1)TH BOND VECTORS
C
        DO 104 K=I-1,ni
        ELCX(K)=ELY(K)*ELZ(K-1)-ELZ(K)*ELY(K-1)
        ELCY(K)=-(ELX(K)*ELZ(K-1)-ELZ(K)*ELX(K-1))
        ELCZ(K)=ELX(K)*ELY(K-1)-ELY(K)*ELX(K-1)
c       WRITE(2,*)ELCX(K),ELCY(K),ELCZ(K),k
104     CONTINUE
C       WRITE(2,*)'***********************************************'


C       MAGNITUDE OF CROSS PRODUCT OF (I)TH AND (I-1)TH BOND
C       VECTORS
```

```
      DO 105 K=I-1,ni
      ELCM(K)=ELM(K)*ELM(K-1)*SIN(TH(K)*3.141592654/180.)
c     WRITE(2,*)'ELCM',ELCM(K),K
105   CONTINUE
C     WRITE(2,*)'ELM*********************************************'


C     DOT PRODUCT OF TWO CROSS PRODUCTS

193   if(i.lt.7)then
      go to 197
      endif

      DO 502 K=I,ni
      ELCD(K)=ELCX(K)*ELCX(K-1)+ELCY(K)*ELCY(K-1)
     + +ELCZ(K)*ELCZ(K-1)
c     WRITE(2,*)'ELCD',ELCD(K)
502   CONTINUE
C     WRITE(2,*)'*********************************************'

      DO 3456 K=I,ni
      GPM(K)=ELCX(K-1)*ELX(K)+ELCY(K-1)*ELY(K)+ELCZ(K-1)*ELZ(K)
c     WRITE(2,*)'GPM',GPM(K),'K',K
3456        CONTINUE


C     TORSIONAL ANGLE FOR (I)TH BOND

      DO 503 K=I,ni
      FAYY(K)=((-ELCD(K)/ELCM(K)/ELCM(K-1)))
c     WRITE(2,*)'FAYY',FAYY(K),K,JA
      IF(FAYY(K).GT.1.)THEN
      FAYY(K)=1.
      ENDIF
      IF(FAYY(K).LT.-1.)THEN
      FAYY(K)=-1.
      ENDIF
      FY(K)=(ACOS(FAYY(K))*180./3.141592654)
c     WRITE(2,*)'FY',FY(K)
C
      IF(GPM(K).LT.0.0000000)THEN
      FY(K)=-FY(K)
      ENDIF
503   CONTINUE

C     WRITE(2,*)'*************************************************'

C     DEFINITION FOR EKTH(I), NECESSARY FOR THE CALCULATION OF
C     THE FORCE DUE TO BOND BENDING


197   if(i.lt.6)then
      go to 198
```

```
      endif

      DO 106 K=I,ni
      EKTH(K)=CKTH*(COS(TH(K)*3.141592654/180.)
     + -COS(CTH*3.141592654/180.))/ELM(K)/ELM(K-1)
106   CONTINUE
C     WRITE(2,*)'***********************************************'


C     DEFINITION FOR E(I), NECESSARY FOR THE CALCULATION OF THE
C     FORCE  DUE TO BOND BENDING

      DO 107 K=I,ni
      EX(K)=ELX(K)/ELM(K)**2
      EY(K)=ELY(K)/ELM(K)**2
      EZ(K)=ELZ(K)/ELM(K)**2
107   CONTINUE


C     DEFINITION FOR A(IJ), NECESSARY FOR THE CALCULATION OF
C     THE FORCE  DUE TO BOND  ROTATIOND


      DO 210 K=I-1,ni-1
      DO 211 L=K+1,ni
      A(K,L)=(ELM(K)**2*ELM(L)**2-D(K,L)**2)
      A(L,K)=A(K,L)
211   CONTINUE
210   CONTINUE
C     WRITE(2,*)'***********************************************'


C     DEFINITION FOR EKFY(I), NECESSARY FOR THE CALCULATION OF
C     THE FORCE DUE TO BOND ROTATION,1/A/B


198   if(i.lt.7)then
      go to 199
      endif

      DO 212 K=I,ni
      EKFY(K)=-1./ELCM(K)/ELCM(K-1)
c     WRITE(2,*)'EKFY(K)',EKFY(K)
212   CONTINUE
C     WRITE(2,*)'***********************************************'

C     CONTRIBUTION TO ROTATIONAL FORCE ON (I)TH  ATOM
C     FROM THE ROTIONAL FORCE ON (I+1)TH ATOM DUE TO
C     PRESENCE OF Xi,Yi AND Zi IN THE GENERALIZED COORDINATE,
C     ROTATIONAL ANGLE Fi+1

C
      if(i.gt.(nbonc-1))then
```

```
      go to 1911
      endif

      ACAX=D(I,I-1)*ELX(I-1)-ELM(I-1)**2*ELX(I)
      ACAY=D(I,I-1)*ELY(I-1)-ELM(I-1)**2*ELY(I)
      ACAZ=D(I,I-1)*ELZ(I-1)-ELM(I-1)**2*ELZ(I)

      ACBX=D(I+1,I)*ELX(I)-ELM(I)**2*ELX(I+1)
      ACBY=D(I+1,I)*ELY(I)-ELM(I)**2*ELY(I+1)
      ACBZ=D(I+1,I)*ELZ(I)-ELM(I)**2*ELZ(I+1)

      ACCX=D(I+1,I)*ELX(I+1)-ELM(I+1)**2*ELX(I)
      ACCY=D(I+1,I)*ELY(I+1)-ELM(I+1)**2*ELY(I)
      ACCZ=D(I+1,I)*ELZ(I+1)-ELM(I+1)**2*ELZ(I)

      ACOM=ELM(I)**2*D(I-1,I+1)-D(I,I-1)*D(I,I+1)

C     WRITE(2,*)'ACOM',ACOM
C     WRITE(2,*)'***********************************************'

      ACOMX=-D(I,I-1)*ELX(I+1)+2.*ELX(I)*D(I-1,I+1)
     + +ELX(I)*D(I,I-1)-ELX(I-1)*ELM(I)**2-ELX(I-1)*D(I,I+1)

      ACOMY=-D(I,I-1)*ELY(I+1)+2.*ELY(I)*D(I-1,I+1)
     + +ELY(I)*D(I,I-1)-ELY(I-1)*ELM(I)**2-ELY(I-1)*D(I,I+1)

      ACOMZ=-D(I,I-1)*ELZ(I+1)+2.*ELZ(I)*D(I-1,I+1)
     + +ELZ(I)*D(I,I-1)-ELZ(I-1)*ELM(I)**2-ELZ(I-1)*D(I,I+1)
C     WRITE(2,*)'ACOMX',ACOMX
C     WRITE(2,*)'ACOMY',ACOMY
C     WRITE(2,*)'ACOMZ',ACOMZ
C     WRITE(2,*)'***********************************************'

      FFYX(I+1)=((ACAX/ELCM(I)**2+(-ACBX
     + +ACCX)/ELCM(I+1)**2)*ACOM+ACOMX)*EKFY(I+1)

      FFYY(I+1)=((ACAY/ELCM(I)**2+(-ACBY
     + +ACCY)/ELCM(I+1)**2)*ACOM+ACOMY)*EKFY(I+1)
      FFYZ(I+1)=((ACAZ/ELCM(I)**2+(-ACBZ
     + +ACCZ)/ELCM(I+1)**2)*ACOM+ACOMZ)*EKFY(I+1)

C     WRITE(2,*)'FFYX(I+1)',FFYX(I+1)
C     WRITE(2,*)'FFYY(I+1)',FFYY(I+1)
C     WRITE(2,*)'FFYZ(I+1)',FFYZ(I+1)
C     WRITE(2,*)'1ST STEP***************************************'

C     CONTRIBUTION TO ROTATIONAL FORCE ON (I)TH ATOM
C     FROM THE ROTIONAL FORCE ON (I+2)TH ATOM DUE TO
C     PRESENCE OF Xi,Yi AND Zi IN THE GENERALIZED COORDINATE,
C     ROTATIONAL ANGLE Fi+2


1911  if(i.gt.(nbonc-2))then
```

```
      go to 1919
      endif

      ACAX=D(I+1,I)*ELX(I)-ELM(I)**2*ELX(I+1)
      ACAY=D(I+1,I)*ELY(I)-ELM(I)**2*ELY(I+1)
      ACAZ=D(I+1,I)*ELZ(I)-ELM(I)**2*ELZ(I+1)

      ACBX=D(I+1,I)*ELX(I+1)-ELM(I+1)**2*ELX(I)
      ACBY=D(I+1,I)*ELY(I+1)-ELM(I+1)**2*ELY(I)
      ACBZ=D(I+1,I)*ELZ(I+1)-ELM(I+1)**2*ELZ(I)

      ACCX=D(I+2,I+1)*ELX(I+2)-ELM(I+2)**2*ELX(I+1)
      ACCY=D(I+2,I+1)*ELY(I+2)-ELM(I+2)**2*ELY(I+1)
      ACCZ=D(I+2,I+1)*ELZ(I+2)-ELM(I+2)**2*ELZ(I+1)

      ACOM=ELM(I+1)**2*D(I,I+2)-D(I+1,I+2)*D(I,I+1)
C     WRITE(2,*)'***********************************************'


      ACOMX=-D(I,I+1)*ELX(I+2)+2.*ELX(I+1)*D(I,I+2)
     + +ELX(I+1)*D(I+1,I+2)-ELX(I+2)*ELM(I+1)**2
     + -ELX(I)*D(I+2,I+1)

      ACOMY=-D(I,I+1)*ELY(I+2)+2.*ELY(I+1)*D(I,I+2)
     + +ELY(I+1)*D(I+1,I+2)-ELY(I+2)*ELM(I+1)**2
     + -ELY(I)*D(I+2,I+1)

      ACOMZ=-D(I,I+1)*ELZ(I+2)+2.*ELZ(I+1)*D(I,I+2)
     + +ELZ(I+1)*D(I+1,I+2)-ELZ(I+2)*ELM(I+1)**2
     + -ELZ(I)*D(I+2,I+1)

C     WRITE(2,*)'ACOMX',ACOMX
C     WRITE(2,*)'ACOMY',ACOMY
C     WRITE(2,*)'ACOMZ',ACOMZ
C     WRITE(2,*)'***********************************************'

      FFYX(I+2)=-EKFY(I+2)*((((ACAX
     + -ACBX)/ELCM(I+1)**2
     + +ACCX/ELCM(I+2)**2)*ACOM)+ACOMX)

      FFYY(I+2)=-EKFY(I+2)*((((ACAY
     + -ACBY)/ELCM(I+1)**2
     + +ACCY/ELCM(I+2)**2)*ACOM)+ACOMY)

      FFYZ(I+2)=-EKFY(I+2)*((((ACAZ
     + -ACBZ)/ELCM(I+1)**2
     + +ACCZ/ELCM(I+2)**2)*ACOM)+ACOMZ)

C     WRITE(2,*)'FFYX(I+2)',FFYX(I+2)
C     WRITE(2,*)'FFYY(I+2)',FFYY(I+2)
C     WRITE(2,*)'FFYZ(I+2)',FFYZ(I+2)
C     WRITE(2,*)'2ND STEP*********************************************'
```

```
C       CONTRIBUTION TO ROTATIONAL FORCE ON (I)TH  ATOM
C       FROM THE ROTIONAL FORCE ON (I)TH  AND (I+1)ATOM DUE TO
C       PRESENCE OF Xi,Yi AND Zi IN THE GENERALIZED COORDINATE,
C       ROTATIONAL ANGLE Fi AND Fi+3

1919  MA(1)=I
      NA(1)=I-1
      LA(1)=I-2
      MA(2)=I+1
      NA(2)=I+2
      LA(2)=I+3

      DO 213 K=1,2

      if(k.eq.2.and.i.gt.(nbonc-3))then
      go to 213
      endif
      P=(D(MA(K),LA(K))*ELM(NA(K))**2)
     +  -D(NA(K),LA(K))*D(MA(K),NA(K))

      AAX1=(D(MA(K),NA(K))*ELX(NA(K))-ELM(NA(K))**2*ELX(MA(K)))
       AAX2=(ELM(NA(K))**2*ELX(LA(K)))-D(NA(K),LA(K))*ELX(NA(K))
      FFYX(I+3*K-3)=(AAX1*(P)/A(MA(K),NA(K))
     +  +AAX2)*(-1.)**(K+1)*EKFY(I+3*K-3)

      AAY1=(D(MA(K),NA(K))*ELY(NA(K))-ELM(NA(K))**2*ELY(MA(K)))
       AAY2=(ELM(NA(K))**2*ELY(LA(K)))-D(NA(K),LA(K))*ELY(NA(K))
      FFYY(I+3*K-3)=(AAY1*(P)/A(MA(K),NA(K))
     +  +AAY2)*(-1.)**(K+1)*EKFY(I+3*K-3)

      AAZ1=(D(MA(K),NA(K))*ELZ(NA(K))-ELM(NA(K))**2*ELZ(MA(K)))
       AAZ2=(ELM(NA(K))**2*ELZ(LA(K)))-D(NA(K),LA(K))*ELZ(NA(K))
      FFYZ(I+3*K-3)=(AAZ1*(P)/A(MA(K),NA(K))
     +  +AAZ2)*(-1.)**(K+1)*EKFY(I+3*K-3)

213   CONTINUE

C       WRITE(2,*)'*******************************************'

C       FORCE DUE TO BOND ROTATION

      DO 701 K=I,ni

      FYC=CA1+2.*CA2*FAYY(K)+3.*CA3*FAYY(K)**2
     + +4.*CA4*FAYY(K)**3+5.*CA5*FAYY(K)**4

      FYX(K)=CKFY*FFYX(K)*FYC

      FYY(K)=CKFY*FFYY(K)*FYC

      FYZ(K)=CKFY*FFYZ(K)*FYC

C       WRITE(2,*)'FYC',FYC
```

```
C       WRITE(2,*)'FYX(K)',FYX(K),'FYY(K)',FYY(K),'FYZ(K)',FYZ(K)
701     CONTINUE


C       CONTRIBUTION TO BOND STRETCHING FORCE ON (I)TH  ATOM
C       FROM THE BOND STRETCHING  FORCE ON (I) AND (I+1)TH ATOM
C       DUE TO RESENCE OF Xi,Yi AND Zi IN THE GENERALIZED
C       COORDINATE, Li AND Li+1

199     DO 1495 K=1,2

        if(k.eq.2.and.i.gt.(nbonc-1))then
        go to 1495
        endif
        FLX(I+K-1)=(-1.)**(K)*CKL*ELX(I+K-1)*(1.-CEL/ELM(I+K-1))
        FLY(I+K-1)=(-1.)**(K)*CKL*ELY(I+K-1)*(1.-CEL/ELM(I+K-1))
        FLZ(I+K-1)=(-1.)**(K)*CKL*ELZ(I+K-1)*(1.-CEL/ELM(I+K-1))
1495    CONTINUE
C       WRITE(2,*)'*********************************************'


C       CONTRIBUTION TO BOND BENDING FORCE ON (I)TH  ATOM
C       FROM THE BOND BENDING  FORCE ON (I)TH ATOM DUE TO
C       PRESENCE OF Xi,Yi AND Zi IN THE GENERALIZED COORDINATE,
C       BOND ANGLE THi

        if(i.lt.6)then
        go to 9101
        endiF

        FTHX(I)=-EKTH(I)*(ELX(I-1)-D(I,I-1)*EX(I))
        FTHY(I)=-EKTH(I)*(ELY(I-1)-D(I,I-1)*EY(I))
        FTHZ(I)=-EKTH(I)*(ELZ(I-1)-D(I,I-1)*EZ(I))
C       WRITE(2,*)'*********************************************'

9101    if(i.lt.6.or.i.gt.(nbonc-1))then
        go to 191
        endif


C       CONTRIBUTION TO BOND BENDING FORCE ON (I)TH  ATOM
C       FROM THE BOND BENDING  FORCE ON (I+1)TH ATOM DUE TO
C       PRESENCE OF Xi,Yi AND Zi IN THE GENERALIZED COORDINATE,
C       BOND ANGLE THi+1


        FTHX(I+1)=-EKTH(I+1)*(ELX(I+1)-ELX(I)
     + +D(I,I+1)*(EX(I+1)-EX(I)))
        FTHY(I+1)=-EKTH(I+1)*(ELY(I+1)-ELY(I)
     + +D(I,I+1)*(EY(I+1)-EY(I)))
        FTHZ(I+1)=-EKTH(I+1)*(ELZ(I+1)-ELZ(I)
     + +D(I,I+1)*(EZ(I+1)-EZ(I)))
C       WRITE(2,*)'*********************************************'
```

```
191   if(i.lt.6.or.i.gt.(nbonc-2))then
      go to 123
      endif


C     CONTRIBUTION TO BOND BENDING FORCE ON (I)TH  ATOM
C     FROM THE BOND BENDING  FORCE ON (I+2)TH ATOM DUE TO
C     PRESENCE OF Xi,Yi AND Zi IN THE GENERALIZED COORDINATE,
C     BOND ANGLE THi+2


      FTHX(I+2)=EKTH(I+2)*(ELX(I+2)-D(I+1,I+2)*EX(I+1))
      FTHY(I+2)=EKTH(I+2)*(ELY(I+2)-D(I+1,I+2)*EY(I+1))
      FTHZ(I+2)=EKTH(I+2)*(ELZ(I+2)-D(I+1,I+2)*EZ(I+1))
C     WRITE(2,*)'*****************************************'

C     X,Y,Z COMPONENTS OF THE TOTAL FORCE

123   TFX(I)=FLX(I)+FLX(I+1)+FTHX(I)+FTHX(I+1)+FTHX(I+2)
     + +FYX(I)+FYX(I+1)+FYX(I+2)+FYX(I+3)

      TFY(I)=FLY(I)+FLY(I+1)+FTHY(I)+FTHY(I+1)+FTHY(I+2)
     + +FYY(I)+FYY(I+1)+FYY(I+2)+FYY(I+3)

      TFZ(I)=FLZ(I)+FLZ(I+1)+FTHZ(I)+FTHZ(I+1)+FTHZ(I+2)
     + +FYZ(I)+FYZ(I+1)+FYZ(I+2)+FYZ(I+3)

C     WRITE(2,*)'TFX(I)',TFX(I),TFY(I),TFZ(I)

      RETURN
      END



C*******************************************************************************

C     FUNCTION GAUSS RETURNS A UNIFORM RANDOM VARIATE FROM
C     A DISTRIBUTION OF ZERO MEAN AND UNIT VARIANCE

C*******************************************************************************

      REAL FUNCTION GAUSS(idum)
      REAL A1,A3,A5,A9,A7
      PARAMETER(A1=3.949846138,A3=0.25240874)
      PARAMETER(A5=0.076542912,A7=0.008355968)
      PARAMETER(A9=0.029899776)
      DOUBLE PRECISION SUM,R,R2
      INTEGER I
      SUM=0.0
      DO 1000 I=1,12
C      v=RAN(idum)
C     write(6,*)'v',v
```

```
90      CALL RAN2(idum,ranv)
C       write(8,*)'ranv',ranv
        if(ranv.gt.1.or.ranv.lt.0)then
         idum=idum-1
        go to 90
        endif
C       WRITE(2,*)'RANV',RANV
       SUM=SUM+v
1000  CONTINUE
         R=(SUM-6.0)/4.0
        R2=R*R
         GAUSS=((((A9*R2+A7)*R2+A5)*R2+A3)*R2+A1)*R
C      WRITE(8,*)'GAUSS',GAUSS
       RETURN
       END


C*******************************************************************************

C      SUBROUTINE RAN2 RETURNS A RANDOM NUMBER BETWEEN 0
C      AND 1

*******************************************************************************

       subroutine ran2(idum,ran)
       parameter (m=714025,ia=1366,ic=150889,rm=1./m)
       DOUBLE PRECISION ir(97)
       data iff/0/
       if(idum.lt.0.or.iff.eq.0) then
       iff=1
       idum=mod(ic-idum,m)
       do 11 j=1,97
       idum=mod(ia*idum+ic,m)
       ir(j)=idum
11     continue
       idum=mod(ia*idum+ic,m)
       iy=idum
       endif
       j=1+(97*iy)/m
c      if(j.gt.97.or.j.lt.1)pause
       iy=ir(j)
       ran=iy*rm
       idum=mod(ia*idum+ic,m)
       ir(j)=idum
       return
       end
```

Input File for the chain with $\lambda = 0.91$

```
8 1. 1.381E-23 6.023E+23 400. 1.E+5 .014 .5 .5
1. 30000 49 5.E-6 1.3E+7 2.5E+9 6.634E+5 .153 70.53
1. 1.3108 -1.4135 -.3358 2.8271 -3.3885 10000
  0.153000000000000  0.000000000000000  0.000000000000000
  0.037189392742390  0.123318096685324  0.053174111103034
  0.033005999198542  0.051784053758746  0.192209408391067
 -0.047519859279891  0.145685302147094  0.311072352781268
 -0.187014214985297  0.137514643080215  0.305131171743871
 -0.239266325915663  0.281657169798146  0.305705342213924
 -0.184399526931905  0.361763009855380  0.178872067914022
 -0.173747926905847  0.512576620523088  0.189891944795750
 -0.047553365252175  0.540162302595642  0.270321595294652
  0.081082510194386  0.536326544891653  0.198561098218889
  0.194097220547070  0.583512419094977  0.266737590182527
  0.298551942241834  0.585979982551729  0.155514427781004
  0.406750109145059  0.668634364004548  0.193053554571094
  0.517819849936056  0.675598244057358  0.078711175118734
  0.638480480875615  0.722299723548547  0.141006744262968
  0.655286660066536  0.633982230947588  0.237215199417468
  0.772800663833600  0.653894087350062  0.336127994663662
  0.772570613480416  0.753188859102235  0.442366873181529
  0.894160842009936  0.736924533208746  0.547766509650554
  1.007250846450889  0.713869944029158  0.449049061552932
  0.999252671357704  0.801888889891373  0.331840986277307
  1.075767360022740  0.740056174473580  0.201913309233852
  1.203617242851564  0.701920311999400  0.272968339667363
  1.301581360303376  0.621619217570701  0.188074575150938
  1.422733603330274  0.584383867460669  0.288475148739376
  1.406266808440649  0.453450893740522  0.353825027080228
  1.501510592404770  0.403701627225291  0.450068682798854
  1.639449557340825  0.359258386549955  0.407513303865502
  1.725227156695967  0.274411941934645  0.501438080146117
  1.827694413502477  0.213818219214874  0.402698738289838
  1.953084079052413  0.145555699704187  0.492625410308671
  2.026362078224821  0.243624551389885  0.568901170894597
  2.142775462875083  0.217084670271999  0.664851430121629
  2.076254663695608  0.143980810402456  0.777488809157132
  1.990911500982778  0.038682633210978  0.760224665029278
  2.065315689289692 -0.081720466909308  0.703987424144919
  1.985779770099492 -0.204058521330056  0.693380598203139
  1.896538294367176 -0.158337258335406  0.592145998410392
  1.971866662511638 -0.126409065793620  0.465415985822154
  1.934795856769193 -0.050223516739218  0.354140501791383
  2.029689596272331 -0.081846865368381  0.250639019649465
  2.011505905392287 -0.238792471979091  0.193639642978731
  2.063470223912165 -0.296626817791114  0.324968718621234
  2.228310153395206 -0.245646059662115  0.344422217221760
  2.214059346670165 -0.088371204637817  0.352356417003817
  2.365336214041560 -0.047780962960556  0.383960725732734
  2.353338826106337  0.116036730828180  0.408007954904516
  2.234693223750724  0.165377971260148  0.505780349726884
  2.291209000000000  0.147447000000000  0.661719600000000
```

Output file for calculation of bond $M_2(t)$

for the chains with

$\lambda = 0.37$	$\lambda = 0.91$	$\lambda = 1.38$	$\lambda = 2.00$	t(ns)
1.000	1.00	1.00	1.00	0.00
5.218495e-1	5.273262e-1	5.016978e-1	4.767273e-1	1.5e-2
3.706808e-1	3.772515e-1	3.482617e-1	3.454201e-1	3e-2
2.706408e-1	2.864779e-1	2.567928e-1	2.814035e-1	4.5e-2
2.083523e-1	2.258148e-1	2.034001e-1	2.370042e-1	6e-2
1.680483e-1	1.801113e-1	1.648633e-1	2.057527e-1	7.5e-2
1.409149e-1	1.461392e-1	1.367962e-1	1.833272e-1	9e-2
1.206145e-1	1.23808e-1	1.159052e-1	1.719057e-1	1.05e-1
1.071512e-1	1.091021e-1	1.026226e-1	1.60552e-1	1.2e-1
9.5698416e-2	9.9069536e-2	9.2541099e-2	1.496928e-1	1.35e-1
8.2063794e-2	9.0826392e-2	8.2869828e-2	1.394649e-1	1.5e-1
7.7150106e-2	8.563e-2	7.979393e-2	1.359208e-1	1.65e-1
7.1061373e-2	7.7462375e-2	7.8735948e-2	1.354957e-1	1.8e-1
6.1887741e-2	6.7756832e-2	7.4189961e-2	1.328595e-1	1.95e-1
5.4243386e-2	6.1491489e-2	6.7968726e-2	1.330768e-1	2.1e-1
4.6675384e-2	5.422312e-2	6.38659e-2	1.334973e-1	2.25e-1
3.8849473e-2	5.623275e-2	5.9708416e-2	1.294026e-1	2.4e-1
3.5118759e-2	5.5428088e-2	5.3936183e-2	1.275842e-1	2.55e-1
3.2580495e-2	5.3616405e-2	5.0982654e-2	1.224868e-1	2.7e-1
2.6157081e-2	5.1434159e-2	3.8194954e-2	1.150309e-1	2.85e-1
1.9540846e-2	4.3825328e-2	3.4254134e-2	1.204764e-1	3e-1
1.7051399e-2	4.4773579e-2	3.175813e-2	1.249334e-1	3.15e-1
1.4808476e-2	4.2550623e-2	2.9920995e-2	1.268353e-1	3.3e-1
1.1440575e-2	4.3303251e-2	2.9209077e-2	1.310399e-1	3.45e-1
1.4181018e-2	3.7376523e-2	2.9772162e-2	1.327216e-1	3.6e-1
2.0035684e-2	3.5419047e-2	2.6919842e-2	1.392437e-1	3.75e-1
1.8268883e-2	3.2838523e-2	2.6791275e-2	1.423075e-1	3.9e-1
1.1950135e-2	2.948302e-2	2.6364863e-2	1.411485e-1	4.05e-1
8.6049438e-3	2.8804243e-2	2.8891921e-2	1.414135e-1	4.2e-1
7.3777437e-3	2.4571121e-2	3.065908e-2	1.398733e-1	4.35e-1
1.3446689e-2	2.0964682e-2	3.1026781e-2	1.398469e-1	4.5e-1
1.616776e-2	1.5211761e-2	3.2424033e-2	1.401225e-1	4.65e-1
1.6348004e-2	2.0803809e-2	3.4784138e-2	1.463239e-1	4.8e-1
1.567173e-2	2.5531352e-2	3.6294878e-2	1.385359e-1	4.95e-1
1.2702525e-2	2.5133967e-2	4.4256032e-2	1.303134e-1	5.1e-1
1.7558157e-2	2.1368146e-2	4.4373274e-2	1.323299e-1	5.25e-1
1.8462539e-2	2.0858169e-2	5.1217198e-2	1.296808e-1	5.4e-1
2.2556365e-2	2.0045042e-2	5.2051783e-2	1.278018e-1	5.55e-1
2.4932265e-2	1.9648075e-2	5.2921593e-2	1.314501e-1	5.7e-1
1.9729555e-2	1.4525294e-2	5.3936601e-2	1.339267e-1	5.85e-1
1.4658272e-2	1.5896022e-2	5.1950216e-2	1.333439e-1	6e-1
1.4530778e-2	1.9738853e-2	4.9185216e-2	1.308763e-1	6.15e-1
1.6864061e-2	1.9511402e-2	4.8172832e-2	1.222264e-1	6.3e-1
2.0301163e-2	1.9354463e-2	4.9186349e-2	1.244133e-1	6.45e-1
1.9948721e-2	1.5434861e-2	4.4503331e-2	1.22425e-1	6.6e-1
1.7311811e-2	1.3703644e-2	4.4363022e-2	1.252635e-1	6.75e-1
1.5302658e-2	1.3586938e-2	4.4468999e-2	1.214041e-1	6.9e-1
1.3510048e-2	1.6161978e-2	4.5624256e-2	1.171191e-1	7.05e-1
1.5355766e-2	1.514709e-2	4.6446443e-2	1.160397e-1	7.2e-1
1.7088234e-2	1.5658081e-2	4.5747697e-2	1.220227e-1	7.35e-1
2.4377227e-2	1.4238e-2	4.4633329e-2	1.273428e-1	7.5e-1
3.0256271e-2	1.418227e-2	4.2330325e-2	1.275524e-1	7.65e-1
2.3023725e-2	1.6013443e-2	3.9731443e-2	1.265208e-1	7.8e-1
1.7842054e-2	1.4716566e-2	3.3336818e-2	1.256709e-1	7.95e-1
1.5975118e-2	1.5956819e-2	2.5391877e-2	1.242403e-1	8.1e-1

1.0550916e-2	1.7733455e-2	2.2618949e-2	1.219915e-1	8.25e-1
8.3901882e-3	1.9427478e-2	1.9009054e-2	1.147157e-1	8.4e-1
7.621944e-3	1.592195e-2	2.6502132e-2	1.068682e-1	8.55e-1
3.8020611e-3	1.6757667e-2	2.9529214e-2	1.05162e-1	8.7e-1
2.3687482e-3	1.1080801e-2	3.2032013e-2	1.036519e-1	8.85e-1
-3.0643642e-3	1.0082304e-2	3.3951819e-2	1.092771e-1	9e-1
-2.6007295e-3	6.2230825e-3	3.3216536e-2	1.089848e-1	9.15e-1
2.6111007e-3	4.3973923e-3	3.4160852e-2	1.071438e-1	9.3e-1
4.7103167e-3	3.4868121e-3	3.1420887e-2	1.0502e-1	9.45e-1
3.3980012e-3	5.3149462e-3	3.254348e-2	1.066138e-1	9.6e-1
4.3699741e-3	5.6826472e-3	3.495425e-2	1.090601e-1	9.75e-1
9.4454885e-3	7.3953867e-3	3.4527063e-2	1.070691e-1	9.9e-1
1.0670781e-2	1.0590732e-2	3.3416212e-2	1.062509e-1	1.005e+0
6.2799454e-3	8.1858039e-3	3.3701658e-2	1.046005e-1	1.02e+0
3.7173033e-3	1.0210752e-2	3.8518965e-2	1.097665e-1	1.035e+0
-1.1951327e-3	1.2814939e-2	3.5124838e-2	1.139965e-1	1.05e+0
-8.6642504e-3	1.7529845e-2	3.2655656e-2	1.101868e-1	1.065e+0
-1.0005295e-2	2.2690535e-2	3.6668777e-2	1.028019e-1	1.08e+0
-1.1910528e-2	2.2763789e-2	4.036504e-2	9.6365213e-2	1.095e+0
-1.4456064e-2	1.9598722e-2	4.0930688e-2	9.4705701e-2	1.11e+0
-9.659946e-3	1.5559137e-2	4.1073918e-2	9.7648501e-2	1.125e+0
-6.2693655e-3	1.3980687e-2	4.2545319e-2	9.3761146e-2	1.14e+0
-2.6465654e-3	8.9752078e-3	4.6371639e-2	9.389323e-2	1.155e+0
2.4129748e-3	7.373631e-3	4.5543969e-2	9.80407e-2	1.17e+0
5.454421e-4	1.9497275e-3	4.2707086e-2	9.9345446e-2	1.185e+0
-3.5768747e-3	4.5210123e-3	3.9045453e-2	1.016266e-1	1.2e+0
-8.8450611e-3	4.3005943e-3	4.1970909e-2	1.025045e-1	1.215e+0
-1.0616213e-2	4.3343306e-3	5.1106453e-2	1.087911e-1	1.23e+0
-7.4266791e-3	4.4549704e-3	5.4872572e-2	1.113632e-1	1.245e+0
-5.8255494e-3	1.0112762e-2	5.410558e-2	1.057609e-1	1.26e+0
-1.0216027e-2	8.2079172e-3	5.5224001e-2	1.063261e-1	1.275e+0
-1.4113039e-2	7.3469877e-3	5.9413075e-2	1.057978e-1	1.29e+0
-1.1792153e-2	7.1977377e-3	6.0913861e-2	1.003149e-1	1.305e+0
-8.0595315e-3	7.2968006e-3	6.5420091e-2	1.004381e-1	1.32e+0
-7.0121884e-3	9.2658997e-3	6.0714722e-2	9.6223056e-2	1.335e+0
-4.5880079e-3	6.9041848e-3	5.5378616e-2	9.166193e-2	1.35e+0
-4.0898621e-3	9.3214512e-3	5.9328258e-2	9.8134935e-2	1.365e+0
-3.4830868e-3	8.7853074e-3	4.8197031e-2	1.056347e-1	1.38e+0
-2.684623e-3	9.550631e-3	4.7093213e-2	1.099245e-1	1.395e+0
-4.0147305e-3	5.2261949e-3	4.6127796e-2	1.091328e-1	1.41e+0
-8.4141791e-3	4.8542619e-3	4.2907357e-2	1.114109e-1	1.425e+0
-8.6109936e-3	9.5705986e-3	4.2793214e-2	1.162561e-1	1.44e+0
-4.4513047e-3	1.0030627e-2	4.2528152e-2	1.142645e-1	1.455e+0
-6.4411759e-4	4.6693683e-3	3.6590815e-2	1.159851e-1	1.47e+0
-4.0271878e-3	8.54671e-4	3.4929752e-2	1.114042e-1	1.485e+0
-5.3104758e-4	-8.0417395e-3	3.5382926e-2	1.101642e-1	1.5e+0
3.0383468e-3	-5.3825676e-3	3.817457e-2	1.144014e-1	1.515e+0
8.5368156e-3	-7.8978539e-3	4.0791452e-2	1.129647e-1	1.53e+0
1.0828853e-2	-1.0001928e-2	4.060483e-2	1.139693e-1	1.545e+0
8.7489486e-3	-5.9194565e-3	3.4397364e-2	1.166868e-1	1.56e+0
9.3573928e-3	1.6282201e-3	3.2328129e-2	1.147872e-1	1.575e+0
3.6864281e-3	2.7062893e-3	3.5290718e-2	1.104633e-1	1.59e+0
9.7119808e-3	4.7087669e-6	3.67679e-2	1.101836e-1	1.605e+0
2.7796626e-3	4.2170286e-4	3.5288692e-2	1.068218e-1	1.62e+0
-5.4234862e-3	5.4953694e-3	3.4627497e-2	1.050307e-1	1.635e+0
-6.3046217e-3	8.2038045e-3	3.543514e-2	1.05865e-1	1.65e+0
-8.8592768e-3	7.5892806e-3	3.4306705e-2	1.042363e-1	1.665e+0
-9.8738968e-3	8.5229278e-3	3.8573802e-2	9.7944915e-2	1.68e+0
-7.2189867e-3	6.8038702e-3	3.9180577e-2	9.0833366e-2	1.695e+0
-2.4455786e-3	5.928576e-3	4.3464601e-2	9.555769e-2	1.71e+0
-3.9171875e-3	3.5792589e-3	5.3308487e-2	9.4791234e-2	1.725e+0
-5.0114095e-3	-1.2806356e-3	5.7711601e-2	9.4349802e-2	1.74e+0
-8.6507201e-3	-4.0921569e-4	5.8791697e-2	9.3252063e-2	1.755e+0
-7.3055029e-3	1.8554926e-4	5.443567e-2	9.6434534e-2	1.77e+0
-4.5337081e-3	-1.9052625e-3	5.1630855e-2	1.014637e-1	1.785e+0
8.6188316e-4	1.3113022e-6	4.0444493e-2	9.87553e-2	1.8e+0
3.0913353e-3	-2.2908151e-3	3.694725e-2	9.8890483e-2	1.815e+0
1.0024548e-2	-7.314235e-3	3.5774648e-2	1.028816e-1	1.83e+0
6.7358017e-3	-1.0335356e-2	3.5987437e-2	1.035607e-1	1.845e+0
3.4087896e-3	-4.3888092e-3	3.7418008e-2	1.109363e-1	1.86e+0

4.3188334e-3	-3.0430555e-3	3.7440717e-2	1.199147e-1	1.875e+0
8.3395839e-3	-1.601696e-3	4.5003295e-2	1.259761e-1	1.89e+0
7.4833035e-3	-1.5827715e-3	5.1586926e-2	1.227909e-1	1.905e+0
2.6649237e-3	-3.2486022e-3	5.8268726e-2	1.230773e-1	1.92e+0
-8.9359283e-4	-2.7229786e-3	6.1501205e-2	1.252584e-1	1.935e+0
-5.3268373e-3	8.7535381e-4	5.7668924e-2	1.281695e-1	1.95e+0
-2.2453964e-3	3.9749742e-3	5.5416584e-2	1.281273e-1	1.965e+0
-6.3052773e-4	5.9010386e-3	5.2823842e-2	1.238208e-1	1.98e+0
3.2203197e-3	3.8682818e-3	5.2541912e-2	1.241043e-1	1.995e+0
1.1031985e-2	2.4202466e-3	5.0442457e-2	1.260976e-1	2.01e+0
1.4882445e-2	-1.625061e-3	4.7965944e-2	1.236819e-1	2.025e+0
1.6244054e-2	-2.464354e-4	4.5251966e-2	1.299424e-1	2.04e+0
1.3554335e-2	-8.366704e-4	4.3321371e-2	1.246923e-1	2.055e+0
8.9636445e-3	-8.7985396e-4	4.2620182e-2	1.18786e-1	2.07e+0
6.4564347e-3	2.9925108e-3	4.513824e-2	1.153363e-1	2.085e+0
5.8264732e-3	5.3251386e-3	4.2177022e-2	1.108179e-1	2.1e+0
6.6204071e-3	1.2527704e-3	3.839767e-2	1.144995e-1	2.115e+0
4.5974851e-3	-1.6838312e-3	3.7617207e-2	1.201053e-1	2.13e+0
8.8453293e-5	-3.9405823e-3	3.6819518e-2	1.1768e-1	2.145e+0
-8.8216066e-3	-4.7549009e-3	4.0284872e-2	1.150593e-1	2.16e+0
-4.2965114e-3	-2.1279752e-3	3.5214722e-2	1.172784e-1	2.175e+0
-6.8930984e-3	-9.585917e-4	3.5276115e-2	1.194549e-1	2.19e+0
-4.4074655e-3	2.8246641e-3	3.8079679e-2	1.165819e-1	2.205e+0
-9.0622902e-4	3.3448339e-3	3.5574913e-2	1.226752e-1	2.22e+0
-7.8555942e-4	6.9781542e-3	3.7686586e-2	1.20894e-1	2.235e+0
9.6023083e-4	1.0924339e-2	4.1796207e-2	1.278673e-1	2.25e+0

Output file for calculation of $M_1(t)$

for the chains with

$\lambda = 0.37$	$\lambda = 0.91$	$\lambda = 1.38$	$\lambda = 2.00$	t(ns)
1.000	1.00	1.00	1.00	0.00
7.784261e-1	7.819575e-1	7.654946e-1	7.580264e-1	1.5e-2
6.758767e-1	6.809513e-1	6.601701e-1	6.726103e-1	3e-2
5.998288e-1	6.087325e-1	5.905019e-1	6.26658e-1	4.5e-2
5.411134e-1	5.540718e-1	5.437995e-1	5.955027e-1	6e-2
5.011939e-1	5.093446e-1	5.099077e-1	5.725367e-1	7.5e-2
4.699048e-1	4.734723e-1	4.844558e-1	5.566602e-1	9e-2
4.436026e-1	4.472985e-1	4.652547e-1	5.456008e-1	1.05e-1
4.223665e-1	4.264518e-1	4.497441e-1	5.367628e-1	1.2e-1
4.038131e-1	4.117484e-1	4.389499e-1	5.306199e-1	1.35e-1
3.831119e-1	3.967986e-1	4.278911e-1	5.24362e-1	1.5e-1
3.691666e-1	3.831475e-1	4.216373e-1	5.215786e-1	1.65e-1
3.561335e-1	3.712097e-1	4.17344e-1	5.197479e-1	1.8e-1
3.447056e-1	3.630731e-1	4.119154e-1	5.181395e-1	1.95e-1
3.337185e-1	3.546102e-1	4.044199e-1	5.18088e-1	2.1e-1
3.216291e-1	3.451549e-1	3.984148e-1	5.171509e-1	2.25e-1
3.121261e-1	3.414248e-1	3.928927e-1	5.116842e-1	2.4e-1
3.043718e-1	3.345407e-1	3.873614e-1	5.08637e-1	2.55e-1
2.969061e-1	3.275141e-1	3.840607e-1	5.106016e-1	2.7e-1
2.898264e-1	3.241692e-1	3.786952e-1	5.082731e-1	2.85e-1
2.844643e-1	3.156744e-1	3.762643e-1	5.093336e-1	3e-1
2.78051e-1	3.079249e-1	3.738657e-1	5.089824e-1	3.15e-1
2.745326e-1	2.97506e-1	3.719839e-1	5.085791e-1	3.3e-1
2.673885e-1	2.920503e-1	3.681411e-1	5.102321e-1	3.45e-1
2.589439e-1	2.854602e-1	3.632674e-1	5.113897e-1	3.6e-1
2.539639e-1	2.791091e-1	3.620166e-1	5.133441e-1	3.75e-1
2.459312e-1	2.738166e-1	3.611493e-1	5.150314e-1	3.9e-1
2.379111e-1	2.65622e-1	3.605575e-1	5.179213e-1	4.05e-1
2.306051e-1	2.591971e-1	3.60176e-1	5.188209e-1	4.2e-1
2.24215e-1	2.513982e-1	3.557435e-1	5.18505e-1	4.35e-1
2.21094e-1	2.446586e-1	3.536236e-1	5.169677e-1	4.5e-1
2.186923e-1	2.38006e-1	3.517983e-1	5.167311e-1	4.65e-1
2.189749e-1	2.365212e-1	3.529812e-1	5.184657e-1	4.8e-1
2.166898e-1	2.347495e-1	3.574858e-1	5.163279e-1	4.95e-1
2.148222e-1	2.30121e-1	3.623047e-1	5.124706e-1	5.1e-1
2.102915e-1	2.265376e-1	3.662751e-1	5.122122e-1	5.25e-1
2.066721e-1	2.260593e-1	3.721576e-1	5.11483e-1	5.4e-1
2.056842e-1	2.25026e-1	3.700516e-1	5.110406e-1	5.55e-1
2.040873e-1	2.235909e-1	3.695175e-1	5.12154e-1	5.7e-1
2.004159e-1	2.216561e-1	3.708203e-1	5.138078e-1	5.85e-1
1.985742e-1	2.217654e-1	3.717736e-1	5.125002e-1	6e-1
1.946093e-1	2.189026e-1	3.706926e-1	5.11358e-1	6.15e-1
1.929075e-1	2.161962e-1	3.709017e-1	5.076892e-1	6.3e-1
1.897011e-1	2.110733e-1	3.679354e-1	5.097782e-1	6.45e-1
1.848239e-1	2.067499e-1	3.650792e-1	5.095729e-1	6.6e-1
1.800898e-1	2.047832e-1	3.657766e-1	5.118502e-1	6.75e-1
1.760281e-1	2.043725e-1	3.666536e-1	5.115994e-1	6.9e-1
1.726117e-1	2.038287e-1	3.676848e-1	5.09063e-1	7.05e-1
1.71043e-1	1.997384e-1	3.680588e-1	5.103441e-1	7.2e-1
1.702569e-1	1.997043e-1	3.655607e-1	5.107475e-1	7.35e-1
1.668744e-1	1.972036e-1	3.645785e-1	5.13815e-1	7.5e-1
1.65733e-1	1.964066e-1	3.635565e-1	5.132148e-1	7.65e-1
1.625104e-1	1.952488e-1	3.651781e-1	5.115635e-1	7.8e-1
1.59696e-1	1.932705e-1	3.630653e-1	5.122936e-1	7.95e-1
1.579849e-1	1.915358e-1	3.586462e-1	5.095545e-1	8.1e-1
1.560155e-1	1.898207e-1	3.56461e-1	5.060203e-1	8.25e-1
1.558795e-1	1.888824e-1	3.555718e-1	5.002815e-1	8.4e-1
1.550595e-1	1.891659e-1	3.574672e-1	4.972106e-1	8.55e-1

1.533341e-1	1.878568e-1	3.582142e-1	4.965944e-1	8.7e-1
1.510208e-1	1.851714e-1	3.593929e-1	4.959914e-1	8.85e-1
1.474179e-1	1.832329e-1	3.620924e-1	4.998662e-1	9e-1
1.44045e-1	1.823316e-1	3.658018e-1	4.985821e-1	9.15e-1
1.424224e-1	1.822047e-1	3.683485e-1	4.980223e-1	9.3e-1
1.389077e-1	1.80615e-1	3.675113e-1	4.977096e-1	9.45e-1
1.324074e-1	1.789943e-1	3.663441e-1	4.985108e-1	9.6e-1
1.291577e-1	1.74523e-1	3.667971e-1	5.024704e-1	9.75e-1
1.282248e-1	1.705017e-1	3.654125e-1	5.011585e-1	9.9e-1
1.2721e-1	1.677674e-1	3.65029e-1	4.977615e-1	1.005e+0
1.250759e-1	1.681497e-1	3.689994e-1	4.973895e-1	1.02e+0
1.222407e-1	1.690575e-1	3.751288e-1	4.99737e-1	1.035e+0
1.195893e-1	1.70303e-1	3.771777e-1	4.985258e-1	1.05e+0
1.200439e-1	1.715265e-1	3.796648e-1	4.973291e-1	1.065e+0
1.1911e-1	1.751945e-1	3.809806e-1	4.938528e-1	1.08e+0
1.164849e-1	1.761601e-1	3.824347e-1	4.915671e-1	1.095e+0
1.161986e-1	1.76555e-1	3.842604e-1	4.918327e-1	1.11e+0
1.172399e-1	1.735045e-1	3.85079e-1	4.927867e-1	1.125e+0
1.181402e-1	1.69305e-1	3.86513e-1	4.91669e-1	1.14e+0
1.20975e-1	1.681969e-1	3.880657e-1	4.924846e-1	1.155e+0
1.230521e-1	1.670129e-1	3.85714e-1	4.935829e-1	1.17e+0
1.217429e-1	1.632387e-1	3.823036e-1	4.923549e-1	1.185e+0
1.193348e-1	1.609619e-1	3.817497e-1	4.943575e-1	1.2e+0
1.193672e-1	1.588814e-1	3.828733e-1	4.946442e-1	1.215e+0
1.206391e-1	1.592588e-1	3.870002e-1	4.976877e-1	1.23e+0
1.233079e-1	1.595561e-1	3.894958e-1	4.967838e-1	1.245e+0
1.256185e-1	1.646558e-1	3.864699e-1	4.946658e-1	1.26e+0
1.24467e-1	1.664984e-1	3.853002e-1	4.936674e-1	1.275e+0
1.225455e-1	1.67523e-1	3.839541e-1	4.923612e-1	1.29e+0
1.212754e-1	1.661481e-1	3.83065e-1	4.919615e-1	1.305e+0
1.231153e-1	1.637636e-1	3.816025e-1	4.924459e-1	1.32e+0
1.235121e-1	1.60832e-1	3.780833e-1	4.899641e-1	1.335e+0
1.257509e-1	1.572538e-1	3.77257e-1	4.886682e-1	1.35e+0
1.258935e-1	1.541552e-1	3.771491e-1	4.920868e-1	1.365e+0
1.256706e-1	1.52402e-1	3.712758e-1	4.960183e-1	1.38e+0
1.233856e-1	1.526197e-1	3.673163e-1	4.996778e-1	1.395e+0
1.189572e-1	1.534406e-1	3.618176e-1	4.980168e-1	1.41e+0
1.1484e-1	1.53426e-1	3.614573e-1	4.981961e-1	1.425e+0
1.105134e-1	1.560214e-1	3.633267e-1	4.994862e-1	1.44e+0
1.059106e-1	1.589227e-1	3.635144e-1	4.998655e-1	1.455e+0
1.032945e-1	1.60575e-1	3.590609e-1	4.994408e-1	1.47e+0
1.030258e-1	1.604335e-1	3.575564e-1	4.940294e-1	1.485e+0
1.011579e-1	1.585925e-1	3.572968e-1	4.940125e-1	1.5e+0
9.9446535e-2	1.590368e-1	3.562687e-1	4.959496e-1	1.515e+0
9.6454926e-2	1.580695e-1	3.575962e-1	4.961908e-1	1.53e+0
9.3749844e-2	1.575904e-1	3.577922e-1	4.967678e-1	1.545e+0
9.188696e-2	1.59786e-1	3.578585e-1	4.972114e-1	1.56e+0
8.9168526e-2	1.612657e-1	3.590735e-1	4.96883e-1	1.575e+0
8.6917996e-2	1.61257e-1	3.628401e-1	4.968061e-1	1.59e+0
8.6744085e-2	1.580672e-1	3.636446e-1	4.982127e-1	1.605e+0
8.4532507e-2	1.54051e-1	3.634501e-1	4.964944e-1	1.62e+0
8.6307451e-2	1.532924e-1	3.634422e-1	4.97012e-1	1.635e+0
8.7161079e-2	1.53689e-1	3.625956e-1	4.962356e-1	1.65e+0
8.9966506e-2	1.547168e-1	3.597046e-1	4.964263e-1	1.665e+0
9.3690887e-2	1.539605e-1	3.60766e-1	4.935999e-1	1.68e+0
9.760689e-2	1.532911e-1	3.648465e-1	4.898914e-1	1.695e+0
1.00637e-1	1.518024e-1	3.701916e-1	4.931482e-1	1.71e+0
9.9107303e-2	1.475775e-1	3.762429e-1	4.932079e-1	1.725e+0
9.6526764e-2	1.430345e-1	3.813673e-1	4.911086e-1	1.74e+0
9.774258e-2	1.43301e-1	3.84597e-1	4.907098e-1	1.755e+0
9.6470065e-2	1.398082e-1	3.843177e-1	4.910053e-1	1.77e+0
9.3705058e-2	1.357471e-1	3.812213e-1	4.937013e-1	1.785e+0
9.1141082e-2	1.335697e-1	3.723777e-1	4.94489e-1	1.8e+0
9.2020229e-2	1.300185e-1	3.684085e-1	4.938429e-1	1.815e+0
9.4249785e-2	1.283443e-1	3.663525e-1	4.943933e-1	1.83e+0
9.3837731e-2	1.26379e-1	3.671605e-1	4.970477e-1	1.845e+0
9.8761819e-2	1.244926e-1	3.684462e-1	4.979185e-1	1.86e+0
1.022887e-1	1.248639e-1	3.67727e-1	5.026094e-1	1.875e+0
1.046797e-1	1.231875e-1	3.729376e-1	5.067813e-1	1.89e+0
1.062444e-1	1.18417e-1	3.758128e-1	5.06921e-1	1.905e+0

1.073846e-1	1.123791e-1	3.786172e-1	5.082785e-1	1.92e+0
1.056611e-1	1.110438e-1	3.814349e-1	5.095062e-1	1.935e+0
1.046747e-1	1.106424e-1	3.760138e-1	5.092807e-1	1.95e+0
1.056025e-1	1.093526e-1	3.710993e-1	5.055113e-1	1.965e+0
1.090451e-1	1.105069e-1	3.682586e-1	5.029485e-1	1.98e+0
1.111414e-1	1.081283e-1	3.682724e-1	5.038472e-1	1.995e+0
1.164746e-1	1.078883e-1	3.670062e-1	5.053343e-1	2.01e+0
1.214473e-1	1.081701e-1	3.670024e-1	5.061788e-1	2.025e+0
1.247869e-1	1.086127e-1	3.681351e-1	5.088812e-1	2.04e+0
1.232267e-1	1.099941e-1	3.700357e-1	5.061107e-1	2.055e+0
1.221254e-1	1.084183e-1	3.728246e-1	5.028092e-1	2.07e+0
1.186607e-1	1.104648e-1	3.712761e-1	5.010432e-1	2.085e+0
1.166236e-1	1.104327e-1	3.689531e-1	4.984106e-1	2.1e+0
1.146288e-1	1.123661e-1	3.669775e-1	4.995146e-1	2.115e+0
1.128901e-1	1.149723e-1	3.65691e-1	5.020851e-1	2.13e+0
1.135395e-1	1.181957e-1	3.61853e-1	4.977359e-1	2.145e+0
1.142485e-1	1.168409e-1	3.620491e-1	4.951165e-1	2.16e+0
1.13043e-1	1.142555e-1	3.622319e-1	4.956191e-1	2.175e+0
1.143931e-1	1.149962e-1	3.67351e-1	4.963885e-1	2.19e+0
1.162495e-1	1.149832e-1	3.69514e-1	4.955236e-1	2.205e+0
1.177736e-1	1.094988e-1	3.683645e-1	4.977662e-1	2.22e+0
1.216433e-1	1.063648e-1	3.748669e-1	4.964685e-1	2.235e+0
1.202524e-1	1.02352e-1	3.799421e-1	5.012991e-1	2.25e+0

Output file for the calculations of:

D(t) directivity
S(t) sense of mobility
C(t) orientation-mobility amplitude
M(t) mobility amplitude

for a chain of 50 numbber of bonds with λ =0.37

D(t)	S(t)	C(t)	M(t)	t(ns)
-4.1409419e-3	-4.3772761e-2	-1.3176148e-2	7.119375e-1	5e-3
-2.8922036e-3	-4.1098319e-2	-8.6745918e-3	5.218491e-1	1.5e-2
-1.9274736e-3	-3.8911987e-2	-7.5884876e-3	4.126891e-1	2.5e-2
-1.4182369e-3	-3.4968361e-2	-5.7540075e-3	3.332182e-1	3.5e-2
-7.3041132e-4	-3.3508915e-2	-6.7860787e-3	2.706403e-1	4.5e-2
1.6655775e-3	-3.1819034e-2	-5.9333537e-3	2.275355e-1	5.5e-2
2.369565e-3	-2.9553495e-2	-4.510053e-3	1.913676e-1	6.5e-2
1.1906388e-4	-2.9530235e-2	-2.2408613e-3	1.680491e-1	7.5e-2
4.0650292e-4	-2.8301701e-2	-1.8210327e-3	1.479985e-1	8.5e-2
-8.2562596e-4	-2.8711492e-2	-3.374723e-4	1.359359e-1	9.5e-2
-2.8285193e-3	-3.0226376e-2	1.5524445e-3	1.206134e-1	1.05e-1
-3.0838042e-3	-3.0278834e-2	1.5444485e-3	1.100481e-1	1.15e-1
-3.931717e-3	-3.1162027e-2	9.0700638e-4	1.046552e-1	1.25e-1
-5.5307732e-3	-3.4127783e-2	-5.421454e-4	9.569741e-2	1.35e-1
-2.2623083e-3	-3.263877e-2	-8.6630008e-4	8.5834309e-2	1.45e-1
-2.8789858e-3	-3.3549957e-2	-2.4083862e-3	8.124169e-2	1.55e-1
-8.2189348e-5	-3.2131836e-2	-2.9607215e-3	7.7153459e-2	1.65e-1
2.4249055e-3	-3.0129416e-2	-3.6479114e-3	7.2959639e-2	1.75e-1
3.5443339e-3	-2.9784698e-2	-4.6554497e-3	6.6949904e-2	1.85e-1
3.5196913e-3	-2.8281767e-2	-5.1808422e-3	6.1888497e-2	1.95e-1
4.0653707e-3	-2.6164612e-2	-5.2224956e-3	5.5656344e-2	2.05e-1
4.5824237e-3	-2.5687503e-2	-5.7995813e-3	5.2870002e-2	2.15e-1
4.3278066e-3	-2.651177e-2	-5.2447366e-3	4.6678793e-2	2.25e-1
4.5145215e-3	-2.6920896e-2	-4.7053262e-3	4.1858252e-2	2.35e-1
4.2606303e-3	-2.8045438e-2	-5.4848418e-3	3.7594777e-2	2.45e-1
4.9164258e-3	-2.6421372e-2	-4.7703274e-3	3.5121534e-2	2.55e-1
7.0523829e-3	-2.6053485e-2	-5.6588212e-3	3.2950498e-2	2.65e-1
5.3377454e-3	-2.6200939e-2	-5.8855307e-3	3.133988e-2	2.75e-1
3.9089122e-3	-2.4709349e-2	-5.4177898e-3	2.6155159e-2	2.85e-1
5.0843903e-3	-2.3981258e-2	-5.3123464e-3	2.041715e-2	2.95e-1
6.3941632e-3	-2.349389e-2	-6.6197854e-3	1.6795209e-2	3.05e-1
7.8940243e-3	-2.1862024e-2	-6.5170708e-3	1.7049775e-2	3.15e-1
6.6033904e-3	-2.3128657e-2	-6.3590356e-3	1.651785e-2	3.25e-1
4.8289937e-3	-2.326387e-2	-5.3290613e-3	1.4197241e-2	3.35e-1
8.7723567e-4	-2.5637014e-2	-5.2427552e-3	1.1443191e-2	3.45e-1
-5.3155172e-6	-2.7178381e-2	-4.416313e-3	1.381248e-2	3.55e-1
-5.8875751e-4	-2.7862715e-2	-4.4504208e-3	1.6507924e-2	3.65e-1
-1.4271684e-3	-2.9468799e-2	-5.017479e-3	2.003799e-2	3.75e-1
-9.6661726e-4	-2.9684924e-2	-5.4820133e-3	2.105926e-2	3.85e-1
-6.856164e-4	-2.9679926e-2	-5.4799942e-3	1.6365103e-2	3.95e-1
-4.2302319e-4	-2.8748766e-2	-4.4222474e-3	1.1952486e-2	4.05e-1
1.6356293e-3	-2.5699694e-2	-2.9894314e-3	1.0188647e-2	4.15e-1
2.6951635e-3	-2.4896789e-2	-3.3674142e-3	6.7155613e-3	4.25e-1
1.2308736e-3	-2.6738297e-2	-3.5057741e-3	7.3788604e-3	4.35e-1
4.4476023e-4	-2.7761934e-2	-4.0814611e-3	1.1424015e-2	4.45e-1
-2.1914995e-4	-2.7956441e-2	-4.095837e-3	1.5704351e-2	4.55e-1
-1.7375e-3	-2.8018313e-2	-3.1357331e-3	1.6167901e-2	4.65e-1
-4.1468441e-3	-3.0018568e-2	-3.2103469e-3	1.7108474e-2	4.75e-1
-4.275593e-3	-3.06013e-2	-3.3444262e-3	1.6480593e-2	4.85e-1
-6.367512e-3	-3.1670395e-2	-1.9484846e-3	1.5670605e-2	4.95e-1

Output file for the calculations of:

D(t) directivity
S(t) sense of mobility
C(t) orientation-mobility amplitude
M(t) mobility amplitude

for a chain of 50 numbber of bonds with λ =0.91

D(t)	S(t)	C(t)	M(t)	t(ns)
--6.9572283e-3	-6.4471245e-2	1.9156743e-2	7.106462e-1	5e-3
-3.5921638e-3	-6.5794148e-2	1.5917007e-2	5.273244e-1	1.5e-2
-5.0740759e-4	-6.4013481e-2	1.3595317e-2	4.171677e-1	2.5e-2
2.8661091e-3	-6.2523864e-2	1.1942774e-2	3.436728e-1	3.5e-2
5.1979143e-3	-5.924565e-2	1.2871034e-2	2.864805e-1	4.5e-2
6.2348456e-3	-5.8300719e-2	1.2797487e-2	2.436797e-1	5.5e-2
7.9796715e-3	-5.6827422e-2	1.3000986e-2	2.10582e-1	6.5e-2
9.9223992e-3	-5.6325015e-2	1.0925249e-2	1.801148e-1	7.5e-2
1.3066508e-2	-5.6406949e-2	8.8714296e-3	1.553714e-1	8.5e-2
1.4940145e-2	-5.6526806e-2	6.3827513e-3	1.382068e-1	9.5e-2
1.5194953e-2	-5.6420393e-2	5.6795473e-3	1.238104e-1	1.05e-1
1.6696436e-2	-5.5174168e-2	4.8714108e-3	1.14461e-1	1.15e-1
1.6550727e-2	-5.5676263e-2	5.0273179e-3	1.05336e-1	1.25e-1
1.450917e-2	-5.5026423e-2	6.7019542e-3	9.9068955e-2	1.35e-1
1.4387596e-2	-5.5745147e-2	6.9315811e-3	9.4799913e-2	1.45e-1
1.200958e-2	-5.6230973e-2	7.3449593e-3	8.9387394e-2	1.55e-1
1.0772453e-2	-5.7143457e-2	6.8122623e-3	8.5628904e-2	1.65e-1
1.1658855e-2	-5.5734672e-2	6.5110009e-3	8.2087204e-2	1.75e-1
1.2410996e-2	-5.581256e-2	5.8102049e-3	7.2832368e-2	1.85e-1
1.1796402e-2	-5.6803644e-2	4.7725793e-3	6.7758486e-2	1.95e-1
1.2044842e-2	-5.6168199e-2	4.6171458e-3	6.2768146e-2	2.05e-1
1.2598231e-2	-5.5978306e-2	4.2032707e-3	5.9212103e-2	2.15e-1
1.3754756e-2	-5.5960223e-2	2.0837903e-3	5.4226413e-2	2.25e-1
1.4071615e-2	-5.543945e-2	1.6082543e-3	5.4280046e-2	2.35e-1
1.4920075e-2	-5.6672081e-2	9.3727099e-4	5.7760183e-2	2.45e-1
1.6201835e-2	-5.5070605e-2	2.0140898e-3	5.5430926e-2	2.55e-1
1.6477436e-2	-5.2449644e-2	4.0199608e-3	5.3554703e-2	2.65e-1
1.5870824e-2	-5.2532785e-2	3.6458352e-3	5.2945949e-2	2.75e-1
1.5220163e-2	-5.2263048e-2	4.0585352e-3	5.1432826e-2	2.85e-1
1.6468147e-2	-5.4070313e-2	2.8937366e-3	4.6249509e-2	2.95e-1
1.6472334e-2	-5.1354613e-2	4.6886527e-3	4.3204982e-2	3.05e-1
1.590188e-2	-5.2111872e-2	5.4797977e-3	4.4776481e-2	3.15e-1
1.534238e-2	-5.1619634e-2	7.0699546e-3	4.3912265e-2	3.25e-1
1.5321173e-2	-5.1887844e-2	7.6547195e-3	4.4469539e-2	3.35e-1
1.4928387e-2	-5.1962733e-2	8.0950307e-3	4.3305676e-2	3.45e-1
1.337599e-2	-5.274358e-2	8.6324709e-3	4.1219305e-2	3.55e-1
1.3253471e-2	-5.4201376e-2	7.5576496e-3	3.4252778e-2	3.65e-1
1.2886958e-2	-5.2488737e-2	8.1675705e-3	3.5420854e-2	3.75e-1
1.3356574e-2	-5.5144206e-2	7.0495554e-3	3.4070943e-2	3.85e-1
1.4173828e-2	-5.4259967e-2	7.744649e-3	3.217775e-2	3.95e-1
1.3636909e-2	-5.2578051e-2	7.500106e-3	2.9482741e-2	4.05e-1
1.310946e-2	-5.2227233e-2	7.8528114e-3	2.6196264e-2	4.15e-1
1.3903248e-2	-5.0988577e-2	8.2568619e-3	2.8052347e-2	4.25e-1
1.4970625e-2	-5.1244918e-2	6.8732356e-3	2.4572019e-2	4.35e-1
1.4430027e-2	-5.1961906e-2	6.3516391e-3	2.1284398e-2	4.45e-1
1.516179e-2	-5.0978668e-2	5.5279066e-3	1.8114209e-2	4.55e-1
1.5791297e-2	-5.0530959e-2	6.5618139e-3	1.5209817e-2	4.65e-1
1.5204899e-2	-4.9748179e-2	7.1920548e-3	1.8947335e-2	4.75e-1
1.5957531e-2	-4.8874144e-2	6.468961e-3	2.3897797e-2	4.85e-1
1.5701607e-2	-5.0215926e-2	7.3223389e-3	2.5532309e-2	4.95e-1

Output file for the calculations of:

D(t) directivity
S(t) sense of mobility
C(t) orientation-mobility amplitude
M(t) mobility amplitude

for a chain of 50 numbber of bonds with λ =1.38

D(t)	S(t)	C(t)	M(t)	t(ns)
-7.9116188e-3	-9.9274337e-2	1.343313e-1	6.86406e-1	5e-3
-3.1752107e-3	-1.103728e-1	1.172702e-1	5.016984e-1	1.5e-2
3.2530422e-3	-1.141854e-1	1.026925e-1	3.896826e-1	2.5e-2
8.565777e-3	-1.135617e-1	9.4297528e-2	3.13162e-1	3.5e-2
1.3061217e-2	-1.143053e-1	8.6812496e-2	2.567902e-1	4.5e-2
1.6089045e-2	-1.14393e-1	8.096914e-2	2.204886e-1	5.5e-2
2.1377787e-2	-1.136319e-1	7.3314816e-2	1.883001e-1	6.5e-2
2.5972482e-2	-1.122159e-1	6.776841e-2	1.648654e-1	7.5e-2
2.9219393e-2	-1.121943e-1	6.2533729e-2	1.461585e-1	8.5e-2
3.1048492e-2	-1.136457e-1	5.8178935e-2	1.275348e-1	9.5e-2
3.2320477e-2	-1.137081e-1	5.5529959e-2	1.159035e-1	1.05e-1
3.4279563e-2	-1.144987e-1	5.3396344e-2	1.08886e-1	1.15e-1
3.505424e-2	-1.144201e-1	5.1897608e-2	9.9184267e-2	1.25e-1
3.6816385e-2	-1.13611e-1	5.1120471e-2	9.2542104e-2	1.35e-1
3.8588408e-2	-1.143985e-1	4.9283519e-2	8.5087374e-2	1.45e-1
3.8197625e-2	-1.146751e-1	4.9594346e-2	7.8871928e-2	1.55e-1
3.8296193e-2	-1.141874e-1	5.0111435e-2	7.9792053e-2	1.65e-1
3.9582301e-2	-1.138827e-1	4.8774865e-2	7.8499414e-2	1.75e-1
4.0870193e-2	-1.117946e-1	4.899117e-2	7.6695815e-2	1.85e-1
4.1230317e-2	-1.124574e-1	4.7924027e-2	7.4191548e-2	1.95e-1
4.0838182e-2	-1.12382e-1	4.7023248e-2	6.8264268e-2	2.05e-1
4.2020015e-2	-1.131557e-1	4.6663892e-2	6.51296e-2	2.15e-1
4.3197289e-2	-1.128348e-1	4.6867423e-2	6.3865505e-2	2.25e-1
4.3132912e-2	-1.135241e-1	4.4813871e-2	5.907451e-2	2.35e-1
4.3256171e-2	-1.130035e-1	4.3890793e-2	5.7389289e-2	2.45e-1
4.5261592e-2	-1.116237e-1	4.2860884e-2	5.3938661e-2	2.55e-1
4.67261e-2	-1.11115e-1	4.1178692e-2	5.1515479e-2	2.65e-1
4.8121992e-2	-1.103332e-1	3.978245e-2	4.4863429e-2	2.75e-1
4.8116468e-2	-1.13669e-1	3.5428446e-2	3.8197912e-2	2.85e-1
4.7284395e-2	-1.15364e-1	3.4832492e-2	3.4817509e-2	2.95e-1
4.872274e-2	-1.136893e-1	3.5211589e-2	3.2479417e-2	3.05e-1
4.8795242e-2	-1.147255e-1	3.3320159e-2	3.1758763e-2	3.15e-1
4.8932541e-2	-1.139759e-1	3.5010666e-2	3.0014887e-2	3.25e-1
4.7704354e-2	-1.140914e-1	3.5933312e-2	2.9730052e-2	3.35e-1
4.9342368e-2	-1.146828e-1	3.6188371e-2	2.9209774e-2	3.45e-1
5.1606923e-2	-1.141419e-1	3.4701195e-2	2.906643e-2	3.55e-1
5.08641e-2	-1.140502e-1	3.4541443e-2	3.0698674e-2	3.65e-1
5.2678406e-2	-1.113997e-1	3.3856977e-2	2.6924191e-2	3.75e-1
5.1456857e-2	-1.118418e-1	3.4355398e-2	2.7081432e-2	3.85e-1
5.1244717e-2	-1.099121e-1	3.4748469e-2	2.4955759e-2	3.95e-1
5.1468607e-2	-1.064311e-1	3.7396997e-2	2.6366014e-2	4.05e-1
5.1043767e-2	-1.062002e-1	3.848264e-2	2.9292151e-2	4.15e-1
5.1618118e-2	-1.046843e-1	3.9056875e-2	2.8691363e-2	4.25e-1
5.2772615e-2	-1.021098e-1	4.0270533e-2	3.065821e-2	4.35e-1
5.278698e-2	-1.017876e-1	4.1713025e-2	3.132816e-2	4.45e-1
5.2600116e-2	-1.021403e-1	4.2682767e-2	3.0494388e-2	4.55e-1
5.197034e-2	-1.028212e-1	4.1692935e-2	3.2425027e-2	4.65e-1
5.1709589e-2	-1.033386e-1	4.1978721e-2	3.2126002e-2	4.75e-1
4.9215555e-2	-1.031902e-1	4.2754013e-2	3.5426054e-2	4.85e-1
4.8311524e-2	-1.042481e-1	4.3272711e-2	3.6292847e-2	4.95e-1

Output file for the calculations of:

D(t) directivity
S(t) sense of mobility
C(t) orientation-mobility amplitude
M(t) mobility amplitude

for a chain of 50 numbber of bonds with λ =2.00

D(t)	S(t)	C(t)	M(t)	t(ns)
-5.1857675e-3	-1.581395e-1	2.435548e-1	6.630935e-1	5e-3
6.0414625e-3	-1.8191e-1	2.017669e-1	4.767312e-1	1.5e-2
1.7693091e-2	-1.879085e-1	1.798088e-1	3.818356e-1	2.5e-2
2.4870403e-2	-1.900169e-1	1.634354e-1	3.178402e-1	3.5e-2
2.988182e-2	-1.907324e-1	1.533568e-1	2.814041e-1	4.5e-2
3.5158392e-2	-1.897793e-1	1.440619e-1	2.51943e-1	5.5e-2
4.125065e-2	-1.903631e-1	1.362501e-1	2.275052e-1	6.5e-2
4.4209592e-2	-1.904039e-1	1.286787e-1	2.057534e-1	7.5e-2
4.7526829e-2	-1.904276e-1	1.229327e-1	1.898975e-1	8.5e-2
4.9486902e-2	-1.899279e-1	1.195882e-1	1.810507e-1	9.5e-2
5.1631138e-2	-1.886305e-1	1.179622e-1	1.719059e-1	1.05e-1
5.3347059e-2	-1.89844e-1	1.130506e-1	1.639062e-1	1.15e-1
5.5544503e-2	-1.908966e-1	1.097953e-1	1.559398e-1	1.25e-1
5.6164369e-2	-1.916429e-1	1.084198e-1	1.496936e-1	1.35e-1
5.7770394e-2	-1.930833e-1	1.042701e-1	1.419661e-1	1.45e-1
5.9743807e-2	-1.94543e-1	1.015137e-1	1.362917e-1	1.55e-1
5.9617378e-2	-1.948688e-1	9.999293e-2	1.359216e-1	1.65e-1
5.9761904e-2	-1.940924e-1	1.006456e-1	1.364236e-1	1.75e-1
6.1092671e-2	-1.94163e-1	9.912210e-2	1.343448e-1	1.85e-1
6.2441103e-2	-1.935738e-1	9.867867e-2	1.328607e-1	1.95e-1
6.2452942e-2	-1.913252e-1	9.955223e-2	1.351247e-1	2.05e-1
6.3227385e-2	-1.919425e-1	9.950551e-2	1.362027e-1	2.15e-1
6.3224323e-2	-1.922221e-1	9.858854e-2	1.335007e-1	2.25e-1
6.2686361e-2	-1.936718e-1	9.805267e-2	1.31305e-1	2.35e-1
6.3476607e-2	-1.926222e-1	9.659596e-2	1.281879e-1	2.45e-1
6.5117873e-2	-1.909619e-1	9.569814e-2	1.275866e-1	2.55e-1
6.6961303e-2	-1.938659e-1	9.330680e-2	1.209122e-1	2.65e-1
6.7596003e-2	-1.932107e-1	9.355713e-2	1.174718e-1	2.75e-1
6.7254595e-2	-1.936982e-1	9.248182e-2	1.1503e-1	2.85e-1
6.5387644e-2	-1.912084e-1	9.621231e-2	1.196323e-1	2.95e-1
6.5848231e-2	-1.888441e-1	9.713695e-2	1.194732e-1	3.05e-1
6.5036789e-2	-1.871587e-1	9.828531e-2	1.249337e-1	3.15e-1
6.5436691e-2	-1.875909e-1	9.895151e-2	1.275004e-1	3.25e-1
6.5600723e-2	-1.858806e-1	1.010581e-1	1.296972e-1	3.35e-1
6.4627029e-2	-1.850363e-1	1.032804e-1	1.31043e-1	3.45e-1
6.3788243e-2	-1.85544e-1	1.032286e-1	1.305844e-1	3.55e-1
6.1216328e-2	-1.843633e-1	1.060728e-1	1.376433e-1	3.65e-1
5.9380326e-2	-1.834931e-1	1.073081e-1	1.392428e-1	3.75e-1
5.877997e-2	-1.821857e-1	1.080381e-1	1.416555e-1	3.85e-1
5.9684996e-2	-1.809086e-1	1.080699e-1	1.425734e-1	3.95e-1
5.9208263e-2	-1.847052e-1	1.072956e-1	1.411529e-1	4.05e-1
6.0017962e-2	-1.866601e-1	1.073776e-1	1.414447e-1	4.15e-1
6.099746e-2	-1.865193e-1	1.079444e-1	1.425417e-1	4.25e-1
6.1596651e-2	-1.874353e-1	1.074919e-1	1.398725e-1	4.35e-1
6.1617624e-2	-1.877201e-1	1.07233e-1	1.434135e-1	4.45e-1
6.1362807e-2	-1.887772e-1	1.076771e-1	1.410659e-1	4.55e-1
6.0417544e-2	-1.884975e-1	1.073662e-1	1.40124e-1	4.65e-1
6.0356747e-2	-1.860967e-1	1.089522e-1	1.465904e-1	4.75e-1
6.1310686e-2	-1.864748e-1	1.074643e-1	1.443947e-1	4.85e-1
6.3436814e-2	-1.852238e-1	1.060932e-1	1.385355e-1	4.95e-1

Output file for hazard plot

$\lambda = 0.37$		$\lambda = 0.91$		$\lambda = 1.38$		$\lambda = 2.00$	
Cum.hz.	t(ns)	Cum.hz.	t(ns)	Cum.hz.	t(ns)	Cum.hz.	t(ns)
3.369555e-1	5e-3	2.679586e-1	5e-3	2.737752e-1	5e-3	2.365897e-1	5e-3
4.847662e-1	1e-2	3.820179e-1	1e-2	3.820364e-1	1e-2	3.124864e-1	1e-2
6.473255e-1	1.5e-2	4.688547e-1	1.5e-2	4.772498e-1	1.5e-2	3.983052e-1	1.5e-2
7.46891e-1	2e-2	5.538669e-1	2e-2	5.829155e-1	2e-2	5.090594e-1	2e-2
8.426781e-1	2.5e-2	6.665064e-1	2.5e-2	6.773447e-1	2.5e-2	6.045866e-1	2.5e-2
9.41743e-1	3e-2	7.520819e-1	3e-2	7.526505e-1	3e-2	6.710908e-1	3e-2
1.007789e+0	3.5e-2	8.365585e-1	3.5e-2	8.126882e-1	3.5e-2	7.691868e-1	3.5e-2
1.085453e+0	4e-2	9.391253e-1	4e-2	8.660949e-1	4e-2	8.473389e-1	4e-2
1.169269e+0	4.5e-2	1.047702e+0	4.5e-2	9.279314e-1	4.5e-2	8.891829e-1	4.5e-2
1.229303e+0	5e-2	1.162356e+0	5e-2	9.817411e-1	5e-2	9.392024e-1	5e-2
1.268786e+0	5.5e-2	1.29253e+0	5.5e-2	1.051712e+0	5.5e-2	9.987074e-1	5.5e-2
1.310005e+0	6e-2	1.405679e+0	6e-2	1.12678e+0	6e-2	1.091699e+0	6e-2
1.36175e+0	6.5e-2	1.467847e+0	6.5e-2	1.177526e+0	6.5e-2	1.201864e+0	6.5e-2
1.416319e+0	7e-2	1.534348e+0	7e-2	1.231398e+0	7e-2	1.288675e+0	7e-2
1.47404e+0	7.5e-2	1.62694e+0	7.5e-2	1.287878e+0	7.5e-2	1.374218e+0	7.5e-2
1.524734e+0	8e-2	1.765844e+0	8e-2	1.339328e+0	8e-2	1.445706e+0	8e-2
1.578327e+0	8.5e-2	1.896648e+0	8.5e-2	1.421735e+0	8.5e-2	1.559614e+0	8.5e-2
1.634744e+0	9e-2	1.984985e+0	9e-2	1.490414e+0	9e-2	1.671445e+0	9e-2
1.670181e+0	9.5e-2	2.064844e+0	9.5e-2	1.553834e+0	9.5e-2	1.712361e+0	9.5e-2
1.719785e+0	1e-1	2.133851e+0	1e-1	1.657063e+0	1e-1	1.78453e+0	1e-1
1.785042e+0	1.05e-1	2.207976e+0	1.05e-1	1.758067e+0	1.05e-1	1.845786e+0	1.05e-1
1.826333e+0	1.1e-1	2.28804e+0	1.1e-1	1.812634e+0	1.15e-1	1.878044e+0	1.1e-1
1.854905e+0	1.15e-1	2.375079e+0	1.2e-1	1.841206e+0	1.2e-1	1.928619e+0	1.15e-1
1.884316e+0	1.2e-1	2.445425e+0	1.25e-1	1.870618e+0	1.3e-1	2.000093e+0	1.2e-1
1.930244e+0	1.25e-1	2.495425e+0	1.45e-1	1.94882e+0	1.35e-1	2.077073e+0	1.25e-1
2.011844e+0	1.3e-1	2.548057e+0	1.5e-1	2.087164e+0	1.4e-1	2.13874e+0	1.35e-1
2.100176e+0	1.35e-1	2.603612e+0	1.55e-1	2.183458e+0	1.5e-1	2.204945e+0	1.4e-1
2.157156e+0	1.45e-1	2.662436e+0	1.6e-1	2.292365e+0	1.55e-1	2.300292e+0	1.45e-1

2.21799e+0	1.5e-1	2.758269e+0	1.65e-1	2.411676e+0	1.65e-1	2.434568e+0	1.5e-1
2.282301e+0	1.65e-1	2.863031e+0	1.75e-1	2.464308e+0	1.75e-1	2.554802e+0	1.55e-1
2.327756e+0	1.7e-1	2.939954e+0	1.8e-1	2.549275e+0	1.85e-1	2.694729e+0	1.6e-1
2.375375e+0	1.75e-1	3.023288e+0	1.95e-1	2.641187e+0	1.9e-1	2.853154e+0	1.65e-1
2.425375e+0	2.05e-1	3.114197e+0	2e-1	2.707854e+0	2.15e-1	2.944063e+0	1.85e-1
2.505785e+0	2.1e-1	3.214196e+0	2.05e-1	2.817744e+0	2.2e-1	3.044063e+0	1.9e-1
2.623636e+0	2.3e-1	3.325308e+0	2.1e-1	2.984993e+0	2.25e-1	3.155174e+0	1.95e-1
2.721552e+0	2.35e-1	3.450308e+0	2.15e-1	3.130447e+0	2.3e-1	3.280174e+0	2.1e-1
2.792981e+0	2.4e-1	3.593165e+0	2.25e-1	3.241559e+0	2.35e-1	3.423031e+0	2.3e-1
2.869904e+0	2.55e-1	3.759831e+0	2.35e-1	3.366559e+0	2.4e-1	3.589698e+0	2.55e-1
3.099197e+0	2.65e-1	3.959831e+0	3.05e-1	3.509416e+0	2.5e-1	3.914698e+0	2.75e-1
3.380257e+0	3.05e-1	4.209831e+0	3.1e-1	3.676082e+0	2.55e-1	4.373031e+0	3e-1
3.523114e+0	3.1e-1	4.543165e+0	3.2e-1	3.876082e+0	2.6e-1	4.873031e+0	3.35e-1
3.689781e+0	3.15e-1	5.043165e+0	3.45e-1	4.126082e+0	2.65e-1	5.873031e+0	3.95e-1
3.889781e+0	3.55e-1	6.043165e+0	3.85e-1	4.459416e+0	3.3e-1		
4.139781e+0	3.8e-1			4.959416e+0	3.4e-1		
4.473114e+0	4.3e-1			5.959416e+0	3.75e-1		
4.973114e+0	5.15e-1						
5.973114e+0	5.45e-1						